Report No. CG-D-53-77

092

ADA044197

CONTINUING DEVELOPMENT OF THE VULNERABILITY MODEL

FINAL REPORT
FEBRUARY 1977

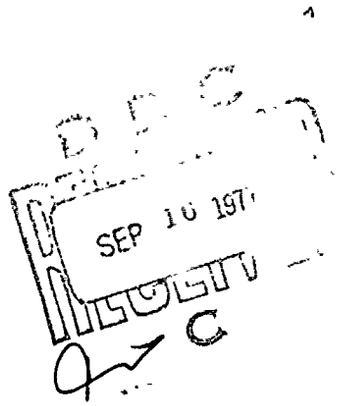

Prepared for

DEPARTMENT OF TRANSPORTATION
UNITED STATES COAST GUARD
Office of Research and Development
Washington, D.C. 20590

NOTICE

This document is disseminated under the sponsorship of the U. S. Department of Transportation in the interest of information exchange. The United States Government assumes no liability for the contents or use thereof.

The United States Government does not endorse products or manufacturers. Trade or manufacturers' names appear herein solely because they are considered essential to the object of this report.

(10) A. H./Rausch,
Norman A./Eisenberg
Cornelius J./Lynch

Technical Report Documentation Page

(18) 1. Report No. USCG-D-53-77 (19)	2. Government Accession No.
3. Recipient's Catalog No.	
(6) 4. Title and Subtitle: Continuing Development of the Vulnerability Model.	(11) 5. Report Date: February 1977
	6. Performing Organization Code
7. Author(s): A. H. Rausch, N. A./Eisenberg, C. J., Lynch	8. Performing Organization Report No.
9. Performing Organization Name and Address: Enviro Control, Inc. One Central Plaza 11300 Rockville Pike Rockville, Maryland (12) 340p.	10. Work Unit No. (TRAIS) 3142
	(15) 11. Contract or Grant No. DOT-CG-33377-A
12. Sponsoring Agency Name and Address: U. S. Coast Guard Headquarters Office of Research and Development Washington, D. C. 20590	13. Type of Report and Period Covered (9) Final Report,
	14. Sponsoring Agency Code G-DSA-1/TP44

15. Supplementary Notes

The U. S. Coast Guard's Research and Development Technical Representative for the work performed herein was Dr. M. C. Parnarouskis.

16. Abstract

This report describes the continuing development of the Vulnerability Model (VM), a computer simulation which provides a quantitative measure of the consequences of a marine hazardous chemical spill. Included are improvements in the modeling of fires, injury to indoor populations, additional toxicological analysis and modeling of ingestion of contaminated water.

17. Key Words	18. Distribution Statement
Vulnerability Model Damage Assessment Marine Spills	Unlimited

19. Security Classif. (of this report)	20. Security Classif. (of this page)	21. No. of Pages	22. Price
Unclassified	Unclassified	333	

Form DOT F 1700.7 (8-72) Reproduction of completed page authorized

CONTENTS

CONTENTS
(continued)

LIST OF FIGURES

LIST OF FIGURES (continued)

LIST OF FIGURES (continued)

LIST OF FIGURES (continued)

LIST OF TABLES

LIST OF TABLES (continued)

INTRODUCTION

BACKGROUND

This report describes the continuing development of the Vulnerability Model (VM), a computer simulation intended to provide quantitative measures of the consequences of maritime spills of hazardous materials. The VM is being developed for the U.S. Coast Guard under Contract DOT-CG-33377-A. Its first stage of development in described in [1].

The VM is a research tool, one of whose uses is in the USCG Risk Management Program. It has been designed to treat virtually all of the large class of materials carried in bulk in marine transport. Since many of the cargoes of particular hazard are carried as bulk liquids, the VM can provide useful information even in its current stage of development.

The simulation starts with a description of the nature of the spill itself, continues through the dispersion of the hazardous material, and ultimately includes assessment of the immediate effects of the spill on surrounding vulnerable resources; namely, people, property, and the environment.

The VM requires three types of descriptive data that define: (1) the spill, (2) the physical setting in which the spill occurs, and (3) the vulnerable resources that are subject to the effects of the spill. The spill is described in terms of its location and spill rate, the physical and chemical properties of the spilled material, and the quantity of the spill. The physical setting is described in terms of the geometric configuration of the shoreline(s), hydrologic/oceanographic properties, and meteorological data. Vulnerable resources are described in terms of demographic distribution, property distribution, and land/water use. The geographic area of concern may represent any user-defined location, a rectangular area measuring 10 miles in length and 5 miles in width being typical of anticipated applications. The physical setting and the distribution of vulnerable resources are described in terms of mutually exclusive geographic cells that cover the entire area of concern.

The VM operates in two phases. Phase I simulates the spill itself, the physical and chemical transformations of the spilled substance and its dissemination in space. This phase covers the time period from the

---

[1] Eisenberg, N. A., C. J. Lynch, and R. J. Breeding, *Vulnerability Model: A Simulation System for Assessing Damage Resulting From Marine Spills*, CG-D-136-75; NTIS AD-A015245, prepared by Enviro Control, Inc., for the Department of Transportation, U.S. Coast Guard, June 1975.

initiation of the spill until a user-specified time has elapsed. The time interval between simulation calculations is specified by the user but may be overridden by certain submodels (such as the explosion submodel).

Phase I of the VM consists of submodels interconnected by an executive routine, with built-in logic dictating the sequence of submodel processing as a function of the spill development. At the present time, submodels depicting spill development simulate the following phenomena: (1) cargo venting, (2) surface spreading (with or without evaporation), (3) water mixing, (4) sinking and boiling, (5) air dispersion, and (6) fire and explosion. Some of these submodels had been designed previously under USCG sponsorship, and others were designed specifically for the VM. A time-history file of the spill sequence simulated during the first phase is retained in computer storage on magnetic tape and disk.

In Phase II the computer first superimposes this time-history file upon the vulnerable resources map and then assesses the effects of toxicity, explosion and/or fire on the vulnerable resources as a function of time. Estimates of deaths and nonlethal injuries to people and of damage to property are presented in computer-generated tables. A summary of the types of Phase II damage assessment is given below.

PHASE II DAMAGE ASSESSMENT

DAMAGE-CAUSING EVENT	VULNERABLE RESOURCE	TYPE OF INJURY OR DAMAGE	
TOXICITY	People	Death	
		Nonlethal Injury	
		Irritation	
EXPLOSION	People	Death	
		Nonlethal Injury	Eardrum rupture
			Bone fracture
			Puncture
			Multiple injury
	Structures	Structural Damage	
		Glass Breakage	
POOL BURNING FLASH FIRE	People	Death	
		First-Degree Burn	
	Structures	Ignition	

SCOPE OF THIS WORK

The development phase of the VM described in this report consists of three major tasks:

TASK I.

- *A. Expand and Improve Spill Development Modeling*
- *B. Improve Flash Fire Modeling*
- *C. Improve Ignition Source Treatment*

TASK II.

- *A. Model Injury to Indoor Populations*
- *B. Improve Structural Ignition Criteria*

TASK III.

- *A. Model Secondary Fires of Special Hazards*
- *B. Model Injury from Inhalation of Toxic Combustion Products*
- *C. Model Ingestion of Water Containing Toxic Concentrations*
- *D. Model the Boiling Fireball*
- *E. Toxicological Analysis of Additional Cargoes*
- *F. Model Injury by Asphyxiation*

Chapter 1 of this report treats secondary fires and the boiling fireball. Chapter 2 extends the flash fire modeling, while Chapter 3 outlines the basic theory of ignition criteria and probabilistic interpretation. In Chapter 4 an improved method of structural ignition is outlined.

Toxicology of additional hazardous cargoes along with asphyxiation are treated in Chapter 5, while the related subject of toxic hazards from combustion products constitutes Chapter 6.

Chapter 7 treats the ingestion hazards from toxic material spilled in water; Chapter 8 deals with injury to indoor populations; and Chapter 9 details all changes, additions, and modifications of the VM computer program and includes accompanying flow diagrams. Included among these are the results of Task I-A, the expansion and improvement of spill modeling.

CONCLUSION

The improvements described in this report affect both the scope and the resolution of the system; the former by widening the available physical and chemical scenarios in both Phase I and Phase II, and the latter by increasing the accuracy of prediction outputs via an increase in physical-chemical-geometrical input. An example of a model that vastly increases the scope of the VM is the roiling fireball (Chapter 1), and an example of a model change that increases accuracy is the improved method of structural ignition (Chapter 4).

Chapter 1
SECONDARY FIRES

INTRODUCTION

This chapter treats the phenomenology and analytical aspects of secondary fires, their causes and effects. In particular, we look at three chemical classes of secondary fires: light hydrocarbons, polymers, and cellulose products. Where apropos, especially virulent hazards such as fireball formation or catastrophic container failure are discussed.

A secondary fire is one which is started because of the presence of a large *primary* fire, as previously simulated in Phase I of the Vulnerability Model (VM). Should the primary radiation intensity and duration at the secondary site exceed threshold values specific to each secondary chemical or containment configuration, a secondary fire is assumed to occur. The criteria and outputs of such an event are very similar to those of structural ignition in Phase II of the VM. Among the outputs are: radiation intensity, fire size, and duration of burning. With the exception of the fireball treatment, all analytical and empirical results have been computerized and inserted as VM subroutines. For further details on computer aspects, the reader is referred to Chapter 9.

It is concluded from the work that follows that, while the polymers are the easiest to ignite from far-removed external radiation sources, the hazard to structures and personnel arising from such a fire is small compared to that from a fire of a light hydrocarbon. This is due primarily to the much larger specific energy content of a hydrocarbon and its great ease of burning, reflected largely by its rapid combustion kinetics. Indeed, the most hazardous fire-specific configuration studied thus far in connection with the VM is the fireball that frequently forms during any large propane fire. Its radiation intensity and view factor combine so as to maximize the damage and killing potential in the surrounding area. Fortunately, the containment mechanics of such fuels, through tankage, make the ignition of such a fire more difficult than in the case of open storage of some polymer and cellulose materials.

To summarize briefly what the Secondary Fire Model does, we list the following computational steps in the order in which they are actually performed by the computer.

(1) Radiation intensity and duration from primary fires are calculated at secondary fire sites, to determine whether a secondary chemical ignites.

(2) If ignition occurs, duration, fire size, radiation, etc., are calculated.

(3) Results are stored or sent to appropriate subroutines to await retrieval by Phase II to determine hazard to people and structures.

A. *LIGHT HYDROCARBONS*

One of the main problems concerning tank farm design for light liquid fuels, such as gasoline or butane, is that the required distance between tanks be sufficient to prevent fire spread by radiation from adjacent tanks. To this end, investigators have gained knowledge through both analysis and experimentation on the burning behavior of liquid fuel in open tanks, made either by intent or accident.

Heat released from a burning tank of liquid fuel will be transferred by radiation as well as by convection, but particularly by the former. Convective heat transfer will become important only under strong-wind conditions and will not be considered here.

We will briefly discuss burning rate, flame size, and radiation intensity for a liquid fuel tank fire, and we will give formulas for each. We will thus be able to determine (for a given spill size and diameter) the burning duration and effective intensity for a given liquid fuel fire, information that will be stored and sent to the View Factor Submodel of Phase I of the VM and, subsequently, to Phase II of the VM to determine hazard to personnel and structures from the secondary liquid fuel fires. Finally, we will briefly discuss the Enclosure Model.

1. *Burning Rate*

By correlating burning velocity in centimeters per second with the ratio of heat of combustion to latent heat, $\Delta H_C/\Delta H_V$, Burgess and Hertzberg [2] were able to gain an expression for burning rate of large hydrocarbon fires.

The formula obtained by them was:

$$V_\infty = .000076\ \Delta H_C/\Delta H_V \qquad (1\text{-}1)$$

---

[2] Burgess, D., and M. Hertzberg, Radiation from pool flames, pp. 407-451, in Afghan and Beer (eds.), *Heat Transfer in Flames*, John Wiley & Sons, New York, 1974.

where V_∞ is the limiting, large fire (m/s) velocity of burning of the hydrocarbon fire, ΔH_C is the heat of combustion to CO_2 and water vapor, and ΔH_V is the heat of vaporization. This expression correlates with the data for butane, gasoline, and even LNG for pool burning in a large open tank under low-wind conditions. It turns out that further work on the part of Burgess suggested a modification of (1-1) based on a burning rate, V_p, of grams of fuel per square centimeter per minute.

$$V_p = .007 \frac{\Delta H_C}{\Delta H_V} \tag{1-2}$$

According to the revised scheme, gasoline will have a value of V_p equal to 0.6 and butane 0.5, as will benzene. These figures tend to be conservative, in that they will overestimate the hazard due to fire from these fuels.

2. Flame Size

There are theoretical and experimental studies [3] on hand, demonstrating that the relation between relative flame height, L, and the Froude number, F, may be described by the following exponential equation

$$\frac{L}{d} = CF^{0.2} \tag{1-3}$$

where d is the tank diameter and C is a constant that depends on the fuel being used. Here F is given as

$$F = \frac{V^2}{gd} \tag{1-4}$$

where V is the vapor velocity of fuel and g is the acceleration of gravity. Since V varies from about 10 to 20 mm/s and tank diameters range from about 10 to 100 meters, F is of the order of 10^{-6} to 10^{-7}. From these considerations, it can be shown that the ratio L/d is in the range of one to two [4]. Since the error introduced by inaccurate determination of flame height is not large, we will take the conservative figure of two and thereby end up by slightly overestimating the hazard of tank fires.

---

[3] Putnam, A. A., and C. F. Speich, A model study of the interaction of multiple turbulent diffusion flames, in *Ninth Symposium on Combustion*, Academic Press, New York, 1963.

[4] Atallah, S., and D. S. Allan, Safe separation distances from liquid fires, *Fire Technol.* 7(1): 47-56, 1973.

3. Radiation to Surroundings

The thermal radiation of a hydrocarbon flame is composed of the radiation of individual components of combustion gases, in particular CO_2 and H_2O, which absorb and emit in narrow wavelength bands between one and eight microns. In addition, soot radiates in all frequency ranges according to the Stefan-Boltzmann law modified for gray emission. The spectral intensity of gas radiation depends on temperature, thickness of flame layer, and the partial pressure of the corresponding constituent gas. There are luminous and nonluminous flames, depending on whether soot formation and consequently soot radiation are present or not.

For most engineering purposes, the radiant effective fire surface flux, I_r, can be expressed as follows [5].

$$I_r = I_m \, (1 - e^{-bd}) \tag{1-5}$$

where I_m is the maximum surface radiation for hydrocarbon fires and b is the attenuation coefficient representing the fact that the fire becomes optically thick at a value of d such that $e^{-bd} \ll 1$. For our purposes, $I_m = 142{,}000 \text{ J m}^{-2} \text{ s}^{-1}$ and $b = 0.18$ 1/m Thus, for d of the order of 30 meters, e^{-bd} is of the order of 10^{-2} to 10^{-3} and hence can be neglected for large tanks. Recall d is diameter of tank and thus flame size.

We summarize the steps needed to determine hazard from a liquid hydrocarbon fuel tank fire here, given that it occurs due to structural failure caused by the primary fire resulting from the marine spill.

(1) Determine mass burning rate, V_p, from equation (1-2). ΔH_c and ΔH_v will be in the Properties File for a given hydrocarbon.

(2) From the known contents of the tank, determine burning time by dividing by $(\pi d^2 V_p)/4$. Call this t_{eff}.

(3) Determine flame height/diameter from equation (1-3) or use the conservative value of 2.0. In all cases of interest, L/d is between one and two.

(4) Determine I_r from (1-5) where $I_r = 142{,}000 \, (1 - e^{-0.18 \, d})$.

Flame height, diameter, burning time, and radiation intensity, I_r, are stored and sent to the View Factor Submodel to assess hazard at points exterior to the tank. The results are subsequently sent to Phase II of the VM to determine hazard to personnel and structures.

---

[5] Welker, J. R., *LNG Safety Program*, Interim Report on Phase II Work, American Gas Association, 1974.

4. Enclosure Model

An Enclosure Model, which determines structural stability of a container of flammable loadings such as liquefied petroleum gases and gasoline is described here. The model has the following features.

- Provision for boiling of lading to take place.
- Allowance for venting of lading whenever relief valve setting is surpassed.
- Consideration of dual-wall container.
- Consideration of three general shapes of containers: spherical shell, vertical cylindrical shell, and horizontal cylindrical shell.
- Capability of treating cases involving time-dependent thermal radiation influx.
- Capability of calculating time when container failure occurs.
- Stress and strength analysis of container material and specification of failure criteria.
- Flexibility of accommodating a variety of liquid flammable ladings, provided their thermodynamic properties are known.

To provide an integral picture of the model, a brief discussion of the model is presented here before rigorous treatment of the problem in subsequent sections of Appendix A. To facilitate discussion, a flowchart of the model is shown in Chapter 9. The model can be divided into four submodels, namely: (1) dual-wall container with thermal insulation, (2) spherical container, (3) vertical cylindrical container, and (4) horizontal cylindrical container. It is believed that these four submodels should cover most containers commonly used.

The strength of the outer wall of an insulated dual-wall container submitted to external thermal radiation will deteriorate if the temperature of the outer wall is sufficiently high. However, the inner wall, due to heat insulation, may remain in its normal condition throughout part of or the whole period of external thermal radiation. The structural stability of a dual-wall container depends heavily on the wall material, design criteria, construction, external thermal radiation influx, and time duration. The time-history of temperature of the outer wall is related to material properties and to characteristics of thermal radiation (discussed in detail in Appendix A). Stress and strength analysis is also discussed in Appendix A. Comparison of stress with failure criteria determines the structural stability of the container.

Submodels (2), (3), and (4) resemble each other, notwithstanding their differences in geometry, because none of them has insulation or fire retardant between the container shell and inside lading. These

submodels are therefore treated equally in Appendix A and amended separately to accommodate variations in container geometry. Envisioning sequential events that occur to the container system is important for their successful simulation in a computer. Thermal radiation energy incident upon the container wall is transmitted to the inner surface primarily by conduction. The primary driving force for heat conduction is the temperature difference between outer and inner surfaces of the container. Part of the heat is absorbed in the shell wall and causes the wall temperature to rise. The rest of the conducted heat is used to heat inside liquid lading and lading volume in the ullage volume. If external thermal radiation influx persists for a sufficiently long time, the temperature difference between the inner surface of the shell and liquid lading becomes large enough to cause boiling of liquid lading to commence. The temperature rises in both liquid lading and ullage vapor and the vaporization of liquid lading cause significant buildup of internal pressure. The buildup of internal pressure, coupled with differential thermal expansion of outer and inner surfaces of the container shell, induces extra stresses on the wall material, while the wall material deteriorates in strength due to elevated temperature. The combined effect may cause failure of the wall material.

Containers of flammable materials are usually provided with relief valves, regulatory valves, or similar devices to regulate internal pressure and to control venting of lading. Depending on design pressure, safety factor, and relief-valve setting, venting of lading may be initiated before the container fails structurally. Venting flammable vapor or liquid may catch on fire. A torch resulting from ignition of flammable material venting becomes an emission source of thermal radiation. From full-scale fire tests of a railroad tank car carrying liquefied propane [6], the temperature of a propane torch is approximately 1100°C (2010°F) which can contribute a significant level of thermal radiation to the vicinity of the relief valve. Failure of the tank car under test was initiated not by valve failure but by the preexistence of an acicular type of microstructure, according to a fragmentation and metallurgical follow-up analysis [7]. At the moment of tank failure, the temperature at the location where the failure is believed to have commenced was about 1000°C (1830°F), which is comparable to the temperature of a propane torch. It is conceivable that, under proper conditions, thermal radiation from a torch may significantly deteriorate the seals or gasket of relief valves, causing subsequent failure of the container shell.

---

[6] Anderson, C., W. Townsend, J. Zook, and C. Cowgill, *The Effects of a Fire Environment on a Rail Tank Car Filled with LPG*, prepared for U.S. Department of Transportation, Federal Railroad Administration by Ballistic Research Laboratories, September 1974.

[7] Anderson, C., and E. B. Norris, *Fragmentation and Metallurgical Analysis of Tank Car RAX 201*, prepared for U.S. Department of Transportation, Federal Railroad Administration by Ballistic Research Laboratories, April 1974.

During one of the railroad tank car fire tests, it was observed visually and recorded by motion pictures that seals of valves were burned out at about 870°C (1600°F) before the internal pressure could rise to 270 psig, the pressure required to force open the relief valve [8]. Thus the criteria for structural failure are considered to be met whenever venting and ignition of flammable material occur, since it is assumed that the proximity of the resulting torch flame will be sufficient to raise the tank skin temperature to thermal failure.

5. Boiling Fireball

When a tank containing a liquid petroleum gas such as propane, butane, or for that matter a rich LNG, i.e., one containing a large fraction of heavy hydrocarbons, fails in an accident situation, the internal energy of the pressurized content causes the fuel to expand rapidly and mix with ambient air. Within a few seconds, a large cloud of fuel and air is formed. Such a tank failure of the type described here would be of the catastrophic variety caused by a detonation wave from exterior sources or by extreme heating from a nearby fire. It is likely that, once the tank has started to fail, the internal pressure of the contents will accelerate the failure.

One of the primary hazards from this type of mishap occurs when the cloud of fuel and air is ignited and results in the formation of a fireball. Such a fireball is to be noted for its extreme thermal radiation capability which can result in damage to personnel and structures at distances far exceeding those intuitively felt to be safe for a conventional fire. Many bystanders and inexperienced fire fighters have paid for this mistake with their lives or by suffering third-degree burns over major portions of their bodies.

In this section, a thermal and largely empirical model that describes the heat load on an object at the center of the fireball and at various distances from the fireball is developed. The results are in fairly good agreement with experimental observations. The method of development is essentially that of Hardee and Lee [9].

---

[8] Anderson, C., W. Townsend, J. Zook, W. Wright, and G. Cowgill, *Railroad Tank Car Fire Test: Test No. 7*, prepared for U.S. Department of Transportation, Federal Railroad Administration by Ballistic Research Laboratories, December 1973.

[9] Hardee, H. C., and D. O. Lee, Thermal hazard from propane fireballs, *Transp. Plann. Technol. 2*:121-128, 1973.

a. *Assumptions of model*

The formation of the fireball begins with the ignition of a small amount of fuel. Such ignition will occur more likely by contact with hot container metal than by radiation from another nearby fire. The fuel and air continue to mix and burn at or very near one atmosphere of pressure. Initially the fireball is an expanding hemisphere; however, as buoyant forces begin to act on the hot gases, the fireball starts to rise and approaches a spherical shape. When most of the fuel and air have reacted, expansion decreases and the buoyant forces that now begin to predominate may cause the fireball to rise from the ground. After this point, drag and natural convection currents cause the fireball to assume the familiar mushroom shape.

We assume that the following conditions hold during and after the fireball formation.

(1) Rate of fuel insertion to fireball is roughly constant. This is consistent with experimental observation.

(2) A stoichiometric mixture exists at ignition. This will result in a calculation that tends to overestimate the resulting hazard and therefore represents a worst-case condition.

(3) All available fuel participates in the reaction. Again, this leads to a conservative safety estimate.

(4) The fireball is an isothermal, homogeneous body that is spherical at all times. The cause of this condition is a high degree of turbulence and probably vorticity. This assumption is in accord with detailed analysis which concluded that effects of nonspheroidicity can be neglected [10].

(5) The fireball radiates as a blackbody, which is caused by luminous carbon particles that are abundant even for oxygen-rich fires [11]. In addition, many fireballs will easily exceed in size the optical path length of their associated fires, which justifies the assumption that the emissivity, ε, equals unity.

(6) Burnout time, τ_b, and lift-off time coincide because rapid outward expansion ceases at the termination of fuel addition. Of all the assumptions, this is perhaps the weakest and most difficult to justify experimentally; however, it does

---

[10] Van Nice, L. J., and H. J. Carpenter, *Thermal Radiation from Saturn Fireball*, TRW Systems, NAS 9-4810, December 1965.

[11] Street, J. C., and A. Thomas, Carbon formation in premixed flames, *Fuel 34*:4, January 1955.

not seem to alter the overall analytical results significantly. An analysis based on a rigorous hydrodynamic model would determine lift-off as a function of stability and separation.

(7) The reference state for the fuel-air mixture is 537°R and 1 atmosphere of pressure. For propane, which will be the fuel analyzed here, this implies an adiabatic flame temperature of almost 4000°R.

b. The model

The first consideration to be encountered is how to relate lift-off time to size of fire or, more precisely, to the weight of fuel and air participating in the reaction, W_b. Results of Bader et al. [12] show that:

$$\tau_b = 0.6\ W_b^{1/6} \tag{1-6}$$

The average growth rate, R, for liquid fuel fireballs must be, according to assumption (1) and equation (1-6),

$$R = \frac{W_b}{\tau_b} = 1.67\ W_b^{5/6} \tag{1-7}$$

For a spherical fireball of density ρ, this implies a radius, r, as a function of time, t, of

$$r = \left(\frac{0.75\ W_b t}{\pi \rho \tau_b}\right)^{1/3} \tag{1-8}$$

Thus we see that the radius of the fireball grows as the one-third power of time, t, starting with the fire's inception.

The energy balance of the fireball considers enthalpy of entering mass, radiation heat loss, and addition to energy accumulation from within. This is expressed by

$$\frac{dW}{dt}\, h_{in} - q_r = \frac{d}{dt}\,(W h_{FB}) \tag{1-9}$$

where h_{in} is enthalpy of combusted mixture, $W = (W_b/\tau_b)t$, $q_r = \sigma A T^4$ for a blackbody and surface area, A, and h_{FB} is instantaneous enthalpy

[12] Bader, B. E., A. B. Donaldson, and H. C. Hardee, Liquid-propellant rocket abort fire model, *J. Spacecr. Rockets* 8:1216-1219, December 1971.

of fireball. To calculate A in this context, we use (1-8) for r and obtain

$$A = 4\pi \left(0.75 \frac{W_b}{\pi \tau_b}\right)^{2/3} \left(\frac{t}{\rho}\right)^{2/3} \tag{1-10}$$

If we express time as a dimensionless parameter, $\theta = t/\tau_b$, and let the instantaneous value of enthalpy of the fireball be h_{FB}, we obtain, after considerable manipulation,

$$\theta\left(h_{in} - h_{FB}\right) = \frac{0.6\,\sigma}{W_b^{1/6}} (36\pi)^{1/3} \int_0^{\theta} \left(\frac{\theta'}{\rho}\right)^{2/3} T^4 d\theta' \tag{1-11}$$

We must express ρ in terms of T to solve the integral equation numerically for a given value of W_b, i.e., spill size. Values of θ of interest are between zero and one.

For propane, Hardee and Lee [9] have calculated the average density, ρ, for the fireball from the relation

$$\rho = \frac{P}{RT} \cdot MW \tag{1-12}$$

where R is the molar gas constant and MW is the average molecular weight which, for propane and air, is given as 28.3. This gives for the case at hand

$$\rho = \frac{38.8}{T} \tag{1-13}$$

Inserting this value for ρ in (1-11), we obtain finally

$$\theta\left(h_{in} - h_{FB}\right) = \frac{0.253\,\sigma}{W_b^{1/6}} \int_0^{\theta} \theta'^{2/3} T^{14/3}\, d\theta' \tag{1-14}$$

The numerical solution to (1-14) is shown graphically in Figure 1-1 for W_b = 1000 lb of propane. In the graph, the fireball temperature, T, is given as a function of θ for a stoichiometric mixture. All other mixtures would yield curves below the one shown; hence, they would be cooler for equal values of θ.

It is of interest to show what the thermal flux resulting from such a fireball is at a point interior to the fireball. Utilizing Figure 1-1 and the relationship, $q_0 = \sigma A T^4$, one can plot the internal heat flux, as shown in Figure 1-2.

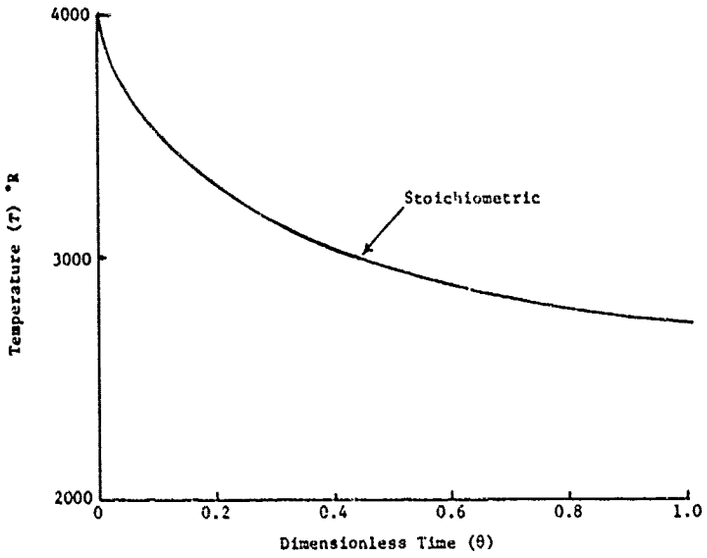

FIGURE 1-1. Fireball Center Temperature Versus Dimensionless Time for 1000 Pounds of Propane

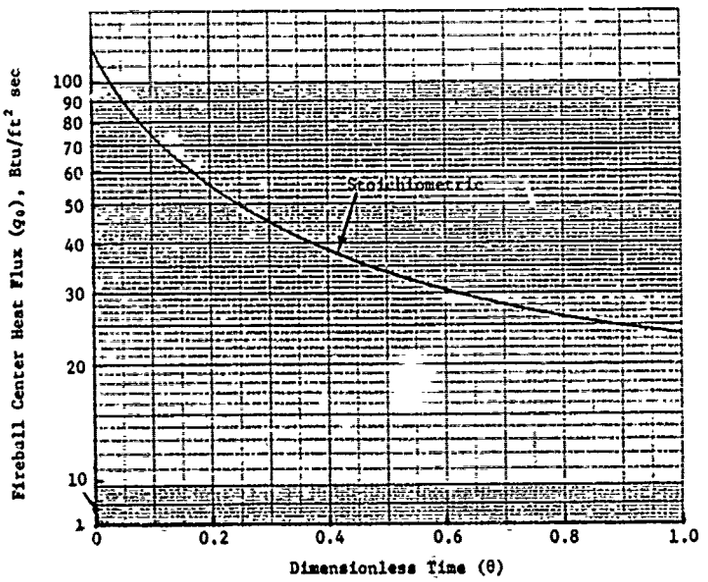

FIGURE 1-2. Fireball Center Heat Flux Versus Dimensionless Time for 1000 Pounds of Propane

The heat received by a body located at a distance, d, from the fireball center can also be significant, as is well known. To calculate this, it is necessary to include a view factor, F_{12}, such that

$$q_{ext} = F_{12} q_0 \tag{1-15}$$

where for $d > r$

$$F_{12} = 1/2 \left[1 - \{1 - (r/d)^2\}^{1/2}\right] \tag{1-16}$$

The total incident radiation on a body outside the fireball is

$$Q = \tau_b \int_0^1 q_{ext} d\theta \tag{1-17}$$

or

$$Q = \tau_b \int_0^1 q_0/2 \left[1 - \{1 - (r/d)^2\}^{1/2}\right] d\theta \tag{1-18}$$

Let the ratio of d to the maximum fireball radius, r_b, be L

$$\frac{d}{r_b} = L \tag{1-19}$$

Then, from equation (1-8), we have

$$\frac{r}{r_b} = \theta^{1/3} \tag{1-20}$$

giving

$$\frac{r}{d} = \frac{\theta^{1/3}}{L} \tag{1-21}$$

Substituting (1-21) into (1-18), we obtain

$$Q = \frac{\tau_b}{2} \int_0^1 q_0 \left[1 - \left(1 - \frac{\theta^{2/3}}{L^2}\right)^{1/2}\right] d\theta \tag{1-22}$$

Equation (1-22) has been integrated for propane fires of up to one million pounds for a stoichiometric mixture for $L = 0$, 1, 1.5, and 2. The results are shown in Figure 1-3. It should be emphasized that these curves represent the worst possible case as compared to fuel-rich or fuel-lean cases. As such, Figure 1-3 can be used as a basic thermal model for hazard prediction for propane fires and, with suitable modification, for other light hydrocarbons capable of fireball generation. For regions outside the fireball, the final radius is needed as a function of W_f. It turns out that for spills in our interest range, 1000 pounds or greater, r_b is given as

$$r_b = 7\, W_f^{1/3} \tag{1-23}$$

where W_f is the total weight of the propane spilled. For instance, for a 200,000-pound spill, $r_b = 7(200{,}000)^{1/3} \simeq 400$ ft. If a stoichiometric propane-air mixture of this size were ignited, a heat load of absorption of 20 Btu/ft^2 would occur at a distance of 800 feet from the fire over a time of the order of 5 seconds. This is far more than enough to kill a person without cover. Indeed, a 10-Btu exposure over a few seconds will cause third-degree burns, which in this case would occur at a distance of the order of 1200 feet. This is in tragic accord with actual accident experience of this type, especially on the part of onlookers wearing only light clothing. It is also evident from these figures that numerous wood dwelling and brush fires will be ignited within a radius of 800 feet, just from radiation alone.

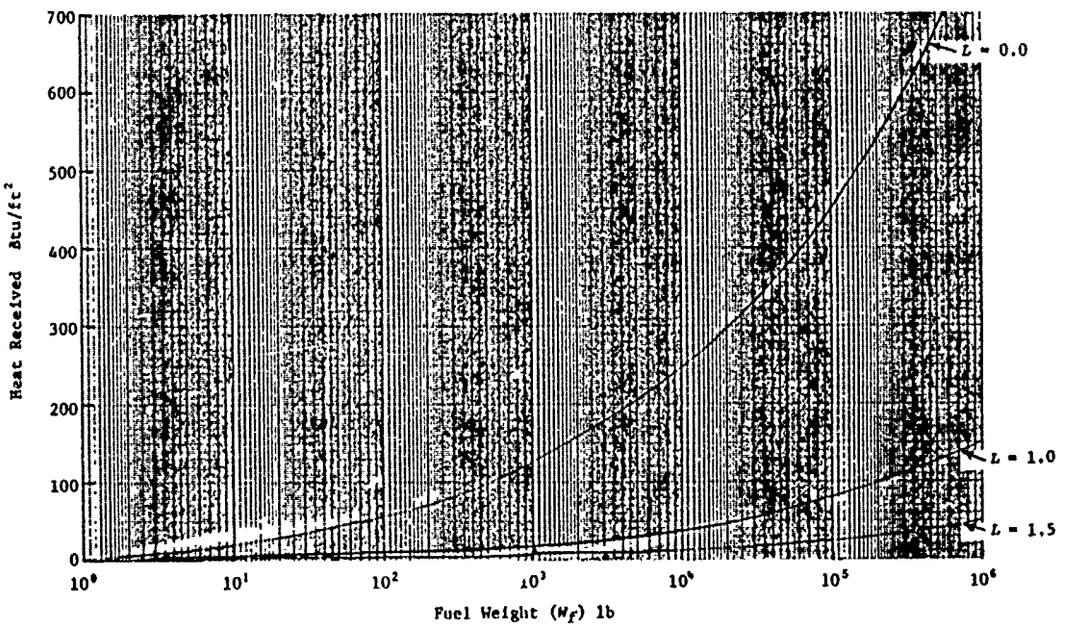

FIGURE 1-3. Heat Received Versus Fuel Weight for Various Distance Ratios for Fuel Burned Stoichiometrically in Air

B. *POLYMERS*

There are four areas of investigation that are important with respect to the study of flammability of solid materials in general and polymers in particular. They are:

- The time and energy required for ignition under a given heat load.
- The burning rate of combustible material, given that ignition has occurred.
- The rate of energy release and total quantity of energy released during combustion.
- The rate of release of toxic products and the quantity of toxic products released during pyrolysis and combustion.

This section addresses the first three areas; toxic substance release is not to be treated in this stage of VM development.

Most polymers will burn. Almost everyone agrees on this point. However, with few exceptions, the degree of flammability hazard of plastics is still under active discussion and investigation. It has been pointed out by some authorities that the autoignition temperatures of most polymers are hundreds of degrees higher than those of ordinary combustible materials. This being true, it does not follow that the resulting fire hazard is necessarily small or inconsequential. Indeed, most of the fire-fighting community now have enough field experience with polymers to add the weight of their reports on the actual behavior of polymers. Although a polymer may be hard to ignite and slow burning, it can be extremely difficult to extinguish when glowing combustion burrows deep into a pile of plastic powder, dust, beads, chips, etc.

In this section, we will model the ignition of several polymers due to external radiation. This will be followed by a discussion of and expressions for burning rates and radiation heat emission.

1. *Ignition of Polymers*

The literature contains little data for the ignition of polymers. The following discussion is patterned after the work of Welker [13] and Hallman et al. [14].

---

[13] Welker, J. R., Ignition of combustible solids, in *Advances in Fire Retardants*, pt. 1, vol. 2, Progress in Fire Retardancy Series, Technomic Publishing Co., Westport, Conn., 1972.

[14] Hallman, J. R., J. R. Welker, and C. M. Sliepcevich, *J. Fire Flammability* 2:321, 1971.

The ultimate objectives of devising a model for the process leading up to the ignition of polymers are: to find an algorithm for predicting whether or not ignition will occur under a given set of radiation and material conditions and, if ignition does occur, to predict how long it will take. Since it is not physically or mathematically possible to model the ignition process exactly, we are forced to resort to correlation techniques based on experimental results. It is shown in reference [13] that the time of ignition, t_i, for a given polymer subjected to an effective constant radiation flux, I_r, and thermal inertia ($\kappa\rho c$) is

$$t_i = \frac{\psi(\kappa\rho c)^a \ \Delta T_s{}^b}{(I_r)^d} \tag{1-24}$$

where ψ is a constant; and a, b, and d are to be determined experimentally; and ΔT_s is equal to $(T_s - T_i)$. Here T_s is the exposed surface temperature, which will turn out to be equivalent to the ignition temperature, and T_i is the initial specimen temperature and is a constant. κ, ρ, and c are respectively the thermal conductivity, density, and specific heat of the polymer. Hallman et al.[14] used the ignition data from tests on a dozen polymers to evaluate ψ, a, b, and d. The incident radiation, sample densities, and ignition times were measured directly for each polymer tested. Literature data for κ, ρ, and c as well as ignition temperature, T_s, were used. A least squares analysis showed that the ignition data are best represented by

$$t_i = \frac{160(\kappa\rho c)^{0.75}\,\Delta T_s}{(I_r)^2} \tag{1-25}$$

It is important to point out that (1-25) is a dimensional equation, the units being:

$$t_i = \text{sec}$$

$$\kappa = \frac{\text{cal}}{\text{cm sec } ^\circ\text{C}}$$

$$c = \frac{\text{cal}}{\text{gm } ^\circ\text{C}}$$

$$\Delta T_s = ^\circ\text{C}$$

$$I_r = \frac{\text{cal}}{\text{cm}^2 \text{ sec}}$$

The following practical procedure would be employed with (1-25) to determine if ignition of a given polymer would occur for a given radiation intensity, I_r, of duration, t_{eff}.

(1) Calculate the surface temperature, T, of the polymer from the relation [15]

$$T \simeq T_i + \frac{2 I_r t_{eff}^{1/2}}{(k\rho c)^{1/2}} \tag{1-26}$$

This assumes that the thickness of the polymer is infinite and that the absorptivity is unity.

(2) For the given polymer, if the value of T from (1-26) exceeds T_s, proceed to calculate t_i from equation (1-25). If t_{eff} exceeds or equals t_i, ignition is assumed to occur.

Thus, two simultaneous criteria must be satisfied

$$T \geq T_s \tag{1-27}$$

$$t_{eff} \geq t_i \tag{1-28}$$

Average values of $(k\rho c)$ and T_s can be used to calculate the quantities needed to determine ignition without large error. T_i can be taken as the ambient air temperature. Values of $(k\rho c)$ and T_s are given in Table 1-1 and can be employed in the calculations in lieu of averages, if the user so desires.

TABLE 1-1. THERMAL INERTIA AND IGNITION TEMPERATURE DIFFERENCES OF SEVERAL POLYMER MATERIALS

Material	$(k\rho c)^{0.75}$	ΔT_s
Gum Rubber	$[(2.9 \times 10^{-4})(0.99)(0.475)]^{0.75} = 1.26 \times 10^{-3}$	240
Cellulose Acetate Butyrate	$[(6.0 \times 10^{-4})(1.2)(0.35)]^{0.75} = 2.0 \times 10^{-3}$	180
Lexan	$[(4.6 \times 10^{-4})(1.19)(0.30)]^{0.75} = 1.45 \times 10^{-3}$	800
Bakelite	$[(5.5 \times 10^{-4})(1.37)(0.375)]^{0.75} = 2.18 \times 10^{-3}$	460
Silicone Rubber	$[(5 \times 10^{-4})(1.35)(0.35)]^{0.75} = 1.90 \times 10^{-3}$	720
Polypropylene	$[(3.5 \times 10^{-4})(0.905)(0.50)]^{0.75} = 1.41 \times 10^{-3}$	410
Polyethylene	$[(10 \times 10^{-4})(0.933)(0.55)]^{0.75} = 3.41 \times 10^{-3}$	250
Plexiglas	$[(5 \times 10^{-4})(1.19)(0.35)]^{0.75} = 1.73 \times 10^{-3}$	260
PVC	$[(5 \times 10^{-4})(1.40)(0.24)]^{0.75} = 1.48 \times 10^{-3}$	220
Polystyrene	$[(2.9 \times 10^{-4})(1.63)(0.325)]^{0.75} = 1.38 \times 10^{-3}$	350
Polymide (Nylon 6/6)	$[(5.9 \times 10^{-4})(1.14)(0.4)]^{0.75} = 2.10 \times 10^{-3}$	460
Polyoxymethylene Delrin	$[(5.5 \times 10^{-4})(1.43)(0.35)]^{0.75} = 2.36 \times 10^{-3}$	320

[15] Carslow, H. S., and J. C. Jaeger, *Conduction of Heat in Solids*, 2nd ed., Oxford Press, 1959.

2. *Pool Fires of Polymers*

The model for pool burning of polymers that follows is based on the presentation by Kanury [16]. Essentially, he conducted experiments on and analyzed the results of convective diffusional burning of eight different polymeric solids in the geometry of circular pools. By taking into account variance principles by means of dimensionless numbers, he was able to scale the results to large fire sizes from laboratory-scale results.

A simple one-dimensional diffusion flame theory is used to correlate mass transfer rates, history of burning, and radiant emission rates.

It should be noted that, at this time, much experimental field work remains to be done on large-scale polymer fires, in order to pin down precisely the fire and radiation hazard emanating therefrom. Since this is not the case at present, we will have to content ourselves with the following treatment until further results are forthcoming.

In 1936 Saunders [17] studied natural convection heat transfer from a vertical flat plate by employing an ingenious technique, in which the *effective height of the flat plate was varied by varying the ambient gas-phase pressure*. Thus, scaling techniques could be applied, and it was possible to deduce the behavior of large-scale phenomena from small-scale laboratory effects. Considering the fire spread and steady burning aspects, in which heat and mass transfer processes are considerably slower than combustion reaction kinetics, de Ris et al. [18] demonstrated that Saunders' technique may be used successfully to model large-scale fires at elevated ambient pressures. The modeling prescriptions evolve from the invariance of certain dimensionless groups between the small-scale model and the full-scale prototype fires. It is from this point of view that we justify our presentation here.

Because most fires usually consist of free convection flows, the inherent fluid mechanical characteristics of geometrically similar fires are governed by the Grashof number, a dimensionless group, which is defined as

$$G = \frac{g L^3 \beta \Delta T \rho^2}{\mu^2}$$

---

[16] Kanury, A. M., Modeling of pool fires with a variety of polymers, in *Fifteenth Symposium on Combustion*, The Combustion Institute, Pittsburgh, Pa., 1974.

[17] Saunders, O. A., The effect of pressure upon natural convection in Air, pp. 278-291, in *Proceedings of Royal Society*, vol. A157, London, 1936.

[18] de Ris, J., A. M. Kanury, and M. C. Yen, Pressure modeling of fires, pp. 1033-1044, *Fourteenth Symposium on Combustion*, The Combustion Institute, Pittsburgh, Pa., 1973.

where g is the acceleration due to gravity, ρ the density, and $\beta\Delta T$ the volumetric expansion ratio at constant pressure. Since the viscosity, μ, molecular weight, M, and the flame, wall, and ambient temperatures are essentially independent of pressure, G remains invariant if the product of length cubed and pressure squared (L^3P^2) is kept invariant between the model and prototype. If any externally controlled velocities, v, are present, invariance is preserved only when either the Reynolds number, $R = \rho vL/\mu$, or the Froude number, $F = \Delta\rho gL/\rho v^2$, is also held invariant; this in turn implies that all the forced velocities have to be so adjusted such that the product Pv^3 is invariant. Perhaps the best way to understand this intuitively is to recall that G represents the ratio of buoyant forces to viscous forces, R the ratio of inertial forces to viscous forces, and F the ratio of gravitational forces to inertial forces.

Upon scaling these fires with adjusted ambient pressures and forced velocities, the dependent dimensionless numbers associated with the convective heat and mass fluxes, the Nusselt and Sherwood numbers, and the solid- and gas-phase characteristic time scales represented by the Fourier numbers will remain invariant. This is all proven by dimensional analysis in reference [18].

For modeling purposes, the following statements are assumed to hold.

(1) c_p, i.e., specific heats, for all gas-phase chemical species are equal.

(2) The problem is one-dimensional in z-direction.

(3) Heat and mass transfer resistance takes place over a thickness of dimension $\delta = \kappa/h$ where κ is the thermal conductivity of the gas phase and h the convective coefficient of heat transfer under turbulent conditions.

(4) Chemical reactions occur infinitely fast, producing a very thin flame sheet.

(5) Flame sheet radiates as an optically thick body at temperature, T_f.

(6) The radiant fluxes transferred from the flame (subscript f) to the polymer surface (subscript w) and to the ambient (subscript ∞) are respectively, $\dot{q}_{rf}$, $\dot{q}_{rw}$, and $\dot{q}_{r\infty}$.

From these considerations, the energy and species conservation equations are:

$$\kappa \frac{d^2T}{dz^2} - \dot{m}c_p \frac{dT}{dz} + \dot{q} = 0 \qquad (1\text{-}29)$$

and

$$\frac{\kappa}{c_p} \frac{d^2Y_i}{dz^2} - \dot{m} \frac{dY_i}{dz} + \dot{W}_i = 0 \qquad (1\text{-}30)$$

where z is the coordinate normal to polymer surface, $\dot{m}$ is the mass transfer rate, Y_i is species i mass fraction (with $i = F$ for fuel, O for O_2, P for combustion products, and I for inerts), and $\dot{q}$ and $\dot{w}_i$ are, respectively, the heat and species source-sink terms. The radiant flux to the surface, $\dot{q}_{rw}$, enters in the energy boundary condition as

$$\dot{m}''Q = \kappa \left.\frac{dT}{dz}\right|_{z=w} + \dot{q}_{rw} \tag{1-31}$$

where Q is the overall "effective" latent heat of degradative depolymerization of the polymer.

The radiative loss suffered by the flame toward the ambient as well as polymer surface will reduce the flame temperature. Within the scope of the model considered here, this is accounted for by defining an apparent heat of combustion, $\Delta H(1-\sigma)$, where σ is the ratio of the total heat radiated by the flame and the heat produced by combustion.

$$\sigma = \frac{\dot{q}_{r\infty}}{\dot{m}\Delta H} \tag{1-32}$$

Here σ will be assumed to be a constant of combustion for a given polymer in air.

The boundary conditions for species conservation at the fuel surface, $z=w$, take the form

$$(Y_{iw} - Y_{iR})\dot{m}_i'' = \frac{\kappa}{c_p} \left.\frac{dY_i}{dz}\right|_{z=w} \tag{1-33}$$

where the subscript R refers to the polymer supply state, $\dot{m}_i''$ is the mass flux of i across the fuel interface. Because O_2, H_2O, CO_2, and N_2 are assumed not to permeate through the fuel surface, $\dot{m}_O'' = \dot{m}_P'' = \dot{m}_I'' = 0$. For a pure fuel, $Y_{FR} = 1$; whereas $Y_{OR} = Y_{PR} = Y_{IR} = 0$. Since O_2 is absent in a diffusion flame, both Y_{OW} and its gradient vanish at the flame surface. The product and inert mass fraction and their respective gradients at the wall, however, are nonzero, their convective and diffusional fluxes being equal and opposite. Thus, the diffusional flux at w of N_2, CO_2, and H_2O is proportional to:

$$\left.\frac{dY_i}{dz}\right|_{z=w}$$

whereas $\dot{Y}_i$ represents the convective flux, and we have

$$\dot{Y}_i \sim -\frac{dY_i}{dz}$$

The fast, single-step, simple chemical reaction leads to the relation

$$fF + O \rightarrow (1+f)P + f\Delta H(1-\sigma) \tag{1-34}$$

where f is the number of grams of fuel, F, per one gram of oxygen, O; P is the product, say H_2O and CO_2; and the last term represents the heat of reaction. Thus, from this, the following relationships between source and sink for (1-29) and (1-30) obtain.

$$\frac{\dot{W}_F}{f} = \dot{W}_O = -\frac{\dot{W}_P}{(1+f)} = \frac{-\dot{q}}{f\Delta H(1-\sigma)} \tag{1-35}$$

$$\dot{W}_I = 0 \tag{1-36}$$

Using (1-35) and (1-36) in (1-29) and (1-30) along with the boundary conditions, composition and temperature profiles as well as combustion rate and flame location can be obtained. The mechanics are rather complicated and will not be given here [19]. The most significant of the results is the following equation for burning rate, $\dot{m}$,

$$\frac{\dot{m}c_p}{h} = \ell n(B+1) \tag{1-37}$$

$$B = \frac{f\Delta H(1-\sigma)Y_{O\infty} + c_p(T_\infty - T_W)}{Q(1-\psi)} \tag{1-38}$$

where Q is the latent heat of depolymerization. B is called the mass transfer driving force and was originally defined in almost the same form by Spaulding [20]. The quantity, $\psi = \dot{q}_{rw}/\dot{m}Q$, is the radiative fraction of the feedback. If radiative effects are missing, the radiative and convective contributions to B may be separated by neglecting the flame temperature reduction and approximating $(1-\psi)^{-1}$ by $1+\psi$ in (1-38) and using (1-37) to eliminate $\dot{m}$. There results

$$B \sim B_C + \frac{B_C}{\ell n(B_C+1)} \cdot \frac{\dot{q}_{rw}}{hQ/c_p} \tag{1-39}$$

---

[19] Penner, S. S., *Chemistry Problems in Jet Propulsion*, pp. 276-292, Pergamon Press, New York, 1957.

[20] Spaulding, D. B., The combustion of liquid fires, pp. 847-864, in *Fourth Symposium on Combustion*, The Williams and Wilkins Co., Baltimore, Md., 1953.

Here,

$$B_C \equiv \frac{f\Delta H\ Y_{O\infty} + c_p(T_\infty - T_W)}{Q} \tag{1-40}$$

Perhaps a more lucid way of expressing (1-37) for small $\dot{q}_{rw}$ or ψ is to separate the mass flux according to its radiative and convective feedback effects.

$$\dot{m} \simeq \frac{\dot{q}_{rw}B_C}{Q\,\ell n\,(B_C+1)} + \frac{h}{c_p}\,\ell n(B_C+1) \tag{1-41}$$

In this way, one can see that for large values of (B_C+1) convection dominates the determination of the mass rate, $\dot{m}$; the radiative term dominates the determination of $\dot{m}$ for small values of (B_C+1), as might be expected.

In order to correlate the Grashof number with B, which will in turn allow us the knowledge of $\dot{m}$ through (1-37), it is necessary to relate the Nusselt number (hd/κ) to the Grashof number and the Prandtl number $(\mu c_p/\kappa)$. Since the latter is of the order unity in our context, we will neglect it and write, as in reference [21],

$$\frac{hd}{\kappa} = 0.14\ G^{1/3}\left(\frac{\mu c_p}{\kappa}\right)^{1/3} \simeq 0.14\ G^{1/3} \tag{1-42}$$

Here d is a characteristic dimension of the order of the fire diameter. Substituting (1-42) into (1-37), we get

$$\frac{4\dot{m}}{(\pi d^2)}\ \frac{d}{\mu}\ \frac{1}{\ell n(B+1)} = 0.14\ G^{1/3} \tag{1-43}$$

This expression correlates well with the experimental data as shown by Kanury [16]. Constant values of viscosity, surface temperature, and flame temperature are assumed, when in fact they are expected to vary from material to material. This is an unfortunate aspect of the infant state of the technology, where better information is not available. Upon establishing that equation (1-43) is valid, Kanury was able to establish a B number for several materials. These are listed in Table 1-2. Thus, we have a seemingly reliable expression for burning rate, $\dot{m}$.

$$\dot{m} = \frac{h}{c_p}\,\ell n(B+1) \tag{1-44}$$

---

[21] McAdam, W. H., *Heat Transmission*, 3rd ed., p. 180, McGraw-Hill, New York, 1953.

TABLE 1-2. PROPERTIES OF POLYMERS AND THEIR FIRES [16]

	f	ΔH Kcal/gm	B	γ	Ψ	B_c	Q cal/gm
Polymethylmethacrylate (Plexiglas)	0.523	6.03	1.412	0.177	0.070	1.32	385
Polyamide (Nylon 6/6)	0.191	7.17	0.818	0.038	0.015	0.81	220
Polycarbonate (Lexan)	0.440	7.36	1.206	0.102	0.040	1.16	455
Polypropylene	0.292	11.00	0.940	0.213	0.084	0.87	534
Polyethylene	0.276	9.84	0.640	0.215	0.085	0.59	622
Polyoxymethylene (Delrin 500)	0.938	3.47	0.813	0.079	0.031	0.79	720
XX Phenolic, Natural	0.414	7.16	0.448	0.191	0.076	0.42	750
Fir (Wood)	0.938	4.00	0.572	0.169	0.067	0.54	710

The burning history or time correlation obeys the form

$$m = m_0 \left[1 - \left(\frac{G^{1/3}\phi}{m_0}\right) t\right] \tag{1-45}$$

where m_0 is the initial fuel mass, and

$$\phi = 0.14 \ln(B+1) \frac{\mu \pi d^2}{4d} \tag{1-46}$$

The expression (1-45) correlates well with burning data and thus seems reliable for model use.

The radiative loss undergone by the flame is proportional to the rate of burning, $\dot{m}$, and thus to the rate of heat release by combustion. This is again validated by Kanury's experimental work. The proportionality constant, γ, which is different for different materials, is shown in Table 1-2. The most prominent feature of the table is the partition of materials into two groups, the first being comprised of strong emitters, where γ is in the range of 18% to 25%, and the second being comprised of weak emitters, where γ is in the range of 4% to 8%. Other investigators have attained values of up to 33% for some materials [22]. We therefore can write for the radiative emission, $\dot{q}_r$,

$$\dot{q}_r = \gamma \dot{m} \Delta H \tag{1-47}$$

---

[22] Twarson, A., and R. F. Pion, Flammability of plastics, I, Burning intensity, to be submitted to *Combust. Flame*.

Values for ΔH can be gleaned from Table 1-2 or averaged to account for most polymers; this can be a user's option. Similar remarks hold for γ. For $\dot{m}$, we differentiate (1-45) with respect to time and obtain

$$\dot{m} = - G^{1/3}\phi \tag{1-48}$$

For G, Kanury reports a value of

$$G = 1105.2 \times d^3 \tag{1-49}$$

where d is the diameter of the pool that is burning, in inches.

To summarize, for a pool fire the following steps should be taken.

(1) Calculate $\dot{m}$ using $\dot{m} = -G^{1/3}\phi$ where $G = 1105.2\ d^3$ where d is in inches for the pool, and $\phi = 0.14\ \ell n(B+1)\{(\mu\pi d^2)/4d\}$. B can be obtained from Table 1-2 or given default value at user's option. μ is 3.215×10^{-4} gm/cm sec.

(2) Calculate the radiation intensity, $\dot{q}_r$, from the formula

$$\dot{q}_r = \gamma \dot{m} \Delta H$$

γ and ΔH can be obtained from Table 1-2 or given default values at user's option.

(3) Calculate burning time, t_{eff}, from the relation

$$t_{eff} = \frac{m_0}{G^{1/3}\phi}$$

This relation assumes complete burning, where m_0 is the original mass of polymer.

The radiation intensity, $\dot{q}_r$, along with t_{eff} will be stored along with the pool fire's dimensions, radius and height, to be used in the View Factor Subroutine already present in the VM to determine hazard to personnel and structures nearby.

C. *CELLULOSE*

In this section we consider the secondary fire hazard posed by cellulose materials. We have in mind here wood and cotton fires in particular. While such substances are classified chemically as polymers, their special properties and experience with regard to fire hazard, particularly wood, warrant their special, although brief, treatment here.

We consider first the ignition criteria for three substances for which experimental data are available--cotton, α cellulose, and wood. We then go on to treat the resulting fire with regard to both size and radiation emission and also, where possible, to give an estimate of burning rate and time duration of the fire.

1. Ignition Criteria

Perhaps the most efficacious manner in which to portray ignition criteria for cellulose fire is to utilize the technique posed by Lawson and Simms in an important paper published in 1952 [23]. They considered two types of ignition due to radiation, piloted and unpiloted.* Here we will do likewise where possible, giving a threshold radiation intensity and a threshold irradiation time for the two types of ignition for each of the three materials considered. In the case of wood, this has already been done in the VM [1]; hence, the results will not be repeated here. It will be recalled that for spontaneous ignition of wood the radiation intensity, I_r, must exceed

$$I_S = 2.54 \times 10^4 \frac{J}{m^2 \text{ sec}} \tag{1-50}$$

and the duration of radiation intensity must exceed, in seconds,

$$t_S = \left(\frac{8.37 \times 10^4}{I_r - I_S}\right)^{5/4} \tag{1-51}$$

Similar relations for piloted ignition are

$$I_p = 1.34 \times 10^4 \frac{J}{m^2 \text{ sec}} \tag{1-52}$$

$$t_p = \left(\frac{7.64 \times 10^4}{I_r - I_p}\right)^{3/2} \tag{1-53}$$

If these values are exceeded in each of the respective cases, ignition is assumed.

For cotton fabric, the following figures comprise the ignition criteria of spontaneous ignition [24].

---

[23] Lawson, D. I., and D. L. Simms, The ignition of wood by radiation, *Br. J. Appl. Phys.* 3:288-292, 1952.

[24] Welker, J. R., H. R. Wesson, and C. M. Sliepcevich, Ignition of α cellulose and cotton fabric by flame radiation, paper presented at Annual Meeting of NFPA, 1968.

*Piloted ignition is one in which fire is started by being adjacent to open flame simultaneously with exposure to radiation.

$$I_S = 1.254 \times 10^4 \frac{J}{m^2 \text{ sec}} \tag{1-54}$$

$$t_S = 5.96 \times 10^8 \, I_r^{-1.64} \tag{1-55}$$

where I_r is the radiation intensity due to the primary fire, be it pool or of flash origin. No similar criteria are given for piloted ignition because the differences are negligible in this case and for α cellulose, better known as paper.

For α cellulose, or paper, we use the following to determine whether ignition occurs:

$$I_S = 1.672 \times 10^4 \tag{1-56}$$

$$t_S = 3.67 \times 10^{17} \, I_r^{-3.64} \tag{1-57}$$

It should be recalled that, if $I_r \geq I_S$ and if the duration of burning of the primary fire, t_{eff}, obeys $t_{eff} \geq t_S$, the secondary materials--in this case wood, cotton, and paper, respectively--are assumed to be ignited.

2. Burning Rate and Effective Time

As for polymers, the burning rate for cellulose materials can be given by

$$\dot{m} = - G^{1/3} \phi \tag{1-58}$$

where G is the Grashof number and ϕ is $0.14 \, \ell n(B+1)(\mu\pi d)/4$. The value of G given by Kanury [16] is $1105.2 \, d^3$. For present use, $B = 0.572$ and $\mu = 3.215 \times 10^{-4}$ gm/cm sec. Here, d is given in inches and is the diameter of the fire.

The effective fire duration time, t_{eff}, is

$$t_{eff} = \frac{m_0}{G^{1/3} \phi} \tag{1-59}$$

where m_0 is the original mass of the cellulose combustible.

2. Radiation Intensity and Flame Size

The radiation for cellulcse materials, as for other polymers, is given as

$$I_r = \gamma \dot{m} \Delta H \tag{1-60}$$

Values for γ and ΔH are, respectively, 0.169 and 4.00 K cal/gm. Again, expression (1-60) and the values for γ and ΔH were extracted from Kanury's paper [16].

Values for the ratio of flame height, L, to diameter, d, have been correlated for wood fires by Thomas [25]. The ratio is given by the expression

$$\frac{L}{d} = 4.4 \left(\frac{\dot{m}^2 \times 10^6}{d^5} \right)^{0.30} \tag{1-61}$$

where $\dot{m}$ and d must be given in Cgs units in order to evaluate (1-61).

Once ignition is determined to exist for a cellulose material that is untreated, the following steps will be taken to calculate fire hazard due to radiation.

(1) Calculate $\dot{m}$ from (1-58).

(2) Calculate radiation intensity, I_r, from (1-60).

(3) Calculate effective duration of burning, t_{eff}, from (1-59).

(4) Calculate ratios of L/d or fire height from (1-61).

The radiation intensity, I_r, duration, t_{eff}, and fire dimensions, L and d, will be stored and used in the View Factor Subroutine already present in the VM, to determine hazard to personnel and structures nearby.

---

[25] Thomas, P. H., The size of flames from natural fires, in *Ninth Symposium on Combustion*, The Combustion Institute, Pittsburgh, Pa., 1962.

Chapter 2

EXTENSION OF FLASH FIRE MODELING

INTRODUCTION

Damage from fire is modeled as affecting the vulnerable resources, people and structures. The damage assessed to structures is burning; the damages assessed to personnel are death and nonlethal burns. For all types of damage, the two parameters of importance are (1) level of radiation and (2) duration of radiation.

For the pool fire, *actual* levels of radiation intensity and duration of intensity are computed for *each* cell center. For the flash fire, on the other hand, *effective* levels of radiation intensity and duration of intensity are computed *only* for the cell in which the flash fire takes place.

The purpose of this chapter is to derive the model necessary for calculating for the flash fire the effective radiation intensity and duration for *each* and *any* cell, as for the pool fire. To accomplish this, it is necessary to calculate the *view factor* for the distance separating the flash fire center and the center of an arbitrary cell of interest. Effective time duration for a flash fire remains unaffected by this extension.

THE MODEL

We start by recalling several important formulas from the VM [1]. The flash fire radiation intensity, I_r, is

$$I_r = \sigma(T_g^4 - T_a^4) \tag{2-1}$$

where

σ = Stefan-Boltzmann constant, 5.67×10^{-8} J/°K^4 m^2 s

T_g = $(T_i + T_a)/2$

T_a = air temperature

T_i = the initial temperature of the gas layer immediately after combustion, a computed value

For the effective duration, t_{eff}, of radiation, we have as before

$$t_{eff} = 3\, t_{1/2} \tag{2-2}$$

$$t_{1/2} = \frac{1}{2\, a\, T_a^3} \left[\tan^{-1} \frac{1}{\beta} - \tan^{-1} \left(\frac{2}{\beta + 1} \right) - \frac{1}{2} \ell n \left(\frac{\beta + 1}{\beta + 3} \right) \right] \tag{2-3}$$

where

$$\beta = \frac{T_i}{T_a}$$

$$a = \frac{A_r\, \sigma}{c_p\, \rho\, V_r}$$

$$A_r = \frac{2\pi}{3} \left(r_U^2 + r_L^2 \right) \left(\sigma_x^2 + \sigma_y^2 + \sigma_z^2 \right) \tag{2-4}$$

$$V_r = \frac{2\pi}{3}\, \sigma_x\, \sigma_y\, \sigma_z \left(r_L^2 - r_U^2 \right) \tag{2-5}$$

For radiation at a distance from the flash fire, we calculate the effective flame radiation intensity over the effective time, $3\, t_{1/2}$, and multiply by the view factor for an ellipsoid, which is the true shape of burning puff model concentrations. A generally conservative estimate of the view factor from an ellipsoid to a vertically oriented differential element, dA_1, is given by a hemisphere. Damage calculated in such a manner will generally be overestimated. Referring to Figure 2-1, it can be shown that the view factor pertaining to our configuration is [26]

$$F_{12} = \frac{1}{2H^2} \tag{2-6}$$

where

$$H = \frac{\ell}{r} = \frac{1}{\sin \phi}$$

ℓ = distance from fire center to arbitrary cell center

r = radius of sphere

The error introduced by taking the ellipsoid as a sphere is small since, in general, $\sigma_x \approx \sigma_y > \sigma_z$ for the puff model, and only a slight

---

[26] Love, T. J., *Radiative Heat Transfer*, p. 240, Merrill Publishing Co., Columbus, Ohio, 1968.

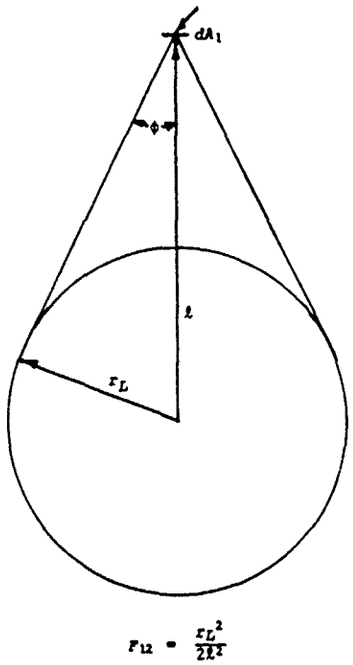

FIGURE 2-1. View Factor for Flash Fire

flattening of the sphere would account for any difference. Only in the case of highly unstable weather would σ_z exceed σ_y and σ_x.

For the value of r, the radius of the spherical approximation of the ellipsoid, we have the radius of the hemisphere containing vapor concentration at the lower flammability limit or greater.

$$r = r_L = \left[2 \ln\left(\frac{1}{(2\pi)^{3/2}} \frac{2m}{\sigma_x \sigma_y \sigma_z K_L} \right) \right]^{1/2} \tag{2-7}$$

Here m is the mass released, K_L is the concentration of the lower flammability limit, and of course $\sigma_{x,y,z}$ are the dispersion coefficients for the puff model.

Thus for the radiation intensity, I_f, at an arbitrary cell center from the flash fire, we have

$$I_f = F_{12} I_r = \frac{r_L^2}{2\ell^2} \sigma (T_g^4 - T_a^4) \tag{2-8}$$

This will be associated with a time duration of

$$t_{eff} = 3\, t_{1/2} \tag{2-9}$$

Both values will be computed, stored, and held for utilization in Phase II to assess injury to people and damage to structures for all cells. A flow diagram detailing the calculation procedure is given in Chapter 9 of this report.

Chapter 3
IGNITION SOURCES

INTRODUCTION

A primary decision made in the VM fire and explosion submodels is whether or not ignition occurs. Three conditions must be satisfied simultaneously for ignition to occur: (1) fuel, (2) oxidizer, and (3) ignition source. Fuel is supplied by the dispersing vapor, the oxidizer by air; while the ignition source presence is specified by the user of the VM for a given grid cell.

A refinement of the model allows gradations in ignition source strength. The user is allowed to specify the ignition potential of a given source so that, for example, a single specification of a set of ignition sources will result in ignition for a highly flammable substance but will not simulate an ignition for a less flammable substance. The gradations used in the VM for ignition sources are based on the NFPA classification for flammable substances. This particular NFPA classification system is based on *liquid flashpoint*. By this criterion, substances with a low flashpoint temperature are considered highly flammable while those with a high flashpoint temperature are considered somewhat safe, or difficult to ignite. In the VM, an ignition source is designated as belonging to a given classification on the basis of the flashpoint of substances it is capable of igniting.

Flashpoint is a material property encompassing a set of physicochemical parameters such as volatility, specific heat, and density. Thus the use of flashpoint to characterize ignition sources is a criterion without strong theoretical basis, since transport properties of the ignition process are not taken into account.

In the sections that follow, two ignition criteria will be presented that explicitly take into account the dynamic or transport nature of the ignition process for a gaseous cloud of known chemical composition. The first will be called the Ignition Energy Model and could prove useful for deciding ignitability in cases where ignition sources can be designated more easily by power densities than by temperature strength. An obvious example would be ignition sources that arise due to electrical arcs. The second criterion discussed is called the Ignition Temperature Model and could prove useful for deciding ignitability in cases where ignition sources can be designated most easily by temperature considerations. Obvious examples would include open flames, smoking materials, and hot material objects.

For a given hazardous cargo of a known concentration between flammable limits, three parameters can be calculated: (1) minimum ignition energy, H_g; (2) ignition temperature, T_{Eg}; and (3) minimum source dimension, d_g.

For a given ignition source, two parameters will have to be known: the minimum source dimension, d_S, and either the effective ignition energy, H_S, or the effective temperature, T_S. If the following inequalities are satisfied, ignition will be assumed to take place.

$$d_S > d_g$$

and either $H_S > H_g$

or $T_S > T_{Bg}$

If $H_S < H_g$ *and* $T_S < T_{Bg}$ or if $d_S < d_g$, ignition will not take place.

Attractive as the two ignition models might seem, however, the two parameters that issue from them are not unique for a given material. As will be seen in the sections that follow, transport properties dominate the determination of ignition energy and temperature and, as is well known, are process-dependent with regard to both rate and path through intermediate thermodynamic states. It is for this reason that the flashpoint retains its role as the preferred ignition criterion. It is unique for a given cargo and is a result of laboratory measurement that is well-understood and agreed upon by a large segment of the combustion community.

The discussion of the two models that follows is intended as a guide to orient thinking regarding ignition hazard and some of its possible ramifications. No computerization of the results has therefore been attempted for insertion in the VM.

The final section of this chapter deals with variable ignition sources; it appears here not for the purpose of its inclusion in the VM but rather for purposes of illustration where explicit account is taken of the stochastic nature of ignition sources. Application is made to the case of a flammable cloud encountering a movable vehicle and the probable consequences of same.

IGNITION ENERGY MODEL

When a combustible gas mixture is ignited by heating a plane slab of gas, it is found that the amount of energy per unit surface area of the slab added to the gas must exceed a definite minimum value for the onset of ignition to occur.

Analysis of the gas ignition problem by various investigators [27], who integrated partial differential equations numerically, shows that

---

[27] Williams, F. A., *Combustion Theory*, p. 188, Addison-Wesley Publishing Co., Reading, Mass., 1965.

for slabs of varying thickness, initially raised to adiabatic flame temperature, two results can be expected:

(1) The temperature of this gas slab decays quickly to the ambient temperature by heat conduction.

(2) For thick slabs, a propagating laminar flame develops.

As a result we can state the following rule. Ignition of a gas slab will occur only if enough energy is added to the gas to heat a slab--about as thick as a steadily propagating adiabatic laminar flame--to the adiabatic flame temperature.

The formula expressing this rule is

$$H = A \delta \rho_0 c_p (T_\infty - T_0) \tag{3-1}$$

where H is the minimum ignition energy, A is the cross-sectional area of the slab, δ is the adiabatic laminar flame thickness, ρ_0 is the initial density of the gas-air mixture, c_p is the constant pressure-specific heat, T_∞ is the adiabatic flame temperature, and T_0 is the initial temperature of the mixture.

The minimum value of A has been related to results of flame-quenching experiments. Flame will not propagate through very narrow channels because of heat loss to the walls. We define a gas flame-quenching distance, d, as the minimum plate separation or dimension in the channel for which flame propagation can be achieved. Thus, the minimum value of A will be d^2.

The value d in turn must be related to fundamental properties of the gas. This can be and has been done through experimentation, where it is found that

$$\sqrt{A} = d = 40 \delta \tag{3-2}$$

The laminar flame thickness, δ, in turn is given by

$$\delta = \frac{\lambda}{c_p \rho_0 V_0} \tag{3-3}$$

Here λ is thermal conductivity and V_0 is the flame velocity. Substituting (3-2) and (3-3) for A and δ respectively in (3-1) gives

$$H = (1.6 \times 10^2 \lambda^3) \left(\frac{T_\infty - T_0}{c_p^2 \rho_0^2 V_0^3} \right) \tag{3-4}$$

Values of H can be calculated or estimated for given types of ignition sources, such as open flame, electric arc, heated wall, etc. If the value of H for a given gas is equal to or less than the value of H for a given or suspected ignition source, ignition will be assumed to occur.

A word should be said about λ and c_p. Correct values of both are very temperature-dependent for gases in the temperature region considered here, namely the adiabatic flame temperature, T_∞. This temperature-dependence can be expressed by the following [28]

$$c_p = A + BT + CT^2 \tag{3-5}$$

where $A = 6.30$ cal/mol, $B = 2.0$ cal/mol°K, $C = -0.43$ cal/mol°K for air, and values for other gases can be found in the literature. In order to calculate the specific heat for a mixture of low-density gases, it will be necessary to take a mass average for the coefficients A, B, and C for the various chemical components and insert in (3-5).

The calculation of λ for a gas mixture as a function of temperature involves a bit more work than the calculation of c_p. It turns out that λ_{mix} can be expressed by [29]

$$\lambda_{mix} = \sum_{i=1}^{n} \frac{X_i \lambda_i}{\sum_{j=1}^{n} x_j \phi_{ij}} \tag{3-6}$$

where X_i is mole fraction of ith component, λ_i is conductivity of ith component, and ϕ is given by

$$\phi_{ij} = \frac{1}{\sqrt{8}} \left(1 + \frac{M_i}{M_j}\right)^{-1/2} \left[1 + \left(\frac{\mu_i}{\mu_j}\right)^{1/2} \left(\frac{M_j}{M_i}\right)^{1/4}\right]^2 \tag{3-7}$$

and M_i and μ_i are, respectively, the molecular weight and viscosity of species i.

It is now necessary to calculate λ_i and μ_i for low-density gases. For μ_i we have for a given species, i,

---

[28] Callen, H., *Thermodynamics*, p. 332, John Wiley & Sons, New York, 1960.

[29] Bird, R. B., W. E. Stewart, and E. N. Lightfoot, *Transport Phenomena*, p. 257, John Wiley & Sons, New York, 1960.

$$\mu_i = 2.6693 \times 10^{-5} \frac{\sqrt{M_i T}}{\sigma_i^2 \Omega_{\mu i}} \tag{3-8}$$

M_i is the molecular weight, σ_i is the collision diameter of the molecule, and $\Omega_{\mu i}$ is a collision term that is a slowly varying function of temperature. $\Omega_{\mu i}$ can be approximated by a term of the order unity or calculated using tabulated values that depend on temperature. The value of σ for air is 3.62 and for methane, 3.82.

For λ_i, we have

$$\lambda_i = \left(c_{pi} + \frac{5}{4} \frac{R}{M_i}\right) \mu_i \tag{3-9}$$

and R is the gas constant.

IGNITION TEMPERATURE MODEL

After what has been said in the foregoing, it is of interest to compute the temperature of ignition of a mixture of combustible gas and air.

The quantity of heat, Q_I, liberated per unit time in a specified region occupied by a combustible mixture in reaction can be written as

$$Q_I = k_0 \, e^{-E/RT} \, f(c) g \cdot V \tag{3-10}$$

where k_0 is the rate constant, E the activation energy, $f(c)$ a function of chemical concentration, g the heat of reaction, and V the volume of the combusting region. We combine the above coefficients by setting

$$Q_I = A \, e^{-E/RT} \tag{3-11}$$

The quantity of heat, Q_{II}, lost by the region of volume V per unit time is given by

$$Q_{II} = h S (T - T_0) \tag{3-12}$$

where h and S are, respectively, the Newton heat conduction coefficient at the boundary of the combusting region and the area of same. T_0 is the ambient temperature, and T is the combustion temperature.

Again, let us combine h and S into one constant, B, and write

$$Q_{II} = B(T - T_0) \tag{3-13}$$

We next plot (3-11) and (3-13) as a function of T as shown in Figure 3-1, where I represents (3-11) and II represents (3-13). Point A represents the fact that $Q_I = Q_{II}$, as do points B and C. It can be shown that only points A and B are stable [30], while point C is unstable and unable to support combustion. Essentially, points A and B express the statement that the heat release due to the chemical reaction of burning is equaled by the heat transfer out of the system due to conduction.

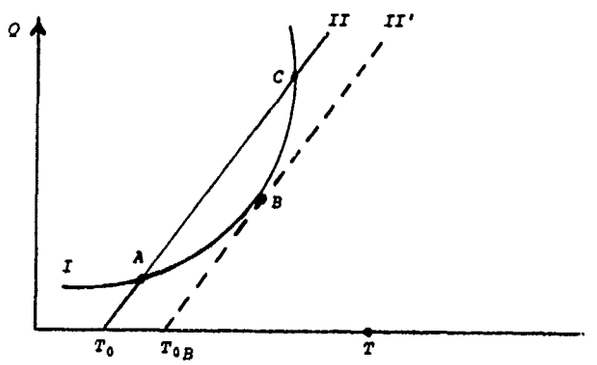

FIGURE 3-1. Combustion Diagram

Let us trace the change in the stable, quasi-stationary state of a system as the ambient temperature, T_0, rises. The values of the stationary temperature will increase continuously, as long as curve II intersects curve I. This displacement of curve II to the right can continue until II is tangent to I at point B. Increasing T_0, such that the curve II' lies to the right of I, causes the stationary process to cease and gives rise to abrupt nonstationary burning of the mixture under conditions of increasing heat accumulations and rising temperature.

It is customary to designate the boundary stationary region of the tangent to the heat liberation curve I and the heat elimination curve II, point B, as the ignition point and the corresponding temperature as the maximum ignition temperature [30]. However, all points along I

---

[30] Vulis, L. A., *Thermal Regimes of Combustion*, p. 18, McGraw Hill, New York, 1961.

between T_A and T_B are also ignition temperatures corresponding to ambient temperatures between T_0 and T_{0B}.

As such it is clear that, since curves *I* and *II* depend explicitly on transport parameters as well as thermodynamic parameters, the dynamic character of the ignition phenomenon and therefore of the ignition temperature itself is manifest. Thus, the ignition temperature of a combustible mixture cannot be thought of as a certain physicochemical constant such as specific heat or density. The ignition conditions for a given species and oxidizer are determined by all the conditions for the evolution of the process in a system rather than by simple properties of the mixture, i.e., heat exchange with surroundings, geometry and size of combustion zone or combustion-containing vessel, and so on.

To be more specific, we will calculate the ignition temperature, T_B, for the case at hand in terms of the parameters A and B. To determine the point of tangency we need, in addition to $Q_I = Q_{II}$, the fact that at point B

$$\frac{dQ_I}{dT} = \frac{dQ_{II}}{dT} \tag{3-14}$$

Thus we have the conditions that must be satisfied simultaneously

$$Q_I = Q_{II} \qquad \text{or} \qquad A\,e^{-E/RT} = B(T - T_0) \tag{3-15}$$

and

$$\frac{dQ_I}{dT} = \frac{dQ_{II}}{dT} \qquad \text{or} \qquad \frac{AE}{RT^2}\,e^{-E/RT} = B \tag{3-16}$$

Combining (3-15) and (3-16), we obtain

$$\frac{E(T - T_0)}{RT^2} = 1 \tag{3-17}$$

which can be recast in the quadratic form

$$T^2 - \frac{ET}{R} + \frac{ET_0}{R} = 0 \tag{3-18}$$

It turns out that the smaller of the two roots of (3-18) is the physically relevant one here, and as a result one obtains for T_B

$$T_B = \frac{E}{2R}\left(1 - \sqrt{1 - \frac{4RT_0}{E}}\right) \tag{3-19}$$

Therefore, ignition can occur in a bounded region of ambient temperature, T_0, given by

$$0 \leqslant T_0 \leqslant E/4R \tag{3-20}$$

When $T_0 = E/4R$, T_B is a maximum and is given by

$$T_{Bmax} = \frac{E}{2R}$$

or twice T_0. This in turn corresponds to the point of inflection for the curve $e^{-E/RT}$ as a function of T.

It is possible to expand (3-19) for low values of T_0, i.e., $T_0 \ll E/4R$, in order to examine more explicitly the behavior of T_B in this region.

$$T_B = \frac{E}{2R}\left[1 - \left(1 - \frac{2RT_0}{E} - \frac{2R^2T_0{}^2}{E^2} - \ldots\right)\right] \tag{3-21}$$

The first approximation yields

$$T_B \approx T_0 = T_{Bmin} \tag{3-22}$$

while the second gives

$$T_B \approx T_0 + \frac{RT_0{}^2}{E} \qquad T_0 \ll \frac{E}{4R} \tag{3-23}$$

Hence, the relative heating of the system which corresponds to the critical ignition region is comparatively small, as can be seen from the fact that

$$T_{Bmax} = \frac{E}{2R} = 2\,T_0 \tag{3-24}$$

Thus,

$$T_0 \leqslant T_B \leqslant 2\,T_0$$

It should be noted that a continuous variation of the parameter, T_0, will not lead to a continuous change in T_B as if it were a function

of T_0, all other parameters remaining the same. T_B varying as a function of T_0 is possible only under the condition that at least one of the parameters which characterize the intersection of curves *I* and *II*, such as λ or k_0, should change simultaneously with T_0. Only one critical value of the ignition temperature, T_B, is possible at a specific value of T_0 when the values of *A*, *B*, and *E* are specified. This can be seen by expressing T_B as a function of *A*, *B*, and *E* by means of (3-16), after which the unique value of T_0 is determined by (3-15). This apparent difficulty exists since, by solving (3-15) and (3-16) simultaneously, we are also solving parametric equations by removing the parameters *A* and *B*. This occurs because of the functional form of both. Had a radiation term of the form $C(\bar{T}^4 - T_0^4)$ been added to the right-hand side of (3-15), such a parametric elimination would not have been possible, and a transcendental solution would have to be resorted to. What the model does show is that, under the assumption of no radiation and a very simple conduction-convection heat transfer model, the critical ignition temperature, T_B, depends to the first order on the activation energy, *E*. This is not surprising because it says, for instance, that methane would have a higher ignition temperature than propane or ethane, a fact in accord with experience.

For open flames of known temperature range and size, the use of T_B as opposed to ignition energy would seem preferable as a criterion of ignitability of gas clouds. For sparks, on the other hand, where the concept of temperature is rather vague, energy import over a volume exceeding δd^2 might be the preferred criterion of cloud ignitability.

VARIABLE IGNITION SOURCES

Any changes to the method of simulating ignition sources in the VM must be made within the framework of a deterministic model. Thus the set of input values completely defines whether ignition will or will not occur. This is in contrast to probabilistic simulation, wherein random numbers are drawn to determine if specified events occur or not. However, in realistic situations ignition sources could very well be probabilistic in nature, such as the lighting of matches or outdoor charcoal grills, the starting of electric machines, or the passing of motor vehicles, trains, motorized boats, etc. The user of the VM has the option of simulating the same scenario twice, the only difference being the presence of ignition sources in one case and the absence of them in another, to evaluate relative destructive consequences. Although this will provide the user with measures of injury and damage for the two cases, it will be necessary to interpret the results in terms of probabilities to evaluate relative risks. It is the purpose of this section to provide the user with a procedure for assigning probabilities to variable ignition sources, in order to interpret VM results in terms of relative risk. This procedure would be used by the analyst external to a computerized simulation of the VM.

A relatively straightforward expression is developed below, one that can be generalized to cover many situations of interest to the VM user. In its simplest form, the expression is:

$$Prob = 1 - [1 - \lambda(t_\lambda)](e^{-\lambda T})$$

where *Prob* is the probability that the moving cloud will come into contact with an active variable ignition source; λ is the average rate of occurrence of the ignition source (such as the number of occasions that the ignition source is turned on randomly per unit time, the frequency of arrival of a moving vehicle at a highway checkpoint, etc.); t_λ is the average length of time that the ignition source is on (for a motor vehicle, e.g., t_λ is the average length of time that it is on the highway in contact with the moving cloud); and T is the time duration of the contact between the cloud and the ignition source, whether the ignition source is turned on or off (for a motor vehicle, T would be the time during which the cloud is in contact with the highway over which the vehicle travels).

For example, if a cloud is in contact with a stationary ignition source for one hour ($T = 1$), and the ignition source is turned on randomly, on the average, 3 times per hour ($\lambda = 3$) for an average time of 6 minutes each ($t_\lambda = 6/60 = 0.10$), then the probability that the ignition source is on (active) sometime during its contact with the cloud is:

$$Prob = 1 - [1 - 3(0.10)][e^{-3(1)}] = 0.97$$

The above expression is also applicable to several ignition sources, each of which may be in a different location within the same VM grid cell, may be of different intensity from the others, may be turned on and off at different frequencies, may be turned on for different average lengths of time, etc. A derivation of the above expression follows.

Derivation

We first consider the case of a stationary ignition source that is turned on and off randomly. Let λ denote the average number of occasions per unit time that this ignition source is turned on. For example, λ might be 1 every five minutes, 1 every hour, 3 every ten minutes, etc. Let t_λ denote the average amount of time that the source remains active, once it is turned on. For example, t_λ might be 10 seconds, 3 minutes, 2 hours, etc. In the following, assume that λ and t_λ are expressed in the same time units, such as hours. For example, λ might be 3 (i.e., 3 occasions per hour) and t_λ might be 0.10 (i.e., the source is on for an average of one-tenth of an hour per hour, or 6 minutes).

Next consider a cloud of ignitable material that passes over and is in contact with this ignition source for a time T (whether the source is on or off). The first problem addressed here is to determine the probability that the ignition source is on during this time T. The ignition source may be on as the cloud passes over initially, or it may have been off initially and subsequently turned on during the time period T.

The probability of this latter occurrence is given by the Poisson distribution as

$$1 - e^{-\lambda T} (\lambda T)^0/0! = 1 - e^{-\lambda T}$$

Note that this expression gives only the probability that the source is turned on during the time period T and is independent of the actual time that the source remains on. If T is 1 hour and λ is (as above) 3, the probability is:

$$1 - e^{-3(1)} = 0.95$$

That is, the probability is 0.95 that the source is turned on during any given one-hour period if, on the average, the source is turned on randomly three times per hour.

On the other hand, the probability that the source is on as the cloud first comes into contact with it is given by the product $\lambda(t_\lambda)$, which effectively is the amount of time, on the average, that the source is on per unit time divided by the unit time. For example, using the above numerical values, $\lambda = 3$ and $t_\lambda = 0.10$, the probability that the source is on when the cloud first comes into contact with it is $3(0.10) = 0.30$. Another way of looking at this probability is that it is the ratio of the time within the one-hour period during which, on the average, the source is on (namely, 3×6 minutes) divided by the number of minutes in an hour: $(3 \times 6)/60 = 0.30$.

The overall probability, then, that the cloud is in contact with an active ignition source is the combination of the above two probabilities. A common practice in combining such probabilities is to take the *complement* of the event that the cloud does *not* come into contact with an active ignition source. The probability that the source is off initially is $[1 - \lambda(t_\lambda)]$; the probability that it is not turned on during the time period T is $[1 - (1 - e^{-\lambda T})] = e^{-\lambda T}$. Since these probabilities are statistically independent, the probability that the cloud comes into contact with an active ignition source *either* initially *or* during the time period T is given by the complement of the above product, namely:

$$1 - [1 - \lambda(t_\lambda)][e^{-\lambda T}] \qquad (3\text{-}25)$$

Using the numerical values as in the above examples, this probability is given by

$$1 - [1 - 3(0.10)][e^{-3(1)}] = 1 - [0.7][0.05] = 0.97$$

That is, for the conditions specified in the example, a cloud that is in contact for one hour with an ignition source that is turned on randomly three times per hour for 6 minutes each time, on the average, has a probability of 0.97 of being in contact with the ignition source while it is on.

Generalization

The above was presented in terms of a stationary ignition source that is turned on and off periodically. However, the results, in terms of expression (3-25), are applicable to situations where the ignition source is moving, such as a vehicle traversing a highway as described below.

Consider Figure 3-2 which depicts a highway perpendicular to the path of the moving cloud. We wish to formulate this situation so that expression (3-25) gives the probability that the cloud comes into contact with a vehicle, V, traveling at a speed, S. In this formulation we approximate the ignitable contours of the cloud as rectangular, denoted as C in the figure.

Let AB denote the ignitable width of the cloud. As the cloud first comes into contact with the highway, between A' and B', it will also come into contact with the vehicle *if* the vehicle is between A' and B'. Let vehicles arrive randomly at point A', once again on the average, at the rate of λ per unit time, traveling at a speed of S. This λ corresponds to the λ of expression (3-25) and $A'B'/S$ corresponds to t_λ of (3-25). The contact time is given by $T = W/U$, where W is the ignitable length of the cloud which is traveling at a speed U. Thus expression (3-25) is applicable in this case for determining the probability that the cloud comes into contact with a vehicle along the highway.

If there is more than one highway within the region of concern (a VM cell), the complement of expression (3-25) gives the probability that the cloud does *not* come into contact with a vehicle for each highway considered separately. The product of these complements gives the corresponding probability of no contact for all highways under consideration. The complement of this product, then, is the probability that the cloud comes into contact with at least one vehicle on one or more of the highways. Of course, λ, t_λ, and T may vary for each highway.

Expression (3-25) is thus applicable to many situations, either as is or with modifications. The user may wish to use this expression to assign probabilities, once the VM has been run and the cloud size and

velocity are known. Any number of ignition sources can be simulated with the computerized version of the VM, merely by defining each ignition source as a cell.

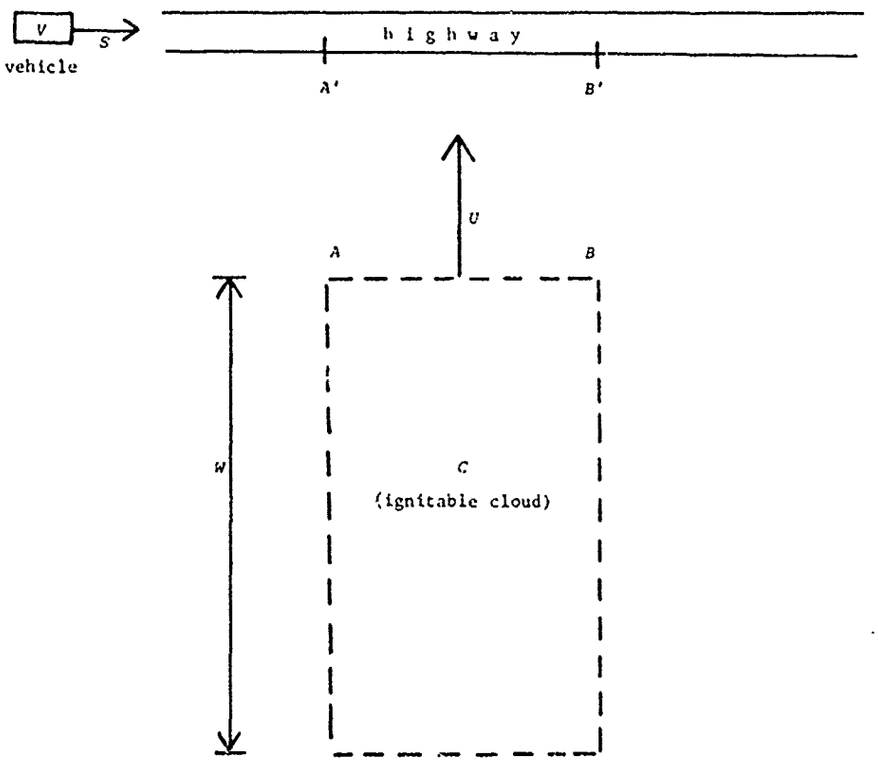

FIGURE 3-2. Highway Perpendicular to Path of Ignitable Cloud

Chapter 4

IMPROVED METHOD FOR STRUCTURAL IGNITION

INTRODUCTION

This chapter describes an improved method for assessing ignition of structures in the Vulnerability Model (VM). Previously, 25% of the structures located within a given cell were assessed as being ignited when the duration and level of thermal radiation were sufficient to cause ignition of wood. As described below, the modeling of structural ignition has been improved in two ways: (1) a better treatment of shielding effects has been formulated and (2) a more precise determination has been made of the fraction of structures in the cell able to be ignited if none were shielded. In addition to the improvements actually made, a general outline for a comprehensive treatment of this problem is given. Since a comprehensive treatment would require computational and data resources beyond the current capabilities of the VM, the intermediate level analysis was selected for use at this time.

The improved analysis is based on several approximations to the actual physical situation. Among the more important assumptions are the following.

(1) For the purposes of this model, the grid cells may be treated as square in shape with one edge directly facing the flame.

(2) The view factor does not change significantly with lateral position (movement normal to the line connecting the flame center and cell center).

(3) A building is considered to be shielded from thermal radiation if a higher building is located between it and the flame; if no higher building is interposed between the flame and a building, the building is considered to be exposed. (Height in this context may be considered to be a generalized measure of shielding ability.)

Although these assumptions limit the physical realism of the model, they permit significant theoretical and computational simplification. At the same time, these assumptions yield a more precise estimate of structural ignition than is currently available in the VM.

In the remainder of this chapter, first a general discussion of the structural ignition problem is given with an outline of the techniques to be followed for a more comprehensive treatment. Then the means for estimating the potential number of structures in a cell subject to ignition is described; essentially, the region of the cell in which ignition may occur is computed. The method for considering shielding is

then stated, and three shielding scenarios are postulated: maximum shielding, minimum shielding, and random shielding. For the case of random shielding, an analysis is performed to relate expected number of structures shielded in terms of number of rows of structures inside the ignition region. The overall model design and computational flow diagram appear in Chapter 9 of this report.

GENERAL TREATMENT OF STRUCTURAL IGNITION

A comprehensive treatment of structural ignition would include consideration of the following factors.

(1) Location of the structure relative to the primary fire (the fire involving the spilled material).

(2) Flame geometry (size, shape, tilt angle, direction of tilt).

(3) Structure orientation with respect to the flame.

(4) Size, shape, and location of obstacles, opaque to thermal radiation, intervening between the structure in question and the fire.

(5) Location and orientation of combustibles inside or on the exterior of the structure.

(6) Ignition characteristics of the exposed combustibles.

The first five factors would be included in a detailed computation of view factor for each location and orientation of combustible materials in or on the building. The ignition characteristics of the exposed combustibles in a comprehensive treatment would go beyond the simple consideration of level and duration of incident radiation, to include such factors as thickness, density, orientation, and point of heating of the combustible material.

The influence of any one of the six factors listed above on determining structural ignition should not be minimized. For cylindrical flames, dependence of view factor on distance between the flame and structure, r, will be generally of the functional form $1/r$ or $1/r^2$. The latter form will always be operative for sufficiently large distances; for very small distances, other functional forms may occur. Regardless of functional form, distance of the exposed structure from the fire is a primary variable determining structural ignition. Similarly, flame geometry has a profound effect on view factor and, hence, an important effect on incidental radiation and ignitability. Obviously, given two structures equidistant from the base of a tilted flame, the structure toward which the flame tilts will receive more radiation than the structure on the upwind side of the flame. Other parameters of flame geometry will also be significant, especially near

the flame. The orientation of the structure with respect to the flame is especially important for structures with noncombustible exteriors. A structure with a windowed wall directly facing the flame is more vulnerable to ignition than are structures with windows at an angle with respect to the flame or structures with a windowless wall facing the flame.

Of paramount concern in this model is, of course, the shielding from thermal radiation effected by structures intervening between the flame and the structure under consideration. Shielding may be complete or partial. If one or more intervening structures prevent all parts of a given building from "seeing" any part of the flame (i.e., receiving any thermal radiation from the flame), then the shielding is complete. For partial shielding two cases arise: (1) some of the given building sees all of the flame, while the rest of the given building sees only part or none of the flame; and (2) none of the given building sees all of the flame, but all or part of the building sees part of the flame. This distinction is not trivial. The intensity of radiation reaching the ignitable substance in or on a building is directly proportional to the view factor for the flame computed at the location of the combustible materials. The view factor, for an infinitesimal receiving element, is equal to an integral over that portion of the emitting body seen by the receptor. When intervening structures shield part of the flame from view by a given receptor, the view factor is accordingly reduced. Shielding can thereby reduce the radiation intensity below the value required for ignition. For structures with combustible exteriors, ignition will occur if the level of thermal radiation (for a given duration) is sufficiently high virtually anywhere on the structure exterior. For structures with noncombustible exteriors, sufficient thermal radiation must penetrate a window or other portal to effect ignition. Consider structure near enough to the flame that the level of thermal radiation incident is sufficient to cause ignition. If an intervening structure shields all of the building to some degree, then the radiation intensity may be reduced enough to prevent ignition of the building. On the other hand, complete or partial shielding of only part of the building, while the remainder is fully exposed, will cause ignition of the building. For buildings with combustible exteriors, Case (2) shielding may prevent ignition while Case (1) shielding, in general, will not. For buildings with noncombustible exteriors, the situation is not as simple: Case (2) shielding may also prevent ignition if the shielding is great enough; Case (1) shielding may also prevent ignition provided the unshielded portion of the building is devoid of windows or other portals. In general, then, a comprehensive accounting of shielding will consider the fraction of the building which is shielded and, for that fraction which is shielded, will consider the fraction of the flame that is obscured. Since the entire building is assessed to be ignited if any part of the building is ignited, a comprehensive treatment would calculate the incident radiation based on view factor for all the various sites on the building where combustibles were

located. At each site, the effects of intervening structures would be taken into account. Obviously, the performance of such a large number of calculations as would be required is beyond the scope of the VM.

In addition to the *degrees* of shielding discussed above, shielding may occur for different reasons. For want of a better terminology, consider horizontal and vertical breaches in shielding. Horizontal breaches in shielding occur when structures in between the fire and the building under consideration are oriented so that spaces between the intervening buildings permit a view of the fire. Vertical breaches in shielding typically occur when a shorter building is between the fire and a taller building. It can also occur when a taller building is between the fire and a shorter building, provided the fire is taller than the taller building. Of course, a comprehensive treatment would use a detailed description of each structure's size, shape, and orientation. A less detailed analysis of shielding is made difficult by the different types of shielding possible, the possible effects of each type, and the different means whereby breaches in shielding can occur. Regardless of the modeling method used, shielding is an important parameter in the determination of structural ignition.

The location and orientation of combustibles inside or on the exterior of a structure have an important influence on ignition of the structure. For structures with combustible exteriors those portions located closer to the flame, directly facing the flame, or located in an unshielded position will be more likely to ignite than other parts of the exterior. The same parameters affect the ignitability of combustibles located inside a structure with a noncombustible exterior. In general studies of fire phenomena, the term usually applied to the hazard of ignition of a structure by nearby fires is "exposure" [31]. Studies of protection against exposure clearly indicate that construction using noncombustible exterior surfaces provides only a small measure of protection if the structure contains a typical number of windows and other portals. Most structures contain combustible materials inside and, unless special precautions are taken (e.g., blank fire walls between buildings, automatically closing steel shutters on windows, outside sprinklers on windows and doors, wired glass in windows, etc.), the hazard presented by the ignition of combustibles inside approaches or exceeds the hazard presented by the ignition of combustible exterior materials. Obviously, then, the location and orientation of these materials are of considerable importance.

In addition to the nature of the exposure experienced by combustible materials, the physical and chemical properties of the materials are important in determining whether ignition results. Table 4-1,

---

[31] Tyron, G. H. (editor-in-chief), *Fire Protection Handbook*, ch. 8, National Fire Protection Association, Boston, 1969.

taken from nuclear weapon effects studies [32], shows the level of radiation required for ignition of various types of materials and three separate radiation pulse durations. Not only is the type of material important, but the thickness and color of the exposed material are also important. For example, heavy dark cotton drapes require higher levels of incident radiation than do black lightweight cotton curtains. In general, denser materials require higher levels of radiation to ignite for the same pulse duration. On the other hand, black lightweight cotton curtains do not require as high a level of incident radiation to ignite as do beige lightweight cotton curtains, because darker hued materials in general absorb radiant energy better. Thus, a detailed knowledge of the physical and chemical nature of the exposed material is required to predict whether ignition occurs. Obviously, the acquisition and processing of data regarding combustibles in and on buildings are beyond the scope of the VM.

TABLE 4-1. IGNITION CRITERIA FOR VARIOUS MATERIALS

Common Kindling Fuels	Weapon Yield (MT)		
	1	5	25
	(cal/cm^2)		
Group I			
Crumpled newspaper, dark picture area	7	9	15
Black lightweight cotton curtains	6	8	11
Dry rotted wood and dry leaves	6	7	10
Group II			
Beige lightweight cotton curtains	32	42	55
Kraft corrugated paper carton	19	22	32
White typing paper	30	42	60
Heavy dark cotton drapes	22	27	50
Group III			
Upholstered furniture	28	40	56
Beds	22	34	52
Pulse duration (seconds)	10.1	22.5	50.5

From the discussion above of factors influencing structural ignition, it is clear that a comprehensive treatment is not feasible at this stage of development of the VM. However, some improvement over the current method in use for assessing structural ignition is possible.

---

[32] Defense Civil Preparedness Agency, *DCPA ATTACK ENVIRONMENT MANUAL, Chapter 3, What the Planner Needs To Know About Fire Ignition and Spread*, CPG 2-1A3, DCPA, June 1973.

The improved method will not consider factors (3) and (5). The assumption is that the primary fires will be large enough and the presence of combustible materials sufficiently ubiquitous that a detailed treatment is unnecessary. Factor (6), the ignition characteristics of the combustible material, will be treated as before by taking an average value for wood or some other material. Factors (1) and (2) will be considered by computation of the view factor. An improvement over the present method will be accomplished by defining more precisely within a cell the region exposed to a level of radiation capable of causing ignition. Factor (4), shielding by intervening structures, will be considered by allowing the user to choose between situations of maximum hazard, minimum hazard, and intermediate hazard. The intermediate hazard is computed by approximating the effect of random shielding.

DETERMINATION OF FRACTION OF THE CELL SUBJECT TO IGNITION

In order to improve the model of structural ignition, first consider how much of a given cell is subjected to radiation levels sufficiently high to initiate ignition. Previously, conditions existing at the cell center were assumed to apply throughout the cell; however, a more precise estimate of structural ignition requires a more detailed level of information. Consequently, variation of radiation levels within the cell are considered. This may be viewed as an automatic subpartitioning of the cell, in which vulnerable resources are distributed proportional to the area of the subpartitions.

Shielding effects will be considered subsequently; the goal here is to define that portion of the cell affected, as if no shielding were occurring. Given a certain size cylindrical flame tilted at some angle to the vertical, a contour may be drawn around the flame such that receptors outside the contour will not be ignited. This "ignition contour" will depend in general on the nature of the receptor as well as on the flame parameters. As mentioned previously, however, the ignition characteristics of the receptor will be treated by assuming an average type of combustible material; thus, in this model the ignition contour will depend only on the flame characteristics. The problem reduces to finding for each cell the fraction of the cell within the ignition contour.

In order to simplify the calculation, the following additional assumptions are made:

(1) The cell is square in shape.

(2) One side of the cell directly faces the flame (i.e., the line between the cell center and the flame center is perpendicular to the side of the cell nearest the flame).

(3) Within each cell, view factor varies primarily with distance from the flame (i.e., within a cell the ignition contour is approximately the arc of a circle).

The user will be required to supply as additional input data the characteristic dimension of each cell. The square representing the cell will be assumed to have a width, W, equal to the characteristic dimension supplied by the user. The characteristic dimension can be taken to be twice the hydraulic radius, i.e.,

$$W = \frac{4A}{P}$$

where A is the cell area and P is the length of the cell perimeter.

However, other less precise ad hoc estimates for W are acceptable. W will be included in the data file giving the cell location and the vulnerable resources within it. Also required for this computation are N, the number of structures in the cell (currently part of the vulnerable resource file), D, the distance of the cell center from the flame (currently computed from the latitude and longitude of the cell center), and a computerized model for calculating view factor (currently SVEIW). A computerized, rather than analytical, model for view factor is used so that any subsequent improvements in view factor models will be easily incorporated into the model.

Given that the cell is square and that the ignition contour is circular over the region of a single cell, five situations are possible.

Case 1. The entire square is outside the ignition contour.

Case 2. The ignition contour intersects the front face of the square.

Case 3. The ignition contour intersects the side face of the square.

Case 4. The ignition contour intersects the rear face of the square.

Case 5. The entire square is inside the ignition contour.

For each of the five cases, the fraction of cell area within the ignition contour, F, and the fraction of the front face within the ignition contour, f, are to be computed.

The computation proceeds as follows. For the computed burning time of the flame, T, find from the ignition criteria (for example, the ignition criteria developed by Lawson and Simms [23] for wood) the critical level of thermal radiation, I_C, required for ignition. Compute the radiation level at the center of the front face of the square, I_1;

i.e., compute the radiation intensity at the distance $(D - W/2)$ using the view factor subroutine and the computed geometrical and emission characteristics of the flame. If I_1 is less than I_C, then the entire cell is outside the ignition contour, $F = 0$ and $f = 0$.

Next, compute the radiation intensity at the rear corner of the cell, I_2; i.e., in the view factor computation, take the distance from flame to receptor, d_2, to be

$$d_2 = \left[\left(D + \frac{W}{2}\right)^2 + \left(\frac{W}{2}\right)^2\right]^{1/2} \tag{4-1}$$

If I_2 is greater than I_C, then the entire cell is within the ignition contour, $F = 1$ and $f = 1$. If I_2 is less than I_C, then the ignition contour intersects the cell and further computation is required.

Compute the radiation intensity at the rear center of the cell, I_3; i.e., in the view factor computation, take the distance to be

$$d_3 = D + \frac{W}{2} \tag{4-2}$$

If I_3 is greater than I_C, then the ignition contour intersects the rear face of the cell and $f = 1$. In order to compute F, a more precise determination of the location of the ignition contour is required. Distances between d_2 and d_3 are chosen according to the formula

$$d_j = \left[\left(D + \frac{W}{2}\right)^2 + \left(\frac{jW}{2n}\right)^2\right]^{1/2} \tag{4-3}$$

Since $I_3 > I_C$ and $I_2 < I_C$ for some choice of j, say $j = k$, I_j will become less than I_C; i.e.,

$$I_k < I_C$$

and

$$I_{k-1} > I_C$$

Then the ignition contour will be assumed to occur at the distance, d_k. The index j varies from 1 to n and n may be taken to be 10, some other convenient number, or $\sqrt{N}$.

Once d_k is determined, the fraction of the area of the square inside the ignition contour may be computed. Referring to Figure 4-1, we have the following relationships.

$$\sin \theta_1 = \frac{W}{2d_k}$$

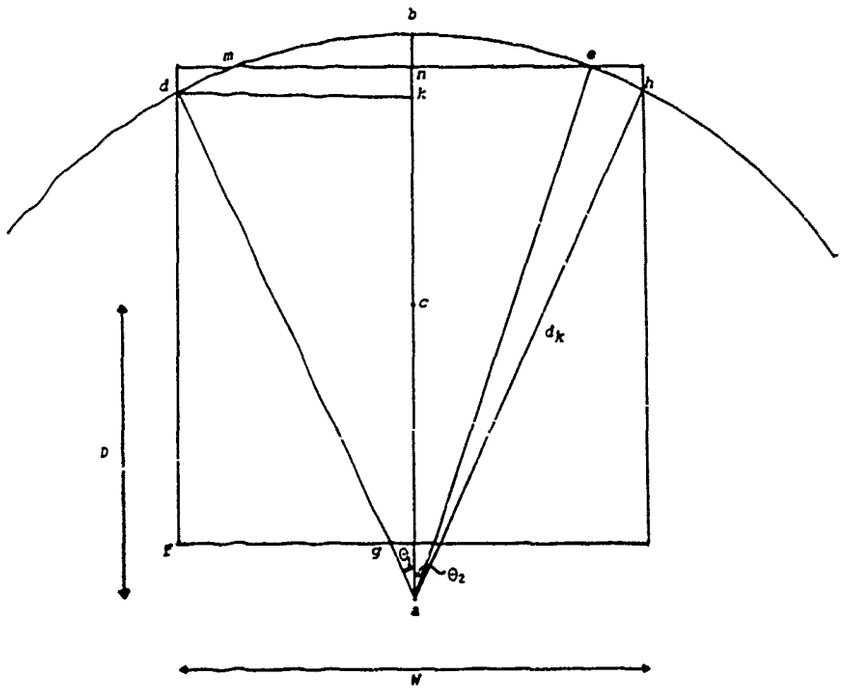

FIGURE 4-1. *Geometry for Case 4 When the Ignition Contour Intersects the Rear Face of the Cell*

$$\cos \theta_2 = \frac{D + W/2}{d_k}$$

$$\widetilde{ak} = d_k \cos \theta_1 = d_k \sqrt{1 - \left(\frac{W}{2d_k}\right)^2}$$

$$\widetilde{a\ell} = D - \frac{W}{2}$$

$$\widetilde{\ell k} = \widetilde{ak} - \widetilde{a\ell} = d_k \cos \theta_1 - D + \frac{W}{2}$$

Area of the sector, *adh*, is

$$A_S = 2\theta_1 d_k^2$$

Area of the triangle, *dfg*, is given by

$$A_B = \frac{1}{2} (\widetilde{\ell k})^2 \tan \theta_1$$

Area of the triangle, *alg*, is given by

$$A_C = \frac{1}{2} (\overline{a\ell})^2 \tan \theta_1$$

Area of the segment, *mben*, is given by

$$A_D = 2d_k^2 \theta_2 - \frac{d_k^2 \sin 2\theta_2}{2}$$

And the area of the exposed portion of the square is

$$A_E = A_S + 2A_B - 2A_C - A_D$$

After some manipulation, this becomes

$$A_E = 2d_k^2 (\theta_1 - \theta_2) + \frac{d_k^2 (\sin 2\theta_1 + \sin 2\theta_2)}{2} - W\left(D - \frac{W}{2}\right) \qquad (4\text{-}4)$$

Hence,

$$F = \frac{A_E}{W^2} = \frac{d_k^2}{W^2} \left[2(\theta_1 - \theta_2) + \frac{1}{2} (\sin 2\theta_1 + \sin 2\theta_2)\right] - \frac{D}{W} + \frac{1}{2} \qquad (4\text{-}5)$$

and obviously $f = 1$ where

$$\theta_1 = \arcsin \frac{W}{2d_k}$$

and

$$\theta_2 = \arccos \frac{D + W}{d_k}$$

Now, if I_3, the intensity computed at the distance $(D + W/2)$, is less than I_C and if I_1, the intensity computed at the distance $(D - W/2)$, is greater than I_C, the ignition contour intersects either the front face or the sides of the cell. To determine which is the case, compute I_4, the radiation intensity at the front corner of the cell; i.e., in the view factor computation, take the distance to be

$$d_4 = \left[\left(D - \frac{W}{2}\right)^2 + \left(\frac{W}{2}\right)^2\right]^{1/2} \qquad (4\text{-}6)$$

If $I_4 > I_C$, the ignition contour intersects the sides of the cell. If $I_4 < I_C$, the ignition contour intersects the front face of the cell. If $I_4 > I_C$ it is desirable to obtain a better measure of the ignition radius. Distances between d_3 and d_4 are chosen according to the formula:

$$d_j = \left[\left(D + \frac{W}{2}\right)^2 - \frac{n-j}{n}\left(2DW - \frac{W^2}{4}\right)\right]^{1/2} \tag{4-7}$$

As before, for some choice of j, say $j = k$, I_j will fall below I_C; i.e.,

$$I_k < I_C$$

and

$$I_{k-1} > I_C$$

Then assume the ignition contour to be the distance, d_k. The upper bound on j, n, may be chosen as before. The area of the cell impacted is computed with reference to Figure 4-2. Observe the following relationships,

$$\sin \theta_1 = \frac{W}{2d_k}$$

$$\overline{fk} = D - \frac{W}{2}$$

$$\overline{ad} = \overline{hk} = d_k \cos \theta_1 - \left(D - \frac{W}{2}\right)$$

Area of the sector, agf, is

$$A_S = 2\theta_1 d_k^2$$

Area of the triangle, ade, is

$$A_B = \frac{1}{2}(\overline{ad})^2 \tan \theta_1$$

Area of the triangle, efk, is

$$A_C = \frac{1}{2}(\overline{fk})^2 \tan \theta_1$$

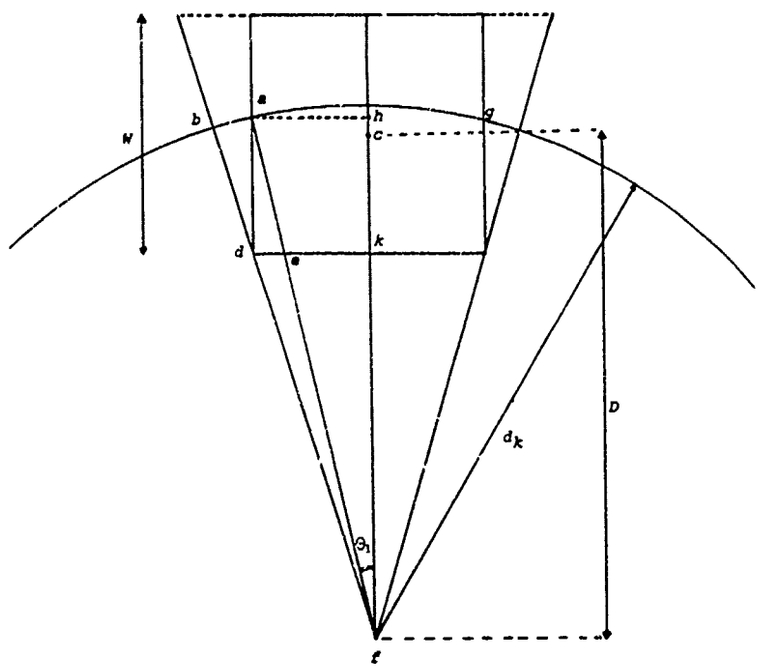

FIGURE 4-2. Geometry for Case 3 When the Ignition Contour Intersects the Side Face of the Cell

Then the area of the impacted part of the cell is

$$A_E = A_S + 2A_B - 2A_C$$

which, after some manipulation, becomes

$$A_E = d_k^2 \left(2\theta_1 + \frac{\sin 2\theta_1}{2}\right) - WD + \frac{W^2}{2} \qquad (4\text{-}8)$$

Hence,

$$F = \frac{A_E}{W^2} = \frac{d_k^2}{W^2} \left(2\theta_1 + \frac{\sin 2\theta_1}{2}\right) - \frac{D}{W} + \frac{1}{2} \qquad (4\text{-}9)$$

where

$$\theta_1 = \arcsin \frac{W}{2d_k}$$

and obviously $f = 1$.

In the event that $I_4 < I_C$ (and, of course, $I_1 > I_C$), then the ignition contour intersects the front face of the cell only. For a more precise determination of the location of the contour, the distance is sequentially varied from $d_1 = D - W/2$ to d_4. Thus let

$$d_j = \left[\left(D - \frac{W}{2}\right)^2 + \frac{j}{N}\left(\frac{W}{2}\right)^2\right]^{1/2} \tag{4-10}$$

in order to find d_k such that

$$I_k < I_C$$

and

$$I_{k-1} > I_C$$

Then, assuming the ignition contour to be d_k, we have with reference to Figure 4-3

$$\cos \theta_1 = \frac{D - W/2}{d_k} \tag{4-11}$$

and the area of the segment, *afbe*, is

$$A_S = d_k^2 \left(2\theta_1 - \frac{\sin 2\theta_1}{2}\right) \tag{4-12}$$

The area of the segment is of course the area affected so that

$$F = \frac{A_E}{W^2} = \frac{A_S}{W^2} = \frac{d_k^2}{W^2}\left(2\theta_1 - \frac{\sin 2\theta_1}{2}\right) \tag{4-13}$$

where

$$\theta_1 = \arccos \frac{D - W/2}{d_k}$$

In this case, $f \neq 1$ since the ignition contour intersects the front face. Again, referring to Figure 4-3, note that

$$\overline{ae} = d_k \sin \theta_1$$

and that

$$f = \frac{2\overline{ae}}{W}$$

which, after some manipulation, becomes

$$f = 2\left[\frac{d_k^2}{W^2} - \left(\frac{D}{W} - \frac{1}{2}\right)^2\right]^{1/2} \qquad (4\text{-}14)$$

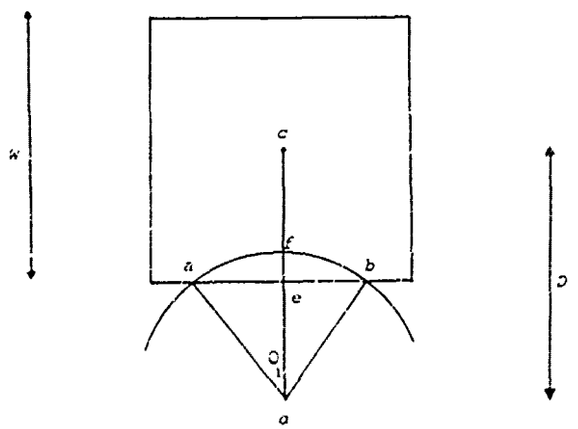

FIGURE 4-3. Geometry for Case 2 When the Ignition Contour Intersects the Front Face of the Cell

These calculations are summarized in a flow chart in Chapter 9. Once the values for F and f are determined, the area potentially experiencing ignition is defined. The calculation now proceeds to consider shielding.

SHIELDING EFFECTS

As explained above, shielding of one structure by another is an important factor influencing ignition; however, a comprehensive treatment is not feasible or desirable at this time. The complexity introduced by the various degrees and types of shielding possible has been discussed above and need not be repeated here. The approach taken here is to define the limiting situations for shielding (maximum and minimum shielding) and then to approximate an intermediate case using an abstract generalization.

The extremum cases for shielding are easily conceptualized. In the event that no structure is shielded by another, every structure within the ignition contour will be ignited. This is likely to be the case

for very high flames and/or topography such that the vulnerable structures are situated on the walls of a valley with the flame in the center of the valley (see Figure 4-4). For the case of minimum shielding, the number of structures ignited is estimated to be

$$N_I = [NF + 1] \tag{4-15}$$

where

- $[X]$ indicates the largest integer in X,
- N_I is the number of structures ignited,
- N is the number of structures in the cell, and
- F is the fraction of the cell area within the ignition contour and calculated according to the formulas given above.

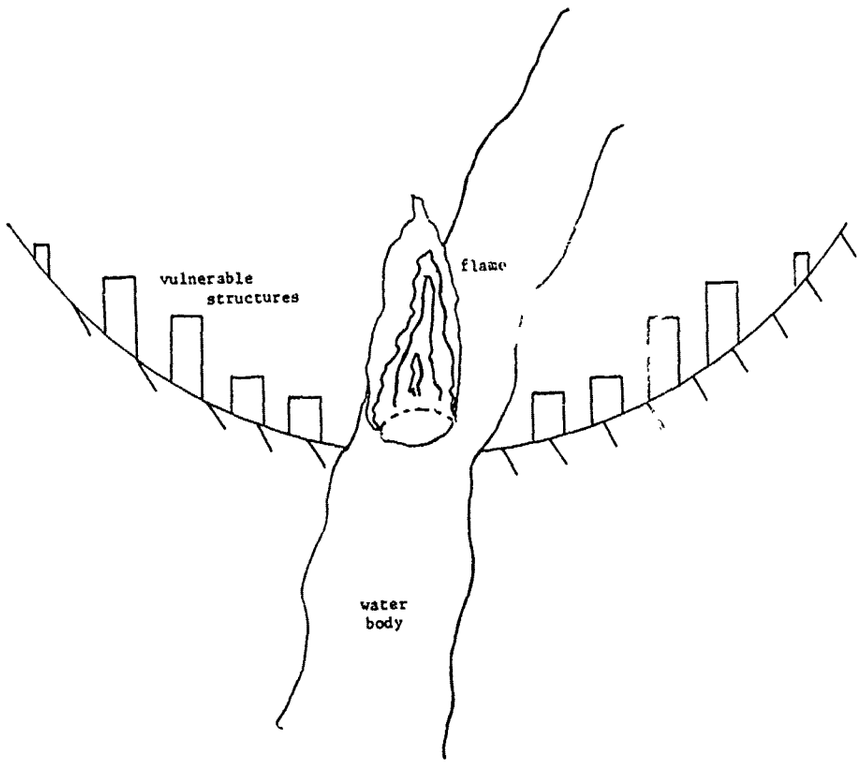

FIGURE 4-4. An Example of the Topography for Which the Minimum Shielding Assumption May Be Appropriate

In the event that the maximum amount of shielding occurs, only those structures that shield the rest will be ignited. In order to estimate the smallest number of structures possible that may shield the remaining structures in the cell, some assumptions must be made about the nature and distribution of the structures in the cell. Let us assume that the structures are uniformly distributed in the cell. Then for N structures in the cell, the structures will be arranged in M rows by M columns where $M = \sqrt{N}$ (in the event that N is not a perfect square, M will be taken to be the next largest or next smallest integer close to $\sqrt{N}$ as is appropriate). The situation corresponding to minimum ignition will be that in which the structures on the row nearest the flame are ignited by shielding all other structures in the cell. It is conceivable, of course, that a single structure in a cell might shield the remainder, but such an event seems improbable. In keeping with other assumptions about the exposure of structures (e.g., that the cell is square), it seems appropriate to assume that the structures are uniformly distributed in the cell and that, for the case of maximum shielding, only those structures in the row nearest the flame are ignited. Then

$$N_I = [Mf + 1] \tag{4-16}$$

where $M = \sqrt{N}$, f is the fraction of the front face of the cell within the ignition contour, and the symbol $[X]$ stands for the largest integer in X (rounding up gives a conservative damage estimate).

Now consider an intermediate case of shielding. As discussed earlier, simple considerations, such as whether an intervening building is wider and/or taller than a potentially shielded building, do not necessarily reveal whether one building will in fact shield another. What is required is that a detailed calculation of view factor be made considering the flame size and intervening building geometry. It is not feasible to perform this calculation. Even so, were such a calculation to be made, the resulting answer would indicate whether a given building was or was not shielded by an intervening building. In other words, for building A to shield building B, building A will possess some measure of shielding ability (depending on its size, shape, and location relative to building B and the flame). The method used here is to equate shielding ability to a numerical value and then to consider random arrangements of these numerical values.

To illustrate this analog, consider three buildings in a line with radiation from the flame parallel to the line of buildings. Suppose each building has a shielding ability represented by the numerical values 1, 2, and 3. There are six possible arrangements of these numerical values. This may be visualized, as in Figure 4-5, by equating shielding ability to height. Now the assumption is made that building A is shielded only if a building B, with a shielding ability greater than that of building A, is between the flame and building A.

Considering the numerical analog, this means that the number of structures ignited depends on the arrangement of the numerical values. Thus, for example, in arrangement 1,2,3 no building is shielded and all three are ignited. In arrangements 3,2,1 and 3,1,2 two buildings are shielded and only the leading building is ignited. In arrangements 1,3,2 and 2,3,1 and 2,1,3 one building is shielded and two are ignited.

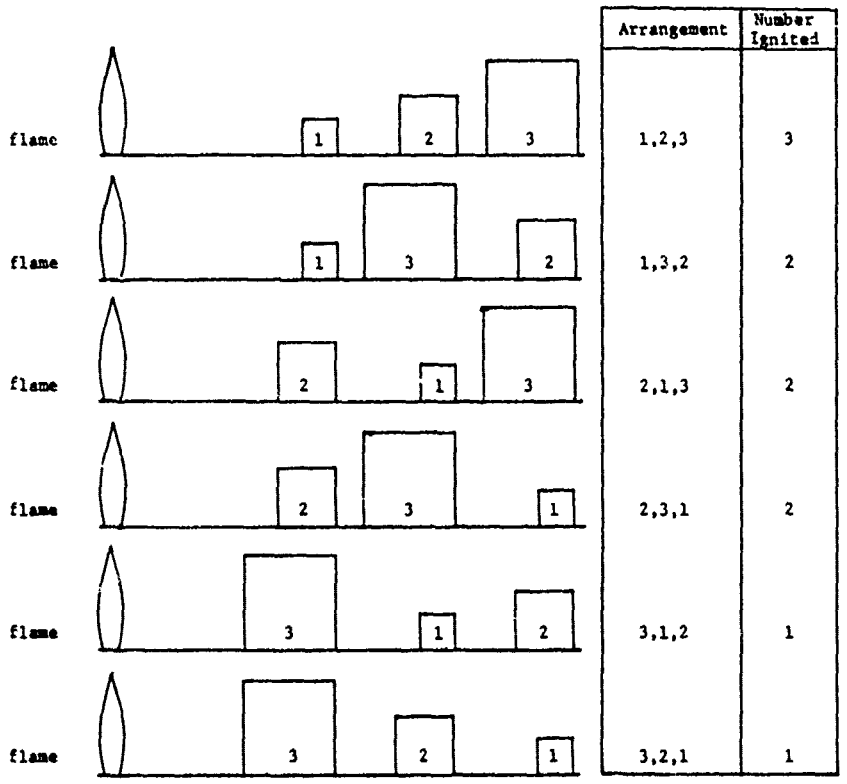

FIGURE 4-5. Visualization of Possible Arrangements of Three Buildings with Three Levels of Shielding Ability

A random arrangement of shielding ability would include all possible arrangements with equal probability of occurrence. For the random arrangement, we may consider the average number of buildings ignited as defined by

$$V = \frac{1}{\nu} \sum_{i=1}^{\nu} n_i \qquad (4\text{-}17)$$

where ν is the total number of different arrangements and n_i is the number of buildings ignited for arrangement i.

For the case of three buildings in a line, $\nu = 3! = 6$ and

$$V = \frac{1}{6}[3 + 1 + 1 + 2 + 2 + 2] = \frac{11}{6} = 1.8333$$

Observe that V lies between 3, the maximum number ignitable, and 1, the minimum number ignitable. What is proposed then is that V be computed for the number of rows of structures inside the ignition contour and that the number ignited in the intermediate case be taken as

$$N_I = [V N_C + 1] \tag{4-18}$$

where N_C is the number of columns. In other words, the average number of rows ignited is multiplied by the number of columns to yield the number of buildings ignited. Three problems remain: (1) what value is to be used for the number of rows, L, since V depends on L; (2) what value is to be used for N_C; and (3) what algorithm is used to compute V given L.

The first two questions are related. The total number of structures within the ignition contour should be equal to the product, $L N_C$.

$$N_C = [Mf + 1] \tag{4-19}$$

where $M = \sqrt{N}$ and $[X]$ stands for the largest integer in X. Then take

$$L = \left[\frac{NF}{Mf} + 1\right] = \left[\frac{MF}{f} + 1\right] \tag{4-20}$$

The number of buildings ignited will then be given by

$$N_I = L N_C V_L \tag{4-21}$$

where V_L is the average number ignited for L buildings in a line.

In order to calculate N_I, an analytic method is required to compute V_L, i.e., the average number of structures ignited for L structures in a row. To formalize the concepts introduced earlier, we proceed as follows. Consider L structures in a line. Each structure will occupy a position of relative proximity to the fire. Each position will be numbered sequentially, depending on its proximity to the fire. The position nearest the fire will be the 1st position; the Lth position will be farthest from the fire. In addition to its position number, each structure will have associated with it a numerical value that gives some measure of the ability of the structure to shield other

structures from thermal radiation. Assume that the numerical value is different for each of the L structures. Also assume that a structure will shield from ignition all structures that are more distant from the fire and that possess a lower shielding value. Conversely, a structure will be ignited if it is located so that no structure intervening between it and the fire has a higher shielding value. This may be stated mathematically as follows. Let the shielding value of the structure in the kth position be S_k. If

$$S_k > S_j \qquad j = 1,2,\ldots,k-1$$

then the kth structure is ignited.

If $S_k < S_j$ for any value of j between 1 and $k-1$, then the kth structure is shielded and is not ignited. Since we have assumed that shielding depends on the relative values of the S_k and not on the absolute magnitude of them, it is convenient to assume, with no loss of generality, that the S_k are integers ranging from 1 to L.

Now we may proceed to state the problem of random arrangements of structures mathematically. Consider an arrangement A_i of the first L integers with each integer I_k occupying a position k. Let

$$T_k = \begin{cases} 1 & \text{if } I_k > I_j \qquad j = 1,2,\ldots,k-1 \\ 0 & \text{if } I_k < I_j \qquad j \in \{1,2,\ldots,k-1\} \end{cases}$$

(If $T_k = 1$, the kth structure is ignited; if $T_k = 0$, the kth structure is shielded from ignition.) Then

$$U_i = \sum_{k=1}^{L} T_k \tag{4-22}$$

where U_i is the value corresponding to arrangement A_i (the analog of the number of structures ignited for arrangement A_i). Then

$$V_L = \frac{1}{\nu} \sum_{I=1}^{\nu} U_I \tag{4-23}$$

where ν is the total number of different arrangements (V_L is the average number of structures ignited).

Now we proceed to develop a formula for V_L, the average number of structures ignited, in terms of L, the number of structures in a line inside the ignition contour. There are $L!$ possible arrangements of L integers. That is, there are L possible ways to fill the first position, $L-1$ possible ways to fill the second position, etc. Thus,

$\nu = L!$ Now V_L may also be computed by the following formula:

$$V_L = \frac{1}{\nu} \sum_{I=1}^{L} \gamma_I \tag{4-24}$$

where γ_I is the number of arrangements in which the Ith integer has the value $T = 1$. That is, γ_I is the number of arrangements in which the Ith structure is ignited. Now,

$$\gamma_I = \frac{L!}{L - I + 1} \tag{4-25}$$

This can be shown as follows. There are $L!$ arrangements. The probability that the Ith structure is ignited is the same as the probability that all $L - I$ larger integers follow it. In other words, out of $L - I + 1$ integers (I and all integers larger), what is the probability that I is first. This probability is

$$\frac{1}{L - I + 1}$$

(the probability that a certain object is chosen from m objects is $1/m$). Since there are $L!$ arrangements and the probability of igniting the Ith structure is $1/(L - I + 1)$, the number of arrangements in which the Ith structure is ignited, γ_I, is given by

$$\gamma_I = \frac{L!}{L - I + 1} \tag{4-26}$$

Substituting this into the formula for V_L gives

$$V_L = \frac{1}{\nu} \sum_{I=1}^{L} \gamma_I = \frac{1}{L!} \sum_{I=1}^{L} \frac{L!}{L - I + 1} = \sum_{I=1}^{L} \frac{1}{L - I + 1} \tag{4-27}$$

In the above, if we let $J = L - I + 1$, then

$$V_L = \sum_{J=L}^{1} \frac{1}{J} = \sum_{J=1}^{L} \frac{1}{J}$$

which is a slightly more convenient form.

It turns out that the psi (digamma) function defined in terms of gamma functions as

$$\psi(z) = \frac{d}{dz}\left(\ell n\, \Gamma(z)\right) = \frac{\Gamma'(z)}{\Gamma(z)} \qquad (4\text{-}28)$$

for integral values reduces to [33]

$$\psi(n) = -\gamma + \sum_{k=1}^{n-1} k^{-1} \qquad n \geq 2 \qquad (4\text{-}29)$$

$$\psi(1) = -\gamma \qquad (4\text{-}30)$$

where γ is Euler's constant, $\gamma = 0.5772156649$. Thus the required value, V_L, may be written in terms of the psi function as

$$V_L = \psi(L+1) + \gamma \qquad (4\text{-}31)$$

where γ is Euler's constant. To compute V_L in the VM, either the simplified summation formula or the formula relating V_L to the psi function may be used, depending upon which is computationally more advantageous. Table 4-2 shows values of V_L for a few values of L. As L increases without bound, V_L also increases without bound. However, V_L increases very slowly. Thus for 100 structures in a row, the average number ignited for all possible arrangements is only a little more

TABLE 4-2. VALUES OF V_L *FOR VARIOUS VALUES OF* L

L	V_L
1	1
2	1.5
3	1.833
4	2.08333
5	2.28333
20	3.59774
50	4.49921
100	5.18738

[33] Abramowitz, M., and I. A. Stegun (eds.), *Handbook of Mathematical Functions*, National Bureau of Standards, 1964.

In order to conceptualize the effect of shielding on structural ignition, it is convenient to equate building height to shielding ability. In this context, the case of maximum shielding (minimum damage) corresponds to the tallest building being nearest the flame and thereby shielding the remainder. The case of minimum shielding (maximum damage) corresponds to the buildings being lined up, in order, with the shortest nearest to the fire and the tallest farthest away; thus, all the buildings are exposed. The case of intermediate shielding corresponds to the average number in a row ignited, the average taken over all possible arrangements of building heights, each with equal likelihood of occurrence. These various shielding situations are illustrated in Figure 4-6. It should be pointed out, however, that equating building height to shielding ability is to be done for conceptual purposes only. As indicated previously, the ability of one building to shield another and prevent ignition is a complicated function of not just building height, but also flame height and size, flame and building location, and building size and shape.

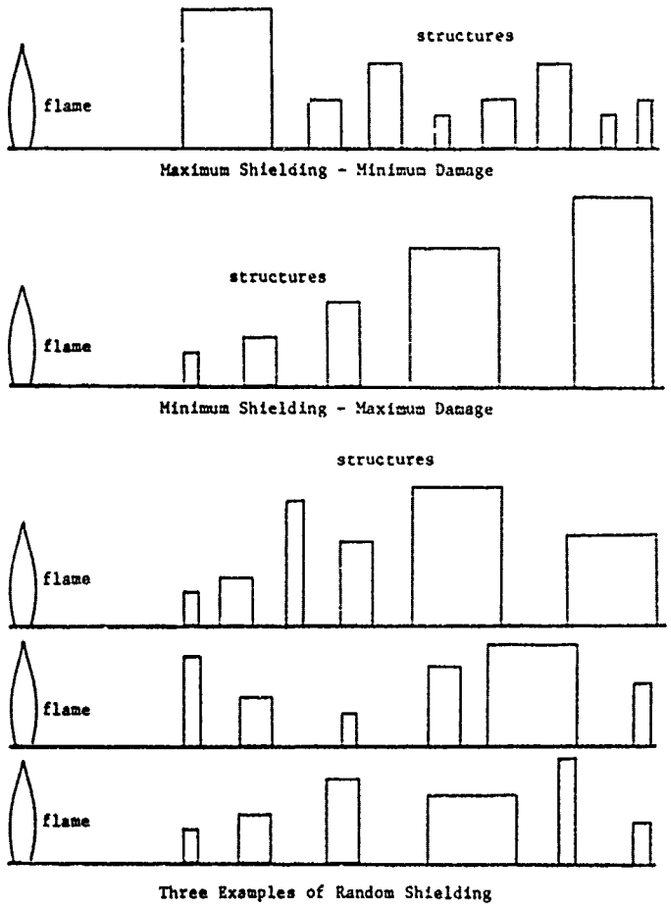

FIGURE 4-6. Conceptualization of Three Different Shielding Situations

CONCLUSION

The Structural Ignition Submodel has been improved by the incorporation of two concepts.

(1) The number of structures ignited within a cell is limited to those structures within the ignition contour of the flame.

(2) The effects of shielding are treated by allowing the user to choose among situations of maximum, minimum, and intermediate shielding.

For both these concepts, implementation relies upon several assumptions and approximations which have been enumerated in the foregoing discussion.

A flow chart of the improved Structural Ignition Submodel is given in Chapter 9 of this report. The user is now required to supply a characteristic dimension for each cell and to choose the desired shielding situation.

Chapter 5

TOXICOLOGY OF ADDITIONAL HAZARDOUS MATERIALS

INTRODUCTION

This chapter is about the effects on the human population of inhaling clouds of toxic substances. It describes how we have developed numbers to translate predicted exposures to a given substance into percentage of people harassed, incapacitated, or killed. Details of the sources of information we used and how the exposure-response relationships were arrived at are given in Appendix B. In this chapter we first discuss the general principles of this work and some of its problems. This has entailed a brief repetition of ground covered in the First Report on the Vulnerability Model [1], but we felt it desirable that the present report should be complete in itself. We then summarize the characteristics and evaluation of each substance and conclude with a short discussion.

The scope here is limited to inhalation because this is the route of most probable exposure and the only one that can be given really satisfactory quantitative evaluation. Ingestion and contact are likely risks to only a small minority of the population at most; and the extent of exposure, if any, is a matter of guesswork requiring a quite different approach from inhalation exposure.

The First Report [1] dealt only with chlorine and anhydrous ammonia. These were the most significant toxic hazards among the five substances initially studied in our Vulnerability Model (VM) development. The other three were LNG (methane), methanol, and gasoline. We provisionally concluded that "LNG is nontoxic in the context of the VM. However, consideration should be given to the risk of asphyxiation in high concentrations of LNG vapor" [1, p. 266]. This has been done in the present report. Methanol was set aside at the time as a low-level toxic hazard, but we recognized that it should be reconsidered. This has not yet been done, and methanol should perhaps be included in a future list of additional hazardous substances. Gasoline presents an intractable problem because "its toxic properties depend mainly on the aromatic hydrocarbon content, which is widely variable" (ibid.). It also might be given future consideration, but the prospects of a fully satisfactory and workable set of exposure-response estimates are not too good. Fortunately, the level of risk is likely to be low in any probable VM incident and negligible in comparison with the fire and explosion hazards.

In the present report, we deal with:

- Acrolein
- Asphyxiating gases - methane and propane
- Carbon tetrachloride

- Hydrogen chloride
- Methyl bromide
- Phosgene

Sections of Appendix B are devoted to each of these materials. They are discussed individually in this chapter after a review of the principles underlying our approach to making best estimates of exposure-response relationships.

OBJECTIVE

If a cloud of toxic substance passes through a populated area, anyone there will inhale some of it unless he is in a totally enclosed space or is wearing a gas mask. The VM predicts, for any grid point, how the concentration would vary with time. It gives us, as required, the peak concentration, or the time above a given level of concentration, or the total exposure ("dosage"; see below). It is the toxicologist's business to decide, from published data on measured or estimated toxic effects for various exposures, how to translate the predicted concentration/time into effects on the population for each toxic substance.

APPROACH

The level of response to inhalation of a given toxic substance may depend on the rate of intake or the total amount taken in, or on both. The rate depends on the concentration. For an individual breathing steadily, the rate at which the toxic gas or aerosol arrives at the respiratory surfaces is directly proportional to the concentration of the substance in the inhaled air at that time. The total amount inhaled (and the amount retained, which is not the same and may be much less) depends on the average concentration and the time of exposure and is directly proportional to the product of concentration and time. This product is often written as Ct and it is called the dosage. This must not be confused with the dose, which is the amount taken in and retained by an individual. Dosage is the same for everyone at a given place: it is the "opportunity" which they have for taking in the substance. What each one actually takes in and retains--the dose--depends on individual characteristics: one may hold his breath, another may breathe faster than usual, and so forth. The usefulness of dosage as a description of exposure is that it is much more easily determined than the actual dose (which may be difficult or impossible to measure) and that effects are often proportional to dosage rather than to the level of concentration or exposure time separately. If response depends entirely on dosage and is completely independent of either concentration or time, we can write, for any given level of response (such as 50% lethality), Ct = constant. This is called Haber's Law. Since it is

strictly true only if the response is entirely independent of the time of exposure, anything which prevents the accumulated dose from exerting its full potential influence must result in a deviation from the law. A common reason for such a deviation is that the toxic substance is slowly eliminated from the body or transformed into something harmless. In that case, Haber's Law holds well enough for short exposures but is increasingly inaccurate as the time of exposure lengthens (and the average concentration drops). Another cause for deviation is if there is more than one mechanism of action: a dosage-dependent one and a concentration-dependent one. In such a case, the dosage-dependent response may hold over a wide range of concentration and the concentration-dependent response (such as acute irritation) may be a significant added stress only at higher concentrations.

In developing exposure-response numbers for the VM, it is obviously convenient if Haber's Law applies, as indeed it does for some substances (especially if the exposure is quite brief as it is in VM circumstances). It is also a tractable problem to deal with purely concentration-dependent conditions. However, hybrid relationships are common, and the preferred approach here is to select ranges of concentration such that Haber's Law can be applied without serious error within each range.

In summary, the general approach to developing numbers for exposure-response to use in the VM is to seek data (or estimates) that can conveniently be embodied in a single exposure-response model or a simple set of models.

PROBLEMS

The toxicologist's work is easy if there are published measurements or well-supported estimates of human exposure-response. There are obviously no experimental data for lethal or highly hazardous human exposures. Accidents occasionally permit estimates to be made of the exposure levels experienced by victims. However, one must usually depend on animal experiments.

There are two difficulties in using animal data. One is the complex problem of extrapolation from species to species. No animal is quite like a man, and those closer to the human (e.g., primates, pigs) are not conveniently usable in the numbers required for a good experiment. The convenient animal models--mouse, rat, guinea pig-- are a lot different from man. The other is the serious lack of suitable data in many cases. Interest in inhalation toxicology is strongly influenced by the needs of occupational and environmental health, where long-term, low-level exposure is the subject of concern. Somewhat more intense, short-term exposures are also of interest in relation to thresholds of tolerance: e.g., now much irritation a worker of member of the public may reasonably be expected to accept. Dangerous exposures are of

concern to the industrial safety officer, but only in relation to prevention of accidents and to emergency actions. He is not interested in knowing that a certain dosage will kill 25% or 75% of those exposed, only that exposure above a certain level is likely to kill some.

The available data base is particularly deficient with respect to the slope of the exposure-response relationship for inhaled toxic substances: i.e., how sensitive the percentage response is to the severity of exposure. This information must be known or estimated if a gradation of exposures predicted by the VM is to be translated into a gradation of percentage responses in the population. A few substances--notably chlorine and phosgene--are well documented. These have been used and extensively studied as war gases, where the area of interest is that of the VM and exactly the reverse of the usual case, being concerned with brief and intense exposure and fatal or incapacitating effects. For the rest, we have resorted to various devices in arriving at best estimates; the reader is referred to Appendix B for details.

Another difficulty is that nearly all the evidence applies to the least sensitive sector of the population, being derived from workers, volunteers, or--indirectly--from selected laboratory animals. There is very little guidance about the very young, old, or sick members of the population, beyond a clear indication that they are significantly more sensitive. We have felt justified in making guesses at the quantitative extent of this extra sensitivity, for two reasons: one is that a reasonable guess is better than ignoring an indisputable factor which would augment casualty rates, and the other is that provision should be made in the VM to accept any better figures that may come along later.

TOXICOLOGICAL EVALUATION OF INDIVIDUAL SUBSTANCES

Appendix B gives the detailed evidential basis and method of analysis for our estimates of exposure-response relationships, and that material is briefly presented here.

Acrolein

Acrolein is a liquid with a boiling point of 52.5°C. It polymerizes readily, especially in light, to form a plastic solid. It has a disagreeable choking odor, and the vapor is strongly irritant to the respiratory mucosa and to the eyes, acting as a powerful lacrimator. It was introduced as a harassing gas by the French in January of 1916 [34] but was soon dropped because its instability made it impractical for field use. Although the vapor has some potential as a lung injuriant, it was considered solely as a temporary incapacitant, which may account in part

---

[34] Prentiss, A. M., *Chemicals in War*, 1st ed., McGraw-Hill Book Co., New York and London, 1937.

for the paucity of estimates for human lethal effects in the literature. The intensity of its irritant property may be judged from the low threshold of concentration which causes irritation of the eyes and respiratory tract within a minute or two. This threshold is generally given as 1 to 3 parts per million [35]. However, acrolein is not to be regarded solely as a primary irritant.

The evidence suggests that two quite different lethal mechanisms may operate in human exposure to acrolein, similarly to the toxicology of chlorine which we reviewed previously [1]. Over a certain range of concentration, the subject is able to continue breathing--although with extreme distress--and accumulates a dangerous dosage in the lower respiratory tract; pulmonary edema develops, and the outcome may be fatal in a day or two. This mechanism would be expected to show a normal type of dose-response relationship. At higher concentrations, the irritation of the upper respiratory tract is so extreme that reflex respiratory spasm causes a hazardous reduction or cessation of breathing, so that resulting fatalities occur immediately or very soon. In those cases, the subject may be regarded as the victim of "strangulation," and the slower deep-lung toxic mechanism cannot of course develop. This lethal mechanism would be expected to be concentration-dependent rather than dosage-dependent. In survivors of the "strangulation" effect, the delayed deep-lung toxicity would develop in those who had accumulated a sufficient inspired dosage.

We have arrived tentatively at the exposure-response estimates of Table 5-1, which structurally resembles the table for chlorine and ammonia in the Final Report of June 1975 [1, p. 86]. It will be clear from the foregoing discussion and the deficiency of estimates for human lethal effects that our estimates are highly judgmental and should be treated accordingly. However, we believe that they present a credible and coherent picture of the possible consequences of acute exposure of the general population to acrolein.

---

[35] Deichmann, W. B., and H. W. Gerarde, *Toxicology of Drugs and Chemicals*, Academic Press, New York, 1969. The meaning of a 1 ppm concentration has been given very effective expression by Deichmann and Gerarde: "One part per million is one drop in 16 gallons or 80 'fifths', a very dry Martini indeed."

TABLE 5-1. EXPOSURE-RESPONSE RELATIONSHIP FOR ACROLEIN

Concentration, mg m^{-3} CH_2:CHCHO	Time	Response	Deaths, %	
			General Population	High-Risk Population
0.4	any	Negligible	0	0
0.4-4	any	Complaint, no risk	0	0
4-20	0.5 hr 1 hr	Severe harassment, risk to susceptibles	0 0	0 25
20-50	0.5 hr 0.5-1 hr 1-2 hr	Severe harassment (risk) Lethal Lethal	0 3 50	25 50 100
50-150	0.5 hr 0.5-1 hr 1-2 hr	Lethal Lethal Lethal	3 50 97	50 100 100
150-450	5 min 5-15 min 15-30 min	Lethal Lethal Lethal	3 50 97	50 100 100

Asphyxiating Gases: General

There are some gases which are nontoxic in the usually accepted sense of the word. That is to say, they do not ordinarily react with the body in any way to cause immediate or delayed irritation or damage. Examples are nitrogen and the inert gases helium, neon, argon, krypton, and xenon. However, they are not necessarily harmless. If present in sufficient concentration, they can dilute the oxygen of the air so much that reduced oxygenation of the blood and hence of the body leads to impaired faculties, unconsciousness, or even death. The body suffers from the lack of oxygen, not from the presence of the diluent gas. The effect is similar to that of high altitude and arises from the same cause: the partial pressure of oxygen in the gas-exchange (alveolar) region of the lung is insufficient to meet physiological needs. The organ most vulnerable to oxygen deficiency is the brain, which normally operates on only a small margin of safety: complete oxygen deprivation causes unconsciousness in a quarter of a minute, irreversible damage in four minutes and death in five minutes.

Gases which act in this way, depriving the lung of oxygen, are called "simple asphyxiants," to distinguish them from substances such as carbon monoxide, which interferes with oxygen transport in the blood (by monopolizing the hemoglobin), and cyanide, which interferes with oxygen use in the cells (by poisoning enzymes). These substances are called "chemical asphyxiants."

Estimation of exposure-response relationships for the VM required two steps: the general one of making best estimates for the effects of different levels of air dilution and the individual one, for each specific substance, of determining that it was a truly nontoxic gas.

The second point proved to be an important one. Methane (CH_4) and ethane (C_2H_6) are generally accepted as simple asphyxiants, and so are propane (C_3H_8) and butane (C_4H_{10}) by some established authorities. It is also generally recognized that pentane (C_5H_{12}) and higher members of the series have a narcotic effect on the central nervous system. The consensus was solid enough to justify our treating methane and propane as simple asphyxiants. We would have left it at that if we had not come by chance on an unpublished paper which showed conclusively that all four members of the methane-butane series have an effect on the central nervous system in mice which rises with increasing molecular weight. It can be neglected for methane, but the simple asphyxiant approach must be modified for propane. In the absence of substantial contrary evidence, we felt that the animal data must be extrapolated to man.

Our basis for the exposure-response estimates was aviation medicine work on the "ceiling" (or limiting ambient air pressure) for unassisted respiration with no impairment, the physiological effects of lower ambient pressures, and the consequences of sudden decompression to still lower pressures. There is an excellent data base and it is to be noted that, in contrast to the situation with all the toxic gases, we were able in this case to work exclusively with data from volunteer exposures. So long as the point of no return, irreversible brain damage, is not reached, even complete oxygen deprivation causes no more than briefly unpleasant aftereffects.

One problem was that decompression immediately reduces the oxygen pressure in the respiratory region of the lung, whereas breathing inert gas washes out the oxygen in successive breaths. An allowance had to be made for this. Unfortunately, no one appears to have done experiments with volunteers and diluted air at sea-level pressure similar to the aviation experiments at reduced pressure. Another problem was that there were, of course, no experimental observations on the time to reach the point of no return at various levels of oxygen deprivation.

Our estimates of exposure-response relationships for simple asphyxiants in air are shown in Table 5-9.

TABLE 5-2. EXPOSURE RESPONSE RELATIONSHIP FOR SIMPLE ASPHYXIANTS

Asphyxiant (%)	Response
42	Ceiling for safe exposure; some mental impairment, but unlikely to result in harm (except to extremely susceptible individuals)
50	Threshold for unconsciousness in the more susceptible segment of the population; a few cases of lasting impairment and perhaps death
60	8 minutes to unconsciousness for an average individual; time to unconsciousness may be about one-half in the more susceptible segment; recovery unlikely in absence of immediate medical aid
65	5 minutes to unconsciousness
70	3 minutes to unconsciousness
75	1.5 minutes to unconsciousness
80	1 minute to unconsciousness
85	0.75 minute to unconsciousness

Asphyxiating Gases: Methane

As already stated, the evidence is that methane does not differ sufficiently from the true simple asphyxiants to warrant modified treatment. We believe that Table 5-2 is applicable for VM purposes.

Asphyxiating Gases: Propane

The evidence to support modified estimates for propane comes solely from one laboratory's experiments with mice. However, it is a solid and coherent body of work. The reader is referred to Appendix B, where it will be seen that the clearest evidence is in a table comparing responses to air diluted with propane and air diluted with nitrogen. "Mild depression" occurred with 40% propane or 60% nitrogen in air. Loss of coordination occurred at 50% or 70%, respectively. Partial lethality was indicated at 60% and less than 80%. We decided to apply a uniform correction factor of 15%, so that the response attributed to 42% simple asphyxiant becomes the response for 42 - 15 = 27% propane, and so forth.

Carbon Tetrachloride

Carbon tetrachloride is a liquid of medium volatility: its boiling point is 77°C, and its vapor pressure at 21°C is 100 mm of Hg. Since the vapor density is high (ca. 5.4), air saturated with it at normal temperatures is about 60% heavier than clean air.

The present discussion is limited to inhalation toxicity. There is also a significant percutaneous hazard from contact with the liquid, and carbon tetrachloride in contact with flames or hot surfaces may form dangerous concentrations of phosgene. Ingestion of the liquid is highly dangerous.

Carbon tetrachloride used to be handled in many industrial and domestic applications which resulted in substantial and repeated inhalation exposures, and it was also used as an anesthetic (being similar to chloroform, though less effective). When it became apparent that chronic exposure, or even a heavy single exposure, might cause serious and lasting injury, a large number of toxicological studies were made. Carbon tetrachloride has been replaced by less toxic solvents for such operations as degreasing and dry cleaning, but the amount manufactured has not changed much because of its extensive use in fluorocarbon manufacture and other applications: U.S. production is about one billion pounds annually.

The literature on inhalation toxicology of carbon tetrachloride is mostly concerned with conditions different from those of the VM: long-term, low-level exposure or a succession of short-term, higher level exposures. In either case, the response is likely to be damage to the liver or kidney, serious and persisting for some time though rarely permanent. VM incidents are more likely to involve an entirely different toxic mechanism, brought on by exposure to higher concentrations and affecting the central nervous system. Initial symptoms include dizziness and sensory disturbance, which may be accompanied by nausea but are not necessarily a disagreeable experience; in fact, carbon tetrachloride has been voluntarily inhaled. Loss of consciousness follows rapidly in heavy concentrations and respiratory failure may occur.

For the purposes of the VM, three levels of response can be distinguished: harassment through sensory disturbance; incapacitation through partial or total loss of consciousness; and death from respiratory failure. Low concentrations would also elicit complaints from some of those exposed; others may find the odor not unpleasant and perhaps experience an agreeable light intoxication.

There is fortunately sufficient evidence from experimental exposure at low levels and from accidental exposures at dangerous levels to permit us to base our analysis entirely on figures for response in man. However, there is extreme variation in individual susceptibility, which

is considerably affected by such things as drinking habits. Consequently, there is considerable scatter between individual exposure-response estimates.

We found that the data did not fit well with Haber's Law but, following the lead of a 1949 paper, we were able to accommodate nearly all the available observations and estimates in a modified relationship, depending on both time and concentration but more heavily on the latter. This was for the immediate effects of sensory disturbance, unconsciousness, and death. We recognized that delayed or long-term injury or even delayed death might occur in some cases but could find no evidence on which to base a quantitative estimate. We did not feel that it was a serious deficiency to ignore these effects in the VM, because the circumstances of exposure would strongly favor short-term casualty effects over lasting injury.

The estimates that we made for carbon tetrachloride are shown in Table 5-3.

TABLE 5-3. EXPOSURE-RESPONSE RELATIONSHIP FOR CARBON TETRACHLORIDE

Response	Concentration, 10^3 mg m^{-3}			
	Time, min			
	5	15	30	60
Complaint, no risk	2.1	1.4	1.0	0.8
Harassment, LC_5 for susceptibles	9.5	6.3	4.5	3.6
Severe harassment, LC_{50} for susceptibles, LC_5 for normals	42	28	20	16
Lethal, LC_{100} for susceptibles, LC_{50} for normals	210	140	100	80

LC_5, LC_{50}, LC_{100} = concentration for 5%, 50%, 100% lethality.

Hydrogen Chloride

The anhydrous gas is transported as a liquid under about 40 atmospheres of pressure; the boiling point at one atmosphere is -85°C. On release into the air, the gas combines with water vapor to form a white cloud of hydrochloric acid droplets; if there is insufficient water vapor, some of the hydrogen chloride (HCl) will remain as anhydrous gas. In either state, the chemical is extremely aggressive because it dissolves in bodily moisture to form strongly acid conditions, reacting with and disturbing the normal alkalinity. The effects are highly irritant and destructive, and the anhydrous gas also has a dehydrating action which augments its aggressiveness. The main sites of attack are the eyes and the moist mucous surfaces of the upper respiratory tract.

The effect of increasing levels of concentration is quite well documented for human exposure. At about 5 parts per million, hydrogen chloride is disagreeable but indefinitely tolerable and not incapacitating. At about 25 ppm it begins to interfere with work, and at about 75 ppm the limit of endurance is being reached. Here there is a gap in the published data and estimates, which take up the story at concentrations of 1000 ppm and more which are dangerous to highly lethal. The hazard is caused by intense irritation, which may cause involuntary stopping of breathing, partially or completely.

Exposure-response estimates for this intense irritant in the VM followed the pattern established for ammonia, another intense irritant. At low concentrations we are concerned with thresholds of harassment, and the time of exposure is unimportant; what matters is the concentration level. At high concentrations, with partial or total cessation of respiration, time also is important and we are concerned with periods measured in minutes rather than hours.

Our estimates of the exposure-response relationship are shown in Table 5-4. We considered also the possibility of long-term or permanent injury but concluded that, although it might well occur, the casualties would be few in proportion to those immediately affected. Furthermore, there is no evidence to support quantitative estimates of persistent injury.

TABLE 5-4. EXPOSURE-RESPONSE RELATIONSHIP FOR HYDROGEN CHLORIDE

Concentration, mg m^{-3}	Time	Response	Deaths, %	
			General Population	High-Risk Population
< 5	any	Negligible	0	0
5-75	any	Complaint, no risk	0	0
75-200	~1 hr	Severe harassment (some risk)	0	25
200-700	< 0.5 hr	Severe harassment/risk	0	25
	0.5-1 hr	Lethal	3	50
	1-2 hr	Lethal	50	100
700-2000	< 0.5 hr	Lethal	3	50
	0.5-1 hr	Lethal	50	100
	1-2 hr	Lethal	97	100
> 2000	< 5 min	Lethal	3	50
	5-15 min	Lethal	50	100
	15-30 min	Lethal	97	100

Methyl Bromide

Methyl bromide is a gas, its boiling point being 4°C; it is shipped in liquid form under 1 atm of excess pressure. It is odorless except at high concentrations, when it has an inoffensive sweetish smell rather like chloroform. It is often described as highly toxic, but this is slightly misleading; for example, the Threshold Limit Value recommended by the American Conference of Governmental Industrial Hygienists for workroom exposure is 20 parts per million, which may be compared with 10 ppm for carbon tetrachloride and 0.1 ppm for phosgene. Methyl bromide is better described as highly *hazardous*, because it is insidious and can produce lasting injury.

Its toxic action has four characteristics that make it exceptionally hazardous:

- No warning; the slight odor and absence of immediate irritation make it possible to experience a fatal exposure without any awareness of exposure at all.
- Delayed action; symptoms are delayed for four to six hours, or even longer.

- Multiple organ targets; in addition to attacking the lungs and central nervous system, it may damage the kidneys and liver.
- Lasting injury; recovery is slow and there may be permanent injury.

The general approach to developing exposure-response estimates for the VM was quite clear. In the absence of immediate irritation or other symptoms, there was no need to consider immediate harassment or incapacitation. Furthermore, it was unlikely that the severity of effects would be proportional to the total intake of methyl bromide and hence to the dosage, with Haber's Law applying. This proved to be the case.

However, the data base was of limited usefulness for our purposes even though it was copious. There were some observations on volunteers at low concentrations. Occupational and accidental exposures with serious or fatal outcome were reported in fair number but had the usual limitation that concentrations and times were generally a matter of guesswork. There were many reports of experimental animal exposure, but they were mostly of single animals or small groups and not presented in a way to assist estimation of exposure-response relationships. One of the best studies is reported in terms of exposure for 100% survival or 100% death only, whereas partial response is more useful for developing response models.

Despite these limitations, we were able to arrive at response models for animals which were gratifyingly consistent, and we felt justified in applying them to an estimate of the 50% lethal dose in man to arrive at exposure-response relationships for lethality and incapacitation. Table 5-5 is based on these. The reader is referred to the detailed presentation in Appendix B and to the caution there as to the limitations of the data base and the analytical method.

TABLE 5-5. EXPOSURE-RESPONSE RELATIONSHIP FOR METHYL BROMIDE

Exposure	Response		Exposure	Response	
Ct,	Lethality		Ct,	Incapacitation	
10^3 mg min m^{-3}	Normal	Sensitive	10^3 mg min m^{-3}	Normal	Sensitive
740	100		340	100	
740-580	90		340-280	90	
580-430	50	100	280-200	50	100
430-340	10	50	200-160	10	50
340-280	0	25	160-130	0	25
280		10	130		10

Phosgene

Phosgene has a boiling point of 8°C and it is transported as a liquid, under less than 1 atm of excess pressure if at 21°C. The gas is much heavier than air (3.4 times) and this, together with the cooling which accompanies evaporation (latent heat, 59 cal g^{-1}), means that the cloud from a spill has a strong tendency to hug the ground.

Phosgene is highly toxic, being lethal at about 1/16 of the concentration required for chlorine, and it is much more insidious than chlorine because it is less irritating and has a delayed effect. A fatal dose can be inhaled without serious discomfort, and there are several cases on record where the victim, even under medical care, was released after first aid only to collapse and die within the next day or two. At concentrations which are in the dangerous zone for prolonged breathing, it passes through the upper respiratory tract with no more than some difficulty in breathing accompanied by slight lacrimation. Higher concentrations cause immediate incapacitating distress, but not to the point of involuntary cessation of respiration as with strong irritants such as hydrogen chloride. The gas which enters the lung is absorbed and reacts slowly with intensely irritant and destructive consequences. There is, therefore, no strong avoidance reflex to protect the victim and no immediate serious symptoms to warn that a hazardous dose has been taken. After some time, from 2 to 24 hours, pulmonary edema develops and the victim, as is often said, drowns in his own body fluid. If this does not occur, there is still a grave risk of pneumonia because the damaged lung tissue's defenses against invasive pathogens are seriously impaired.

Phosgene was introduced as a war gas in December 1915 and it became the preferred lethal agent, retaining this position for many years. It is also an industrial chemical of major importance. Consequently, there is a copious data base with much more thorough observations and estimates for man than we can find for most other substances. Our basis for analysis was the data for human response, and we used the extensive animal data only for estimating the slope of the exposure-response relationship in man.

We found that the evidence favored a two-zone analysis: (a) a harassment zone, primarily concentration-dependent, in which the immediate irritant effect of the gas on eyes and respiratory tract was dominant; and (b) a dangerous-to-lethal zone of more severe exposure, dosage-dependent, in which the delayed damage of lung tissue was dominant. Our estimates are presented in Tables 5-6a and 5-6b.

Long-term and permanent disability was a problem. There is no doubt that a survivor of severe incapacitation might require weeks or months for full recovery, and it is not unlikely that there would be some cases of permanent disability. There is no basis, however, for making quantitative estimates, and the situation is complicated by such factors as the similarity between impaired lung function from this and other causes.

TABLE 5-6a. EXPOSURE-RESPONSE RELATIONSHIP FOR PHOSGENE: HARASSMENT ZONE

Concentration, mg m^{-3}		Time	Response
Normal Population	High-Risk Population		
0-4	0-2	up to 1 hr	Negligible
4-10	2-5	few min to 1 hr	Complaint, but no serious risk
10-20	5-10	up to 15 min	Severe harassment: temporary incapacitation

TABLE 5-6b. EXPOSURE-RESPONSE RELATIONSHIP FOR PHOSGENE: DANGEROUS-TO-LETHAL ZONE

Exposure	Response, %			
Ct, mg min m^{-3}	Normal Population		High-Risk Population	
	Incapacitated	Dead	Incapacitated	Dead
800			15	
1150	15	--	50	--
1600	50	--	85	15
2200	85	15	50	50
3200	50	50	--	90-100
4400	--	90-100		

PROBIT EQUATIONS FOR LETHALITY

The lethality estimates were used to generate probit equations of the form

$$Pr = A + B \ln(Ct^N)$$

Probits are a convenient statistical measure, related to percentage effect, for entering estimates of the intensity of damage from various causes into the VM model. In this equation:

Pr = probit (measure of percent lethality to exposed population)
A = the intercept
B = the slope
C = concentration (in ppm)
t = time (in minutes)
N = best fit power of t
ℓn = natural logarithm

The data, the resulting probit equations, and the correlation coefficients (r, used as a measure of goodness of fit) are presented here. It is to be noted that the estimated power is $N = 1$ for all but carbon tetrachloride, for which $N = 1/2$. Methane and propane are not included since they would require exposures larger than the maximum anticipated in any VM spill to cause lethality.

ACROLEIN		
Concentration (ppm)	Time (minutes)	% Lethality
14.76	45	3
14.76	90	50
42.18	45	50
42.18	90	97
126.53	5	3
126.53	10	50
126.53	22.5	97
Probit = $-9.9315 + 2.0488\ \ell n(Ct)$		
$r = .97$		

CARBON TETRACHLORIDE		
Concentration (ppm)	Time (minutes)	% Lethality
6.46	5	5
4.30	15	5
3.07	30	5
2.46	60	5
32.28	5	50
21.52	15	50
15.37	30	50
12.30	60	50
Probit = $.5443 + 1.0055\ \ell n(Ct^{1/2})$		
$r = .99$		

HYDROGEN CHLORIDE		
Concentration (ppm)	Time (minutes)	% Lethality
1621.30	2.5	3
1621.30	10	50
1621.30	22.5	97
875.50	15	3
875.50	45	50
875.50	90	97
291.83	45	3
291.83	90	50
Probit = $-21.7631 + 2.6518\ \ell n(Ct)$		
$r = .96$		

2500 mg/m^3 (1621.3 ppm) was assumed to be a midpoint for concentrations labeled in the original data as >2000 mg/m^3 (1297.0 ppm).

METHYL BROMIDE		
Concentration (ppm)	Time (minutes)	% Lethality
184.3	1	99
164.4	1	90
125.8	1	50
98.4	1	10
77.2	1	1
Probit = -19.9241 + 5.1565 ℓn(Ct) r = .99		

Since only Ct values are given and since Haber's Law applies, t is arbitrarily chosen as equal to 1.

PHOSGENE		
Concentration (ppm)	Time (minutes)	% Lethality
525.91	1	15
764.96	1	50
1051.82	1	95
Probit = -19.2736 + 3.6861 ℓn(Ct) r = .98		

Since only Ct values are given and since Haber's Law applies, t is arbitrarily chosen as equal to 1.

DISCUSSION

Our evaluation of exposure-response relationships is guided in each case by the kind of mechanisms involved: an immediate irritant effect, a delayed toxic effect, and so forth. When we look over all the substances evaluated in this and the previous report [1], it becomes clear that we have covered the whole range of response categories that the VM is likely to deal with and that the picture is already filled in at all important levels. In addition to the nontoxic effect of a simple asphyxiant, we have two basic kinds of toxic action: immediate irritation and a delayed toxic action (irritant or otherwise). And we have seen that the immediate irritant must be analyzed with concentration primarily in mind and time of exposure important only in the more severe conditions, whereas the delayed toxic action is primarily dosage-dependent--that is, dependent on the product of concentration and time. This way of viewing the inhalation toxicology can be demonstrated by setting out the substances we have evaluated against a graded series of descriptive categories.

Category		*Substance*
Highly irritant	-	Ammonia and hydrogen chloride
Highly irritant, toxic	-	Acrolein
Irritant, toxic	-	Chlorine
Somewhat irritant, toxic	-	Phosgene
Slightly irritant, toxic	-	Carbon tetrachloride
Nonirritant, toxic	-	Methyl bromide
Nonirritant, slightly toxic	-	Propane
Nonirritant, nontoxic	-	Methane

It will be appreciated that there is simplification here which might not be appropriate in an exact and detailed toxicological analysis. But for our strictly practical purposes in the VM, which is workable only if we adopt reasonable approximations and simplifications, this categorization is acceptable. It is useful because it presents the range of response categories in an orderly fashion and explains the need for different approaches to the exposure-response relationships. It also presents an orderly series of increasing likelihood of long-term or permanent injury (apart from the asphyxiating gases, methane and propane). This is due in part to the decreasing intensity of immediate irritation: it is practically impossible to inhale enough ammonia or hydrogen chloride to cause the severe deep-lung damage which would otherwise be possible. (Anhydrous HCl vapor can cause severe skin burns, killing the cells.) Acrolein is a similar but less extreme case: in addition to its conspicuous irritancy, there is clear evidence in animals of its ability to cause delayed deaths through lung damage, lung penetration perhaps being aided by less violent immediate irritation than in man. At the other end of the series, it is easily possible to inhale a dangerous or fatal dose without undue discomfort or even, in the case of methyl bromide, in ignorance of exposure. This is not the whole of the story, because differences in site of attack and biochemical mechanism are also involved. But it is an acceptable aid in clarifying and systematizing the broad picture.

It also suggests a possibly helpful line of thought for future work. Evaluation of new toxic substances and presentation of exposure-response estimates would evidently be assisted if each case could be fitted into one or another of a few standardized response models. It would simplify the initial decision as to which line of approach to take, and it would immediately define what kinds of data would be most useful. For example, a highly irritant substance with possible delayed toxic action (such as acrolein) calls first for data on levels of irritation and threshold of respiratory spasm and only secondarily on delayed effects. In contrast, a substance like methyl bromide, with no immediate irritation but severe delayed effects, calls exclusively for dosage-response data. Analysis in this way on standardized lines would be simplified by focusing on the best numerical constants to fit into a preselected model. The set of models might be reducible to four:

Irritant
Irritant, toxic
Nonirritant, toxic
Nonirritant, nontoxic

Chapter 6

TOXIC HAZARDS FROM COMBUSTION PRODUCTS

In the circumstances to which the Vulnerability Model (VM) applies, fires and explosions could lead to toxic hazards from the products of combustion or from the effects of heat on chemicals present. Serious oxygen depletion can be ignored: in the open it is possible only inside a fire storm, and even in closed spaces it is unusual because oxygen depletion usually interferes with combustion before it impairs human activity. The main products of combustion are carbon dioxide and carbon monoxide. Carbon dioxide begins to have noticeable effect at about 2% by volume, increasing the depth of respiration, but at least 10% can be inhaled without harm and, in fact, this concentration is used therapeutically. It can therefore be neglected as a toxic agent. The next most abundant combustion product, carbon monoxide, would appear to be a more likely toxic hazard because it has significant physiological effects at concentrations of about 0.1%. If later theoretical analysis or actual field observation should indicate the probability of hazardous concentrations, we already have exposure-response relationships for three of the most common toxic products: acrolein, hydrogen chloride, and phosgene (see Appendix B).

It did not seem probable that dangerous concentrations of any toxic combustion product would develop at ground level, downwind of a fire involving the expected range of size and combustible cargoes of VM incidents. The main reason for this immediate feeling was that the intense convection associated with a large fire usually raises the cloud of combustion products well above the surface and promotes mixing with the surrounding air. However, this conclusion required confirmation by more rigorous treatment. This is given in the following analysis of maximum ground-level concentrations to be expected, which is applicable to carbon monoxide or other combustion products. The next section of this chapter is a discussion of the toxicology of carbon monoxide, focusing on the conditions of a VM incident. Finally, we summarize our conclusions. It will be seen that the development of dangerous concentrations at ground level is an improbable event requiring the coincidence of exceptionally unfavorable meteorological conditions.

MAXIMUM GROUND-LEVEL CONCENTRATIONS UNDER VARIOUS METEOROLOGICAL CONDITIONS

The calculation of concentrations downwind of a burning pool takes into account the same factors that apply to evaporation from a pool: emission rates, windspeed, and atmospheric stability. It must also consider another factor which can very greatly reduce ground-level concentrations. This is thermal buoyancy, which raises the combustion cloud above the surface and induces turbulent mixing with the atmosphere. Figure 6-1 shows a typical plume in place and in elevation. It will be seen that the cloud can be imagined as originating above the surface and upwind of the real source. The cloud first touches ground downwind of the source, and maximum ground-level concentration occurs still further downwind. This shows clearly why the ground-level concentrations are likely to be much less than those from an emission originating at the surface and diffusing upwards without the assistance of strong thermal buoyancy. The following analysis investigates these effects quantitatively.

Buoyancy Flux

The buoyancy of a hot plume is derived from the difference of density between the plume and the ambient air. Years of observation on the rises of stack plumes and cooling tower vapor plumes and studies on the thermodynamics of cloud behaviors including cumulus clouds [36-43] reveal that the buoyancy potential of a smoke plume can be represented by its buoyancy flux, F, as follows.

---

[36] Briggs, G. A., I. Van der Hoven, R. J. Engelmann, and J. Haltsky, Processes other than natural turbulence affecting effluent concentrations, ch. 5, in D. H. Slade (ed.), *Meteorology and Atomic Energy 1968*, U.S. Atomic Energy Commission, July 1968.

[37] Briggs, G. A., Plume rise: a recent critical review, consequences of effluent release, *Nucl. Saf. 12*(1):15-24, January-February 1971.

[38] Briggs, G. A., Some recent analyses of plume rise observations, ME 8E, pp. 1029-1032, in *1971 Proceedings of the 2nd International Clean Air Congress*, 1971.

[39] Carpenter, S. B., J. M. Leavitt, F. W. Thomas, J. A. Frizzola, and M. E. Smith, Full scale study of plume rise at large coal-fired electric generating stations, *J. Air Pollut. Control Assoc. 18*(7): 458-465, July 1968.

[40] Slawson, P. R., and G. To Csanady, The effect of atmospheric conditions on plume rise, *J. Fluid Mech. 47*(part 1):33-49, 1971.

[41] Montgomery, T. L., S. B. Carpenter, W. C. Colbaugh, and F. W. Thomas, Results of recent TVA investigations of plume rise, *J. Air Pollut. Control Assoc. 22*(10):779-784, October 1972.

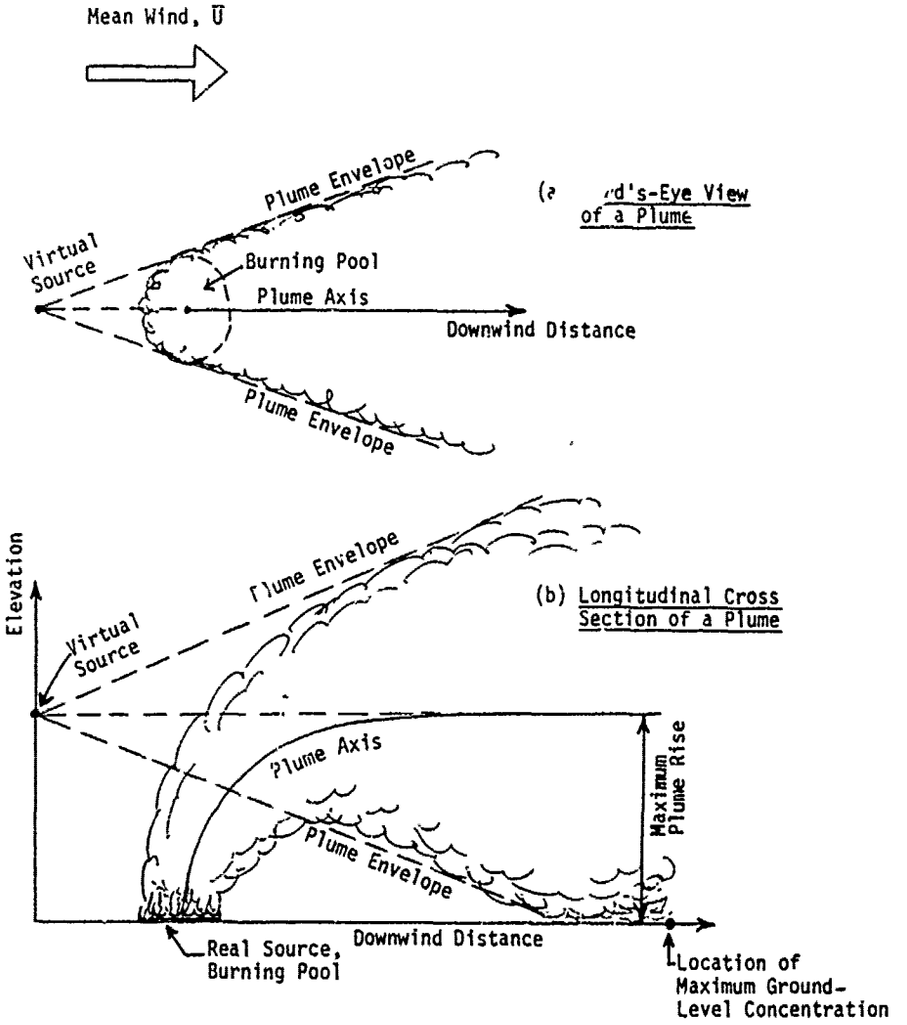

FIGURE 6-1. Typical Plume

[42] Fay, J. A., M. Escudier, and D. P. Hoult, A correlation of field observations of plume rise, *J. Air Pollut. Control Assoc. 20*(6): 391-397, June 1970.

[43] Fay, J. A., D. P. Hoult, and T. Hewett. Laboratory experiments on the motion of a buoyant plume in a stratified flow, ME 8C, pp. 1018-1021, in *1971 Proceedings of the 2nd International Clean Air Congress*, 1971.

$$F = \frac{gQ_H}{\pi c_p \rho_a T} \tag{6-1}$$

where

F = buoyancy flux (m^4/sec^3)

g = gravitational acceleration, 9.8 m/sec^2

Q_H = upward heat emission rate of plume (cal/sec)

c_p = specific heat of air at constant pressure, approximately 0.238 cal/g °K in normal conditions

ρ_a = density of air, approximately 1.18×10^3 g/m^3 in normal conditions

T = ambient temperature in degree Kelvin (°K)

At 25°C and one atmosphere of pressure, equation (6-1) can be approximated by the following equation.

$$F(m^4/sec^3) = 3.73 \times 10^{-5} Q_H(cal/sec) \tag{6-2}$$

The vertical heat emission rate, Q_H, of a smoke plume can be estimated by subtracting heat loss due to radiation from total heat emission rate due to combustion. It must be noted that, as the plume column or pool size increases, the surface area per volume of plume column decreases; therefore the heat loss due to radiation expressed in terms of total heat generation becomes smaller. For very large fires, most of the heat of combustion is convected vertically upward. A conservative estimate of concentrations of combustion products is obtained by assuming all the energy of combustion is convected upward. Neglecting heat loss due to surface radiation, the vertical heat emission rate, Q_H, can be estimated by the following equation.

$$Q_H = f \cdot A_p r_b \rho_c \cdot H_c \tag{6-3}$$

or $[Q_H = f \cdot \pi(R_p)^2 r_b \cdot \rho_c \cdot H_c]$ if the pool of fuel approximates a circle,

where

f = fractional degree of complete combustion

A_p = area of the pool of fuel (m^2)

r_b = burning rate of the fuel or cargo (m/sec)

ρ_c = density of the fuel or cargo (g/m^3)

H_c = unit heat liberated upon complete combustion of the fuel (cal/g)

R_p = radius of the pool (m)

The typical unit heat liberated upon complete combustion of hydrocarbons including petrochemical products averages approximately 11.2×10^3 calories per gram. Based on a burning rate of 1.67×10^{-4} m/sec or 10 mm/min and 90% complete combustion, the heat emission rate ranges from 1.3×10^8 to 1.3×10^{10} calories per second for pool diameters of 10 and 100 meters, respectively. The corresponding buoyancy fluxes are 5×10^3 and 5×10^5 m^4/sec^3, respectively, as indicated by equation (6-2).

Atmospheric Stability and Dispersion

Pool burning can be regarded as a pollution source of local scale, unless the size of the pool becomes large enough to generate a fire storm which significantly alters the atmospheric structure and stability so that the dispersion pattern of the smoke plume is primarily governed by the induced windstorm. Therefore, discussion of atmospheric structure is limited here to the ground layer of 2000 meters or so. The atmospheric structure can be interpreted in terms of atmospheric stability and mixing height. In this section, only atmospheric stability is examined and followed by a discussion of atmospheric dispersion or diffusion.

The classification of atmospheric stability has been thoroughly dealt with in the previous Final Report [1]. However, to obtain more accurate estimates of maximum plume rise and ground-level concentration, stable atmospheric conditions are further divided into six classes: neutral, slightly stable, stable, isothermal, moderate inversion, and strong inversion, in increasing order of stability. Generally, the stability of an atmosphere correlates with its vertical temperature or, more precisely, with the gradient of potential temperature as shown in Table 6-1.

Atmospheres more stable than neutral dampen the upward movement of a plume and thus discourage plume rise. Unstable atmospheres possess greater mixing ability, which quickly dissipates the buoyancy potential of a hot plume and tends to limit plume rise. Therefore, neutral atmosphere gives the highest plume rise for a given size of pool burning. In general, a higher emission height or plume rise results in a lower maximum ground-level concentration, provided the buoyancy flux and the emission strength of the burning pool are constant.

To accommodate the effects of plume rise on predictions of downwind concentrations, the conventional Gaussian model is modified as follows [Slade, 44].

---

[44] Slade, D. H. (ed.), *Meteorology and Atomic Energy 1968*, U.S. Atomic Energy Commission, July 1968.

TABLE 6-1. POTENTIAL TEMPERATURE GRADIENT FOR VARIOUS ATMOSPHERIC STABILITY CLASSES (Carpenter et al. [45])

Atmospheric Stability Class	Potential Temperature Gradient, $\partial\theta/\partial z$ (°K/m)
Neutral	0
Slightly Stable	0.0027
Stable	0.0064
Isothermal	0.01
Moderate Inversion	0.0136
Strong Inversion	0.0173

$$\overline{C}(x,y,z) = \frac{10^6 Q}{2\pi\sigma_y\sigma_z\overline{U}} \left\{exp\left[\frac{-y^2}{2\sigma_y{}^2}\right]\right\}\left\{exp\left[-\frac{(z-h_e)^2}{2\sigma_z{}^2}\right] + exp\left[-\frac{(z+h_e)^2}{2\sigma_z{}^2}\right]\right\} \tag{6-4}$$

where

$\overline{C}$ = time-averaged concentration in a plume (ppm) at a given time and spatial point (x,y,z)

Q = volumetric emission rate of the pool (m^3/sec)

(x,y,z) = the x-, y-, and z-axes, respectively, of the Cartesian coordinate with the positive direction of the x-axis pointing directly downwind and origin at the center of the pool

σ_y, σ_z = standard deviations of plume width (meters) in the crosswind (y) and vertical (z) directions, respectively

h_e = plume rise or effective emission height (m)

By equating y and z to zero in equation (6-4), one obtains an expression for ground-level concentration directly downwind.

$$\overline{C}(x,y=0,z=0) = \frac{10^6 Q}{\pi\sigma_y\sigma_z\overline{U}} \; exp\left[-\frac{h_e{}^2}{2\sigma_z{}^2}\right] \tag{6-5}$$

---

[45] Carpenter, S. B., T. L. Montgomery, J. M. Leavitt, W. C. Colbraugh, and F. W. Thomas, Principal plume dispersion models: TVA power plants, *J. Air Pollut. Control Assoc.* *21*(8):491-495, August 1971.

The σ_y and σ_z are parameters indicating the degree of dispersion or expansion of a plume in crosswind and vertical directions, respectively. σ_y and σ_z values are downwind-distance-dependent and assume power functions generalized as follows.

$$\sigma_y = bx^q \tag{6-6}$$

$$\sigma_z = ax^p \tag{6-7}$$

where a, b, p, and q are constants which vary with stability classes.

For various ranges of downwind distances and atmospheric stability classes, the values of a, b, p, and q are summarized in Table 6-2 [45]. The influence of man's activities such as climatological modification by urbanization and natural terrain on σ_y and σ_z values has been discussed in Chapter 3 of the prior VM report [1].

TABLE 6-2. CONSTANTS a, b, p, *AND* q *IN THE EQUATIONS OF* σ_y *AND* σ_z *(calculated from [45])*

Stability Class	Range of Downwind Distances, x (m)	Constants			
		a	*b*	*p*	*q*
Neutral	$10^2 - 10^3$	7.667	8.681	0.477	0.459
	$10^3 - 10^5$	0.411	0.374	0.744	0.761
Slightly Stable	$10^2 - 10^3$	7.20	8.597	0.398	0.446
	$10^3 - 10^5$	1.423	0.553	0.5	0.692
Stable	$10^2 - 10^3$	9.031	8.397	0.275	0.438
	$10^3 - 10^5$	5.462	0.916	0.256	0.610
Isothermal	$10^2 - 10^3$	9.846	8.20	0.211	0.428
	$10^3 - 10^5$	5.307	0.747	0.230	0.603
Moderate Inversion	$10^2 - 10^3$	9.610	7.875	0.208	0.426
	$10^3 - 10^5$	7.457	1.526	0.175	0.519
Inversion	$10^2 - 10^3$	9.375	7.547	0.204	0.423
	$10^3 - 10^5$	8.758	1.914	0.146	0.478

After examination of the diffusion equation and its prominent features, it is desirable to derive a set of equations which yields the maximum ground-level concentration, C_{max}, and the corresponding downwind distance, x_{max}. This is done by equating the differentiated form of

equation (6-4) to zero and solving for x with the aid of equations (6-6) and (6-7) as follows:

$$x_{max} = \left[\frac{p}{p+q} \cdot \frac{h_e^2}{a^2}\right]^{1/2p} \tag{6-8}$$

and

$$C_{max}(x=x_{max}, y=0, z=0) = \frac{10^6\ Q(e^{-k})}{\pi ab(k^{-k})(h_e^2/2a^2)^k} \tag{6-9}$$

where

$$k = \frac{p+q}{2p}$$

Plume Rise or Effective Emission Height

There are a number of plume rise equations, primarily empirical or semiempirical [36-43]. A critical review of plume rise equations by Briggs [37] generalized a set of equations which describes the behavior of a plume rise rather closely under either stable or neutral atmospheric conditions. They are presented as follows.

(A) Buoyant plume in stable air (stability-limited)

(a) $$h_e = (2.3 \sim 2.9)\left(\frac{F}{\overline{U}S}\right)^{1/3} \tag{6-10}$$

where, under normal conditions,

$$S = \frac{g}{T}\left(\frac{\partial\theta}{\partial z}\right) \approx 0.0329\ \frac{\partial\theta}{\partial z}\left(\frac{^\circ K}{m}\right) \tag{6-11}$$

(b) In very light winds ($\overline{U} \leqslant 1$ meter per second),

$$h_e = 5.0\ F^{1/4}\ S^{-3/8} \tag{6-12}$$

where

h_e = plume rise (m)

F = buoyancy flow (m^4/sec^3)

$\overline{U}$ = mean windspeed (m/sec)

S = buoyant restoring acceleration (sec^{-2}) per unit vertical displacement as given in equation (6-11)

$\frac{\partial\theta}{\partial z}$ = potential temperature gradient of the atmosphere (°K/m)

(R) Buoyant plume in neutral air

$$h_e = 1.6 \frac{F^{1/3} x^{2/3}}{\overline{U}} \qquad \text{when } x < 3.5\ x^*$$

or

$$h_e = 1.6 \frac{F^{1/3} (3.5\ x^*)^{2/3}}{\overline{U}} \qquad \text{when } x > 3.5\ x^* \qquad (6\text{-}13)$$

where

$$x^* = (14 \text{ meters})\{F(m^4/sec^3)\}^{5/8} \qquad \text{when } F < 55(m^4/sec^3)$$

or

$$x^* = (34 \text{ meters})\{F(m^4/sec^3)\}^{2/5} \qquad \text{when } F > 55(m^4/sec^3) \qquad (6\text{-}14)$$

From equations (6-10) and (6-13), one sees that plume rise depends on windspeed, buoyancy flux, and atmospheric stability, of which the last is explicitly addressed in the parameter S.

In neutral atmosphere, the plume rises as the two-thirds power of downwind distance (known as the two-thirds power law) and approaches its maximum height as determined by equations (6-13) and (6-14). Plume rises as a function of downwind distance in neutral atmosphere are presented graphically in Figures 6-2, 6-3, 6-4, and 6-5 for buoyancy fluxes of 500, 5,000, 50,000, and 500,000 m^4/sec^3, respectively. In these figures, four cases with different mean windspeeds are given.

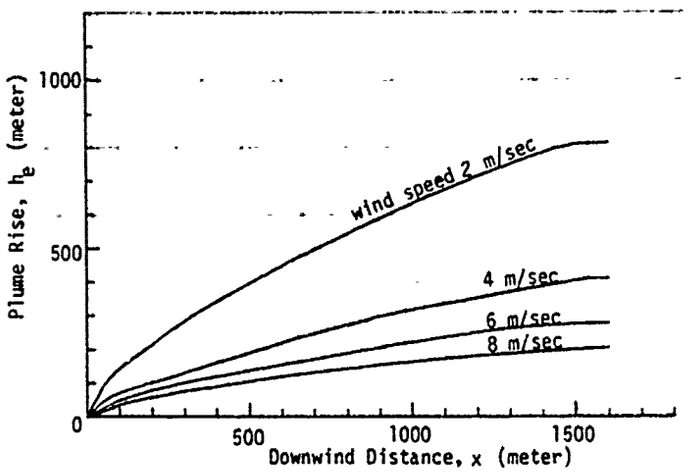

FIGURE 6-2. Plume Rise in Neutral Atmosphere for Buoyancy Flux = 500 m^4/sec^3

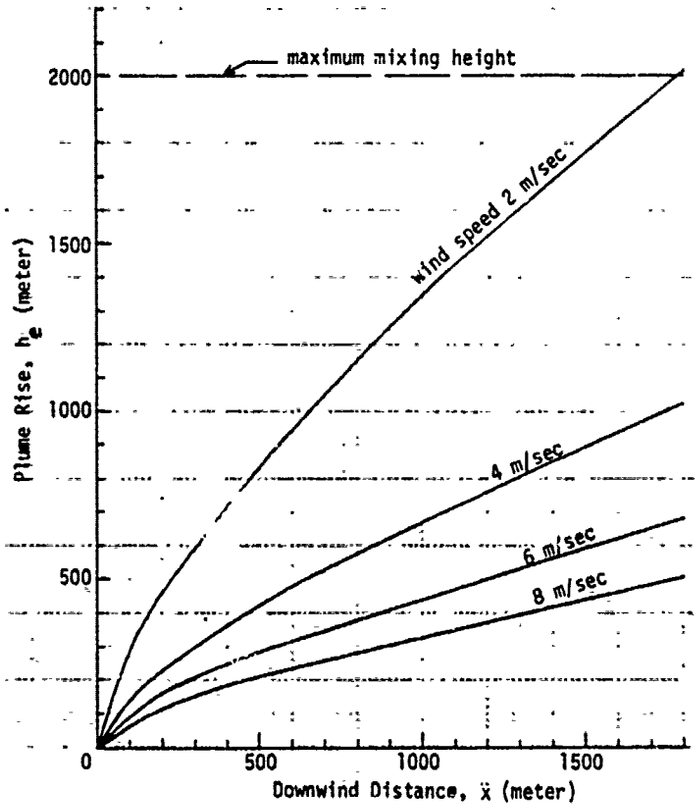

FIGURE 6-3. Plume Rise in Neutral Atmosphere for Buoyancy Flux = 5,000 m^4/sec^3

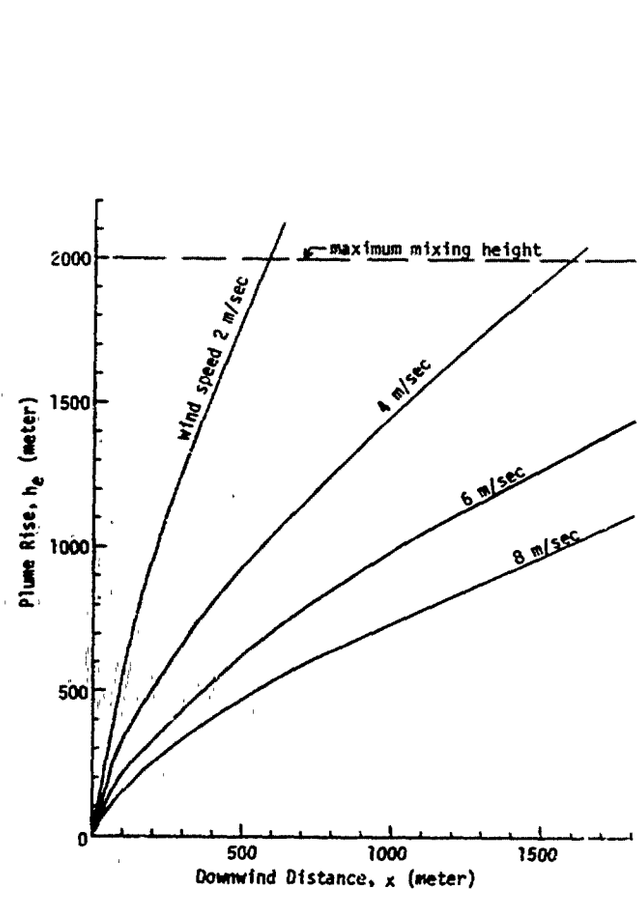

FIGURE 6-4. Plume Rise in Neutral Atmosphere for Buoyancy Flux = 50,000 m^4/sec^3

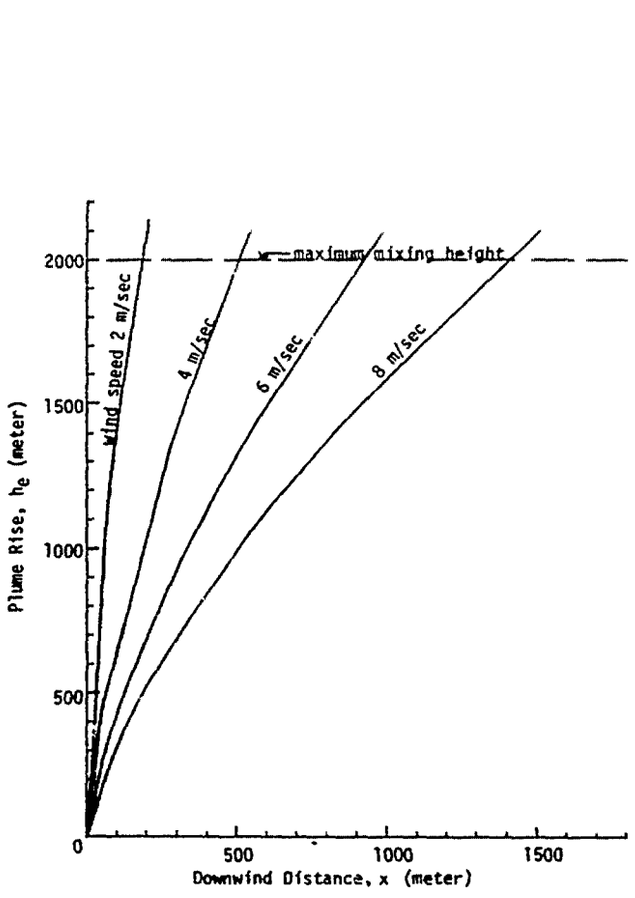

FIGURE 6-5. Plume Rise in Neutral Atmosphere for Buoyancy Flux = 500,000 m^4/sec^3

As noted, the ultimate plume rise in stable air can be calculated from equations (6-10) and (6-12). Maximum plume rises as a function of buoyancy flux and windspeed are presented in Figures 6-6, 6-7, 6-8, 6-9, and 6-10 for slightly stable, stable, and isothermal atmospheres, and atmospheres with moderate and strong inversions, respectively. Only the range of windspeeds which is probable in the given stability category is given in these figures. For a given buoyancy flux, the maximum plume rise decreases with decreasing atmospheric stability and with increasing windspeed.

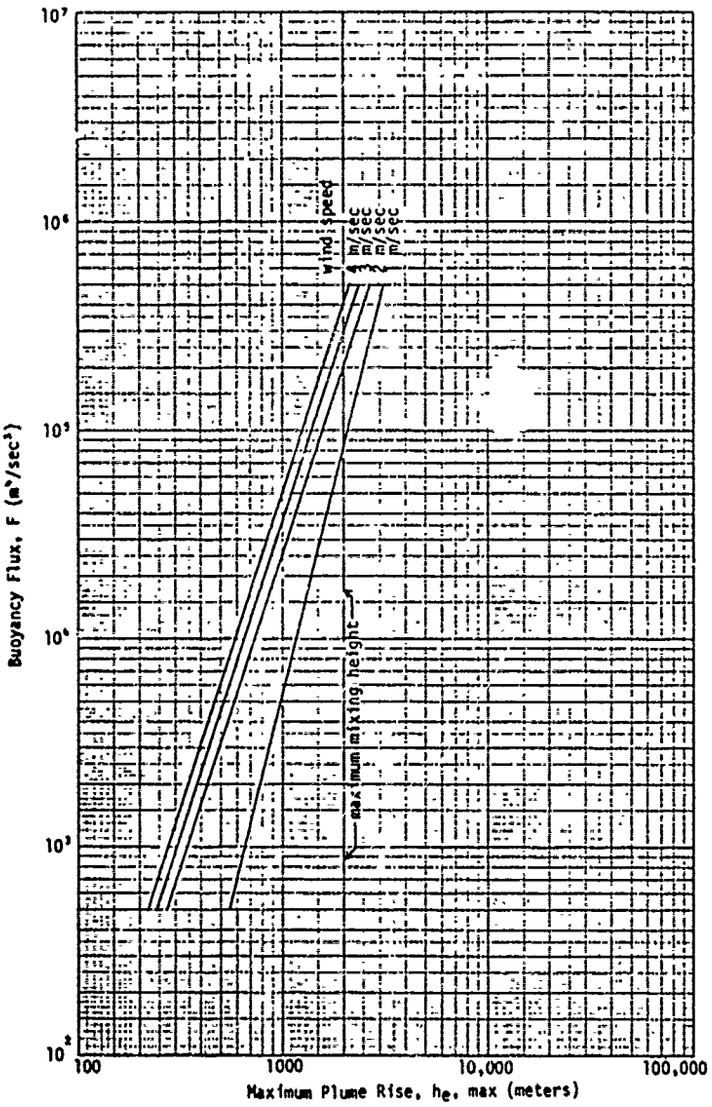

FIGURE 6-6. Maximum Plume Rise vs. Buoyancy Flux in Stable Atmosphere ($\partial\theta/\partial z$ = 0.0064 °K/m)

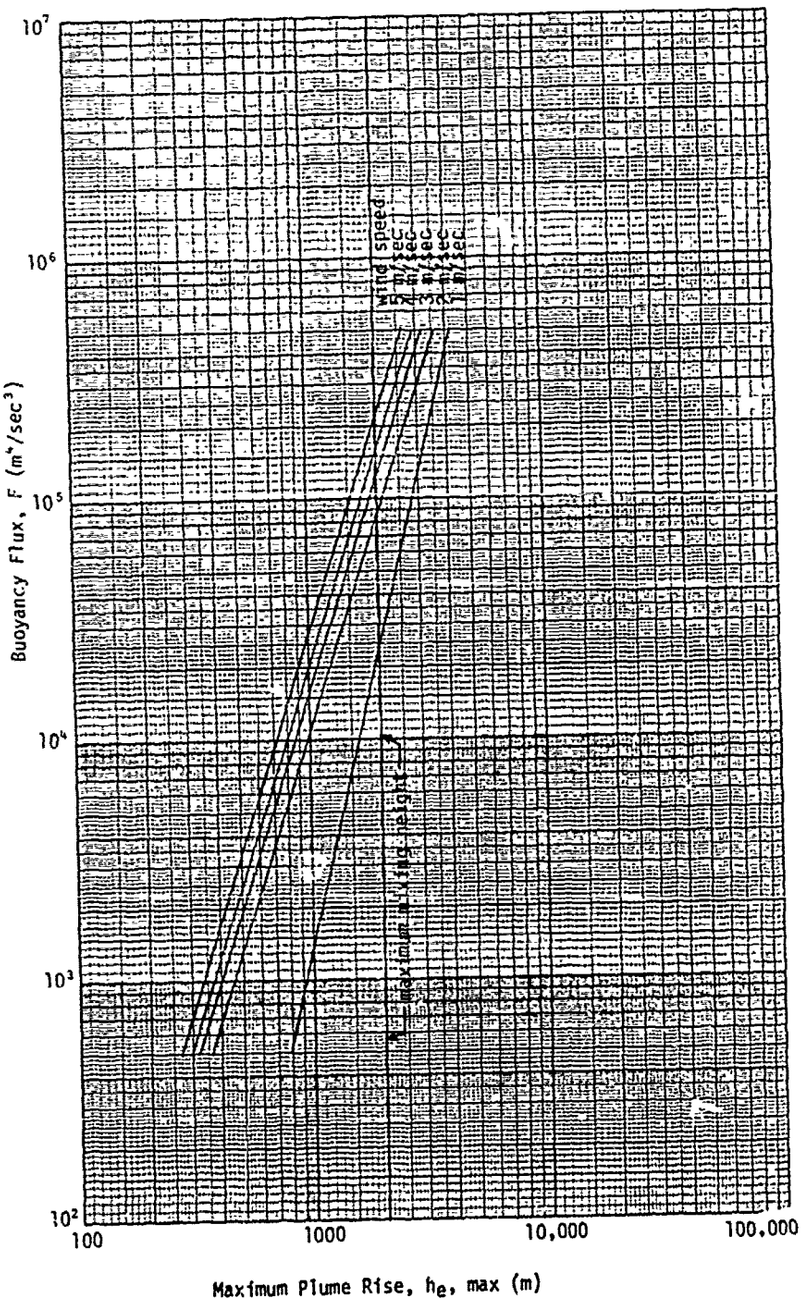

FIGURE 6-7. Maximum Plume Rise vs. Buoyancy Flux in Slightly Stable Atmosphere ($\partial\theta/\partial z$ = 0.0027 °K/m)

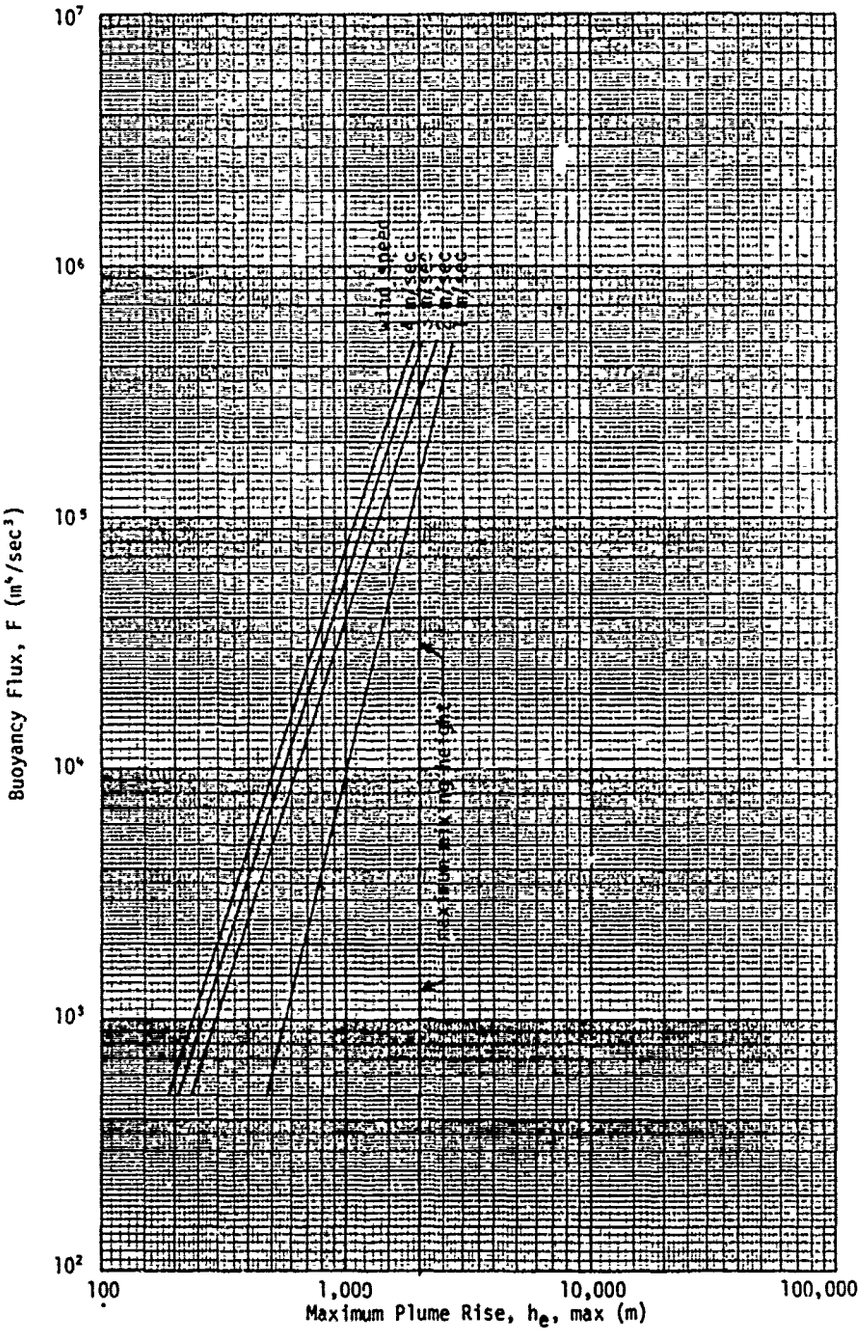

FIGURE 6-8. Maximum Plume Rise vs. Buoyancy Flux in Isothermal Atmosphere ($\partial\theta/\partial z$ = 0.01 °K/m)

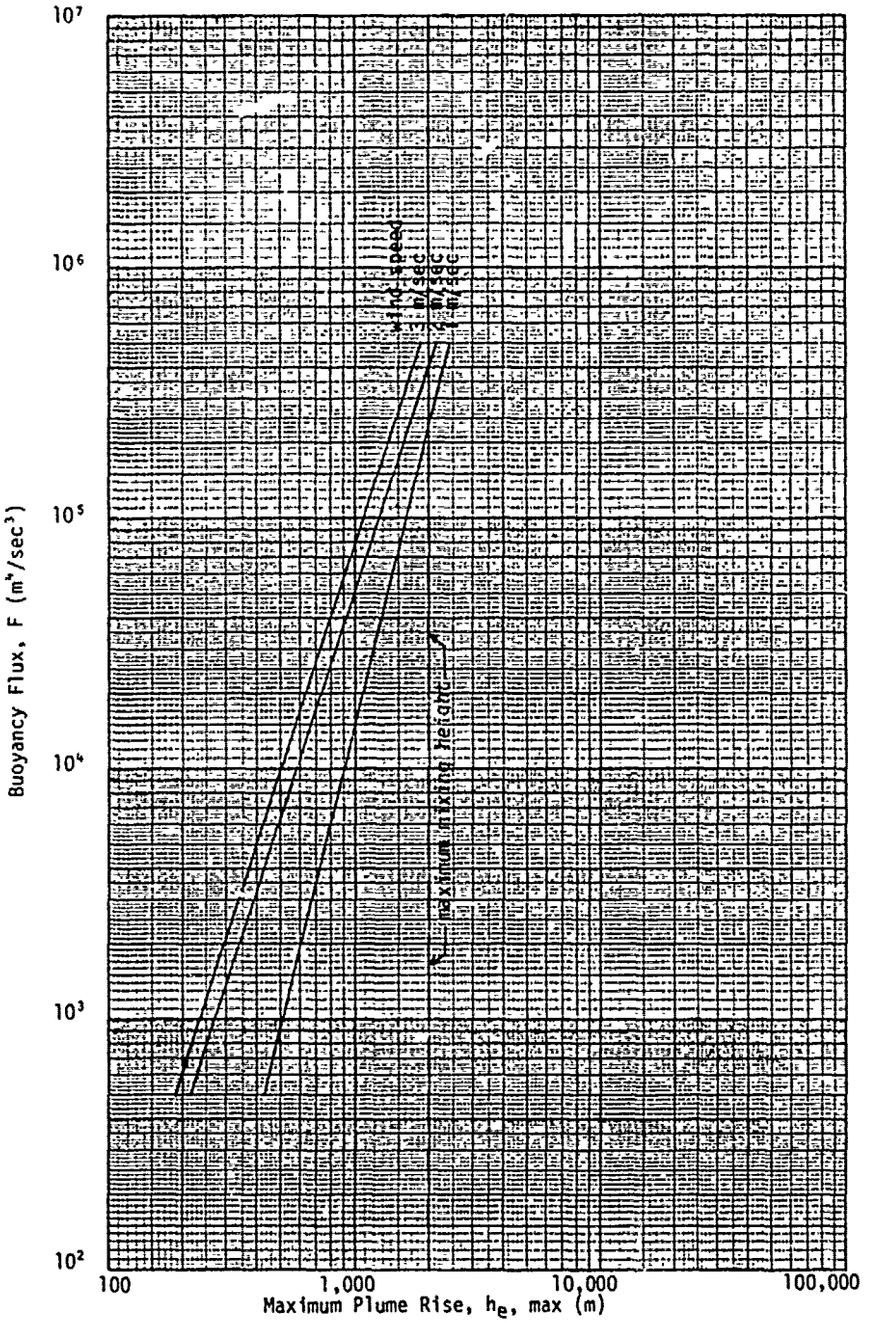

FIGURE 6-9. Maximum Plume Rise vs. Buoyancy Flux in an Atmosphere with Moderate Inversion ($\partial\theta/\partial z$ = 0.0136 °K/m)

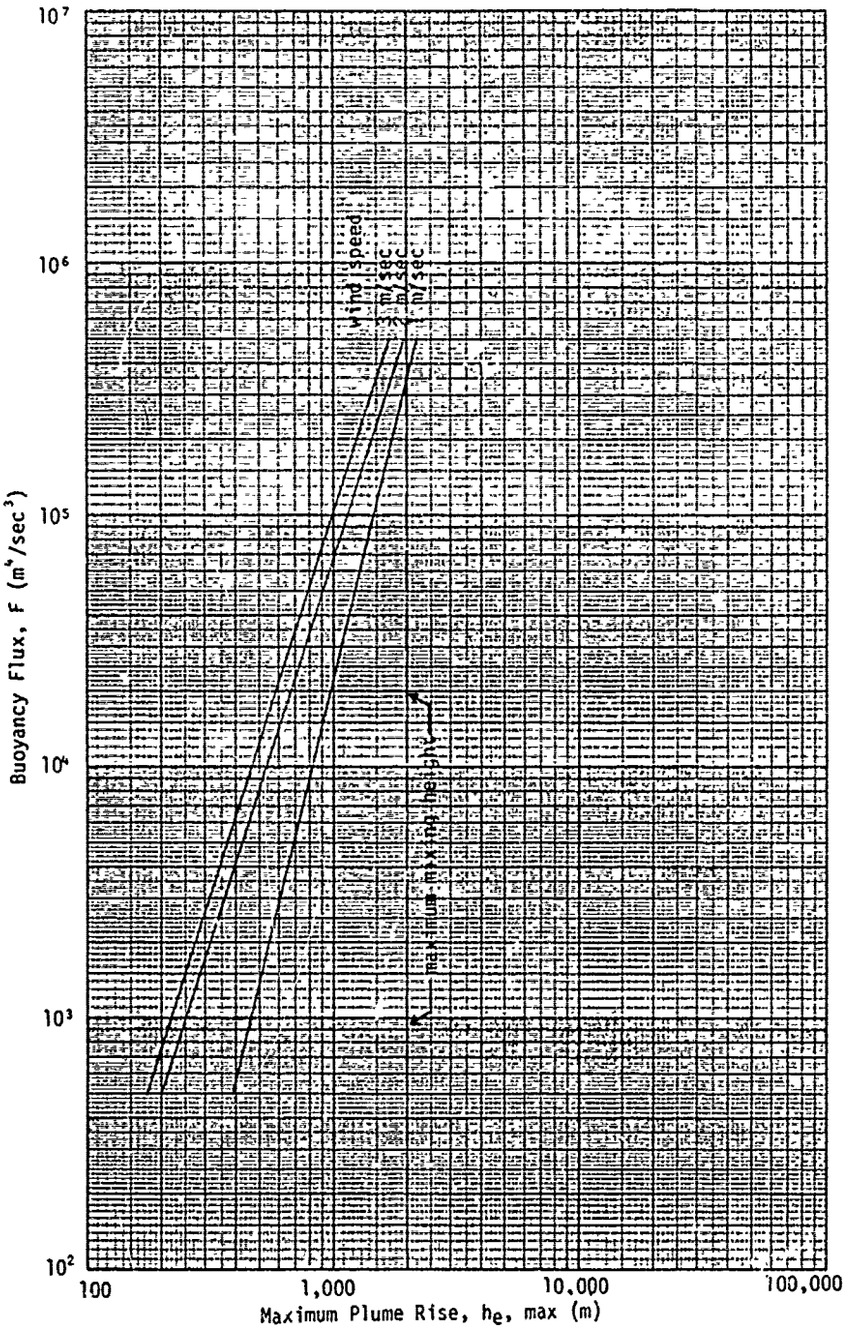

FIGURE 6-10. Maximum Plume Rise vs. Buoyancy Flux in an Atmosphere with Strong Inversion ($\partial\theta/\partial z$ = 0.0173 °K/m)

Atmospheric Structure and Ceiling Height

An atmosphere does not usually have a uniform vertical temperature profile, but rather consists of layers of air with different stabilities. An inversion layer or a strong stable layer aloft can limit the exchange of physical quantities such as humidity, thermal energies, or mechanical turbulence between the upper and lower atmospheres which sandwich the lofting inversion layer. The elevation of the base of a lofting inversion determines the volume of air available for mixing of contaminants from pool burning. The lofting inversion acts like a lid or ceiling, so to speak, which limits the degree of mixing in the ground-level atmosphere. Generally speaking, ceiling height or mixing height ranges from several hundred meters to 2,000 meters or so. However, nocturnal or nighttime radiational loss of heat from the land surface can induce a surface-based inversion of the radiational type. In this case, the mixing height is literally zero. Inversion caused by subsidence of air mass in a high-pressure system usually is more pronounced and stronger than radiational inversion. The base of a subsidence inversion can be as low as 500 meters or less above the ground. The occurrence of a low ceiling equivalent to a mixing height of 500 meters or less is quite frequent, especially along the West Coast, such as in California in the morning of the autumn season. Subsidence inversion can last several days (Hosler [46], Holzworth [47]).

Based on the preceding discussion, the predicted plume rise beyond a thousand meters above the ground surface, or several hundred meters during low-ceiling periods, may not be realistic because the plume rise formula fails to account for situations having shallow mixing height. Under this condition, if the plume has enough thermal energy, it may erode away or penetrate the lofting inversion layer and vent into the upper atmosphere, as shown in Figure 6-11. If the mixing layer is rather deep, so that the plume loses much of its buoyancy before reaching the inversion base, the plume cannot penetrate the inversion layer and may remain lofting close to the inversion base, as shown in Figure 6-12. The plume dispersion is then primarily in the crosswind direction until the positive buoyancy is dissipated at a certain downwind distance, where vertical dispersion downwind begins to equal the magnitude of the crosswind dispersion. In the preceding two cases, the plume never touches ground or reaches ground at considerable downwind distance so that the plume becomes significantly diluted and high concentration at ground level is expected never to occur.

---

[46] Hosler, C. R., Low-level inversion frequency in the contiguous United States, *Mon. Weather Rev. 89*:319-339, September 1961.

[47] Holzworth, G. C., *Mixing Heights, Wind Speeds, and Potential for Urban Air Pollution Throughout the Contiguous United States,* Environmental Protection Agency, Office of Air Programs, Research Triangle Park, N.C., January 1972.

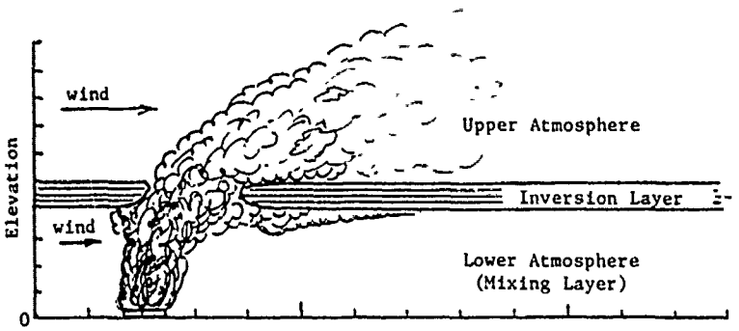

FIGURE 6-11. Complete Erosion of Inversion Layer by the Plume

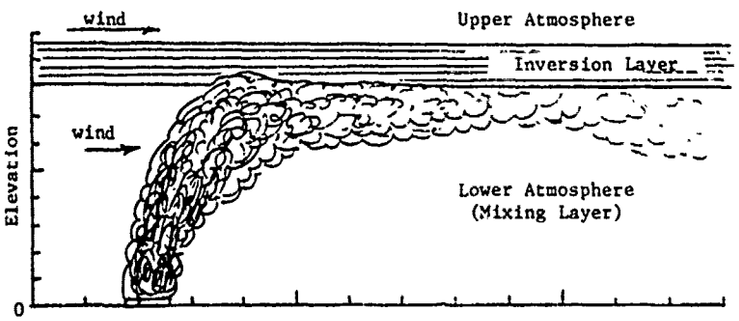

FIGURE 6-12. Partial Erosion of Inversion Layer by the Plume

In the third case, which involves shallow mixing height and a plume of low-buoyancy potential, the plume may become trapped and mixed in the shallow lower atmosphere, as shown in Figure 6-13. Only the less pronounced dilution capacity in the crosswind direction remains to disperse the plume. The resultant ground-level concentration can be very high and persist for a long period. This phenomenon is known as trapping in the terminology of atmospheric pollution. It has been documented that trapping of a plume frequently occurs under subsidence inversion conditions for which a mixing layer as shallow as 500 meters or less can persist two to four hours from midmorning to midafternoon, according to the studies on the Tennessee River Valley Authority's stack plumes (Carpenter et al. [45]).

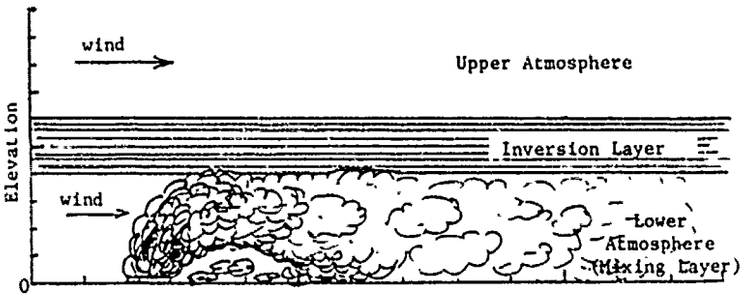

FIGURE 6-13. Trapping of Plume in a Shallow Mixing Layer

The ground-level concentration resulting from plume trapping can be estimated by the following equation.

$$\overline{C}(x,y=0,z=0) = \frac{10^6\, Q}{\sqrt{2\pi}\,\sigma_{yt}\, U\, H_t} \qquad (6\text{-}15)$$

where

H_t = mixing height (m)

and

$$\sigma_{yt} = \sigma_y + 0.47\left(\frac{H_t}{1.11} - 2.15\,\sigma_z\right) \quad \text{all units in meters} \qquad (6\text{-}16)$$

As can be seen from equation (6-15), maximum ground-level concentration results from minimum σ_{yt} value, if the values of windspeed and mixing height are constants. Value of σ_{yt} is determined by the atmospheric stability in the mixing layer discussed previously in the section on atmospheric stability and dispersion. However, whenever trapping occurs due to lofting inversion, the atmosphere in the mixing layer tends to assume neutral stability. If trapping occurs when there is a low cloud ceiling, the mixing layer tends to have a homogeneous temperature or isothermal profile. It is therefore estimated that isothermal condition may possibly result in worst ground-level concentration.

Emission Rates of Contaminants

The emission rate, Q, of a burning pool has a direct influence on ground-level concentration as indicated by equations (6-4), (6-5), (6-9), and (6-15). Emission rate is primarily determined by the burning rate of fuel in the pool, pool size, and degree of complete combustion.

Emission rate of contaminants generally increases with increasing burning rate and pool size. For contaminants such as carbon monoxide from incomplete combustion, emission rate increases with increase in degree of incomplete combustion. Emission rates of contaminants resulting from oxidation of ingredients or impurities, such as sulfur, in the fuel increase with increase in degree of complete combustion. The emission rate for incomplete combustion products can be approximated by the following equation.

$$Q = 22.4 \times 10^{-3} (1 - f)\ A_p\, r_b\, \rho_c / M_w \qquad (6\text{-}17)$$

or

$$Q = 22.4 \times 10^{-3}\ \pi\ (1 - f)\ R_p^{\,2}\, r_b\, \rho_c / M_w \qquad (6\text{-}18)$$

where

f = fractional degree of complete combustion

M_w = molecular weight of the combustion product (g/mole)

and A_p, r_b, ρ_c, and R_p have been defined previously.

It must be noted that more accurate estimates of emission rate of a substance from pool burning can be obtained after a thorough investigation of the flame chemistry, kinetic constants of combustion reactions, and oxygen transfer between the flame and the ambient air.

For a burning rate of 10 mm/min, or 1.667×10^{-4} m/sec, and 10% incomplete combustion of hydrocarbons with molecular weight ranging from 16 to 100 grams per mole, the volumetric emission rate Q is calculated to range from 0.3 to 1.8 m^3/sec for pool diameter of 10 meters and to range from 30 to 183 m^3/sec for a pool diameter of 100 meters.

Case Study

The case study presented in the following includes trapping with isothermal stability in the mixing layer and plume dispersion in neutral, slightly stable, stable, and isothermal atmospheres and in atmospheres with moderate and strong inversion, respectively. They are discussed below.

(A) Trapping of plume

For various combinations of mixing heights and windspeeds, the ground-level concentrations are calculated for a number of downwind distances. The results are presented graphically in Figures 6-14, 6-15, and 6-16. In these figures, ground-level concentration is

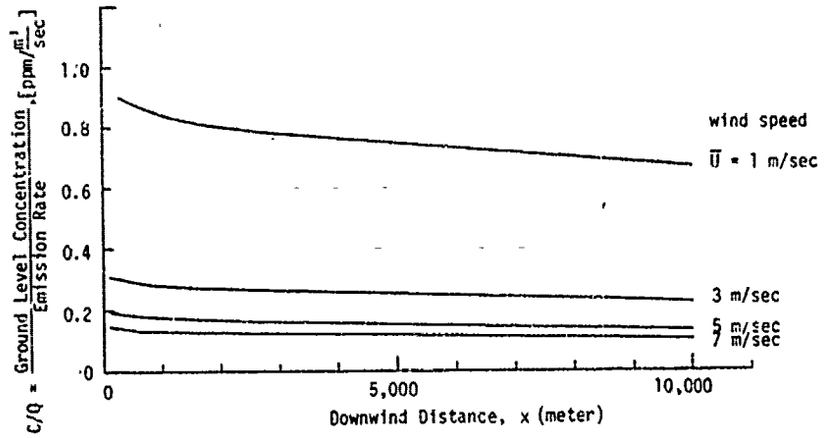

FIGURE 6-14. Ratio of Ground-Level Concentration to Emission Rate Under Trapping Conditions for Mixing Height of 1,000 Meters

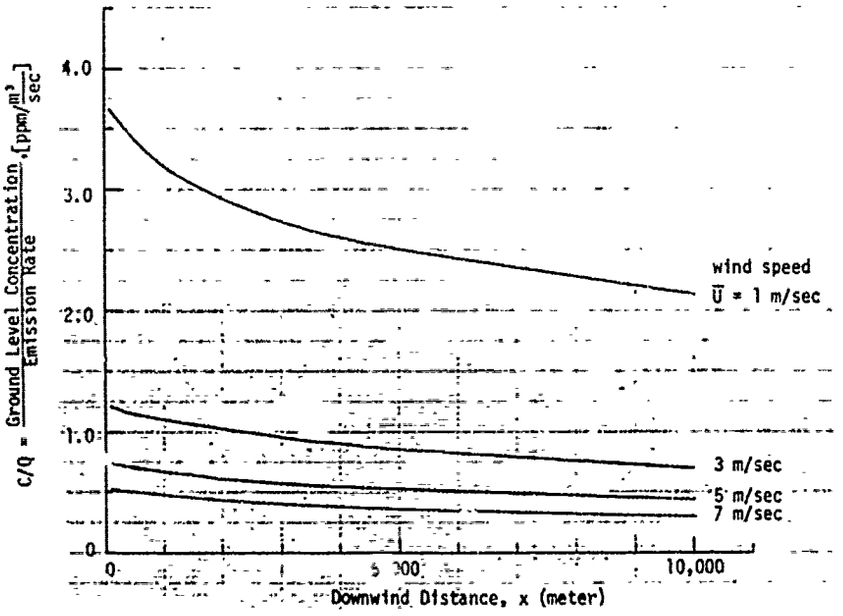

FIGURE 6-15. Ratio of Ground-Level Concentration to Emission Rate Under Trapping Conditions for Mixing Height of 500 Meters

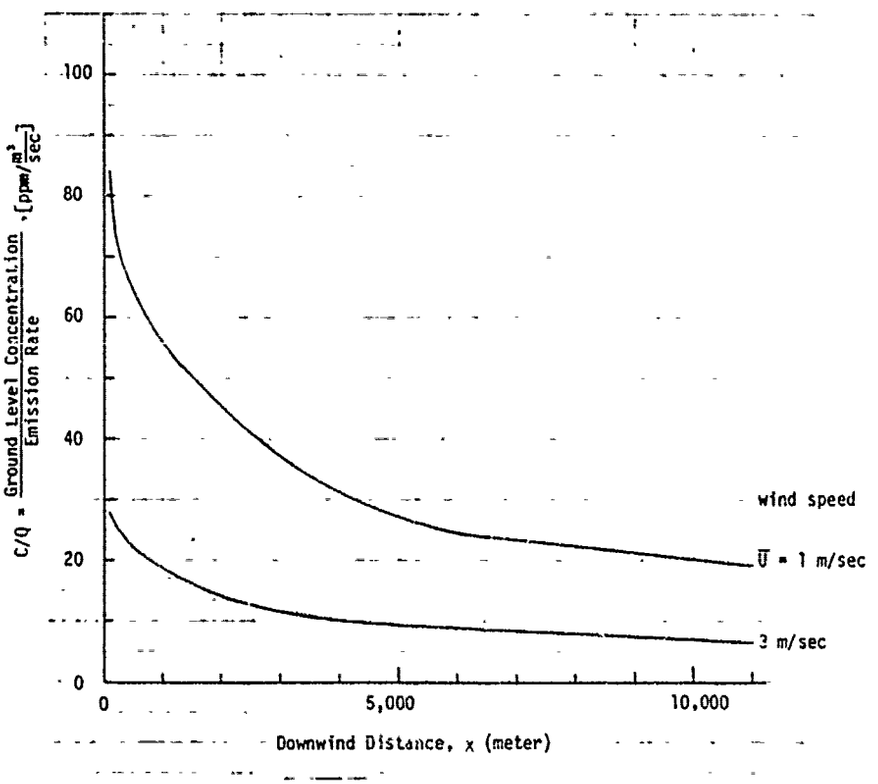

FIGURE 6-16. Ratio of Ground-Level Concentration to Emission Rate Under Trapping Conditions for Mixing Height of 100 Meters

expressed in terms of emission rate, Q. It is concluded that lower mixing height and lighter wind yield higher ratios of ground-level concentration to emission rate, C/Q. Using the emission rates calculated in the section above on emission rates of contaminants, it is determined that the maximum possible ground-level concentration under a trapping situation ranges from 1.56×10^2 to 1.56×10^4 ppm for pool diameters of 10 and 100 meters, respectively.

(B) Dispersion in neutral atmosphere

Using the relevant constants in Table 6-2 and equations (6-8) and (6-9), the maximum ground-level concentration can be calculated by the following simplified equation:

$$C_{max,y=0,z=0} = 0.25 \frac{Q}{\bar{U}(h_e)^{2.02}} \qquad (6\text{-}19)$$

The same procedure is used repeatedly for the derivation of dispersion equations for various atmospheric stabilities as listed below.

(C) Dispersion in slightly stable atmosphere

$$C_{max,y=0,z=0} = 0.96 \frac{Q}{\bar{U}(h_e)^{2.39}} \tag{6-20}$$

(D) Dispersion in stable atmosphere

$$C_{max,y=0,z=0} = 28.8 \frac{Q}{\bar{U}(h_e)^{3.38}} \tag{6-21}$$

(E) Dispersion in isothermal atmosphere

$$C_{max,y=0,z=0} = 57.0 \frac{Q}{\bar{U}(h_e)^{3.62}} \tag{6-22}$$

(F) Dispersion in an atmosphere with moderate inversion

$$C_{max,y=0,z=0} = 170 \frac{Q}{\bar{U}(h_e)^{3.96}} \tag{6-23}$$

(G) Dispersion in an atmosphere with strong inversion

$$C_{max,y=0,z=0} = 536 \frac{Q}{\bar{U}(h_e)^{4.28}} \tag{6-24}$$

Therefore, the equation for maximum ground-level concentrations for cases (B) through (G) takes the following general form.

$$C_{max,y=0,z=0} = \frac{\alpha \cdot Q}{U(h_e)^{\beta}} \tag{6-25}$$

where α and β are constants.

For various combinations of buoyancy flux and atmospheric stability, the ratios of maximum ground-level concentration and emission rate, C_{max}/Q, are tabulated in Table 6-3. Values not reported in Table 6-3 are for those conditions under which, either the maximum plume rise reaches the maximum ceiling height of 2000 meters and thus falls into the trapping category, or high windspeeds are not consistent with the given stability category.

TABLE 6-3 THE C_{max}/Q RATIO FOR VARIOUS COMBINATIONS OF BUOYANCY FLUX AND ATMOSPHERIC STABILITY IN $\left(ppm/\frac{m^3}{sec}\right)$

Atmospheric Stability	Buoyancy Flux, F (m^4/sec^3)		
	5,000	50,000	500,000
Neutral	0.04	--	--
Slightly Stable	0.06	9×10^{-3}	--
Stable	6×10^{-3}	5×10^{-4}	--
Isothermal	4.5×10^{-3}	2×10^{-4}	--
Moderate Inversion	2.4×10^{-3}	1×10^{-4}	--
Inversion	1.6×10^{-3}	1×10^{-4}	--

Using Table 6-3 and the highest possible emission rates calculated in the section on emission rates of contaminants, one obtains the maximum possible ground-level concentrations and their associated physical conditions for cases (E) through (G) as follows.

- Maximum ground-level concentration of 0.1 ppm in slightly stable atmosphere with plume buoyancy flux of 5,000 m^4/sec^3 and emission rate of 1.8 m^3/sec and windspeed of 2 m/sec.
- Maximum ground-level concentration of 1.65 ppm in slightly stable atmosphere with plume buoyancy flux of 50,000 m^4/sec^3 and emission rate of 183 m^3/sec and windspeed of 2 m/sec.

TOXICOLOGY OF CARBON MONOXIDE

In simple terms, carbon monoxide (CO) exerts its toxic effect by displacing oxygen from the blood. This is common knowledge: it is probably the most widely known toxic mechanism by far. The statement as presented is not in fact very accurate and it ignores a great deal of complexity, but it is not a bad popular approximation.

Blood is an effective carrier of oxygen because the hemoglobin (Hb) in the red cells forms oxyhemoglobin (O_2Hb) in a reversible reaction which releases oxygen where the demand is high (i.e., where the local partial pressure of oxygen is low). Hemoglobin also combines with carbon monoxide, forming carboxyhemoglobin (COHb). The two compounds form at similar rates, but CO is bound much more firmly and the rate of dissociation of COHb is much the slower. When hemoglobin is in equilibrium with a mixture of CO and O_2, the ratio of COHb concentration to

O_2Hb depends on (1) the partial pressure of each gas and (2) a factor representing the relative affinity of Hb for the two gases. In equation form,

$$\frac{(COHb)}{(O_2Hb)} = M \frac{P_{CO}}{P_{O_2}}$$

where M is the affinity ratio. This equation was first presented by J. S. Haldane in 1895 [48]. The value determined for M depends on experimental conditions: 210 has been widely used, and we will use it here. This means that, if Hb is in equilibrium with an atmosphere of 210 parts O_2 and 1 part CO, there will be present 50% COHb and 50% O_2Hb. In other words, 0.1% of CO in air (21% O_2) will halve the oxygen-carrying capacity of the blood.

The effect is in fact greater than this because the O_2 is not as readily available as it is in normal blood, being bound more tightly. (This is connected with the fact that Hb has four "acceptors" per molecule, and their affinity depends on how "full" the molecule is. This need not be discussed here but is worth mention, because the symbols--COHb or O_2Hb--suggest a simple one-to-one compound. This is misleading: a more exact representation would be $COHb_4$, $(CO)_2Hb_4$, $(CO)_3Hb_4$, and $(CO)_4Hb_4$.)

It will be evident that CO toxicity is very much the same thing as the hypoxia discussed in relation to the simple asphyxiants (see Appendix B). The difference is that these reduce the supply of oxygen to the lung, whereas CO is a chemical asphyxiant which reduces the ability of the blood to collect and transport oxygen. As far as the tissues needing the oxygen are concerned, the effect is much the same. In fact, some people prefer to call CO nonpoisonous, quoting evidence such as an experiment of Haldane's in which he exposed mice to O_2 at 2 atm of pressure, mixed with enough CO to convert effectively all of their Hb to COHb. The partial pressure of O_2 was enough to keep them alive by the amount of O_2 dissolved in the blood (none being in the red cell reservoirs). We feel that this terminology is contrary to the general conception of a poison as: "Any substance which,...in relatively small amounts, by its chemical action may cause damage to structure or disturbance to function" [49]. Henderson and Haggard [50] sum up the situation very clearly. In man the Hb normally carries about 1 liter of

---

[48] Haldane, J. S., The action of carbonic oxide on man, *J. Physiol. (London) 18*:430-462, 1895.

[49] *Dorland's Illustrated Medical Dictionary*, 24th ed., W. B. Saunders Co., Philadelphia and London, 1965.

[50] Henderson, Y., and H. W. Haggard, *Noxious Gases and the Principles of Respiration Influencing Their Action*, 2nd ed., Reinhold Publishing Corp., New York, 1943.

O_2, or about 4 minutes' supply. Takeup of 10 ml CO preempts 1% of the Hb. At rest, the tissues use about 30% of the arterial O_2; in vigorous exercise, 70% to 80%, reducing the safety margin from a large to a narrow one. CO can obliterate the safety margin.

The resemblance to hypoxic hypoxia (as with the simple asphyxiants) can be seen below.

% Reduction of O_2 by Dilution	*% of Hb in COHb Form*	*Corresponding Physiological Effects*
40	30	Impairment
50	40	Incapacitation
60	50	Unconscious; dangerous
80	70	Rapidly fatal

The resemblance extends also to the type of response, the central nervous system and the cardiovascular system being especially at risk. There is one big difference. The rate of uptake of CO is quite slow, especially at lower concentrations. The lung retains about 50% of the inhaled CO at the beginning of exposure, but it takes many inhalations to build up the concentration, and as equilibrium is approached the back-pressure of blood CO reduces the uptake more and more. The rate of loss after exposure is even slower, with the result that most of the damage from a brief, intense exposure occurs afterwards. Typical figures for uptake are shown below.

Exposure to 0.1% CO	
Time, hr	*% COHb*
1	26
2	41
4	53
Equilibrium (many hr)	66

It will be seen that 50% of the equilibrium concentration is reached in a little over 1 hr. In contrast, it takes 3 or 4 hr for 50% to be lost after exposure unless assisted by treatment or exertion, and again the rate is most rapid at first and slows down. (Exertion may of course do more harm than good, by increasing tissue oxygen demand.) All the CO does not go to COHb: about 20% forms a similar compound with myoglobin, a simpler version of hemoglobin which normally functions as a reserve oxygen store in muscle. This is important in relation to high sensitivity to CO effects. A diseased heart may experience increased demand for blood flow at the same time as its oxygen supply, via the coronary arteries, is depleted and its myoglobin oxygen reserve is diminished. Other sensitive individuals include, as might be expected, those who live on the margin of oxygen insufficiency because of chronic bronchitis

or asthma. The young are more at risk than (healthy) older people, because of higher metabolic activity. (The same thing applies to smaller animals and birds, especially, which is why canaries are used to detect CO in mines.)

Recovery in survivors of a brief, intense exposure is usually complete. "The great majority of victims of carbon monoxide asphyxia recover without any lasting symptoms..." [51]. Patty [52] remarks that this may be true if the victim remains conscious; "Where poisoning is severe enough to cause unconsciousness, however, some damage to the brain, central nervous system and circulation may occur..." As we note when discussing hypoxia, it is the length and intensity of oxygen deprivation which determine whether damage occurs. The CO-Hb reaction is reversible without lasting effect; tissue damage may be irreversible. It should be added that treatment, if promptly applied, considerably improves the prognosis for seriously affected victims; it consists mainly of augmenting O_2 supply, by artificial respiration, administering pure O_2, or (best) O_2 under about 2 atm. However, the need may not be recognized soon enough: the characteristic flush--well known in popular fiction--is more likely to be seen on the autopsy table than in the living patient, who is much more probably pallid or cyanosed.

Effect of VM Conditions

If there is exposure to CO in a VM incident, it will be in conditions quite different from simple experimental exposure.

- The CO concentration will vary throughout; in conjunction with the slow uptake and release, this means difficulty in estimating consequent COHb levels.
- There may be enough O_2 depletion to augment the chemical asphyxiation.
- Other toxic chemicals are likely to be present.
- The people exposed are likely to be more than normally susceptible, because of increased O_2 demand through exertion and fear and because of increased ventilation rate which augments intake of CO.

A simple general expression for the uptake problem in fluctuating concentration is not possible, and the complication of attempting to model it with any accuracy is considered to be not worthwhile. As for the other factors, these are of course well recognized--e.g., by those concerned with firefighting--but do not lend themselves to generalization.

---

[51] Hamilton, A., and H. L. Hardy, *Industrial Toxicology*, 3rd ed., Publishing Science Group, Inc., Acton, Mass., 1974.

[52] Patty, F. W. (ed.), *Industrial Hygiene and Toxicology*, Interscience Publishers, New York, 1962.

Dose-Response Estimates

In the previous discussion, we have expressed CO concentrations in percentages (volume/volume) because this is common practice in the literature about CO. The unit of parts per million (ppm) is also commonly used, 10,000 ppm obviously equaling 1%. (There is also a rather odd unit that used to be applied to CO concentrations quite widely: parts per 10,000.) For the present discussion of dose-response, we will also use weight/volume concentrations when desirable, 0.01% or 100 ppm being approximately 110 mg m^{-3}.

We have already noted that uptake of CO is most rapid at first, approaching equilibrium asymptotically, and is more rapid at high than at low concentrations (see Figure 6-17).

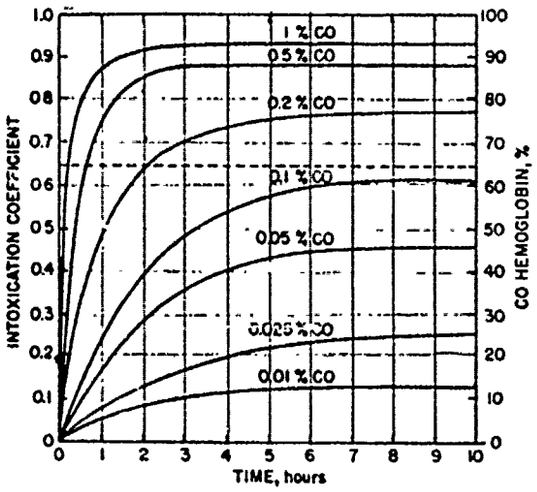

FIGURE 6-17. Speed of Saturation of Hemoglobin with Different Concentrations of CO Until Equilibrium Between the Concentration of CO in Air and Blood Is Produced (from Von Oettingen [53])

It follows that response, in terms of blood COHb concentration, is dependent on both concentration and time and differs from the simple dosage (concentration multiplied by time) proportionality of Haber's Law.

---

[53] Von Oettingen, W. F., U.S. Public Health Bulletin, No. 290, 1944.

This is clearly shown in the experimental results of Peterson and Stewart [54]; see Figure 6-18 below.

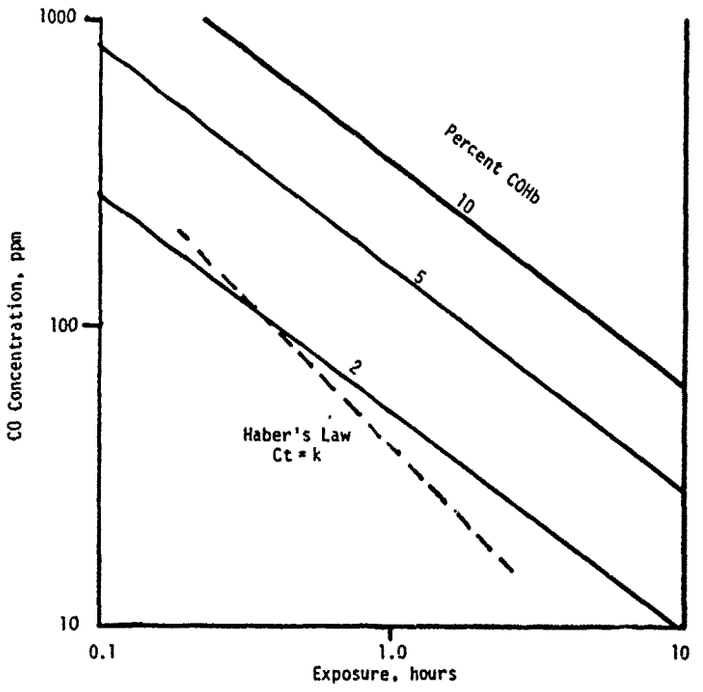

FIGURE 6-18. Concentration and Time To Develop Given COHb Levels in Sedentary Men (from Peterson and Stewart [54])

Although lines for a given COHb concentration do not correspond with constant *Ct*, attempts have been made to propose *Ct*-type relationships. Henderson and Haggard [50] give the following rough guide, which is a reasonable approximation for times around 1 hr but not for much longer or shorter times:

Dosage, ppm hr	*Physiological Response*
300	None perceptible
600	Just perceptible
900	Headache and nausea
1,500	Dangerous to life

[54] Peterson, J. E., and R. D. Stewart, *Absorption and Elimination of Carbon Monoxide by Inactive Young Men*, report prepared under Contract CRC-APRAC, Project No. CAPM-3-68, Coordinating Research Council, Inc., 1969.

In an earlier publication [55], Henderson et al. give similar figures, with extension above and below:

100 ppm	Allowable for several hours
4,000 ppm	Fatal in less than 1 hour

Their figures have been adopted, directly or with some modification, by several authorities. Sax [56] gives

Concentration, ppm	*Time, hr*	*Effect*
400-500	1	None appreciable
600-700	1	Barely appreciable
1,000-1,200	1	Dangerous
4,000 up	< 1	Fatal

Braker and Mossman [57] tabulate similar figures, but they rate 1,000 to 1,200 ppm for 1 hr as "unpleasant but not dangerous" and 1,500 to 2,000 ppm as "dangerous."

Dose-response relationships in terms of COHb are more realistic and lend themselves to better agreement among authorities. Figures published by the U.S. Bureau of Mines (Sayers and Yant [58]) are generally acceptable and are shown below.

Blood Saturation in % of COHb	*Symptoms*
0-10	No symptoms
10-20	Tightness across forehead; possibly slight headache, dilation of cutaneous blood vessels
20-30	Headache and throbbing in temples
30-40	Severe headache, weakness, dizziness, dimness of vision, nausea, vomiting, and collapse

---

[55] Henderson, Y., et al., *J. Ind. Hyg.* 3:79-137, 1921.

[56] Sax, N. I., *Dangerous Properties of Industrial Materials*, 3rd ed., Van Nostrand Reinhold Co., New York, 1968.

[57] Braker, W., and A. L. Mossman, *Effects of Exposure to Toxic Gases--First Aid and Medical Treatment*, Matheson Gas Products, East Rutherford, N. J., 1970.

[58] Sayers, R. R., and W. P. Yant. U.S. Bureau of Mines, Reports Investigations No. 2476, 1923.

Blood Saturation in % of COHb	*Symptoms*
40-50	Same as previous item with more possibility of collapse and syncope, and increased respiration and pulse
50-60	Syncope, increased respiration and pulse, coma with intermittent convulsions, and Chenye-Stokes respiration
60-70	Coma with intermittent convulsions, depressed heart action and respiration, and possibly death
70-80	Weak pulse and slow respiration, respiratory failure, and death

We are interested in the range of COHb from around 25% (harassing discomfort) up to about 75% (rapidly fatal); in between, concentrations around 40% correspond with incapacitation and 60% with unconsciousness and death if prolonged. The problem is to relate these COHb concentrations with ambient CO concentrations and times of exposure. Forbes [59] gives a useful graphic display (Figure 6-19), in which it will be seen that exposure for 1 hr is likely to be hazardous only at concentrations far above 0.1% (of the order of 1.0%).

We estimated the CO concentrations for 20% to 80% COHb in various exposure times, using data from Von Oettingen [53].

COHb, %	*% CO To Give Corresponding COHb Concentrations in*		
	2 hr	*1 hr*	*0.5 hr*
20	0.04	0.07	0.15
30	0.06	0.12	0.18
40	0.10	0.16	0.25
50	0.14	0.22	0.36
60	0.18	0.34	0.50
70	0.28	0.45	0.70
80	0.42	0.70	1.0

These figures had to be estimated from a graphical presentation. However, they are probably quite good; data from two other sources (limited to the lower end of the range) correspond closely.

---

[59] Forbes, W. H., Carbon monoxide uptake via the lungs, in R. F. Coburn (ed.), Biological Effects of Carbon Monoxide, *Ann. N.Y. Acad. Sci. 174*, 1970.

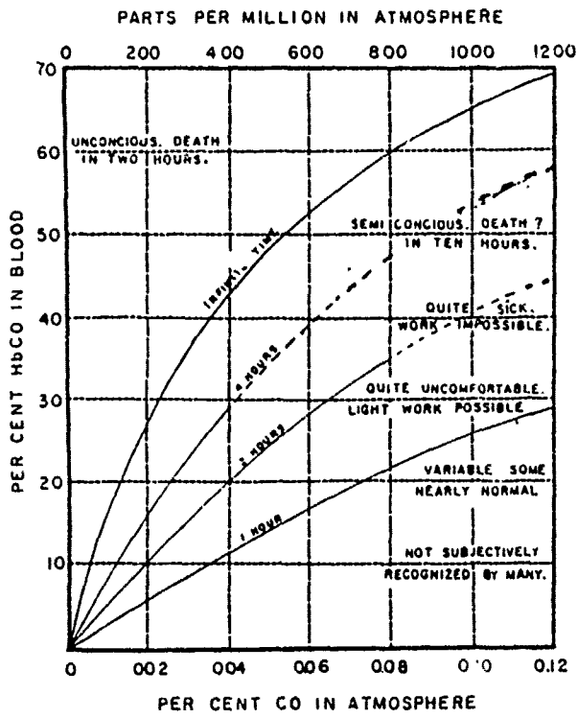

FIGURE 6-19. Percent COHb in Blood vs. Atmospheric CO at One Hour, Two Hours, Four Hours, and Infinite Time (from Forbes [59])

It will be seen that, in this time range, harassing to incapacitating effects are not to be expected below about 0.1% to 0.25% CO (1,000-2,500 ppm, or 1,100-2,800 mg m^{-3}), and serious to fatal consequences at about twice this level. For exposures of 15 min, CO concentrations would probably be about 50% higher than for 30 min.

It will be obvious that figures for hazardous exposure in man are obtainable only from accidents, experimental exposure being acceptable only at lower levels. However, the relation between response and COHb level can be accurately determined, provided that blood samples are taken fairly soon and properly handled and analyzed. The area of uncertainty is in the respiratory exposure needed to establish high COHb levels.

A note on lower COHb levels may be of interest. Nonsmokers, unexposed to CO, have about 0.5% COHb. The healthy body produces about 0.4 ml of CO per hour, and the steady outward flow of this to the expired air maintains this low level of COHb. In hemolytic disease,

the level is higher. Heavy smokers are likely to be at 5% COHb or more, up to 10%. The NIOSH-recommended occupational exposure limit is an 8-hour average of 35 ppm of CO, which will establish about 5% COHb in the nonsmoker; a ceiling of 200 ppm for brief exposure is recommended. Hamilton and Hardy [51] note that "an international committee" proposed a 1-hr ceiling of 400 ppm and a 20-min ceiling of 1,000 ppm. The significance of this for us is that a 0.1% exposure for 20 min was considered safe; this agrees with figures shown above from Von Oettingen [53].

Summary on dose-response

The concentration-time relationships for developing various levels of blood COHb are complicated. It is, however, possible to make a reasonable estimate of exposure levels, below which there would be no significant hazard. Using the figures tabulated earlier, exposures for discomfort level are:

% CO by Volume	*ppm*	*Time, hr*
0.04	400	2
0.07	700	1
0.15	1,500	0.5
0.25	2,500	0.25

These exposures would cause headache in normal persons and would be hazardous only to the most sensitive individuals ("last straw" cases). Below these levels of exposure, CO can be neglected in the VM.

CONCLUSION

The calculations of maximum ground-level concentrations gave, for trapping with isothermal stability in the mixing layer, 156 to 15,600 ppm. For dispersion into atmospheres with slightly stable temperature profile, the figures were 0.1 to 1.65 ppm.

The estimates of carbon monoxide exposures with discomfort but no hazard in normal subjects ranged from 400 ppm and 2-hr exposure to 2,500 ppm and 0.25-hr exposure.

We conclude that the threshold for minimal harassment can be reached only in trapping conditions and that hazardous concentrations will occur only in extreme cases. The likelihood that these conditions will coincide with a cargo fire of appropriate dimensions appears low enough to justify neglecting it for the present. The probability is calculable from available climatological data for various regions of the United States, and this might be undertaken at some future time.

Chapter 7

INGESTION HAZARDS FROM TOXIC MATERIALS SPILLED INTO WATER

INTRODUCTION

There is clearly some risk that the contaminated water resulting from a hazardous material spill will be swallowed, either by bystanders or by those directly involved with the venting vessel, spill mitigation, or emergency operations. The purpose of this chapter is to describe how to assess potential injury to the population exposed, to describe a method for estimating this type of injury in the VM, and to present some numerical values to be used as inputs to the VM.

Injury resulting from water ingestion is significantly more difficult to quantify than are other injury mechanisms treated by the VM, because of the significantly greater uncertainty regarding how much tainted water any particular individual ingests. Thus, in addition to strictly toxicological considerations, the definition of hazardous levels for contaminated water must take into account the probable amount of water ingested by individuals. The results of this chapter are summarized in convenient terms in Table 7-6.

EXPOSURE SUBCLASSES OF THE POPULATION

In the event of a major spill, the local water treatment authority would usually have ample time after the spill to prevent contaminated water from reaching consumers, or at least to warn the public against consumption. Also, most adults are unlikely to drink deliberately from navigable waters at any time. There are, however, some people who may be exposed to incidental and unintentional ingestion, for example, emergency personnel or swimmers. Ships' crews and shore-based personnel directly involved in the incident should be aware of the hazards but might not be able to avoid them. Others not directly involved, such as recreational swimmers, might receive timely warning of some contaminants through perception of abnormal odor, taste, or appearance so that they could avoid ingestion.

In general, then, we might consider three subclasses of the population exposed to this toxic hazard, each subclass having a significantly different rate of ingestion of contaminated water. The three subclasses are described below.

(1) The general population drinking contaminated water as part of the normal daily intake of fluid, not realizing that a toxic threat exists.

(2) A small segment of the population in intimate contact with the water by virtue of work or recreation (ships' crews,

fishermen, swimmers, etc.), performing their activities without the knowledge that a toxic threat exists.

(3) A very small segment of the population involved in emergency activities on or near the water, pursuing these activities with a knowledge of the hazard and taking pains to avoid water ingestion.

AMOUNT OF INGESTION

The first step in developing a method for assessing toxic injury resulting from water ingestion is to estimate how much water might be swallowed. As the upper limit, we take unrestricted drinking and assume that warning of the risk will be given within 24 hours of the spill; one day's intake is unlikely to exceed 2500 ml, except during prolonged heavy exercise [60]. At the other extreme, the probable intake for a large part of the local population is obviously zero. What, however, is the probable intake for those directly exposed to the contamined water? Two categories can be distinguished. For unalerted swimmers or those accidentally immersed in the water, 250 ml (about a cupful) is a reasonable estimate. Fully trained and equipped personnel would probably ingest less than this, but it would not be advisable to assume that their intake would be zero. We will assume that they cannot avoid swallowing amounts up to 2.5 ml.

These figures are relevant to the intake of water containing dissolved or dispersed toxicants. Immiscible toxicants that would definitely sink (e.g., phosphorus) present a negligible ingestion hazard. Those that would float and are not soluble (e.g., ethyl ether) could be swallowed, but the complications of assessing the hazard from ingestion of these compounds are beyond the scope of the current study and are not discussed here.

TOXICOLOGICAL MECHANISMS

In this aspect of the VM, the concern is with water ingestion. Although the process under consideration seems simple and unequivocal from an operational or physical point of view, the process of water ingestion is not necessarily so straightforward from a toxicological point of view. The following discussion illustrates some of the toxicological complexities that exist but are unable to be treated currently.

By definition, absorption means the transport, either active or passive, through a cellular surface or membrane into the cell. From

---

[60] Guyton, A. C., *Textbook of Medical Physiology*, 3rd ed., W. B. Saunders, Philadelphia, 1967.

here an absorbed substance may be metabolized, excreted, or passed through another cell wall to another cell, the circulatory system, or the lymphatic system. Absorption of material usually implies transport through the intestinal wall but may also occur through the skin or via other portals.

Absorptive toxicity may be broken down further, depending upon the mode of action of the chemical in question. When the agent is absorbed and not transported further, the action site is considered local and injury is confined to the site of absorption. The opposite mode of action is a systemic effect. In this case, the toxic chemical is absorbed through one portal, enters one of the body's circulatory mechanisms, and then exerts its effect on specific cells, organs, or other body tissue. It is possible that the compound may return to the absorbing tissue where it may also be susceptible to damage. During the interval between absorption and distribution, the chemical may have undergone metabolic transformation resulting in increased, decreased, or no effect on the chemical toxicity of the original compound. These chemicals and/or their metabolites may then be deposited into depot tissue for storage or eliminated using any combination of the body's excretory mechanisms--urine via the kidney and bladder, feces via intestinal secretion, bile from the liver, pancreatic secretions, respiratory gases via the lungs, and sweat via the skin.

Other body fluids including saliva may also play a role in the excretory process for some compounds. Excretion of a compound from a body tissue may not eliminate the toxicity problem for that specific chemical, since it may be reabsorbed as it passes by other tissue. For example, compounds excreted via saliva and bile may be reabsorbed by the small intestine.

TOXICOLOGICAL ASSUMPTIONS

A fundamental toxicological consideration in assessing damage from water ingestion is the dose-response of the impacted population. Since a miniscule amount of data exists for the toxicological response of humans in the lethal range, recourse is made to data from experiments on animals (i.e., use is made of "animal models"). The chemicals considered were taken from a list of cargoes of particular hazard (COPH). Toxicological data exist and are compiled for many of the substances on the list; however, most of the data are obtained from animal models of human toxicity. To make the transition from animal data to human assessment, several assumptions are made. One group of assumptions concerns the animal model, the other group concerns the population at risk. Chemicals are administered intragastrically to healthy experimental animals who had no previous exposure to the test chemicals. Hence no effects on oral or esophageal tissue are observed. Test animals are an inbred strain, selected for many generations on the basis of uniformity in physical and biochemical parameters. Human populations may be the exact opposite in every case in terms of exposure conditions.

The second group of assumptions are made about the population at risk and associated conditions, since an adequate data base does not exist to assess the effects of these conditions.

(1) The population prone to exposure has no prior exposure in the case of cumulative toxins or in hypersensitization.

(2) The population exposed to risk is normal and healthy.

(3) All chemical absorption occurs through ingestion, with no added load due to absorption via other portals.

(4) Potential synergistic effects of chemical combinations are also ignored.

(5) Other aspects of receiving water quality such as pH, organic load, etc., are not considered.

DOSE-RESPONSE DATA

The present treatment deals only with toxicants on the list of hazardous chemicals, COPH, which are either soluble in water or readily dispersible to form a suspension (if any). LD_{50} values are available for most of these which are based mainly on experiments using rats or other small mammals. There are also some available data for other levels of effect. Human data are limited to experimental exposure well below the threshold of lethality; accidental exposure at lethal or sub-lethal levels does not yield useful quantitative data except on rare occasions. It is thus necessary to estimate human dose-response values from animals exclusively for lethality and mainly so for other responses. We do this by assuming equal response for equal dose per unit of body weight. LD_{50} values and other data for the substances of interest are shown in Table 7-1. Lethality data for some of the chemicals of interest do not exist in the published literature [61].

Four "end points" (levels of effect) are used, corresponding to tenfold differences in dose (see Table 7-2). These levels of effect are defined as follows. At the LD_{50} level, 50% of the exposed population are killed, 45% are incapacitated, and the remaining 5% experience irritation. Incapacitation can be temporary or permanent and necessitates, as a minimum, first aid assistance. Irritation is temporary and can range from consciousness of discomfort to near-incapacitation. At the threshold of lethality, 5% of the exposed population are killed (being the most susceptible individuals in a heterogeneous population), 45% are incapacitated, and 50% experience irritation. At the threshold of incapacitation, 5% are incapacitated and 90% experience irritation. At

---

[61] Environmental Protection Agency, Designation and determination of removability of hazardous substances from water, *Fed. Regist.* *39*(164):30466 (part IV), 1975.

TABLE 7-1. TOXICITIES AND CHEMICAL PARAMETERS FOR HAZARDOUS MATERIALS

Chemical Compound	Synonym	LD_{50} 1/ (mg/kg)	Comment	Hazard in Water	BP (°C)	Solubility (g/l)	Density
LNG		NA		no	NA	-	NA
LNH_3		-		yes	-33.3	899.	6.77
Ammonium hydroxide		250	cat				
LCl_2		NA		yes	-34.6	14.6	3.21
Gasoline		600	human - mixture of compounds	yes	variable	variable	variable
Methanol		1400	human	yes	64.9	∞	0.79
Acetaldehyde		1930		yes	20.8	∞	0.78
Acetone cyanohydrin	2-hydroxy 2-methyl nitrile propanoic acid	17		yes	82	>100. (very)	0.93
Acrolein	propenol	46		yes	525	very	0.84
Acrylonitrile	nitrilepropenoic acid	93		yes	801	300	0.81
Allyl chloride	3-chloropropene	700		yes	NA	3	0.90
Butadiene	1, 3-butadiene	NA		no-insoluble	-44	insoluble	0.62
Butane		NA		no-insoluble	-0.5	negligible	0.58
Butene		NA		no-insoluble	3.7	insoluble	0.62
Butylene oxide	epoxybutane	300 (est)	LD_{low} 3000	yes	-60	decomposes (hot)	0.83
Carbon disulfide		150		yes	46	2.2	1.26
Chlorosulfonic acid		NA		yes	158	decomposes	1.77
Sulfuric acid		2140		yes	151-286	∞	~1.70
Hydrochloric acid		NA		yes	~85-100	∞	~1.10
Dimethylamine		540		yes	7.4	>100 (very)	0.68
Epichlorohydrin	1-chloro -2,3-epoxy propane	90		yes	116	slightly	1.18
Ethane		-		no-gas	-88.6	insoluble	0.57
Ethylene	ethene	-		no-gas	-103	insoluble	-
Ethylene oxide	1,2-epoxy ethane	330		yes	13.5	soluble	0.88
Ethyleneimine	aziridin	15		yes	56	∞	0.83
Ethyl ether	diethyl ether	2200		no-low solubility	34.5	slightly	0.71
Hydrofluoric acid		80	guinea pig, same as hydrogen fluoride	yes	19.5	∞	0.99
Hydrogen chloride		NA		yes-reacts	-85	823	1.19
Hydrocloric acid		NA		yes	-85 to +110	∞	1.10
Methyl acetylene	propyne	NA		no	-23.2	slightly	0.71
Methyl bromide		NA		yes-decomposes	3.6	slightly	0.71
Methanol		1400	human	yes	64.9	∞	0.79
Hydrobromic acid		NA		yes	NA	very	NA
Methyl chloride		1800		yes	-24	5	0.92
Lead alkyls		-	general class	-	-	-	-
Tetraethyl lead		100 (est)	ip LD_{50} 10	no-low solubility	110	0.3	~1.6
Oleum		-		yes-decomposes	77 to 122	∞	~1.85
Sulfuric acid		2140		yes	151 to 280	∞	~1.70
Sulfur trioxide		NA		yes	44.8	decomposes to H_2SO_4	1.92
Phosphorus		-		no	-	-	-
Phosphoric acid		7	rabbit	yes	NA	>1000	1.83
Propane		-		no	-42	negligible	0.53
Propylene	propene	NA		yes	-47.4	very	0.52
Propylene oxide	1, 2-epoxy propane	1140		yes	34.3	∞	0.86
Sulfur dioxide		NA		yes	-10	228	1.43
Sulfurous acid		NA		yes	variable	soluble	~1.03
Toluene diisocyanate		NA		yes	251	NA	NA
3, 5-diaminotoluene		NA		yes	284	very	NA
Vinyl chloride	chloroethylene	NA	TC 380 ppm	no	-13.4	slightly	0.91

1/Source is reference 63, unless otherwise noted.

the threshold of irritation, 5% experience irritation and the remaining 95% experience no noticeable symptoms. Permanent or long-term incapacitation may occur among those incapacitated at the LD_{50} and threshold of lethality levels, but may be neglected at the threshold of incapacitation level for most substances. The effects for relative dose levels were estimated by examining the dynamic range between LD_{50} and LD_{Low} values [62,63] or experimental data from selected compounds [64]. (No percentage response is proposed for long-term effects because they are so much a function of the specific agent that they cannot be generalized, even in a preliminary discussion.) In discussing these levels of effect, the responses indicated have included corrections for double counting; that is, percent response to a lesser effect is reduced by the percent of individuals experiencing a more severe effect.

TABLE 7-2. END POINTS

Effect	Relative Dose (grams)
LD_{50}	1000
Threshold of lethality	100
Threshold of incapacitation	10
Threshold of irritation	1

For example, at the LD_{50} dose level, 95% of the population has experienced incapacitation, but a value of 45% for this category of response is given because 50% of the population has passed beyond the incapacitation response to a lethal response. Similarly, virtually the entire population experiences irritation, but the response is limited to that for only 5% of the population; 95% of the population experiences more severe effects. In the following, it is important to bear in mind that two types of dose-response functions are discussed: (1) dose-response actually observed and (2) dose-response expected, were more severe response categories ignored. In other words, dose-response relationships both with and without corrections for double counting are considered.

---

[62] Stecker, P. G. (ed.), *Merck Index*, 8th ed., Merck and Company, Rahway, N.J., 1968.

[63] Christensen, P. G. (ed.), *The Toxic Substances List*, 1974 ed., U.S. Department of Health, Education, and Welfare, Rockville, Md., 1974.

[64] Becker, B. A., and G. L. Plaa, *Toxicol. Appl. Pharmacol.* 7:804, 1965.

Figure 7-1 depicts the log-linear dose-response approximations to the relationships described above. The solid curves represent the response without regard to the fact that some of the population may be responding to a more severe response; i.e., the solid curves represent the response *uncorrected* for double counting. The dashed curves (which are asymptotic to the solid curves in the low-response region) represent the expected observed response; i.e., the dashed curves represent the response *corrected* for double counting. For example, at a concentration of 0.4 LD_{50}/liter the solid curves indicate that 5% of the population is killed, 50% is incapacitated, and 95% is irritated; clearly, more than 100% of the population cannot respond. The 95% irritated includes persons also killed or incapacitated, while the 50% incapacitated includes some persons killed. The actual response expected to be observed is given by the two dashed curves and the solid curve for lethality. The response at 0.4 LD_{50}/liter is 5% killed, 45% incapacitated, and 45% irritated. Thus, double counting has been avoided. Since separate procedures have been developed to prevent double counting in the VM, it is the dose-response relationships uncorrected for double counting that are required as input to the VM.

DOSE-RESPONSE INPUTS FOR THE VM

One suitable basis for input to the VM is the ingestion of 250 ml that was estimated for swimmers and others accidentally exposed (i.e., directly involved persons who fall into the water). Table 7-2 can then be restated in terms of concentration, rather than mass of toxic material ingested. Table 7-3 lists the expected response to an intake of 250 ml at various levels of concentration expressed as LD_{50} mass units per liter.

TABLE 7-3. RESPONSES AT VARIOUS CONCENTRATIONS (250-ml intake)

Exposure		Response (expected to be observed)		
Dose (mass units)	Concentration	Killed %	Incapacitated %	Irritated %
LD_{50}	$4(LD_{50})$/liter	50	45	5
$(LD_{50})/10$	$0.4(LD_{50})$/liter	5	45	45
$(LD_{50})/100$	$0.04(LD_{50})$/liter	0	5	90
$(LD_{50})/1000$	$0.004(LD_{50})$/liter	0	0	5

This can be modified into a more convenient form for VM use, by estimating ranges of concentration which would average out to these levels of effect and by extending the overall range above and below (Table 7-4).

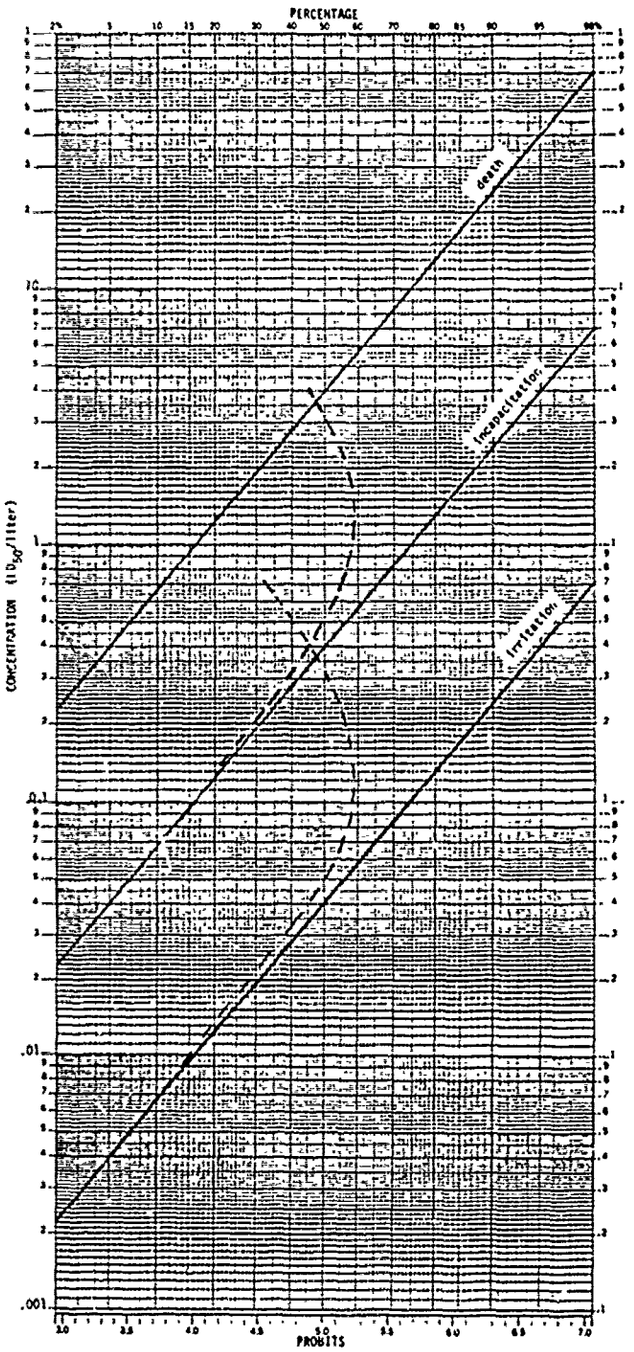

Note: Dashed lines indicate expected observed response and implicitly correct for more severe responses. Solid lines indicate hypothetical responses when no allowance is made for double counting, i.e., individuals may be in more than one response category.

FIGURE 7-1. Dose Response Curves for Ingestion Effects

TABLE 7-4. RESPONSES FOR VARIOUS CONCENTRATION RANGES

Exposure	Response, % (for 250 ml ingested)					
Concentration, LD_{50}/liter	Killed	Incapacitated		Irritated		No Response
		expected observed	unadjusted	expected observed	unadjusted	
40	95	5	100	--	--	0
4	50	45	95	5	100	0
0.4	5	45	50	45	95	5
0.04	0	5	5	45	50	50
0.004	0	0	0	5	5	95

TABLE 7-5. TOXICITY LEVELS[a] FOR KNOWN COMPOUNDS[b]

Chemical Compound	LD_{50} dose	
	mg/kg	(g/ℓ) or (kg/m^3)
LNH_3 as ammonium hydroxide	250	70
Gasoline	600	168
Methanol	1400	392
Acetaldehyde	1930	540
Acetone cyanohydrin	17	5
Acrolein	46	13
Acrylonitrile	93	26
Allyl chloride	700	196
Butylene oxide	300	84
Carbon disulfide	150	42
Chlorosulfuric acid as sulfuric acid	2140	599
Dimethylamine	540	151
Epichlorohydrin	90	25
Ethylene oxide	330	92
Ethyleneimine	15	4
Hydrofluoric acid	80	22
Methyl chloride	1800	504
Oleum as sulfuric acid	2140	599
Phosphorus as phosphoric acid	7	2
Propylene oxide	1140	319

[a] Assuming a 250-ml intake and a 70-kg individual.

[b] See Table 7-1 for references and comments.

It might be convenient to express the source strength in LD_{50} units; the wide range of toxicities can then all be treated on the same basis. To simplify the data, Table 7-5 shows the toxicity level of known compounds expressed on an LD_{50} basis and a corresponding kg/m^3 basis. This table assumes that a 70-kg person drank 250 ml of contaminated water. For example, 5 kg of acetone cyanohydrin spilled into a cubic meter of water would result in the death of 50% of the people who drank 250 ml.

LEVELS OF WATER HAZARD

By defining locations upriver or downriver from a spill on a river or contours in lakes and estuaries, regions of one level of water hazard may be determined. Then USCG or local officials may preclude certain activities in certain regions of the water. Table 7-6 shows one possible classification scheme and corresponding official actions. This table is presented for illustrative purposes only, since any regulatory decisions would have to be made by those officials charged with that responsibility.

TABLE 7-6. A CLASSIFICATION SCHEME FOR HAZARDOUS LEVELS OF CONTAMINATED WATER

Concentration (LD_{50}/liter)	Characterization		Response
	Numerical	Verbal	
> 40	5	Extremely dangerous	Too hazardous for emergency personnel to use.
4 - 40	4	Very hazardous	Only emergency personnel allowed to enter into water-related activities, evacuate shore facilities.
0.4 - 4	3	Hazardous	Forbid all but absolutely necessary use of water.
0.04 - 0.4	2	Moderately hazardous	Forbid recreational use of water; limit use for transport.
0.004 - 0.04	1	Unsafe	Advise swimmers of possible effects; issue orders not to use municipal water supply if contaminated.
< 0.004	0	Nominally safe	--

SUBMODEL FOR USE IN THE VM

The dose-response curves depicted in Figure 7-1 were transformed to the concentration units listed in Table 7-4, and the following probit equations were constructed:

$$\text{Lethality: Probit} = 4.0097 + 0.7143 \ln (\text{concentration})$$

$$\text{Incapacitation: Probit} = 5.6546 + 0.7143 \ln (\text{concentration})$$

$$\text{Irritation: Probit} = 7.2994 + 0.7143 \ln (\text{concentration})$$

where concentration is in units of LD_{50}/liter.

The following submodel has been incorporated into the VM for assessing injuries resulting from ingestion. The concentration of the spilled toxic substance is known from the Phase I VM simulation. The LD_{50} for the specific substance under consideration is known from Table 7-1. From these two values, calculate L, the number of LD_{50} units per liter. With L as input, proceed as follows.

(1) Calculate the percent killed, P_K; the percent incapacitated, P_{IC}; and the percent irritated, P_{IR}, from the appropriate probit equation.

(2) To avoid double counting:

set $P_{IR} = P_{IR} - P_{IC}$

$P_{IC} = P_{IC} - P_K$

As an example, let the concentration be measured as 0.1 LD_{50}/liter for a specific toxic substance. Using the above probit equations, the assessed numbers of injuries are calculated as follows.

Type of Injury	*Notation*	*Probit*	*% Corresponding to Probit*	*% Response Corrected for Double Counting*
Lethality	P_K	2.86	2	2
Incapacitation	P_{IC}	4.50	31	29
Irritation	P_{IR}	6.15	87	56

Chapter 8

INJURY TO INDOOR POPULATIONS

INTRODUCTION

The first stage of development of the Vulnerability Model did not extend to assessing injuries to the indoor population. Models have now been developed for assessing such injuries and are part of the Vulnerability Model simulation. This chapter describes the models, their basic assumptions, and explains the rationale behind their development.

Intuitively, we view buildings as mitigating the potential hazard of marine spills, whether that hazard arises from fire, explosion, or the air dispersion of a toxic or asphyxiating chemical. The models developed here affirm the intuitive view that buildings reduce the hazardous external environment, shield the inhabitants, and reduce damage and injury. Although this is true in general, the details of this shielding are neither simple nor straightforward.

In the case of an external fire produced by a flammable cargo, the opacity of the building will shield many inhabitants from burn-producing irradiation. A few persons near apertures, such as windows and doors, will receive some exposure. Further shielding is also provided by structures in between the building in question and the fire.

In the case of explosion, injury is caused by (1) direct blast effects, (2) debris impact, and (3) collision with solid objects after translation of the subject personnel. Structures interfere with the external blast wave, reducing peak pressure and/or altering the rise time of the overpressure. Structures shield their inhabitants from external debris; however, this is partially or fully offset by generation of nearby debris from failing windows or accelerated interior objects at lower pressures and from failing interior and exterior walls at higher pressures. Translation injury may be reduced, because translated bodies are stopped short of full speed by close-in walls (not present outdoors); however, at higher overpressures, high impact speed can be achieved with the probability of impact enhanced. At very high overpressures, walls are demolished so translation injury is reduced but may be replaced by such effects as crushing due to falls from upper stories of high-rise buildings.

In the case of air dispersion of a toxic chemical, buildings tend to reduce injury by limiting the amount of toxic material entering the building and thereby limiting the concentration levels inside. Nevertheless, a rule of thumb in chemical warfare, verified by the model developed here, is that dose (concentration times time) is the same

indoors and out. Thus for those toxic chemicals where dose determines injury, buildings may provide no reduction in hazard. On the other hand, for the highly irritant gases, such as chlorine and ammonia, where peak concentration as well as total dose is important, buildings are expected to lessen injury.

In the following sections of this chapter, models are presented which describe the mitigating effects of buildings on damages caused by (1) air dispersion of toxic or asphyxiant gases, (2) explosion, and (3) fire.

TOXIC INHALATION DAMAGE TO INDOOR POPULATIONS

In order to assess injury to indoor populations resulting from inhalation of toxic material from a marine spill, two separate calculations are required: (1) a computation of concentration as a function of time inside a structure, given the outdoor concentration-time history; and (2) a calculation of injury to the occupants of a structure based on the concentration-time history of the toxic substance in the structure. Conveniently, the second computation is identical to that currently performed by the VM for outdoor populations; that is, given toxic concentration as a function of time, percentages of the exposed population killed and injured are calculated according to the scheme described in Chapter 6 and Appendices E and G of the Final Report on the first stage of development of the Vulnerability Model [1]. Consequently, the following is directed towards a quantitative prediction of the concentration-time history of toxic material *indoors* given the concentration-time history *outdoors*.*

Some Preliminary Considerations

Conveniently, the seepage of gases in and out of buildings has been the subject of considerable study by architects and mechanical engineers in relation to heating and ventilation. For example, a significant load factor in calculating the heating (cooling) requirements of a building is the infiltration of cold (hot) air into the building from outside. The infiltration into buildings takes place through cracks around closed doors and windows, building walls (virtually all are permeable), intentional ventilation openings, open doors and windows, and other structural breaches.

---

*The model developed here can also be used to assess injury to people indoors resulting from the air dispersion of an asphyxiating chemical. This model will calculate the indoor concentration-time history, and injury can then be determined using the algorithm developed in Chapter 5 and Appendix B of this report.

The infiltration rate into any given building is a function of a large number of variables, depending on the feature through which the infiltration occurs [65]. For example, Table 8-1 shows that the infiltration rate through walls depends upon the type of construction, surface area of the wall, and wind velocity. Table 8-2 shows that infiltration rates through doors depend upon the type of door, frequency of use, building height (because of the chimney or stack effect), area of the door, wind velocity, and orientation of the door with respect to wind direction. Table 8-3 similarly shows that infiltration through windows depends on such parameters as type of window, type of weatherstripping, closure condition (locked or unlocked), wind speed, and crack length around the window.

TABLE 8-1. INFILTRATION THROUGH WALLS[a]

Type of Wall	Infiltration Rate, cu. ft. per sq. ft. per hr.		
	Wind Velocity, mph		
	10	20	30
Brick wall[b]			
8-1/2 inch, plain.....	4	12	23
8-1/2 inch, plastered[c].....	0.04	0.11	0.24
13 inch, plain.....	4	12	21
Frame wall, lath and plaster[d]...	0.07	0.18	0.26

[a] From reference [65]; experimental values corrected to allow for pressure buildup in rooms.

[b] Constructed of porous brick and lime mortar--workmanship poor.

[c] Two coats prepared gypsum plaster on brick.

[d] Wall construction: bevel siding painted or cedar shingles, sheathing, building paper, wood lath, and three coats gypsum plaster.

[65] Perry, R. H. (ed.), *Engineering Manual*, pp. 4-12 to 4-13, McGraw-Hill, New York, 1967.

TABLE 8-2. INFILTRATION THROUGH DOORS--WINTER[a] (15 mph wind velocity,[b] doors on one or adjacent windward sides[c])

Description	Infiltration Rate, cfm/ft² of exposed area				
	Infrequent Use	Average Use			
		1- and 2-story building	Tall buildings, ft		
			50	100	200
Revolving door	1.6	10.5	12.6	14.2	17.3
Glass door (3/16" crack)	9.0	30.0	36.0	40.5	49.5
Wood door 3' x 7'	2.0	13.0	15.5	17.5	21.5
Small factory door	1.5	3.0			
Garage and shipping-room door	4.0	9.0			
Ramp garage door	4.0	13.5			

[a] From reference [65]. All values are based on the wind blowing directly at the window or door. When the prevailing wind direction is oblique to the window or doors, multiply the values by 0.60 and use the total window and door area on the windward side(s).

[b] For design wind velocities different from 15 mph, multiply the table values by the ratio of velocities.

[c] Doors on opposite sides increase values 25 percent.

TABLE 8-3. INFILTRATION THPOUGH WINDOWS[a]

Type of Window	Infiltration Rate, cu. ft. per ft. of crack per hr.		
	Wind Velocity, mph		
	10	20	30
Double-hung wood-sash windows (unlocked):			
Total for average window, nonweatherstripped, 1/16-in crack and 3/64-in clearance. Includes wood-frame leakage	21	59	104
Weatherstripped	13	36	63
Double-hung metal windows:			
Nonweatherstripped, unlocked	47	104	170
Rolled-section steel-sash windows:			
Architectural projected, 1/32-in crack	36	86	139
Heavy casement section, projected, 1/32-in crack	24	54	92
Hollow-metal, vertically pivoted window	88	186	242

[a] From reference [65].

For the purposes of the Vulnerability Model it appears ill-advised, at this time, to develop a model incorporating all of these variables. It certainly would seem impractical to develop a data base capable of specifying all the required variables. Instead of detailed calculations of the infiltration rate into individual buildings, a simpler approach, the air-change method, will be used. In this approach, the average number of air changes in a building taking place per unit time is specified. As will be demonstrated shortly, this is a very useful parameter for describing building behavior in a Vulnerability Model scenario. Table 8-4 shows the dependence of air-change rate on type of room within an average residence [66]. After a computation scheme is developed, a method will be presented in which air-change rates are parameterized by indoor-outdoor temperature differential and wind speed. Modeling based on this two-parameter characterization comfortably fits into the present and planned structure of the VM; thus, excessively large data bases are avoided while preserving a modicum of differentiation between disparate environmental conditions and vulnerable resources.

TABLE 8-4. AIR CHANGES TAKING PLACE UNDER AVERAGE CONDITIONS[a] IN RESIDENCES, EXCLUSIVE OF AIR PROVIDED FOR VENTILATION[b]

Kind of Room or Building	Number of Air Changes Taking Place per Hour
Rooms with no windows or exterior doors.....	0.5
Rooms with windows or exterior doors on one side.....	1
Rooms with windows or exterior doors on two sides.....	1.5
Rooms with windows or exterior doors on three sides...	2
Entrance halls.....	2

[a] For rooms with weatherstripped windows or with storm sash, use 2/3 of these values.

[b] From reference [66].

[66] American Society of Heating, Refrigerating, and Air Conditioning Engineers, Inc., *ASHRAE Guide and Data Book*, ch. 25, ASHRAE, New York, 1965.

A Fundamental Model of Infiltration

To model the process of infiltration, consider an enclosed volume with flow in and flow out as shown in Figure 8-1. Our basic assumptions are: (1) the volumetric rate of inflow equals the volumetric rate of outflow; (2) the inflow has a toxic concentration equal to that of the outside atmosphere; (3) the outflow has a toxic concentration obtained by continuous and complete mixing of the inflowing gas with the gas already inside; (4) the infiltration rate does not change during the time of interest; and (5) the toxic material does not react chemically with air or building walls, is not adsorbed or filtered during infiltration, does not settle or precipitate out, and is not otherwise removed from the air. (Assumptions 4 and 5 can be removed at the expense of a mathematically more complex model.)

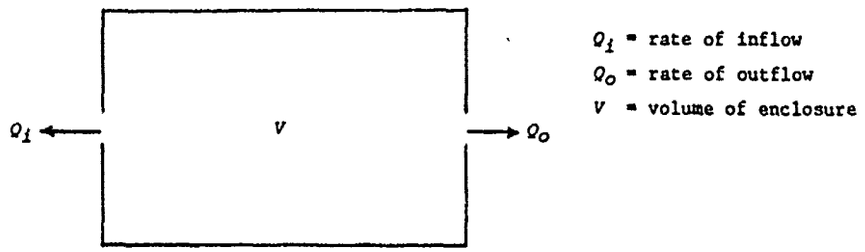

FIGURE 8-1. Schematic for Infiltration Rates into Enclosures

Now the rate of mass of toxic substance flowing into the enclosed space is given by

$$\frac{dm_i}{dt} = C_o Q_i \tag{8-1}$$

where

$\frac{dm_i}{dt}$ is the rate of mass of toxic substance entering

C_o is the concentration of toxic substance outside

Q_i is the rate of inflow

Similarly, the rate of mass of toxic substance flowing out of the enclosed space is given by

$$\frac{dm_o}{dt} = C_i \, Q_o \tag{8-2}$$

where

$\frac{dm_o}{dt}$ is the rate of mass of toxic substance leaving

C_i is the concentration of toxic substance inside the enclosure

Q_o is the rate of outflow

By definition,

$$M_i = C_i \, V \tag{8-3}$$

where

M_i = mass of toxic substance inside the enclosure

V = volume of the enclosure

If we assume that there is no toxic material inside the enclosure at time $t = 0$, then

$$M_i = \int_0^t \left(\frac{dm_i}{d\tau} - \frac{dm_o}{d\tau} \right) d\tau \tag{8-4}$$

This is simply a statement of the principle of conservation of mass. Substituting for M_i from equation (8-3) gives

$$C_i \, V = \int_0^t \left(\frac{dm_i}{d\tau} - \frac{dm_o}{d\tau} \right) d\tau$$

and differentiating yields

$$V \frac{dC_i}{dt} = \frac{dm_i}{dt} - \frac{dm_o}{dt} \tag{8-5}$$

(of course, V is assumed time-invariant).

Substituting from equations (8-1) and (8-2) into equation (8-5) gives

$$V \frac{dC_i}{dt} = C_o Q_i - C_i Q_o$$

but since we assume (assumptions 1 and 4)

$$Q_i = Q_o = Q$$

where Q is the infiltration rate, we may write this result as

$$\frac{V}{Q} \frac{dC_i}{dt} + C_i = C_o$$

or

$$\frac{1}{R} \frac{dC_i}{dt} + C_i = C_o \tag{8-6}$$

where $R = \frac{Q}{V}$ is the air-change rate.

Equation (8-6) is a differential equation determining the inside concentration, C_i, as a function of time given the external concentration, C_o, as a function of time. It is a classic first-order ordinary differential euqation, characteristic of a simple electrical RC (resistance-capacitance) circuit [67].

We may proceed to find a generalized solution of this equation by the use of Laplace transform techniques. Note that the initial condition is

$$C_i (0) = 0 \tag{8-7}$$

That is, the initial concentration of toxic material inside the enclosure is zero. Thus, taking the Laplace transform of equation (8-6) gives

$$\left(\frac{s}{R} + 1\right) \tilde{C}_i (s) = \tilde{C}_o (s)$$

---

[67] Keysig, Erwin, *Advanced Engineering Mathematics*, pp. 72 and 220, John Wiley and Sons, Inc., New York, 1967.

where $\tilde{C}_i$ (s) and $\tilde{C}_o$ (s) are the Laplace transforms of C_i (t) and C_o (t), respectively.

Rewriting, we have

$$\tilde{C}_i\ (s) = \frac{R\ \tilde{C}_o\ (s)}{(S + R)} \tag{8-8}$$

Since

$$L^{-1}\left(\frac{1}{s+R}\right) = e^{-Rt} \tag{8-9}$$

we obtain by the Convolution Theorem (reference [33], p. 1020)

$$C_i\ (t) = R \int_0^t e^{-R\tau}\ C_o\ (t - \tau)\ d\tau \tag{8-10a}$$

or

$$C_i\ (t) = R \int_0^t e^{-R(t - \tau)}\ C_o\ (\tau)\ d\tau \tag{8-10b}$$

Thus given the outside concentration as a function of time, $C_o(t)$, we may in general find the inside concentration by either of the above integral forms. This is the model proposed for use in the VM. R is the air-change (infiltration) rate. The outside concentration as a function of time, $C_o(\tau)$, is currently calculated for all cells in the VM at each time step.

An example

Suppose the outside concentration is a constant value, C^*, beginning at time, $t = 0$, up to time, $t = t^*$, as shown in Figure 8-2. Then, from equation (8-10b),

$$C_i\ (t) = \begin{cases} R \int_0^t e^{-R(t - \tau)}\ C^*\ d\tau & t < t^* \\ R \int_0^{t^*} e^{-R(t - \tau)}\ C^*\ d\tau & t \geq t^* \end{cases}$$

or

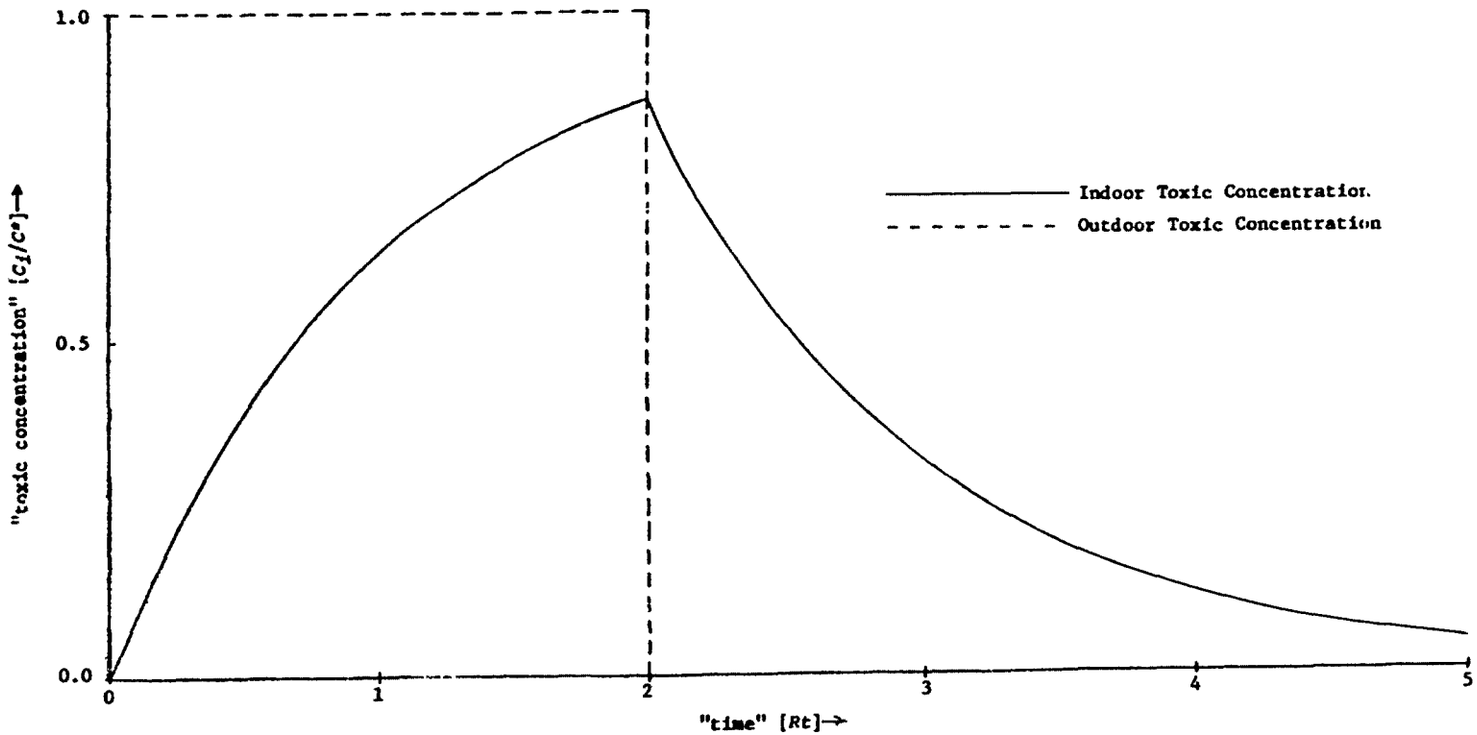

FIGURE 8-2. "Indoor Toxic Concentration" Vs. "Time" (assuming t = 2/R)*

$$C_i(t) = \begin{cases} C^* \left(1 - e^{-Rt}\right) & t < t^* \\ C^* e^{-Rt} \left(e^{Rt^*} - 1\right) & t \geq t^* \end{cases}$$

The inside concentration as a function of time is shown in Figure 8-2, assuming $t^* = 2/R$; the peak inside concentration is attained at time $t = t^*$. In general, the peak concentration is given by

$$C_{i_{max}} = C^* \left(1 - e^{-Rt^*}\right) ;$$

for large values of Rt^*

$$C_{i_{max}} \simeq C^*$$

and for small values of Rt^*

$$C_{i_{max}} \simeq C^* t^* R$$

Computational Algorithm

Although the forms given by equations (8-10a) and (8-10b) are suitable for obtaining the inside concentration given a theoretical variation with time of the outside concentration (as in the previous example), these forms are not so useful for obtaining the inside concentration in the context of the Vulnerability Model. In the VM, the outside concentration will in general be tabulated at discrete time steps. Thus it is necessary to derive an algorithm based on equation (8-10) for use in the VM.

We begin by representing the three time functions, $C_o(t)$, $C_i(t)$, and $f(t) = e^{-Rt}$, by a series of impulses (delta functions). That is, let

$$C_o(t) = \sum_{n=0}^{\infty} A_n \delta (t - nT) \qquad (8\text{-}11a)$$

$$C_i(t) = \sum_{n=0}^{\infty} B_n \delta (t - nT) \qquad (8\text{-}11b)$$

$$f(t) = \sum_{n=0}^{\infty} D_n \delta (t - nT) \qquad (8\text{-}11c)$$

where T is the spacing between the impulse functions. For now, we assume the outside concentration is tabulated at equally spaced time steps.

Further analysis will remove this restriction. For the functions to be adequately represented by the above summations, we require that the area under an impulse over any interval equals approximately the area under the function. That is,

$$\int_{(n-1/2)T}^{(n+1/2)T} C_o(t)\,dt = \int_{(n-1/2)T}^{(n+1/2)T} dt \sum_{n=0}^{\infty} A_n \delta(t - nT) = A_n$$

Therefore, for functions varying sufficiently slowly,

$$A_n \simeq T\,C_o(nT) \tag{8-12a}$$

Similarly for C_i and $f(t)$, we have

$$B_n \simeq T\,C_i(nT) \tag{8-12b}$$

$$D_n \simeq T\,e^{-RnT} \tag{8-12c}$$

Because the functions are undefined for $t < 0$, a better approximation is obtained for the first interval by

$$A_o = \frac{T}{2} C_o(0) \tag{8-13a}$$

$$B_o = \frac{T}{2} C_i(0) \tag{8-13b}$$

$$D_o = \frac{T}{2} \tag{8-13c}$$

Taking the Laplace transforms of equation (8-11), we obtain

$$\tilde{C}_o(s) = \sum_{n=0}^{\infty} A_n\,e^{-snT} \tag{8-14a}$$

$$\tilde{C}_i(s) = \sum_{n=0}^{\infty} B_n\,e^{-snT} \tag{8-14b}$$

$$\tilde{f}(s) = \sum_{n=0}^{\infty} D_n\,e^{-snT} \tag{8-14c}$$

where the A_n, B_n, and D_n are given by equations (8-12) and (8-13). Comparing these forms to equations (8-8) and (8-9), we observe that

$$\sum_{n=0}^{\infty} B_n \, e^{-snT} = R \left(\sum_{n=0}^{\infty} A_n \, e^{-snT} \right) \left(\sum_{n=0}^{\infty} D_n \, e^{-snT} \right) \tag{8-15}$$

The left-hand side is a power series in e^{-sT}, and the right-hand side is a product of two such power series. By equating terms of equal powers [67, p. 15], we obtain the relations:

$$B_0 = R \, A_0 \, D_0$$

$$B_1 = R \, [A_0 \, D_1 + A_1 \, D_0]$$

$$B_2 = R \, [A_0 \, D_2 + A_1 \, D_1 + A_2 \, D_0]$$

$$B_3 = R \, [A_0 \, D_3 + A_1 \, D_2 + A_2 \, D_1 + A_3 \, D_0] \text{ etc.} \tag{8-16}$$

Since the A_n's and D_n's are known functions obtained from equations (8-12) and (8-13), we have an algorithm for obtaining the B_n's which is equivalent to finding C_i as a function of time. In fact, we may write

$$C_i \, (nT) = \text{RT} \sum_{i=0}^{n} A'_i \, D'_{n-i} \qquad n > 0 \tag{8-17a}$$

where

$$A'_k = \begin{cases} C_0 \, (kT) & k > 0 \\ \dfrac{C_0 \, (0)}{2} & k = 0 \end{cases} \tag{8-17b}$$

$$D'_k = \begin{cases} e^{-kRT} & k > 0 \\ 1/2 & k = 0 \end{cases} \tag{8-17c}$$

and

$$C_i \, (0) = \frac{RT}{2} \, C_0 \, (0) \tag{8-17d}$$

These formulas give the internal concentrations for each time step directly in terms of the tabulated external concentrations.

Concurrence of Analysis and Empirically Obtained Principle

A rule of thumb, based on field testing, that has been used for years by the chemical-biological warfare community, is that when considering exposure of people inside buildings to toxic airborne material, the dosage inside equals the dosage outside. Using the notation used previously, we may state this axiom mathematically.

Let $D_o(t)$ represent the cumulative dose experienced outside the building. Then, according to the usual definitions,

$$D_o(t) = \int_0^t C_o(\tau)\, d\tau \tag{8-18a}$$

Similarly, if $D_i(t)$ represents the cumulative dose experienced inside the building, then

$$D_i(t) = \int_0^t C_i(\tau)\, d\tau \tag{8-18b}$$

Now the total dose, inside or out, is the dose received after a very long time, since the toxic material is released for only a finite time. Thus, we may write

$$D_o^T = \lim_{t\to\infty} D_o(t) = \int_0^\infty C_o(\tau)\, d\tau \tag{8-19a}$$

and

$$D_i^T = \lim_{t\to\infty} D_i(t) = \int_0^\infty C_i(\tau)\, d\tau \tag{8-19b}$$

where D_o^T and D_i^T are the total dose outside and inside, respectively. Now the axiom obtained empirically may be stated as

$$D_o^T = D_i^T \tag{8-20}$$

This empirical result will be shown to follow from the model of infiltration presented above. Although this does not validate the model, it does demonstrate that the model does describe correctly key features of the phenomena.

First take the Laplace transform of equations (8-18):

$$\tilde{D}_o(s) = \frac{\tilde{C}_o(s)}{s} \tag{8-21a}$$

and

$$\tilde{D}_i(s) = \frac{\tilde{C}_i(s)}{s} \tag{8-21b}$$

where the standard identity for the Laplace transform of an integral has been used. From equation (8-8) we obtain

$$\tilde{D}_i(s) = \frac{1}{s} \frac{R\tilde{C}_O(s)}{(s+R)} \tag{8-22}$$

Now we make use of the "Final Value" theorem as stated by Kuo [68]:

> "If $f(s)$ is $L\{f(t)\}$ and if $s \cdot f(s)$ is analytic on the imaginary axis and the right half of the s-plane, then
>
> $$\lim_{t \to \infty} f(t) = \lim_{s \to 0} s \cdot f(s)$$

Since the total dose is the limit of the cumulative dose as $t \to \infty$, we will attempt to apply the final value theorem to the functions, $D_O(t)$ and $D_i(t)$.

For $D_O(t)$, the outside dose, we have

$$s \cdot \tilde{D}_O(s) = \tilde{C}_O(s) \tag{8-23}$$

Since the concentration is a bounded, smoothly varying function of time (on the basis of physical reasoning), which vanishes as time becomes sufficiently large, we expect $C_O(s)$ to meet conditions of analyticity specified in the theorem. Consequently, applying the theory we obtain

$$D_O^T = \lim_{t \to \infty} D_O(t) = \lim_{s \to 0} s \cdot \tilde{D}_O(s) = \tilde{C}_O(0) \tag{8-24}$$

In the case of $D_i(t)$, we have

$$s \cdot \tilde{D}_i(s) = \frac{R\tilde{C}_O(s)}{(s+R)} \tag{8-25}$$

Since the function $\frac{R}{(s+R)}$ meets the analyticity condition and $\tilde{C}_O(s)$

---

[68] Kuo, B. C., *Automatic Control Systems*, p. 20, Prentice Hall, Englewood Cliffs, N.J., 1967.

meets the conditions for the reasons discussed above, then the product given in equation (8-25) also meets them. Consequently,

$$D_i^T = \lim_{t \to \infty} D_i(t) = \lim_{s \to 0} \left[\frac{R}{(s+R)}\right] \left[\tilde{C}_O(s)\right] \tag{8-26}$$

From an elementary theorem of calculus,

$$\lim_{s \to 0} \left[\frac{R}{(s+R)}\right] \left[\tilde{C}_O(s)\right] = \left[\lim_{s \to 0} \left[\frac{R}{(s+R)}\right]\right] \left[\lim_{s \to 0} \left[\tilde{C}_O(s)\right]\right]$$

Hence,

$$D_i^T = \tilde{C}_O(0) \tag{8-27}$$

(since $\lim_{s \to 0} \left[\frac{R}{(s+R)}\right] = 1$). Comparing (8-27) and (8-24), we obtain

$$D_O^T = D_i^T \tag{8-28}$$

which is identical to (8-20), Q.E.D.

The agreement between the result obtained from the model and the empirically based rule of thumb adds to the credibility of the model.

Parameterization of Air-Change Rate

Considerable research has been performed on infiltration into buildings by investigators concerned with heating and air conditioning systems, energy conservation, and building design. Infiltration rate has been found to increase with increasing wind speed and with increasing values of absolute temperature difference between indoors and outside. As wind flows around a building, a region of high-pressure stagnation is created on the windward side of the building and a low-pressure region is created on the leeward side. This differential pressure around the building causes infiltration flow through the building. As wind speed increases, the differential pressure increases, as does the resulting infiltration. Some infiltration may be attributed to the direct impingement of wind on breaches in the structure, such as cracks around doors and windows. As the wind speed increases, the dynamic wind pressure forces more air through these openings, so that the resulting infiltration increases. Infiltration rate also increases as the absolute value of the temperature difference between indoors and outside increases; the convective air flow generated by the temperature difference increases the infiltration rate. In the winter, cold outside air

tends to seep into the lower portion of the building and to force the warmer inside air upward and out through structural breaches in the roof and upper building. As the temperature difference increases, so does the buoyancy of the warmer inside air, so the convective flow and resulting infiltration increase. In the summertime the reverse process occurs. Cooler inside air seeps out of breaches in the lower portion of the building and is displaced by warmer outside air entering at a higher level. Again, increased temperature differentials promote natural convection and the resulting infiltration. Since both positive and negative temperature differentials produce infiltration, it is the absolute value of temperature difference that is used to describe the phenomenon.

The number of air changes due to infiltration is obtained from the Achenbach-Coblentz wind speed and temperature correlation [69]:

$$R = A + BU + C\,|\Delta\Theta| \tag{8-29}$$

where

R = infiltration rate in air changes per hour

U = wind speed, in miles per hour

$\Delta\Theta$ = temperature difference between the interior of the residence and the outside, °F

and A, B, and C are empirical constants characteristic of the residence. Their values for a typical house are:

$A = 0.25$

$B = 0.02165$

$C = 0.00833$

To demonstrate the effect of temperature and wind speed variations on the time history of indoor concentration, several cases were examined using the Achenbach-Coblentz correlation, (8-29), and the computer algorithm described in the subsection, Computational Algorithm, above. Typical values of outside toxic concentration near a liquid ammonia spill are used for the values of outside concentration, C_o. The duration of appreciable outside concentrations was for about 5 minutes (beginning about 6 minutes after the start of the simulation), reaching a maximum of 178,000 ppm of ammonia vapor in air. The time history of

---

[69] Department of Housing and Urban Development, *Residential Energy Consumption: Single Family Housing*, p. 72, HUD, March 1973.

outside concentration used in these sample computer runs is given in Table 8-5. The computer calculations give results for combinations of wind speeds of 10, 20, and 30 mph and absolute value of temperature difference of 20°F and 40°F. From the computer results, Figures 8-3, 8-4, and 8-5 were drawn for constant wind velocity, in order to demonstrate the effect of an increase in the temperature difference between indoor and outdoor air. An increased temperature difference produced a quicker initial response of indoor concentration, but the decay of the concentration was faster also. Figures 8-6 and 8-7 were drawn for constant temperatures, in order to show the effect of an increase in the wind velocity. An increased wind velocity also produced a quicker initial response of indoor concentration and a subsequent faster decay, as for the temperature difference. It is to be noted that the damage criteria are based on the integral

$$\int c^n \, dt$$

where $n \simeq 2.25$ and t is time. Since n is greater than unity, the damage criteria of indoor populations appear to be less than the damage criteria of outdoor populations.

TABLE 8-5. TIME HISTORY OF OUTSIDE CONCENTRATION USED FOR THE EXAMPLE

Time (min)	Outside Concentration (ppm)
0	0
1	0
2	0
3	0
4	0
5	8.41
6	17,100
7	178,000
8	115,000
9	15,500
10	840
11	26.5
12	0.414
13	0.0042
14	0.0000326

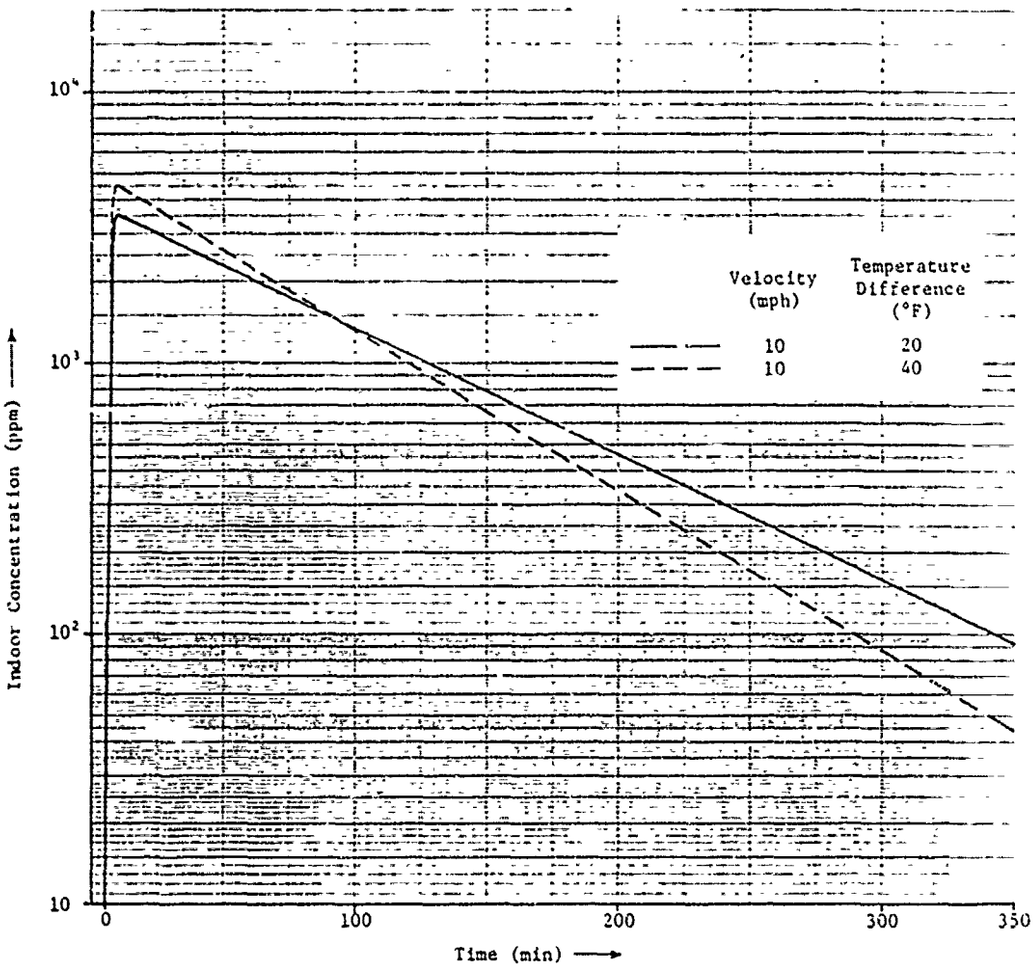

FIGURE 8-3. Concentration Vs. Time

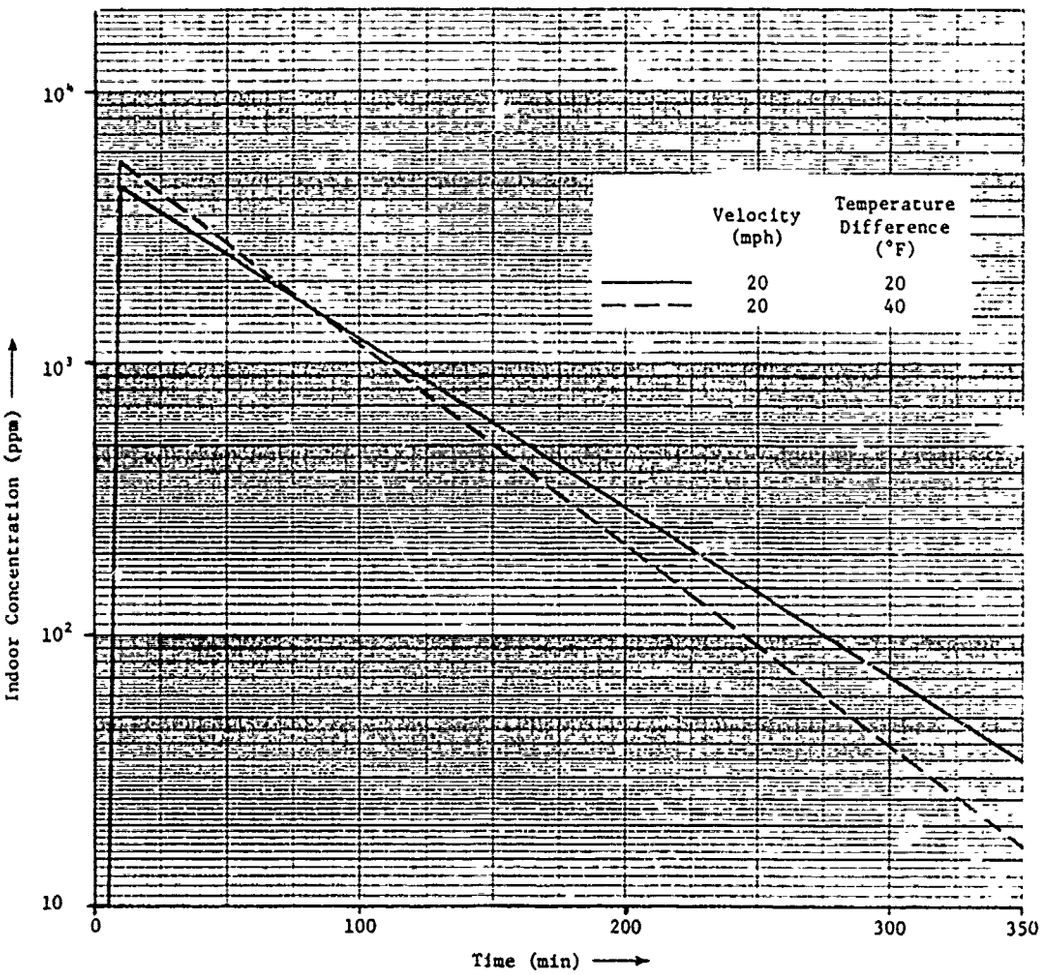

FIGURE 8-4. Concentration Vs. Time

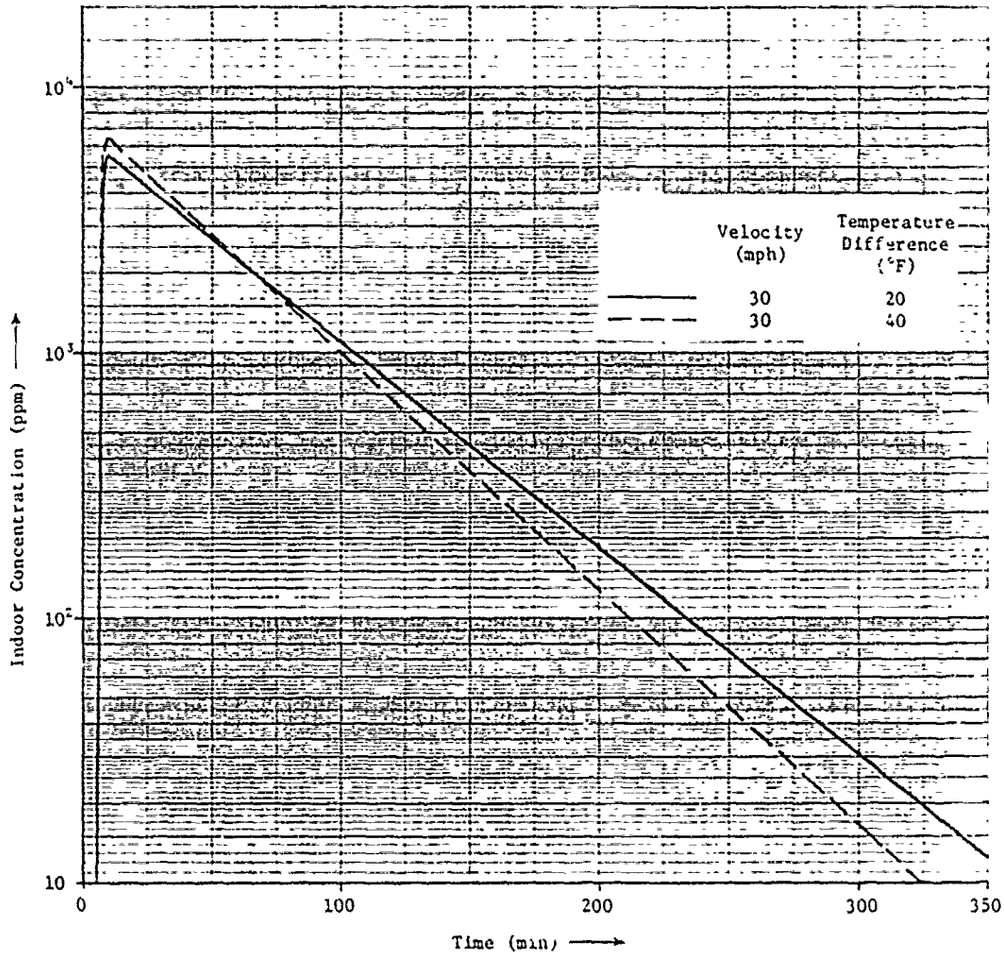

FIGURE 8-5. Concentration Vs. Time

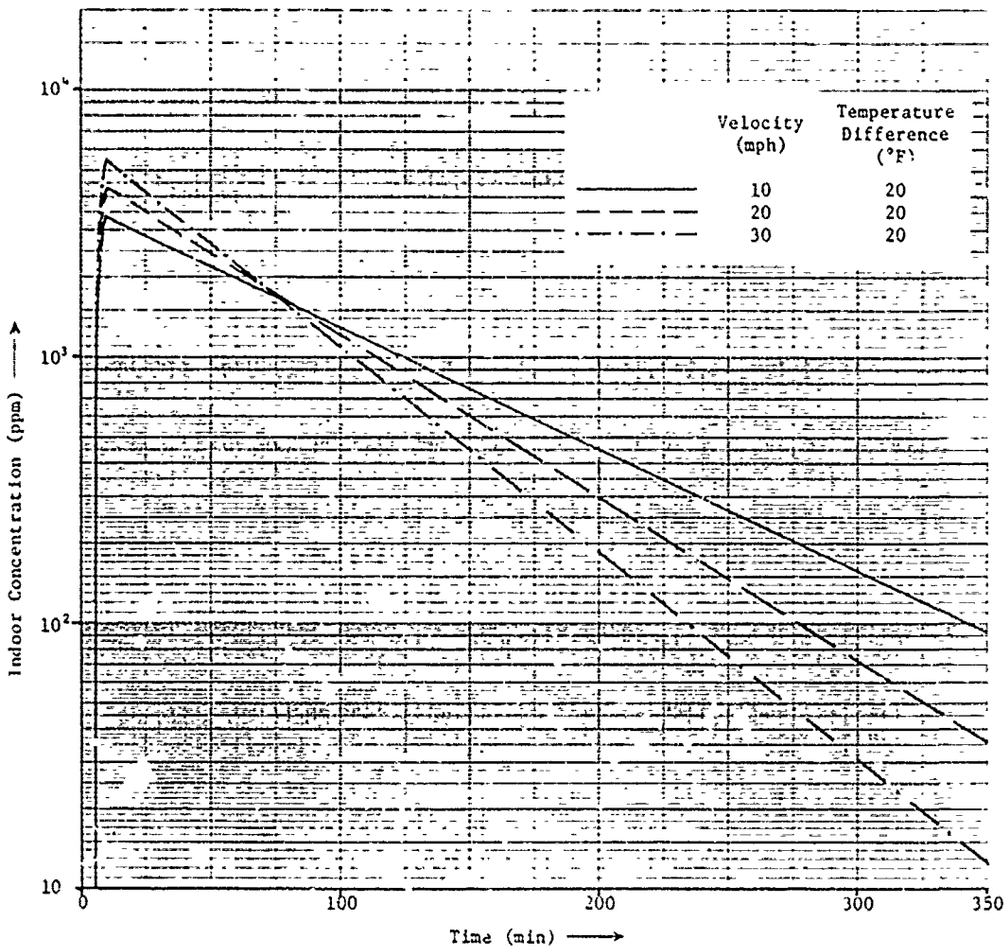

FIGURE 8-6. Concentration Vs. Time

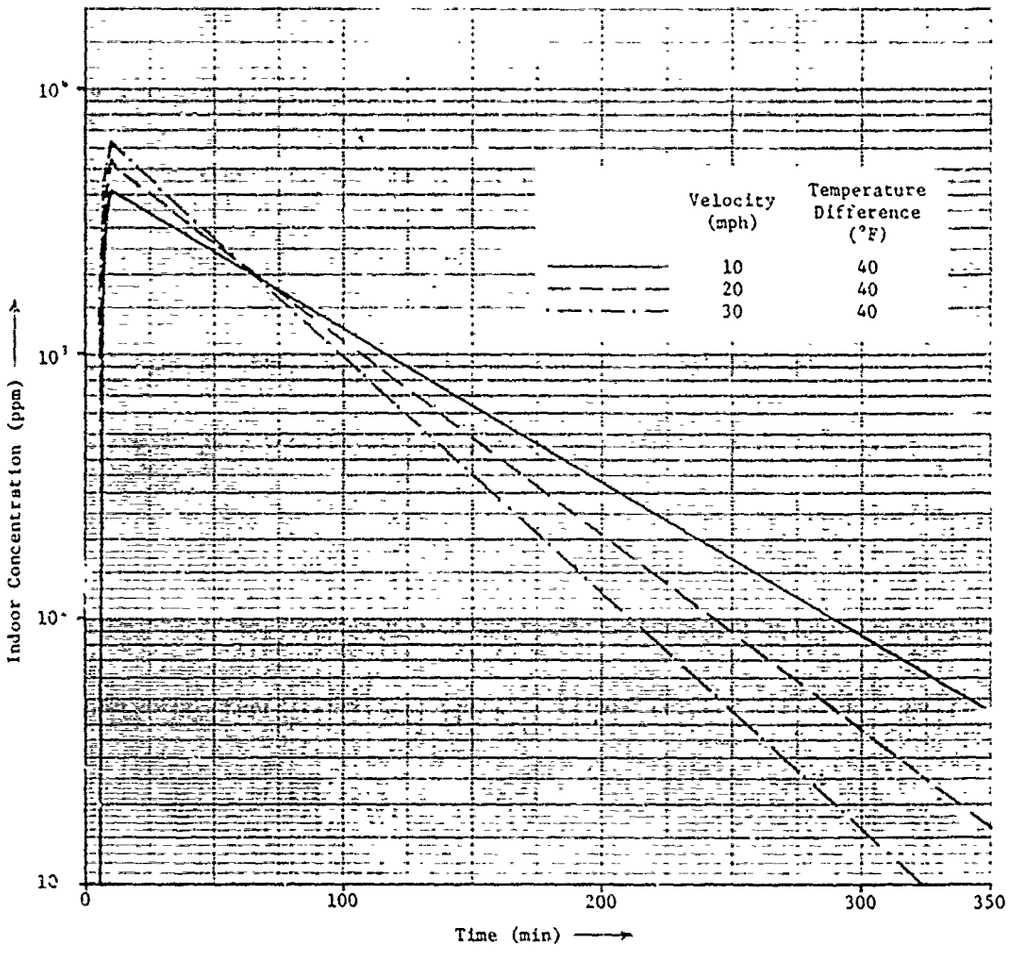

FIGURE 8-7. Concentration Vs. Time

Comparison of Infiltration Analysis With Experimental Data

C. H. Buschmann, in a recent paper [70], has presented experimental data on the infiltration of an air-dispersed gas into a typical residential structure. Freon 12 was used as a tracer to simulate releases of hazardous gases. For the infiltration test, the Freon was released continuously for 10 minutes upwind of a house. The concentration of Freon was measured as a function of time outside the house and at several locations inside the house. The plotted data reproduced from Buschmann's paper are shown in Figure 8-8.

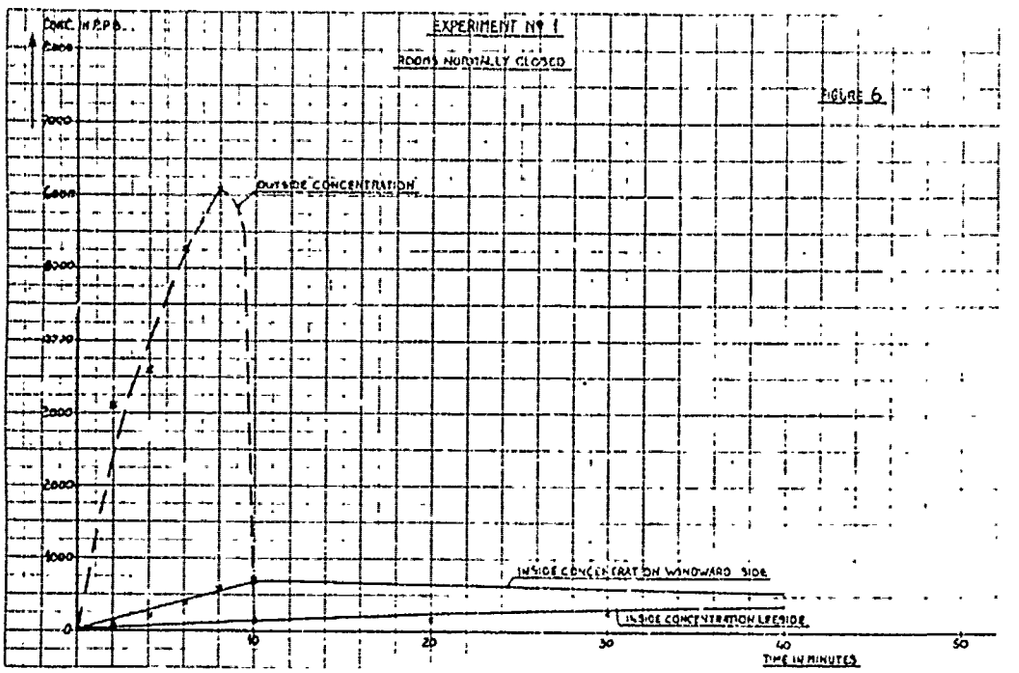

FIGURE 8-8. Buschmann's Plot of Measured Inside and Outside Concentrations [70]

[70] Buschmann, C. H., Experiments on the dispersion of heavy gases and abatement of chlorine clouds, pp. 475 ff., in *Preprints of the Fourth International Symposium on Transport of Hazardous Cargoes by Sea and Inland Waterways*, Jacksonville, Fla., October 26-30, 1975.

The measurements of outside concentration reported by Buschmann were used as input data for the computer program devised to predict inside concentration caused by infiltration. Inside concentrations predicted by the program are compared to the measured inside concentrations in Figure 8-9. Wind speed and ambient temperatures (inside and outside the house) were not reported in the referenced paper; so a wind speed of 10 mph and an absolute temperature difference of 40°F were chosen for this comparison. These choices of wind speed and temperature differential, when inserted into the Achenbach-Coblentz correlation equation, result in an infiltration rate of 0.01333 sec^{-1}. In Figure 8-9 the indoor concentration on both the windward and leeward sides are replotted from Figure 8-8. In addition, the average of these concentrations is plotted. Since the model developed here assumes complete mixing inside the building, it is the average value that is expected to be predicted. The computer-calculated prediction of indoor concentration shows a remarkable agreement with the measured average indoor concentration. Considering the lack of experimental detail given in Buschmann's paper (although he does say--on page 476--that a full report on his experiments is available), the assumptions inherent in this model, and the limitation on accuracy imposed by calculating results at one-minute time steps, the agreement between the analysis and experiment tends to validate the analysis.

Closing Remarks

The model developed here is a relatively simple description of very complex phenomena. Not taken into account are such factors as (1) the effect of interior partitions on the infiltration process, (2) the details of mixing inside the building, (3) possible buoyancy effects (heavy gases may concentrate in the basement), and (4) chemical reaction or infiltration of the toxic material with the walls or other structural features. Neglect of this last phenomenon will overestimate the hazard indoors. Neglect of the other phenomena will, in general, balance the damage assessment, overestimating in some cases and underestimating in others. In any event, the model is believed to be compatible with the anticipated data bases and to be suitable for implementation in the Vulnerability Model.

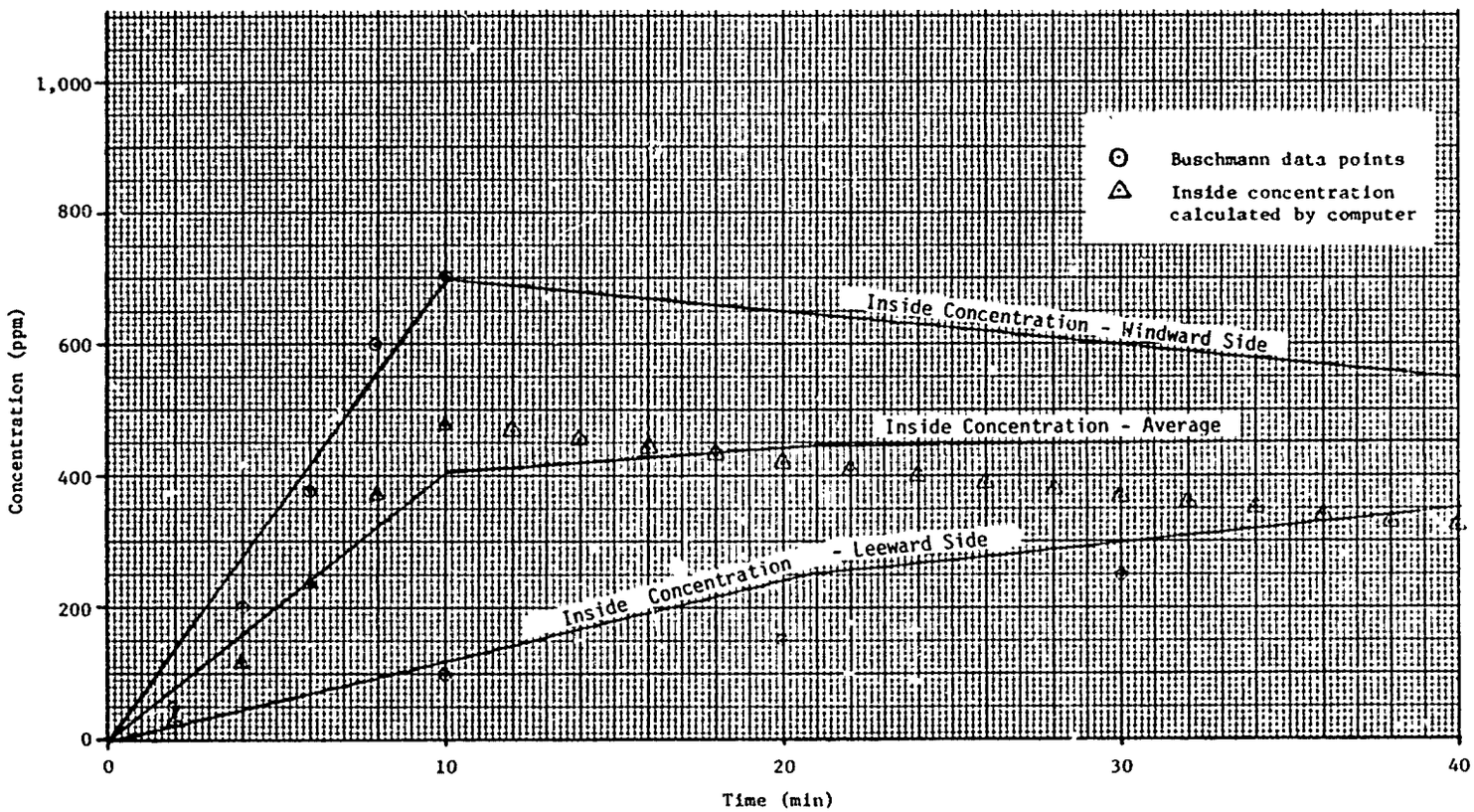

FIGURE 8-9. Comparison of Computer Calculation of Inside Concentration to Measured Data

EXPLOSION INJURY TO INDOOR POPULATIONS

Introduction

This section describes the algorithms used in the Vulnerability Model for assessing injuries to the indoor population that are caused by explosions resulting from maritime spills of detonable chemicals. The algorithms are comprised of two parts:

(1) Calculation of the adverse environment indoors.

(2) Estimation of the resulting injuries.

For the case of gas infiltration, Part 2 is identical to the assessment method used outdoors; i.e., the location of vulnerable resources inside structures modifies the adverse environment experienced but does not affect the response of the vulnerable resources to the environment. Part 1, for the case of gas infiltration, is accomplished by relating gas concentration outside to gas concentration inside through a first-order ordinary differential equation. Although this is not a simple relationship of an algebraic or functional type, the resulting numerical algorithm is readily computable and not excessively complicated.

Unfortunately, the simplifications applicable to the case of gas infiltration do not apply to the case of explosion injury. Specifically, (1) the blast environment indoors is not simply related to, nor easily computed from, data describing the shielding structure and outside blast environment; and (2) the nature of the response of vulnerable resources (people) to the indoor blast environment depends to a large degree on the characteristics of the structure. The current state of the art for assessing blast injury to indoor populations is less advanced, in the sense of yielding uniform, easily interpreted results, and at the same time requires a higher level of computational sophistication to obtain results. Consequently, the assessment of blast injury to indoor populations will necessarily be limited in the degree of confidence placed in the accuracy of the methods used.

Much of the analysis of blast injury to indoor populations has been performed in connection with nuclear weapon effects research conducted by or for agencies such as the Defense Civil Preparedness Agency (DCPA; formerly the Office of Civil Defense, OCD) and the Defense Nuclear Agency (DNA; formerly Defense Atomic Support Agency, DASA). It is from these

sources that assessment methodologies were sought; however, several problems have arisen in the application of this research for use in the VM. The following subsection discusses nuclear weapon effects research on blast effects and problems arising from the application of this research to the VM.

Nuclear Weapon Effects Research

Considerable effort has gone into researching the effects of nuclear weapons on human subjects. A significant part of the research effort has involved blast effects (e.g., see White et al. [71], Bowen et al. [72], Fletcher and Bowen [73]). Unfortunately, the information in these and other references is not directly applicable to the problem of indoor population injury for the following reasons.

1. Injury assessment for people in a given building subjected to a given free-field (outdoor) blast environment requires the use of complex computer codes with a concomitant input data requirement.

2. Aggregated damage assessment criteria for general classes of structures include nonblast damage mechanisms such as prompt nuclear radiation and thermal pulse.

3. Aggregated damage assessment criteria are usually grouped on the basis of shelter area characteristics rather than building type; i.e., basements, lower floors, and upper floors of the same building are placed in different categories.

4. Virtually all the open literature on nuclear weapon effects considers only high-yield explosions (1 megaton or greater); the damage mechanisms are significantly different for the relatively low-yield explosions of interest in the VM.

Each of these problem areas is discussed in turn in the following presentation.

---

[71] White, C. S., R. K. Jones, E. G. Damon, E. R. Fletcher, and D. R. Richmond, *The Biodynamics of Air Blast*, DNA-2738T, Defense Nuclear Agency, Washington, D.C., July 1971.

[72] Bowen, I. G., E. R. Fletcher, and D. R. Richmond, *Estimate of Man's Tolerance to the Direct Effects of Air Blast*, DASA-2113, Defense Atomic Support Agency, Washington, D.C., October 1968.

[73] Fletcher, E. R., and I. G. Bowen, Blast-induced translational effects, *Ann. N.Y. Acad. Sci. 152*:378-403, 1968.

Complexity of computational techniques

The extent of detail in which blast injury to people indoors is computed is surprising. Three steps are involved in computing this injury:

1) deriving the indoor blast environment given the free-field blast incident on the building;

2) deriving the physical response (acceleration, deceleration, collision) of persons indoors subjected to the calculated indoor blast environment; and

3) deriving the biological response, i.e., the degree of mortality or injury, given the physical response of the subject indoor population.

The third step was researched by investigators at The Lovelace Foundation and was reported in the papers cited above [71-73]. The first and second steps were investigated, and are currently under investigation, by researchers at IIT Research Institute [74-76] and Stanford Research Institute [77-78]. Detailed studies of the response of various structures to blast environments were carried out because the extent and nature of the injury inflicted on indoor populations are so contingent on the structure-dependent interior blast environment and because generalizations about the response of structures to blast are difficult to formulate. The approach (upon which is based most of DCPA's casualty predictions) of Longinow et al. [75, p. 20] to computing injury from nuclear weapons is shown in Figure 8-10. The computational steps corresponding to the three steps listed above are so indicated. The additional steps indicated in Longinow's approach have their counterparts in the VM. For example, the combining of casualty predictions for various damage mechanisms of a nuclear weapon make it impossible to subtract easily the results of damage mechanisms not operative in the VM, such as damage from ionizing radiation.

---

[74] Feinstein, D. I., *Casualty Prediction Comparisons*, Project No. J6114 (AD 676183), IIT Research Institute, July 1968.

[75] Longinow, A., G. Ojdrovich, L. Bertram, and A. Wiedermann, *People Survivability in a Direct Effects Environment and Related Topics*, Project No. J6144 (AD 764114), IIT Research Institute, May 1973.

[76] Longinow, A., E. Hahn, A. Wiedermann, and S. Citko, *Casualties Produced by Impact and Related Topics of People Survivability in a Direct Effects Environment*, IIT Research Institute, August 1974.

[77] Wiehle, C. K., and J. K. Bodsholt, *Existing Structures Evaluation*, Project No. 6300, Stanford Research Institute, July 1971.

[78] Wiehle, C. K., and J. K. Bodsholt, *Blast Response of Five NFSS Buildings*, Project No. 1219, Stanford Research Institute, October 1971.

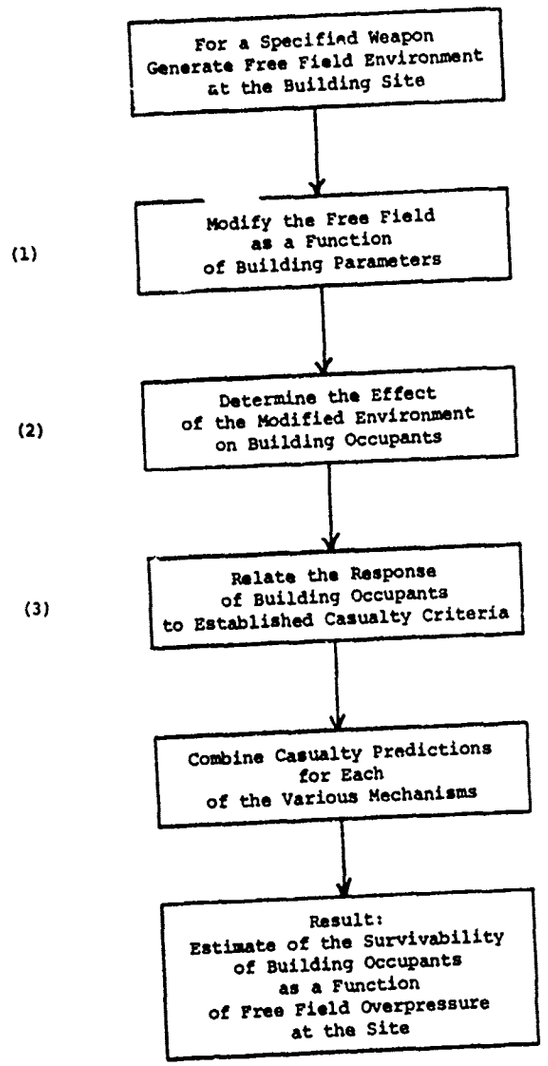

FIGURE 8-10. General Computational Process for Determining Indoor Casualties from a Nuclear Weapon (from [75], p. 20)

To demonstrate the high degree of detail used to calculate personnel injury from nuclear weapons, consider a few examples of the models used to fulfill partially the requirements indicated by computational steps (1) and (2) in Figure 8-10. An important part of defining the blast environment inside the building is the specification of the size, velocity, and location of debris and other moving objects with which the building occupants can collide and thereby be injured. Figure 8-11 shows a flowchart of the computation used to initiate the analysis of debris; this computation, although very complex, is only the beginning. A second analysis, shown schematically in Figure 8-12, traces the trajectory of most of the objects set in motion by the blast wind. Extent of detail with which the calculations represented in Figures 8-11 and 8-12 are manifested is revealed by reference to Figures 8-13 through 8-18 and Table 8 6. Figure 8-13 shows the initial fracture pattern calculated for a wall subject to a given blast loading. Figure 8-14 shows the secondary debris considered by the model to be generated by the failure of the wall. The response of each piece of the secondary debris to the blast wind is calculated and the translation of each piece is determined. Figure 8-15 shows the location of various wall fragments for a given simulation, while Figure 8-16 shows the relation between travel distance and debris weight for the same simulation.

As if these calculations for wall debris were not detailed enough, Longinow has done all parts of his nuclear weapon effects simulation to the same exacting degree. For example, not only are the motions of debris from wall failure computed, but the movements of interior furnishings are treated also. Thus, Figures 8-17 and 8-18 show the velocity histories of various interior furnishings on the first and second floors, respectively, of a building subject to blast loading. Table 8-6 shows the travel distance and flight time obtained by integrating the equations of motion.

Needless to say, the degree of detail only partially revealed by the preceding discussion is far beyond the requirements, capability, and constraints on time and resources currently characteristic of the VM. In fact, the detail represented by Longinow's models is far beyond that found useful for routine weapon effects modeling conducted by the DCPA. Rather than exercising these detailed models for every building in a city under simulated attack, the models have been exercised for a few representative structures or "shelter spaces" and damage estimates for these large classes have been established. Thus, to simulate an attack on a city, only the percentage of each type of shelter space at various distances from the explosion center need be known in order to estimate the damage. The detailed nature of each building (structural type, material, orientation with respect to the blast, etc.) need not be specified as is required for the operation of the detailed models.

It is clear that the detailed models are in theory adaptable for use in the VM, but as a practical matter their use is precluded. Thus, in order to take advantage of the considerable research previously performed

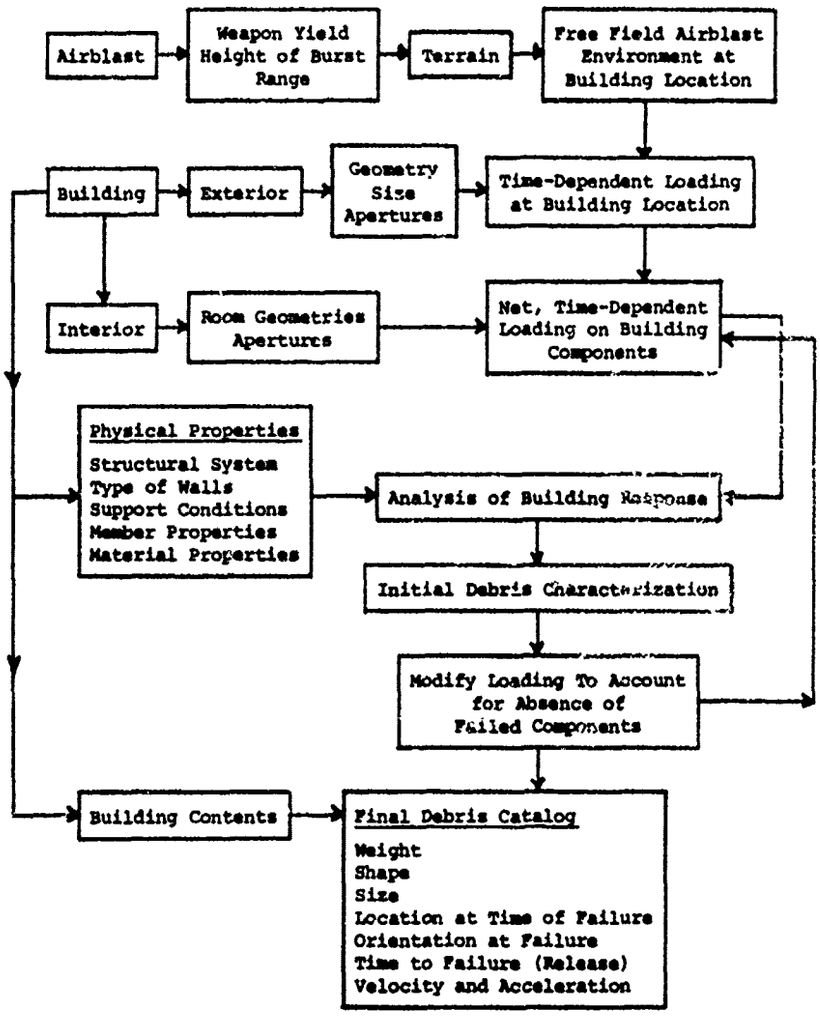

FIGURE 8-11. Loading and Response Analysis
(from [75], p. 45)

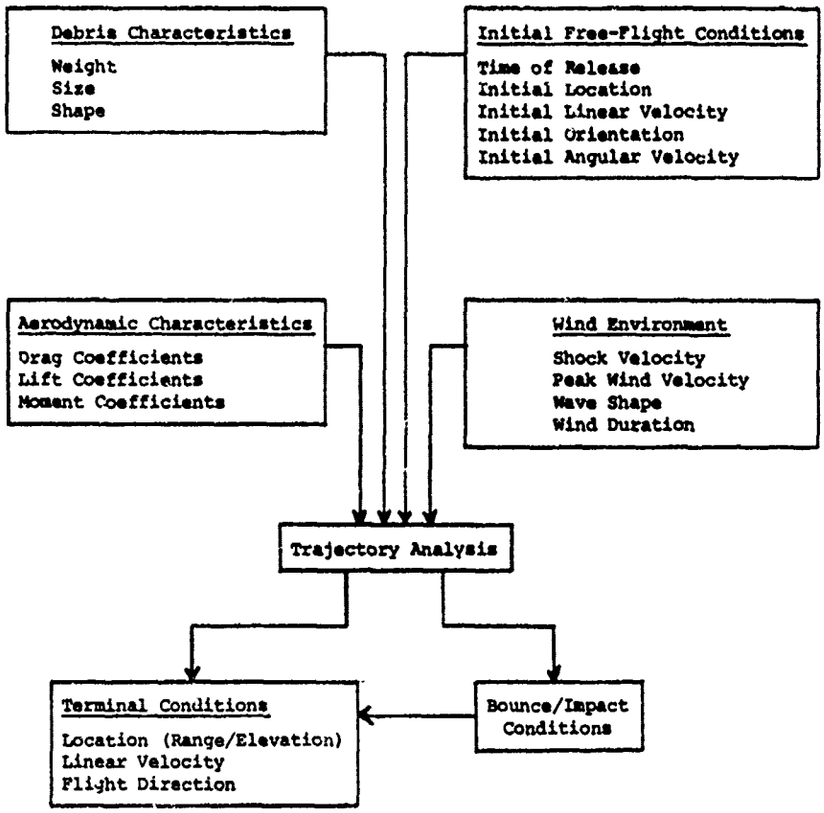

FIGURE 8-12. Debris Transport/Trajectory Analysi.
(from [75])

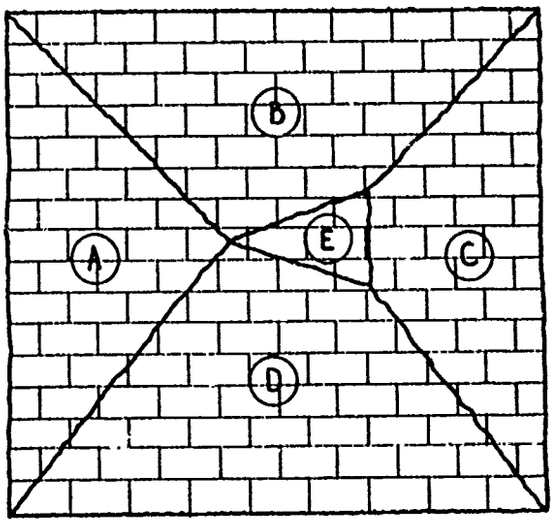

FIGURE 8-13. Wall Failure Pattern
(from [75], p. 57)

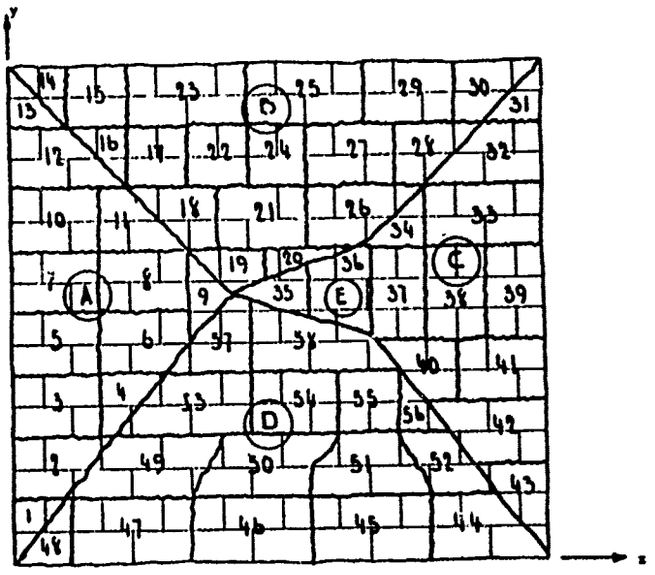

FIGURE 8-14. Secondary Debris Pattern
(from [75], p. 58)

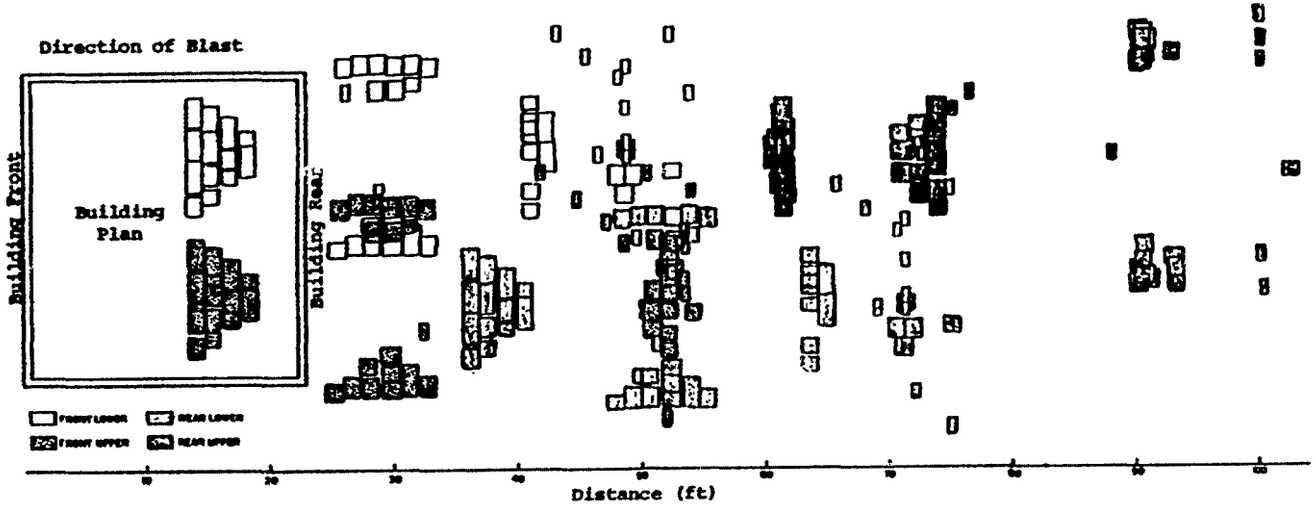

FIGURE 8-15. Distribution of Wall Debris
(from [75], p. 68)

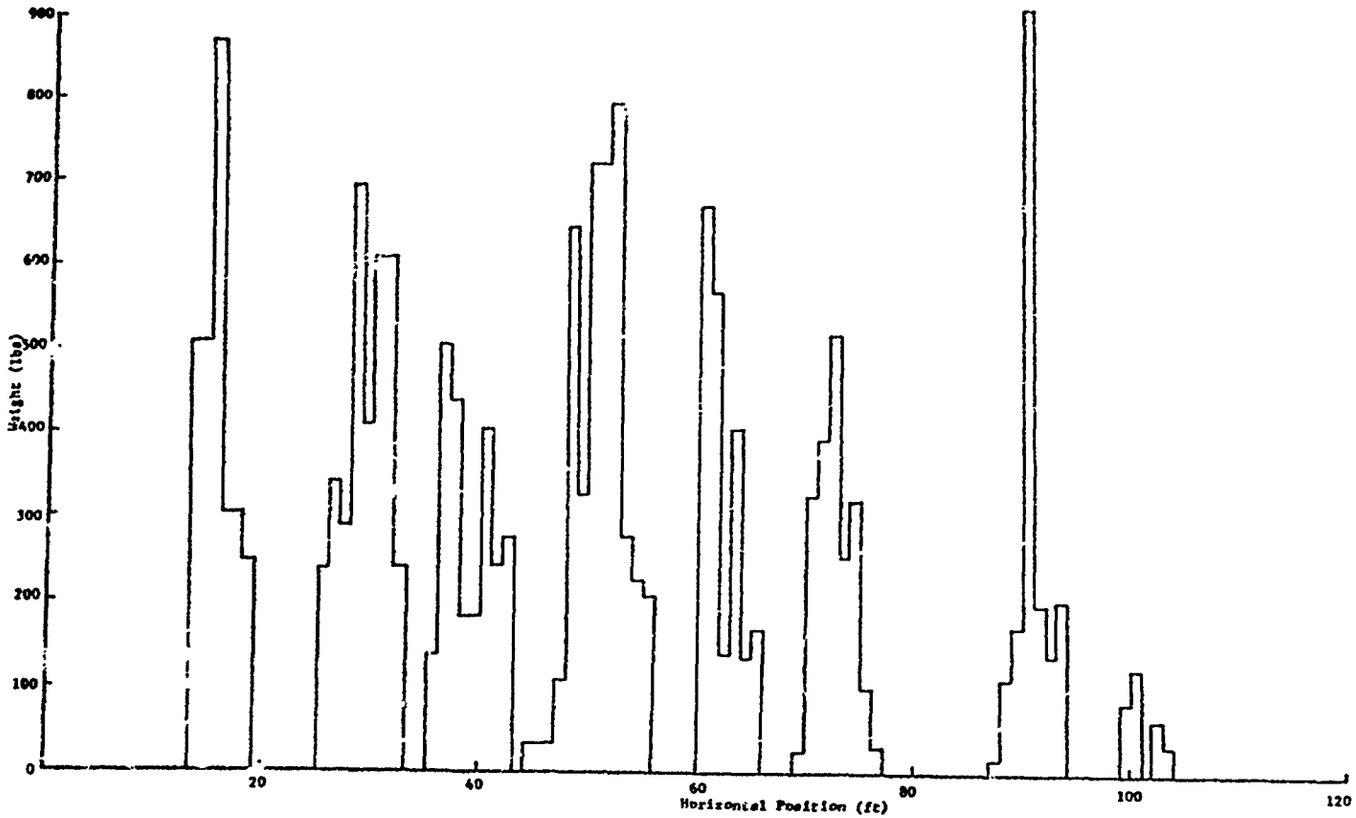

FIGURE 8-16. Weight-Distance Relationship of Wall Debris
(from [75], p. 69)

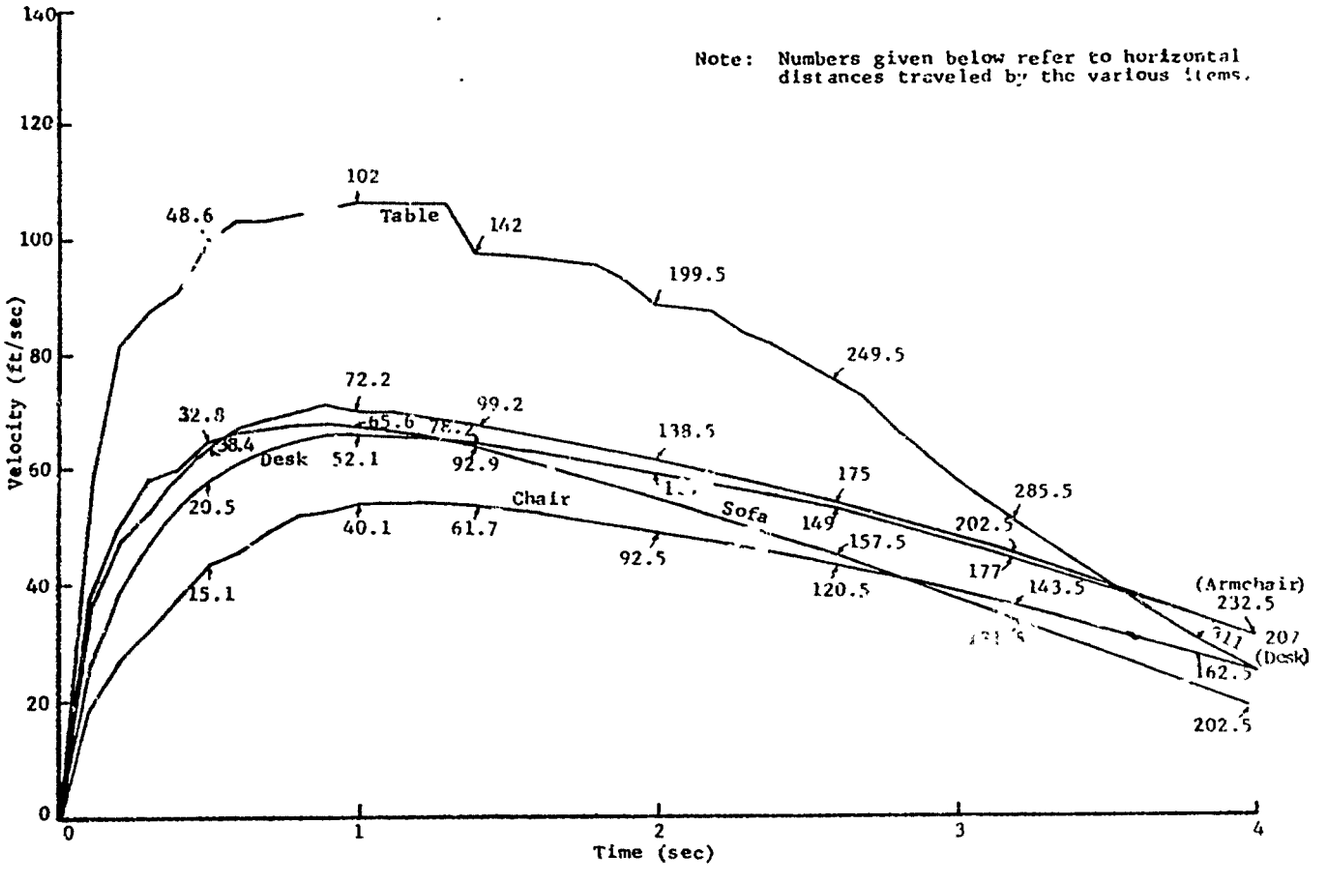

FIGURE 8-17. Velocity Histories of Furniture Items (First Floor)
(from [75], p. 71)

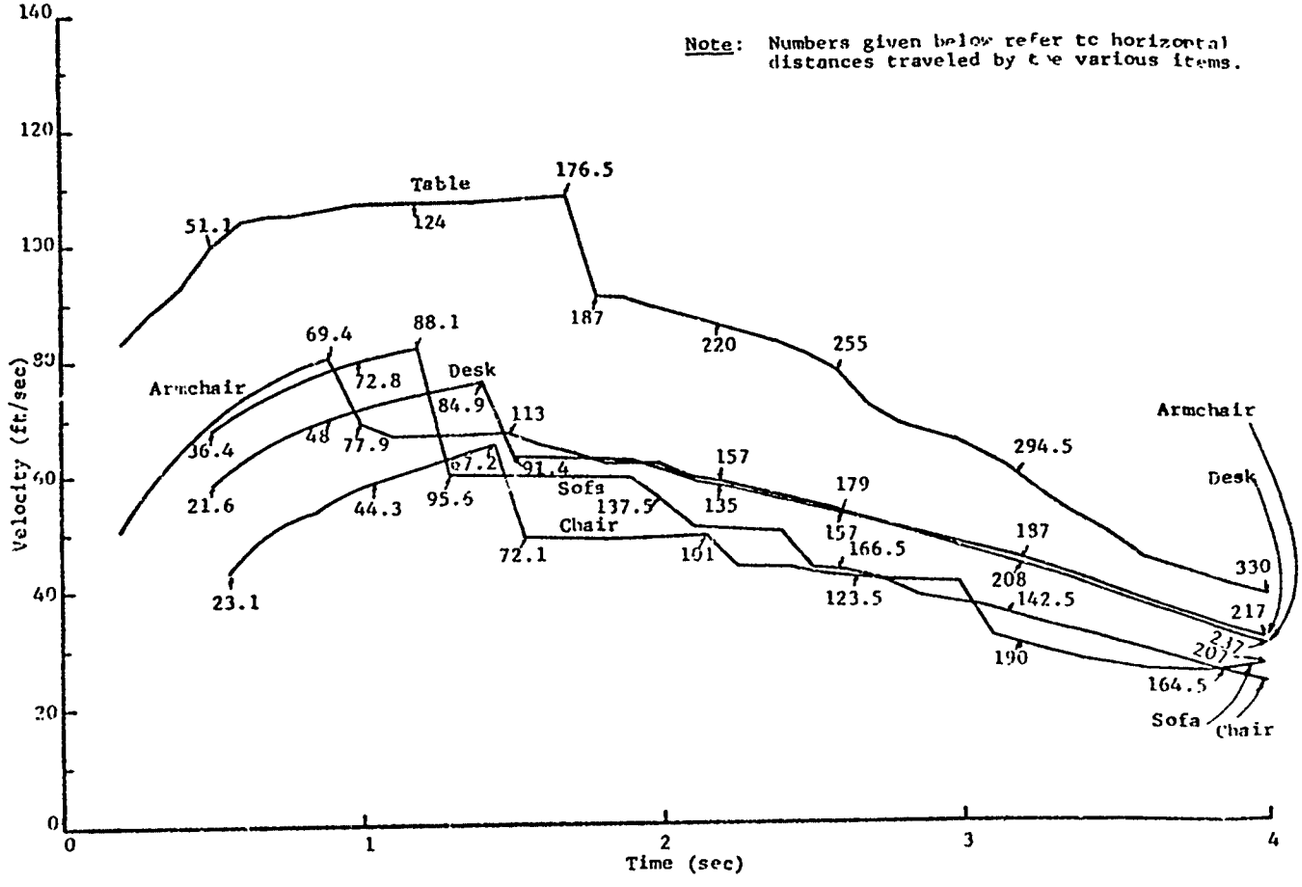

FIGURE 8-18. Velocity Histories of Furniture Items (Second Floor)
(from [75], p. 72)

TABLE 8-6. FINAL POSITIONS AND TIMES OF ARRIVAL OF FURNITURE ITEMS AND STUDWALL DEBRIS
(from [75], p. 70)

	Item	x_i^* (ft)	x_f^{**} (ft)	t_f^{***} (sec)
First Floor	Sofa	8.0	210	5.8
	Table	11.0	328	5.0
	Armchair	14.0	259	7.1
	Chair No.1	1.0	189	5.8
	Chair No.2	14.0	202	5.8
	Chair No.3	20.0	198	5.7
	Desk	2.0	238	6.0
Second Floor	Sofa	8.0	221	5.8
	Table	11.0	373	6.7
	Armchair	14.0	263	6.0
	Chair No.1	1.0	188	5.7
	Chair No.2	14.0	212	5.8
	Chair No.3	20.0	224	5.8
	Desk	2.0	246	6.0
	Plasterboard	11.5	350	6.0
	Stud	11.5	282	6.0

$^*x_i$ - initial position

$^{**}x_f$ - final position

$^{***}t_f$ - time of arrival

regarding nuclear weapon effects, use must be made of the generalized results of the detailed models, similar to the method used for the large-scale attack models. However, use of models based on data generalized and aggregated for nuclear weapon effects studies leads to several problems as described below.

Inclusion of nonblast damage in criteria

The preceding discussion gives examples of the detailed models used to define the indoor blast environment, given characteristics of the structure and the incident free-field blast wave. Similarly detailed models are used to derive the physical response of the personnel located indoors and subject to the blast environment prevailing there. One such model, developed by Longinow and used extensively by him, treats the human body as a rigid body (Figure 8-19) subject to a variety of forces: (1) pressure forces (Figure 8-20) caused by the diffraction of the interior blast wave around the body; (2) aerodynamic drag and lift forces (Figure 8-21) caused by the passage of the blast wind past the body; (3) contact forces caused by the collision of the body with solid impediments (such as floors and walls); and (4) frictional forces caused by the body sliding along the floor. These forces are summed and applied to the subject modeled as a free body (Figure 8-22); the resulting set of simultaneous differential equations are solved numerically to yield the trajectory of the subject as shown in Figure 8-23. As important as the path followed by the subject person is, the impact velocities experienced by the subject during the translation are critical, since these impact velocities have been related to the degree of biological injury [71] (as shown for lethal injury levels in Figure 8-24). Longinow has developed an even more sophisticated model using an articulated three-segment body (Figure 8-25), but this new model has not yet been extensively exercised.

In virtually all summary reports and manageable models used to describe the effects of nuclear weapons, damages caused by various mechanisms are combined to give an aggregate measure of damage for a given level of weapon potency. In addition to the primary and secondary blast mechanisms of interest in the VM, nuclear weapon effects models consider the additional damage mechanisms of ionizing radiation and thermal radiation. For example, see Figure 8-26 for a schematic of the damage mechanisms and effects considered by Longinow. Obviously, nuclear radiation is not a meaningful damage mechanism for the nonnuclear chemical explosions to be simulated by the VM. Although some heat and hot gases usually accompany a chemical explosion, in no case do any phenomena even remotely equivalent to a nuclear fireball occur. In fact, energy used to form a fireball or to radiate heat away from the combustion zone is unavailable for producing blast phenomena; consequently, significant thermal effects occurring simultaneously with significant blast effects are precluded for chemical explosions. The fireball phenomena resulting from spills of combustible liquids are discussed elsewhere and exclude significant blast phenomena. Thus, to be useful in the VM, models should only consider primary and seconda y blast damage.

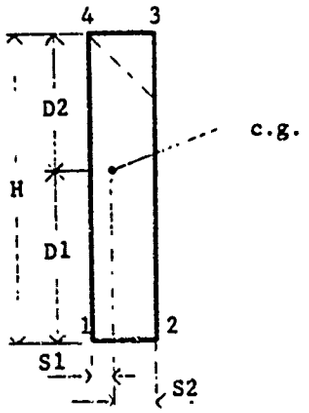

Weight	165 lbs
Height, H	5.77 ft
Height to c.g., D_1	3.20 ft
S_1	0.29 ft
S_2	0.625 ft
Width (out of plane)	1.56 ft
Moment of inertia	8.58 (lb-sec^2-ft)

FIGURE 8-19. Rigid Body Model (from [75], p. 117)

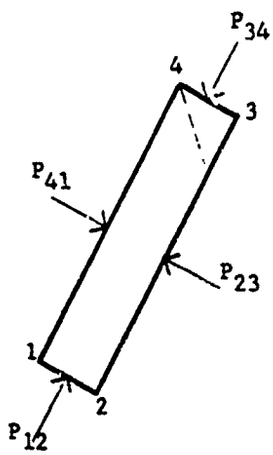

$$P_{12} = 1/2(P_1 + P_2) \cdot (S_1 + S_2) \cdot W$$
$$P_{23} = 1/2(P_2 + P_3) \cdot H \cdot W$$
$$P_{34} = 1/2(P_3 + P_4) \cdot (S_1 + S_2) \cdot W$$
$$P_{41} = 1/2(P_4 + P_1) \cdot H \cdot W$$

FIGURE 8-20. Pressure Force Notation (from [75], p. 117)

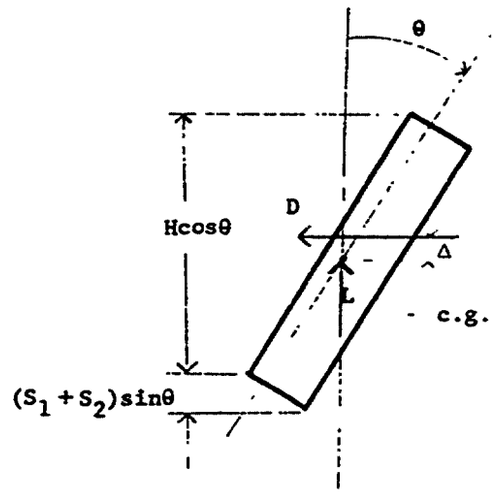

FIGURE 8-21. Drag and Lift Forces
(from [75], p. 119)

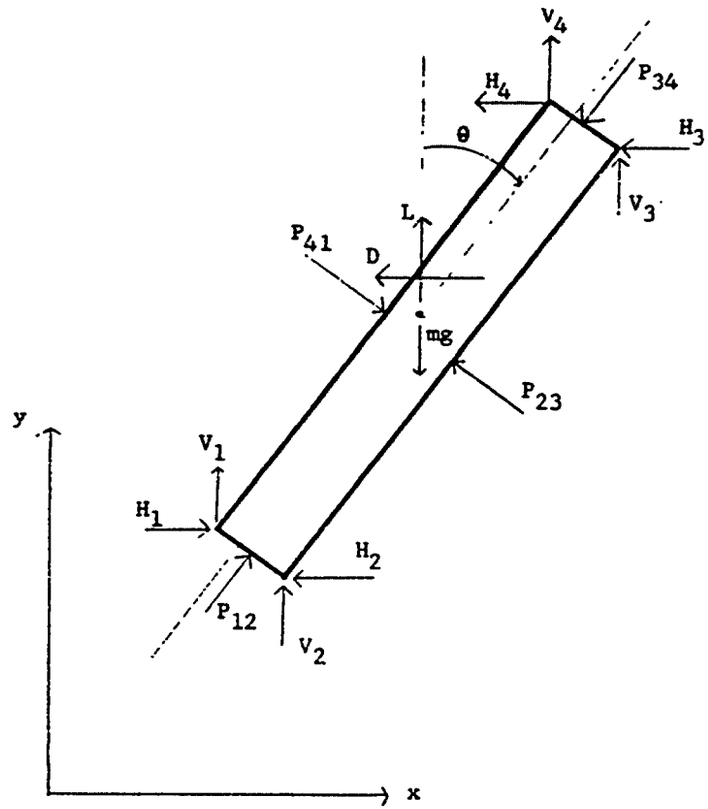

FIGURE 8-22. Tumbling Man -- Free Body
(from [75], p. 122)

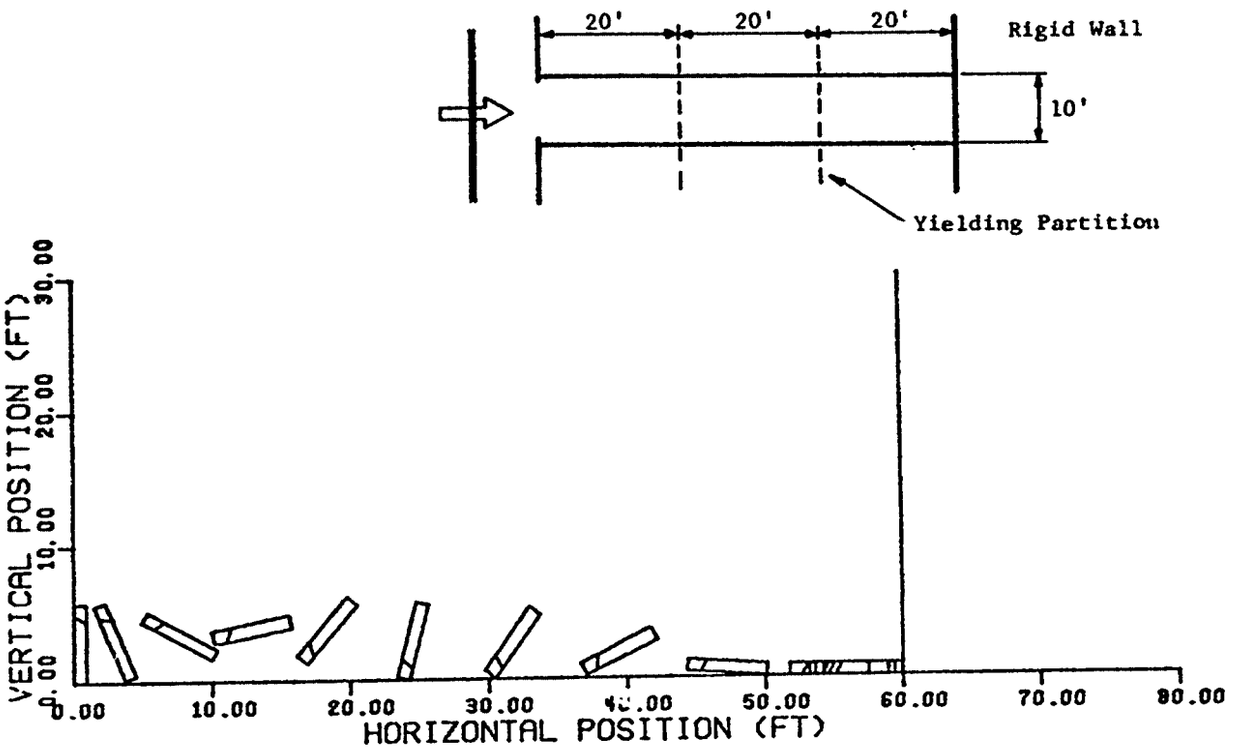

FIGURE 8-23. Sample Trajectory Plot (from [75], p. 124)

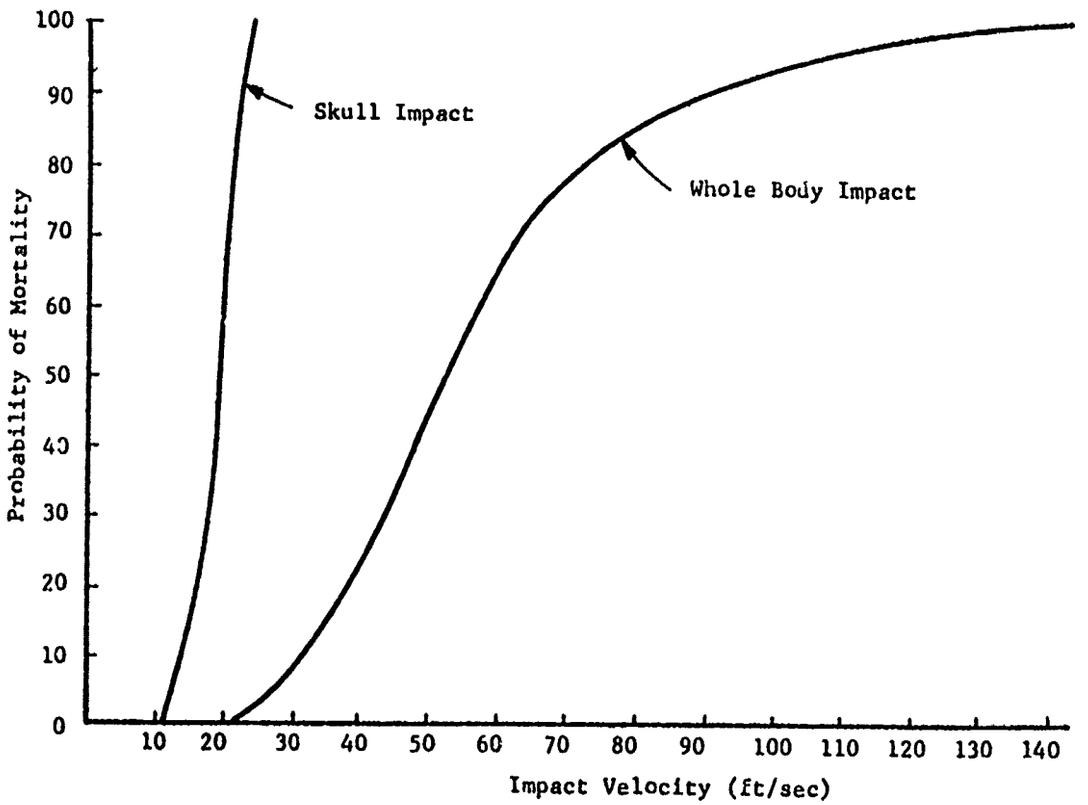

FIGURE 8-24. Impact Fatality Criteria (from [75], p. 126)

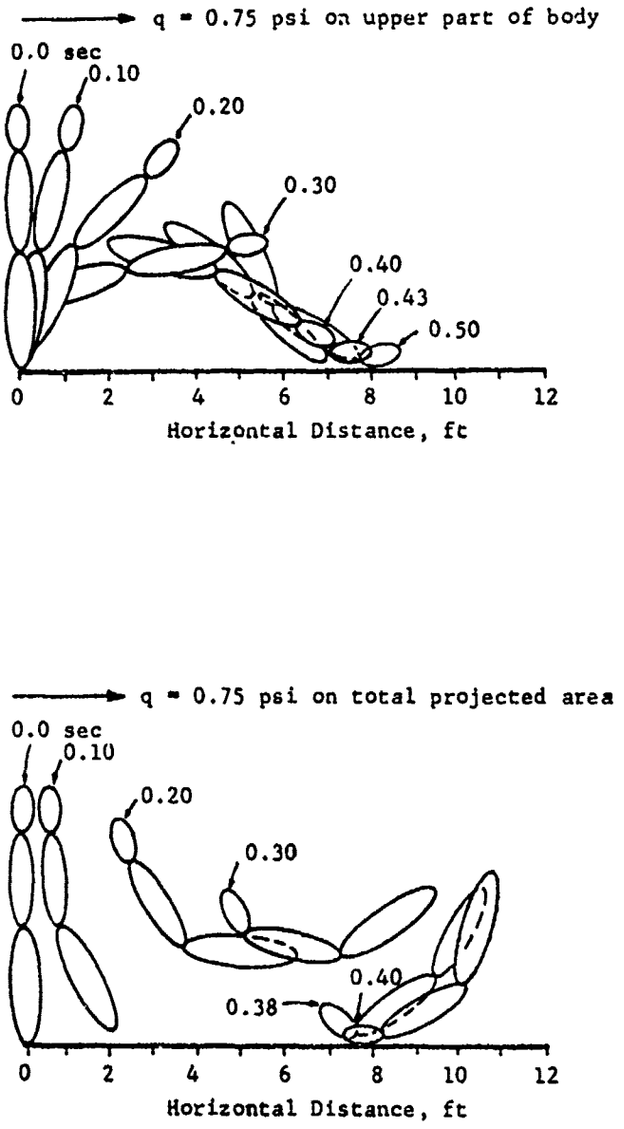

FIGURE 8-25. Trajectory of Articulated Tumbling Man
(from [75], p. 151)

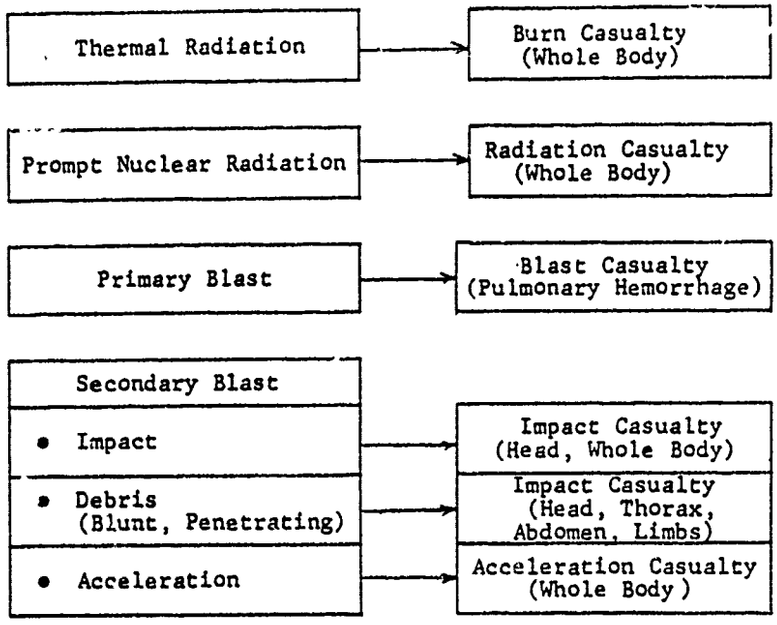

FIGURE 8-26. Effects and Casualty-Producing Mechanisms Considered in the Operational Simulation Model (from [75], p. 15)

Although the models, used to generate the basic data upon which nuclear weapon casualty predictions are based, compute the influence of each damage mechanism separately, published, accessible, manageable casualty models have lumped the influence of all damage mechanisms together. Table 8-7 is a rare instance in which casualty predictions based on each mechanism acting alone were displayed before combining the influence of all mechanisms shown in Table 8-8. Notice that in this case, as in most nuclear weapon effects studies, the level of damage is related to a single parameter characterizing the weapon environment, viz. free-field overpressure. As will be discussed below, for the large explosions (100 kT or greater TNT equivalent) considered by virtually all of these studies, free-field overpressure uniquely specifies both the blast and nonblast environments created by the nuclear weapon. The breakdown of survivability by damage mechanism, as shown in Table 8-7, was performed for illustrative purposes; a more typical display of survivability estimates, in which all damage modes are combined, is shown in Figure 8-27. Unfortunately, from such a display there is no readily apparent means to subtract out damage caused by thermal radiation and nuclear radiation. As shown by the values in the 4th and 7th columns of Table 8-7, effect on mortality of thermal and ionizing radiation is not overwhelming but neither is it negligible. For this reason, the large quantity of damage estimates and related material, generated at great expense over many years to estimate nuclear weapon effects, is not adaptable for use in the VM.

Aggregation of damage criteria by shelter space

A third barrier to the utilization of nuclear weapon effects research in the VM is that damage estimates are aggregated on the basis of shelter space type rather than on the basis of building category. The emphasis on shelter space category in previous work done for the DCPA (previously OCD) was motivated by the desire to determine the benefits of early warning and transfer of the populace to "fallout" shelters. A surprise attack without any warning was not considered to be a very likely occurrence, so that scenario was not given great emphasis. Of course, for the VM, a "complete surprise" scenario is the rule rather than the exception.

The types of shelter spaces considered in the analyses performed by DCPA are listed in Table 8-9 [79]. Different parts of the same building have different shielding capacities, and therefore exposure to the same free-field blast environment will cause different levels of personnel injury depending upon location within the building. For example, the members of the pairs of spaces (D,F) and (H,I) each refer to the same building type but possess different shielding abilities. The differences in blast protection afforded by different locations in the same building are reflected in the value estimated as the mean

---

[79] Defense Civil Preparedness Agency, *DCPA ATTACK ENVIRONMENT MANUAL, Chapter 2, What the Planner Needs To Know About Blast and Shock,* CPG 2-1A3, DCPA, June 1973.

TABLE 8-7. PERCENT SURVIVORS FOR INDIVIDUAL EFFECTS
(from [76], p. A-20)

EXAMPLE BUILDING NO. 1

PERCENT SURVIVORS

OVERPRESSURE (PSI)	DEBRIS (STANDING)	DEBRIS (PRONE)	THERMAL	TRANSLATION (STANDING)	TRANSLATION (PRONE)	IONIZING RADIATION
1	100.0	100.0	100.0	100.0	100.0	100.0
2	100.0	100.0	99.2	99.9	100.0	100.0
3	100.0	100.0	99.2	99.2	100.0	100.0
4	99.2	99.0	98.4	99.0	100.0	100.0
5	76.2	68.9	97.9	80.5	100.0	100.0
6	60.9	55.7	97.1	56.9	100.0	100.0
7	62.9	54.6	96.4	49.5	100.0	100.0
8	58.8	53.6	92.5	47.6	100.0	100.0
9	57.1	53.1	91.1	31.7	100.0	100.0
10	53.9	40.8	91.0	.0	38.9	100.0
11	48.8	37.4	91.0	.0	19.8	100.0
12	43.8	34.1	91.0	.0	17.5	100.0
13	41.2	32.6	91.0	.0	15.3	100.0
14	38.6	31.1	91.0	.0	13.1	100.0
15	39.2	31.4	91.0	.0	6.6	100.0
16	39.8	31.7	91.0	.0	.0	78.2
17	41.3	32.4	91.0	.0	.0	52.8
18	42.8	33.2	91.0	.0	.0	27.4
19	45.6	35.0	91.0	.0	.0	1.9
20	48.4	36.8	91.0	.0	.0	.0

TABLE 8-8. TOTAL SURVIVORS (from [76], p. A-21)

EXAMPLE BUILDING NO. 1

OVERPRESSURE (PSI)	TOTAL SURVIVABILITY STANDING	PRONE
1	100.0	100.0
2	99.1	100.0
3	98.4	100.0
4	96.6	99.0
5	60.0	68.9
6	36.9	55.7
7	29.3	54.6
8	25.9	53.6
9	16.5	53.1
10	.0	15.9
11	.0	7.4
12	.0	6.0
13	.0	5.0
14	.0	4.1
15	.0	2.1
16	.0	.0
17	.0	.0
18	.0	.0
19	.0	.0
20	.0	.0
10 PERCENT	9.39	10.69
50 PERCENT	5.43	9.08
90 PERCENT	4.18	4.30

Frame Type: Reinforced concrete
Plan Dimensions: 53' x 140'
Height: 69'
Number of Floors: 6
Exterior Wall Type: Two-way unreinforced masonry NLBW with arching action
Material: 4" brick, 8" structural clay tile
Typical Strength: 11.6 psi
Aperture Percent: 10
Interior Partitions: Clay tile/wood studwalls

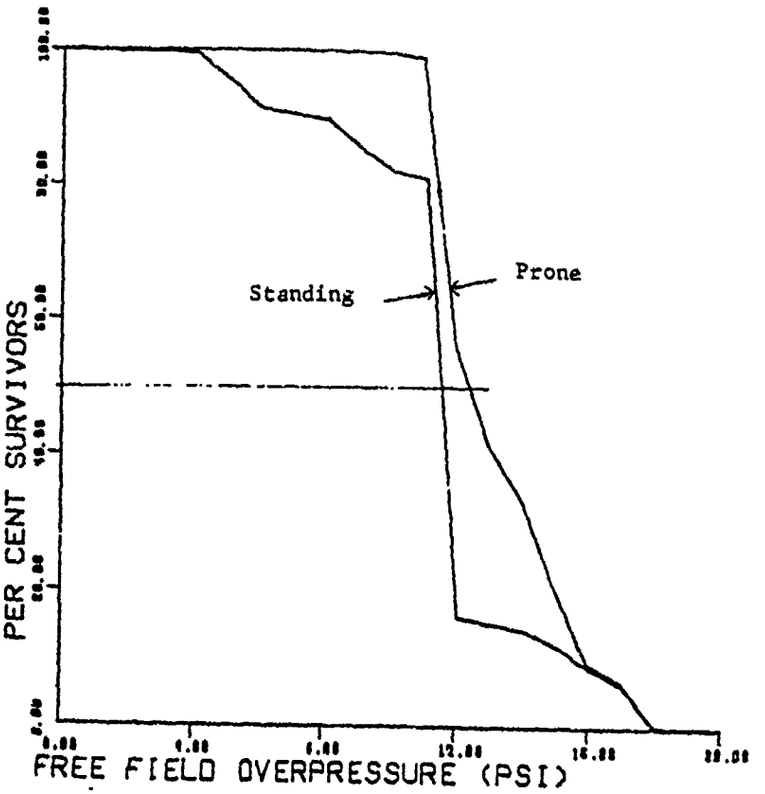

FIGURE 8-27. Upper Floor Survivability Estimates, Building 204, Brady Moving and Storage Building. An example of typical, combined-effects damage criteria. (from [75], p. 27)

TABLE 8-9. TYPES OF SHELTER SPACES
(from [79])

RELATIVE BLAST PROTECTION	
Preference	Description
A	Subway stations, tunnels, mines, and caves with large volume relative to entrances
B	Basements and sub-basements of massive (monumental) masonry buildings
C	Basements and sub-basements of steel and reinforced-concrete framed buildings having flat slab or slab and beam ground floor construction
D	First three floors of buildings with "strong" walls
E	Basements of wood-frame and brick-veneer residences
F	Fourth and higher floors of buildings with "strong" walls
G	Basements of steel and reinforced-concrete framed buildings with flat plate ground floor
H	First three floors of buildings with weak walls, brick buildings and residences
I	Fourth and higher floors of buildings with weak walls

lethal overpressure for that location. The mean lethal overpressure (MLOP) is that free-field overpressure which will result in 50% lethality in the given location. Table 8-10shows the difference between mean lethal overpressure above and below ground in two types of buildings. A more typical example of injury estimates is shown in Table 8-11 [80], where further aggregation has been done (combining various classes of shelter spaces listed in Table 8-9) and primary emphasis is on sheltered areas. The estimates shown in Table 8-11 have been used extensively for nuclear weapon vulnerability studies.

---

[80] Memorandum for Deputy Assistant Director, R&E from George N. Sisson, 8 November 1974, Subject: Revision of Relative Blast Protection Codes, DCPA, Attachment 3.

TABLE 8-10. VARIATION IN MEAN LETHAL OVERPRESSURE WITH LOCATION FOR THE SAME BUILDING (from [79])

BLAST PROTECTION IN CONVENTIONAL BUILDINGS		
Location	Median Lethal Overpressure[a]	
	Residences	NFSS[b] Buildings
Above ground	5 psi	7 psi
Below ground	10 psi	12 psi

[a]The median lethal overpressure is that blast overpressure at which 50 percent of the occupants may be expected to be fatally injured.

[b]National Fallout Shelter Survey.

TABLE 8-11. PERSONNEL INJURY ESTIMATES USED FOR NUCLEAR WEAPON VULNERABILITY STUDIES (from [80], Attachment 3)

	MLOP[a]	MIOP[b]
1. Mines, Caves, Tunnels, etc. (Code A)	35	--
2. Best Available NFSS Basements (Codes B & C)	10	7
3. Upper Story NLBW[c]-A (Codes E & F) (strong-walled - less than 10 stories)	8	2
4. Tall Building Upper Story Space, Weak-Walled Upper Story Space, and Weak Basements (Codes G, H, & I)	5	2
HOMES: (Code I) Above ground	5	2
(Code D) Basements	10	4

[a]Mean Lethal Overpressure.

[b]Mean Injury Overpressure.

[c]Non-Load-Bearing Wall.

Because of the manner in which the data have been aggregated, it is difficult to derive from this information a damage criterion representative of an entire building. Although it might be possible to obtain damage estimates for various portions of a single building, this would require data not currently in the VM data base and would complicate the computation to an undesirable degree.

Low-yield explosion phenomena

The fourth and virtually insurmountable barrier to utilizing nuclear weapon effects studies in the VM is that those studies have assumed weapon sizes of 1 Mt (one megaton TNT equivalent) or larger, while the VM is interested in explosions no larger than, say, 50 kt and usually is interested in much smaller explosions. As the size of an explosion varies over several orders of magnitude, both the blast environment created by the explosion and the effect of that environment on vulnerable resources change. Since the phenomenology involved in producing damage changes as explosion size varies, it is impossible to obtain simple scaling laws for explosion damage and extremely difficult to obtain any measures of how damage criteria change with explosion size.

As an example, consider Figure 8-28 in which the variation of impulse with explosion yield is shown parameterized by overpressure. For a fixed value of overpressure, impulse increases as yield increases. In view of this information, consider a simplistic treatment of personnel injury caused by glass breakage and the impact of broken glass shards on subject personnel. For injury of this type to occur, 1) the glass must be broken and 2) the fragments must be accelerated to a speed sufficient to penetrate the skin. (Of course the fragments must impact on somebody, but this aspect of the problem need not concern us here.) For a blast wave of sufficient duration, the breakage of the glass depends only on the peak overpressure of the the blast wave. An overpressure of 1 psi may be assumed sufficient to shatter a windowpane; but in order to cause injury the fragments must be accelerated, and this can be taken to depend on the impulse of the blast wave. Hence, for a free-field overpressure of 1 psi, injury of this type will certainly occur at high yields but may not or will be reduced at low yields. Obviously, peak overpressure is not a suitable variable to parameterize injury in this situation (contrary to the virtual universal practice in nuclear weapons studies, where high yields are assumed). Then why not use blast wave impulse as the injury parameter? A similar difficulty arises. Suppose we postulate that a minimum impulse level of 100 psi-msec is required to accelerate fragments sufficiently to cause damage. Then for a yield of 30 tons, both overpressure (2 psi > 1 psi) and impulse (= 100 psi-msec) are great enough to cause injury. However, at a higher yield of 0.3 kt, at an impulse of 100 psi-msec the overpressure is too small ($<$1 psi but $>$0.5 psi) to cause injury. Thus, impulse is not a suitable injury parameter alone either. Since two different phenomena, depending on different parameters of the blast wave, cause the injury, a simple parametric relation for injury is precluded and the influence of yield must be considered. Actually, the situation is worse than this. For low-yield explosions, the breakage of glass is no longer solely dependent on peak overpressure but depends also on blast wave duration --

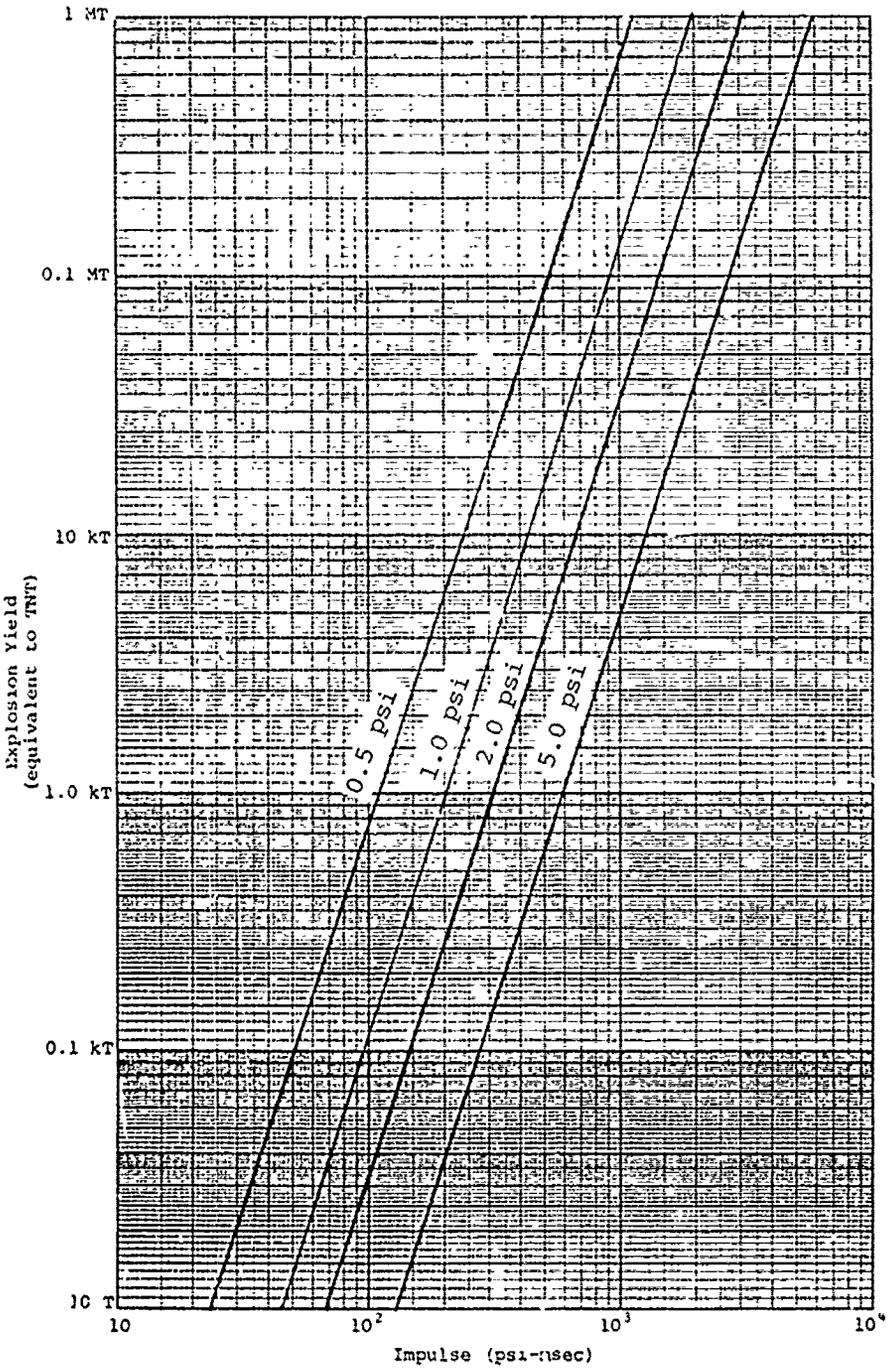

FIGURE 8-28. Variation of Impulse With Yield at Various Overpressure Levels

a yield-related parameter. The influence of yield, at low-yield values, is ubiquitous and must be considered.

The influence of yield on other types of blast injury is similarly universal and complex. For example, wall failure depends in a complex manner on peak overpressure and positive-phase duration of the blast wave. On the other hand, the acceleration of the debris formed by wall collapse depends on impulse or alternatively on blast-wind magnitude and duration. The injury caused by debris to subject personnel depends in a complex manner on both debris formation and acceleration. Injury from translation is similarly complex. Both blast wind and peak overpressure accelerate the subject personnel. However, the degree to which these phenomena occur within the building depends upon the survival, or non-survival, of the building walls. Furthermore, for long-duration blast winds, subject personnel will tend to be accelerated to the prevailing velocity of the blast wind. However, for short-duration blast winds, as will occur in low-yield explosions, the subject personnel may not be accelerated to the prevailing velocity before the wind dies out. Consequently, the entire indoor damage scenario is changed. Thus, obtaining injury criteria for low-yield explosions by simple physical scaling without reiterating years of research into nuclear weapon effects appears to be beyond reach.

Recent Advances by DNA in Low-Yield Damage Estimation

In spite of all the difficulties alluded to above, some progress has been made in determining damage criteria for low-yield explosions. Unfortunately, the report [81] presenting the details of this progress is classified (Confidential), and the results contained therein cannot be fully expounded at this time. An effort was made to have that information most relevant to the VM released, so that the results of the study may be employed, even if the methodology and rationale used to obtain the results remain classified. This effort was successful in obtaining the declassification of certain key information (Figures 2-2 through 2-8 in the referenced report; Figures 8-29 through 8-35 in this report).*

The referenced report uses a method to relate free-field overpressure to damage level that is equivalent to the probit analyses used previously in the VM. The method employed in the report is stated as follows.

---

[81] Fricke, Martin P., Preliminary civilian casualty criteria for low-yield nuclear weapons (U), DNA 3547T, Confidential Report, Defense Nuclear Agency, 1 April 1975.

*Mr. J. F. Moulton, Jr., Chief, Aerospace Systems Division, Defense Nuclear Agency, was most gracious in devoting his time and effort to assist ECI and the USCG in this matter.

The fraction of people experiencing fatality is given by the variable, P, defined by

$$P\left(\frac{D}{D_{50}}, \frac{\sigma}{m}\right) = \frac{1}{\sqrt{2\pi}} \int_{-\frac{1}{\beta} \ln \frac{D}{D_{50}}}^{\infty} e^{-t^2/2}\, dt \tag{8-30}$$

where

D is the value of free-field overpressure experienced

D_{50} is the value of free-field overpressure at which 50% of the population is affected

$\frac{\sigma}{m}$ is a parameter taken by the investigators to have a value of 0.3

and

$$\beta = \left(\ln\left[\left\{\frac{\sigma}{m}\right\}^2 + 1\right]\right)^{\frac{1}{2}} = 0.2936 \tag{8-31}$$

This may be stated more simply as

$$P\left(\frac{D}{D_{50}}, \frac{\sigma}{m}\right) = \frac{1}{2}\left\{1 + erf\left[\frac{1}{\sqrt{2}\beta} \ln\left(\frac{D}{D_{50}}\right)\right]\right\} \tag{8-32}$$

when

$P \geq 0.5$ (i.e., $D \geq D_{50}$)

and

$$P\left(\frac{D}{D_{50}}, \frac{\sigma}{m}\right) = \frac{1}{2}\left\{1 - erf\left[\frac{1}{\sqrt{2}\beta} \ln\left(\frac{D_{50}}{D}\right)\right]\right\} \tag{8-33}$$

when

$P \leq 0.5$ (i.e., $D \leq D_{50}$)

where

$$erf\,(x) = \frac{2}{\sqrt{\pi}} \int_0^x exp\,(-t^2)\, dt \tag{8-34}$$

Also, and quite significantly, we note that the analysis concludes:

$$D_{10} = D_{50} / 1.46 \tag{8-35a}$$

and

$$D_{90} = 1.46\ D_{50} \tag{8-35b}$$

Equations (8-35a) and (8-35b) alone are sufficient to relate these results to a probit analysis.

Note that in terms of a probit, Pr, the fraction of the population affected, P, is given by,

$$P = \int_{-\infty}^{Pr-5} \phi(x)\,dx \tag{8-36}$$

where

$$\phi(x) = \frac{1}{\sqrt{2\pi}}\ e^{-x^2/2} \tag{8-37}$$

Also, equation (8-30) may be rewritten as,

$$P = \int_{-a}^{\infty} \phi(x)\,dx \tag{8-38}$$

where

$$a = \frac{1}{\beta}\,\ell n\ (D/D_{50}) \tag{8-39}$$

If (8-38) and (8-39) are to be equivalent, then

$$\int_{-\infty}^{Pr-5} \phi(x)\,dx = \int_{-a}^{\infty} \phi(x)\,dx = -\int_{a}^{-\infty} \phi(-x)\,dx$$

$$= -\int_{a}^{-\infty} \phi(x)\,dx \qquad \text{(since } \phi \text{ is an even function)}$$

or

$$\int_{-\infty}^{Pr-5} \phi(x)\,dx = \int_{-\infty}^{a} \phi(x)\,dx \qquad (8\text{-}40)$$

Comparing the limits of integration, we find

$$Pr - 5 = a$$

or

$$Pr = 5 + \frac{1}{\beta}\ \ell n(D/D_{50})$$

or

$$Pr = 5 + 3.406\ \ell n(D/D_{50})$$

or

$$Pr = [5 - 3.406\ \ell n(D_{50})] + 3.406\ \ell n(D) \qquad (8\text{-}41)$$

which is the form of injury equation used previously in which D (overpressure) is the causative variable, 3.406 is the slope parameter, and the term in brackets is the location parameter.

Now, so far this analysis as described has shed little light on the problem of low-yield explosions. The significant accomplishment of the DNA study, the part that cannot yet be revealed fully, is relating the value of D_{50} for various shelter spaces to the yield of the explosion. That is to say, for each shelter space (as stated above, the weapon effects community is more interested in survivability as a function of shelter space, rather than as a function of building type) a graph is provided that shows how the mean lethal overpressure (the mean injury overpressure too) varies with explosion yield. By combining the value of D_{50} with equations (8-35a) and (8-35b) or the equivalent preceding relations, the level of injury for any given overpressure may be computed. For use in the VM, the graphs relating D_{50} to explosion yield will be fitted by a functional equation and the equation will be computerized. In this way, indoor blast damage can be computed for any yield explosion by methods not too dissimilar from those used previously. Since the analysis has combined all damage phenomena, the breakdown by the various causative mechanisms (as currently done for outdoor blast damage) will not be possible in the case of indoor population blast injury; this is a minor defect. A more serious problem is that the rationale by which these damage criteria were obtained and estimates of their validity are likely to remain classified for several years. Although less than full disclosure of the bases for the submodels adopted for use in the VM is not consistent with previously followed design guidelines, no other viable alternative appears to be available in this instance.

Derivation of the Assessment Algorithm

Figures 8-29 through 8-35 summarize the numerical results of the DNA study on personnel injury from low-yield explosions. Figure 8-29 shows the variation of D_{50} as a function of explosion yield, for each mechanism causing damage. As can be seen from equation (8-41), a higher D_{50} implies that a proportionally higher value of incident external overpressure is required to produce the same level of personnel injury LD_{50} represents the lethal mean overpressure; BD_{50} represents the mean overpressure producing burdening injuries. For each of the damage mechanisms considered in Figure 8-29, the D_{50} values increase as explosion yield decreases. This indicates that the overpressure environment produced by lower yield explosions is less effective in producing damage than the same overpressure environment produced by higher yield explosions. In general, the damage mechanisms described by this graph are not considered dependent on the type of shelter space. However, the mechanism "sweep" (blowing people out of a building) is lethal only if the distance fallen is over about 10 meters (30 feet); hence, the notation on that curve of "4th floor or higher." Similarly, lung hemorrhage induced by direct blast effects depends upon whether the blast wave is considered reflected ("person against wall") or undisturbed ("person in open"). The horizontal curves marked "glass" and "50% eardrum rupture and lung threshold" indicate limiting overpressure values, independent of yield, for certain damage mechanisms. Figure 8-29 is the basis for all subsequent results. As appropriate, damage curves applicable for the various shelter spaces are superimposed to produce a D_{50} vs. yield curve for each shelter space.

Thus Figures 8-30 through 8-33 represent the composite dependency (from all mechanisms) of lethal injury on yield for the shelter spaces "outside," "residences and multistory buildings," "upper floors of multistory buildings," and "basements and strong-walled buildings," respectively. Figure 8-34 shows the composite dependency of burdening injury on yield for the same four shelter categories. Figure 8-35 summarizes the D_{50} dependency on yield for lethality and injury and for all shelter spaces considered.

For the purposes of the VM, building type is a more relevant parameterization of data than shelter space, as used in Figure 8-35. For the VM we initially consider four classifications of building type: residences, low-rise buildings, high-rise buildings, and outside. To fit the data presented in Figure 8-35 into these categories, we proceed as follows. Basements offer considerable shielding from damage. Typically, however, basements are occupied to a lesser extent than upper stories of residences and other buildings. Thus we assume, conservatively (slightly conservatively, it is believed), that building occupants are all above ground. Thus, curve ③ is taken to describe the LD_{50} vs. yield dependence for residences. Again, for conservatism, we assume both low-rise and high-rise buildings are weak-walled; for

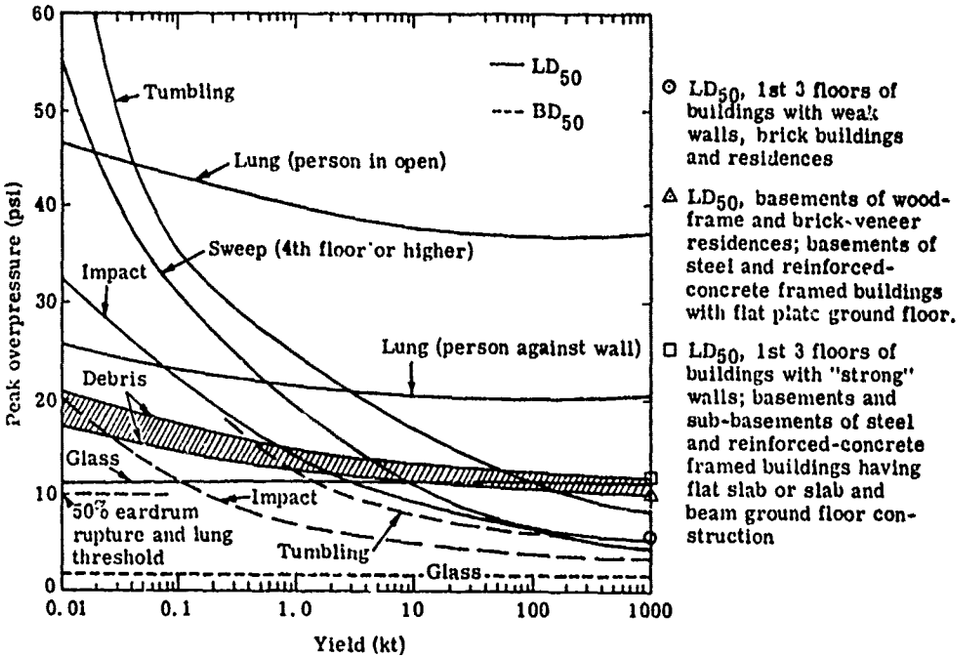

FIGURE 8-29. Values of LD_{50} and BD_{50} for Potential Blast Hazards (Figure 2-2 in [81])

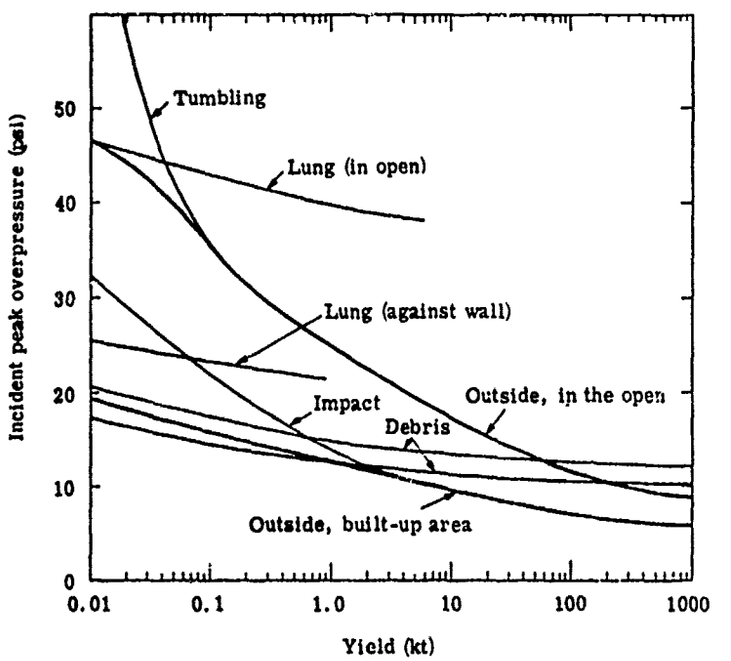

FIGURE 8-30. Selection of LD_{50} Values for Personnel Located Outside (Figure 2-3 in [81])

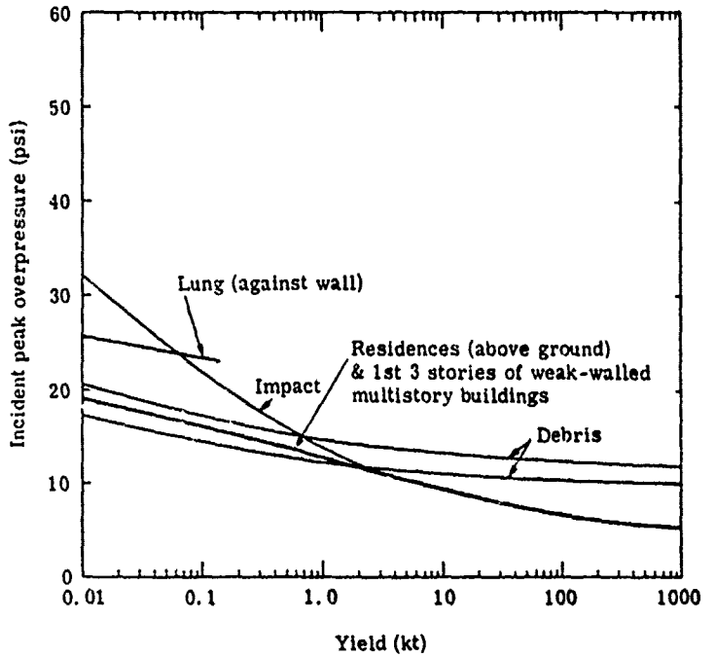

FIGURE 8-31. Selection of LD_{50} Values for Personnel Located in Residences and Multistory Buildings (Figure 2-4 in [81])

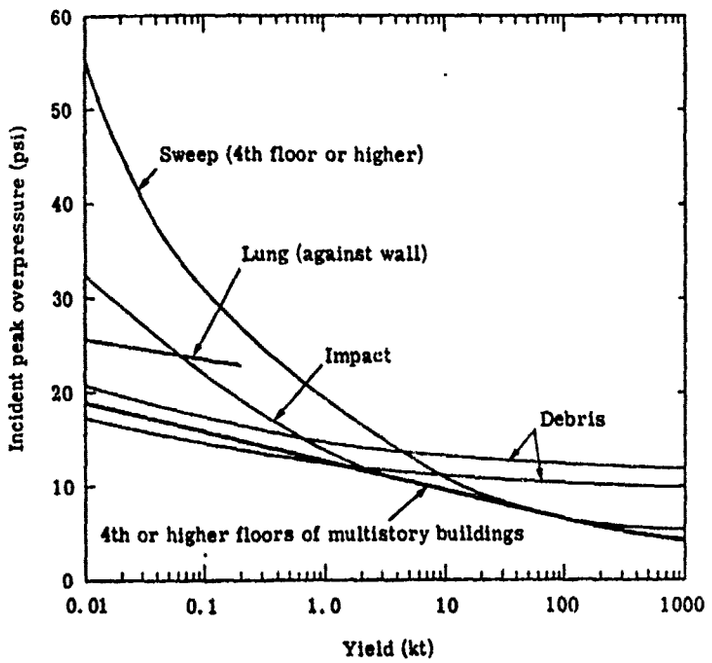

FIGURE 8-32. Selection of LD_{50} Values for Personnel Located on Upper Floors of Multistory Buildings (Figure 2-5 in [81])

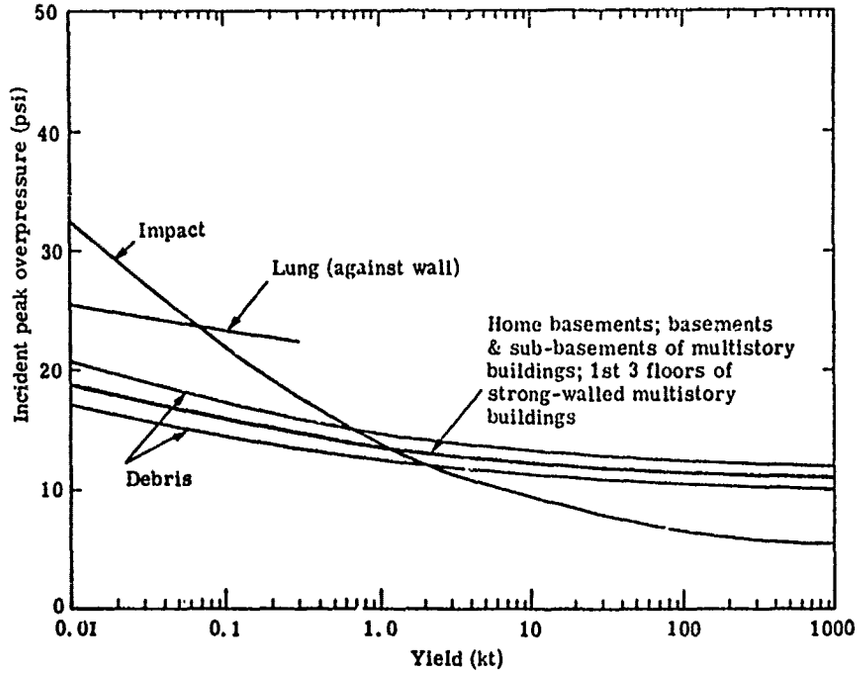

FIGURE 8-33. Selection of LD50 Values for Personnel Located in Basements and Strong-Walled Buildings (Figure 2-6 in [81])

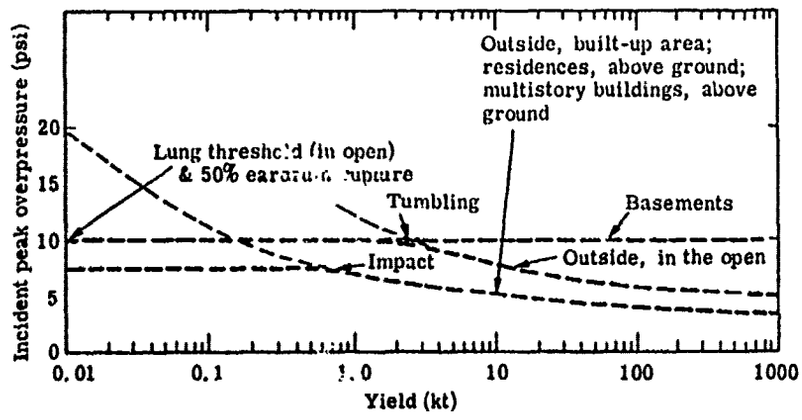

FIGURE 8-34. Selection of BD_{50} Values (Figure 2-7 in [81])

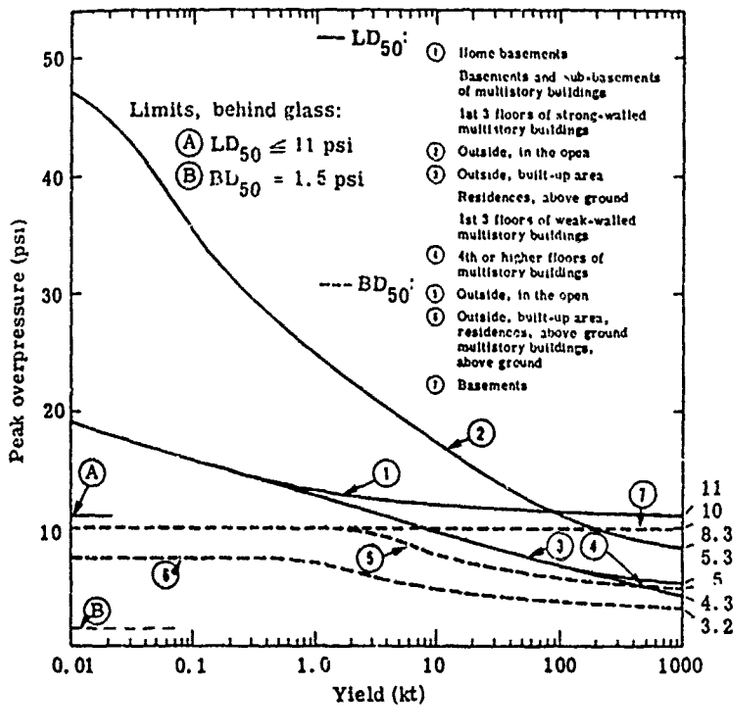

FIGURE 8-35. Personnel Vulnerabilities for Air Blast. The solid curves give the mid-lethal (LD_{50}) free-field peak overpressures for the shelter categories indicated, and the broken curves give the mid-burdening (BD_{50}) peak overpressures. For personnel subject to glass fragments, the LD_{50} and BD_{50} values are limited to maximum values of 11 and 1.5 psi. (Figure 2-8 in [81])

most stores, schools, and low-rise office buildings, this will be the case. Thus, curve ③ is also taken as the LD_{50} vs. yield curve for for low-rise buildings. For high-rise buildings, differences in injury can occur, depending on whether occupants are above or below the 4th floor. These differences are represented by curves ③ and ④ on Figure 8-35. Since these curves diverge only for yields above about 200 kilotons, the difference is largely immaterial for the low-yield chemical explosions considered in the VM. Thus, curve ③ may be taken as describing the LD_{50} vs. yield relationship for high-rise buildings. Curve ② may be used to describe injury to people in the open, but curve ③ is probably more appropriate for describing injury to outside personnel in cities. Curve ① is not used since it describes the damage function for basements and strong-walled spaces, which for purposes of the VM may be conservatively neglected. To describe burdening

injuries, curve ⑤ is used for outside, in the open and curve ⑥ is used for all inside personnel as well as for those outside in built-up areas. Curve ⑦, for basements, is not used for the reasons given above. It is not considered reasonable that all personnel are subject to glass fragments, so the LD_{50} limit of 11 psi and the BD_{50} upper bound of 1.5 psi are not applied. Although this may underestimate injury in specific instances, the exclusion of consideration of basement areas and other conservatisms are expected to compensate sufficiently for this simplification.

Thus, the four categories of buildings to be considered are seen to be described adequately by only four D_{50} vs. yield curves. Two curves describe lethality: curve ③ describes inside personnel and those outdoors in built-up areas; curve ② describes outdoor, in the open, personnel responses to blast. Two curves describe burdening injury: curve ⑥ describes those outdoors in built-up areas and inside personnel; curve ⑤ describes the response of personnel outdoors in the open. These four curves may be described by a polynomial approximation, for use in the computer. Thus we have, for indoors and outside in cities,

lethality (curve ③)

$$LD_{50} = 16.1513 - .8967\,y + .0245\,y^2 - .0002\,y^3 \qquad (8\text{-}42a)$$

injury (curve ⑥)

$$BD_{50} = 7.5979 - .6547\,y + .0511\,y^2 - .0013\,y^3 + .00001\,y^4 \qquad (8\text{-}42b)$$

and for outside in open areas,

lethality (curve ②)

$$LD_{50} = 37.9449 - 7.7497\,y + .7764\,y^2 - .0209\,y^3 + .0002\,y^4 \qquad (8\text{-}43a)$$

injury (curve ⑤)

$$BD_{50} = 10 \text{ psi} \qquad (8\text{-}43b)$$

Equations (8-42) and (8-43) describe, respectively, lethal and injury response to explosion when combined with equation (8-41) and calculated values for yield (Y) and overpressure (D). Equations (8-42b) and (8-43b) are alternative means of expressing the response of outdoor populations, since the VM is already computing that response by other means. The method currently used in the VM separates the response

according to causitive mechanism (direct blast, debris, translation); this method is not refined in that manner. However, the method here is probably more accurate for lower yield explosions. It appears advisable that a user option be allowed in the computer code, so that an individual choice can be made between the two assessment methods.

Closing Remark

The information presented above yields a quantitative method for assessing indoor population injury from explosion. The several limitations and caveats associated with the method have been elucidated above; however, it is felt that this technique is the best available at this time.

FIRE INJURY TO INDOOR POPULATIONS

As with injury from explosion and from inhalation of toxic chemicals, buildings tend to shield occupants from the direct adverse effects of fire resulting from marine spills of hazardous materials. In this stage of development, only direct fire damage is considered; direct fire damage is taken to be that resulting from burning of the cargo itself or from secondary fires of particular hazard as described in Chapter 1. Death and nonlethal injury from burning of the structure itself are not considered at this time, primarily because the degree of injury is highly dependent on the difficulty in predicting response of building occupants and rescue personnel.

Some Preliminary Considerations

In considering injury to indoor populations from fire (as from other mechanisms), we are faced with two separate problems: (1) determination of the indoor thermal radiation environment as a function of the external thermal radiation environment and (2) determination of the response of the indoor population to the calculated thermal environment indoors. As with the other damage modes, it is expected that the personnel response to the same thermal radiation environment will be largely the same regardless of location and that the algorithm for assessing damage devised in the first stage of development can be used. Response of indoor and outdoor populations may be different in cold, winter climates, since persons outdoors generally will be wearing heavier clothing and will be better shielded from the thermal radiation. This possible difference in response will not be taken into account in the model that will be presented below.

The first problem, that of determining the thermal radiation environment indoors as a function of the thermal radiation outside, may be posed quite simply but is difficult to solve. The thermal radiation environment experienced by a person indoors may be obtained by calculating the total flame radiation reaching each portion of the subject's body. In theory, this calculation could be performed for each portion of the body by integrating the received radiation over those radiating surface elements of the flame that are "visible" at the receptor site. The integration would take account of intervening opaque objects and could be modified to account for intervening absorptive media. Essentially, a shape factor analysis would be performed for every potential location of indoor personnel and the flame. Such a large number of detailed calculations are clearly unwarranted. The alternative method of analysis used here is to derive or to estimate average factors for various phenomena that are used to modify the external thermal radiation level, so as to compute the internal level. These reduction factors take into account such phenomena as:

- shielding of occupants by building walls,
- shielding of a given building by other buildings between it and the flame, and
- attenuation by window glass.

Before this model is described in detail, it is advisable to present a model developed by Longinow et al. [75] for indoor burn damage and to describe why that model was deemed unsuitable for use in the Vulnerability Model.

The Longinow Model

The Longinow model was developed to determine indoor burn damage from nuclear weapon attacks [75]. The computational method is shown schematically in Figure 8-36. The computer programming steps, corresponding to the functional blocks identified in Figure 8-36, are shown in Figure 8-37. A comparison of the functional blocks and their corresponding program steps reveals several problems that would contraindicate use of this model in the VM. Among these problems are the following.

(1) The damage calculation depends only on sill height (the distance of the bottom of the window from floor level), and not on window width or on glass area facing the flame.

(2) The model permits no more than 65% mortality, regardless of the radiation environment.

(3) The damage inflicted is related to free-field overpressure for a 1-Mt weapon, rather than to external levels of thermal radiation as required for the VM.

(4) Shielding by intervening structures does not appear to be accounted for.

As shown in the portion of the computer program marked (B) in Figure 8-37, the fraction of body exposed (PERBX) is zero if the sill height (SILHT) is greater than 5.75 feet and increases linearly as sill height is reduced. The fraction of body exposed is 1 when sill height is zero (i.e., the window begins at floor level). Clearly, the width of the window is not taken into account; an individual standing half exposed in front of a floor-to-ceiling window (half shielded by the exterior wall) would conservatively be assessed as being irradiated from side to side.

Statement number 200 in Figure 8-37 indicates that the fraction of body exposed based on the sill height calculation is uniformly multiplied by a factor of 0.4 to obtain the final value for the fraction of body exposed. The thinking behind this value is apparently that body area is distributed 40% front, 40% back, and 10% each side. Thus the

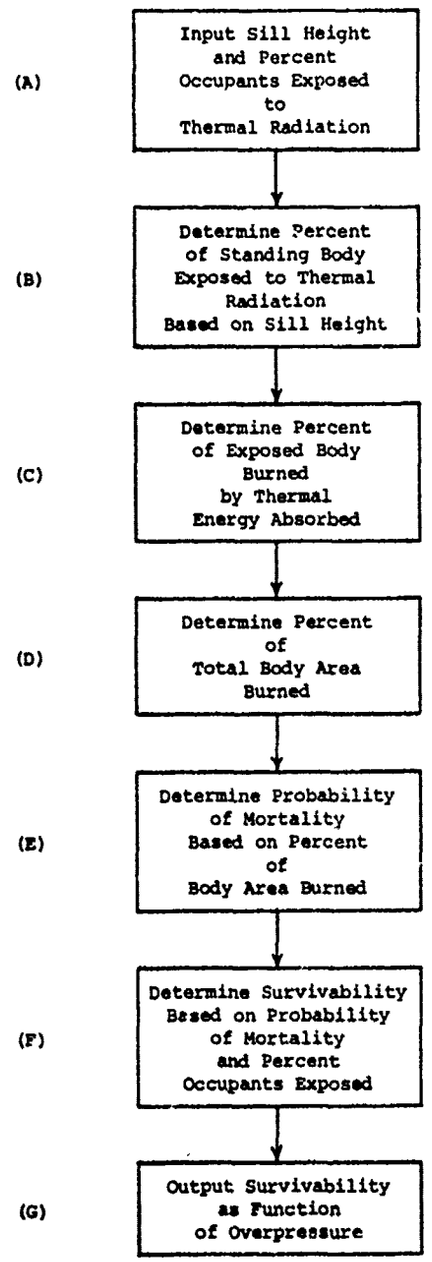

FIGURE 8-36. Flowchart of Thermal Radiation Routine (from reference [75], p. 237)

C.6.2 Thermal Radiation Model - Listing

```
      DIMENSION TQ(19),NAME(10)
      DATA (TQ(N),N=1,19)/367.42,343.96,320.50,301.28,282.07,260.14,
     *238.14,215.50,193.47,176.41,159.33,143.20,127.05,106.52,
     *78.02,60.90,48.25,24.89,13.84/
   25 READ(5,2,END=1000)(NAME(N),N=1,10)
    2 FORMAT(10A6)
(A)-> READ(5,1)PERIX,SILHT
    1 FORMAT(2F10.3)
      WRITE(6,4)(NAME(N),N=1,10)
    4 FORMAT('1',10A6//1X,'THERMAL RADIATION SURVIVABILITY'//)
      WRITE(6,3)PERIX,SILHT
    3 FORMAT(/' PERCENT OCCUPANTS EXPOSED',F7.3//' SILL HEIGHT',F7.2)
      WRITE(6,4)(NAME(N),N=1,10)
      WRITE(6,5)
    5 FORMAT( 5(' '/),18X,'FREE FIELD',9X,'PERCENT'/17X,'OVERPRESSURE',
     *7X,'SURVIVORS'/)
      IF(SILHT.GT.5.76) GO TO 200   <- [PERBX=0 probably by initialization]
(B)   PERBX=1.-(SILHT/5.76)
  200 PERBX=.4*PERBX
      DO 100 IL=1,19
      ENTRAN=.56*TQ(IL)
      IF(ENTRAN.LT.4.) GO TO 40
      IF (ENTRAN.GT.6.) GO TO 41
      BURN=8.35*ENTRAN-33.4
      GO TO 30
(C)   41 IF(ENTRAN.GT.16.7) GO TO 42
      BURN=16.7
      GO TO 30
   42 BURN=1.3*ENTRAN-4.6
      IF(BURN.GT.100.) BURN=100.
      GO TO 30
   40 BURN=0.
(D)-> 30 PERBAB=PERBX*BURN
      PERMOR=.6*PERBAB
      IF(PERBAB.GT.10.) PERMOR=1.4*PERBAB-8.
      IF(PERBAB.GT.20.) PERMOR=2.54*PERBAB-30.77
(E)   IF(PERBAB.GT.33.) PERMOR=1.69*PERBAB-2.68
      IF(PERBAB.GT.49.) PERMOR=1.09*PERBAB+26.5
      IF(PERBAB.GT.60) PERMOR= .4*PERBAB+58.
      IF(PERBAB.GT.80.) PERMOR=100.
(F)-> PERSUR=100.-PERMOR*PERIX
(G)-> FFOP=21-IL
  100 WRITE(6,8)FFOP,PERSUR
    8 FORMAT(20X,F6.2,10X,F7.2/)
      GO TO 25
 1000 STOP
      END
```

FIGURE 8-37. Computer Programming Steps for Thermal Radiation Model (from reference [75], p. 238)

maximum burn area produced by radiation traveling horizontally is 0.4 of total body area. The section of the computer program marked (E) in Figure 8-37 relates percent of body area burned (PERBAB) to percent mortality (PERMOR); this nonlinear relationship is represented by linear segments and is graphed in Figure 8-38. The percent of the exposed body area burned by the thermal radiation is computed by the section marked (C); the percent of the exposed area burned (BURN) multiplied by the fraction of body area exposed (PERBX) yields the percent of body area burned (PERBAB) as computed in section (D). Since BURN $\leq$ 100%, as shown in section (C), and PERBX $\leq$ 0.4, PERBAB $\leq$ 40%. Figure 8-38 reveals that 65% mortality corresponds to a percent body area burned of 40%. Thus, percent mortality is always less than or equal to 65%. Other models of burn damage developed by investigators of nuclear weapon effects and used in the VM to assess burn damage outdoors do not limit percent mortality in this way. This limiting of burn damage appears to be not sufficiently conservative for use in the VM. It appears in the Longinow model apparently because the fraction of body area exposed is limited to 0.4, or it may be due to consideration of hypovolemic shock as the only operative physiological mechanism leading to death from burns.

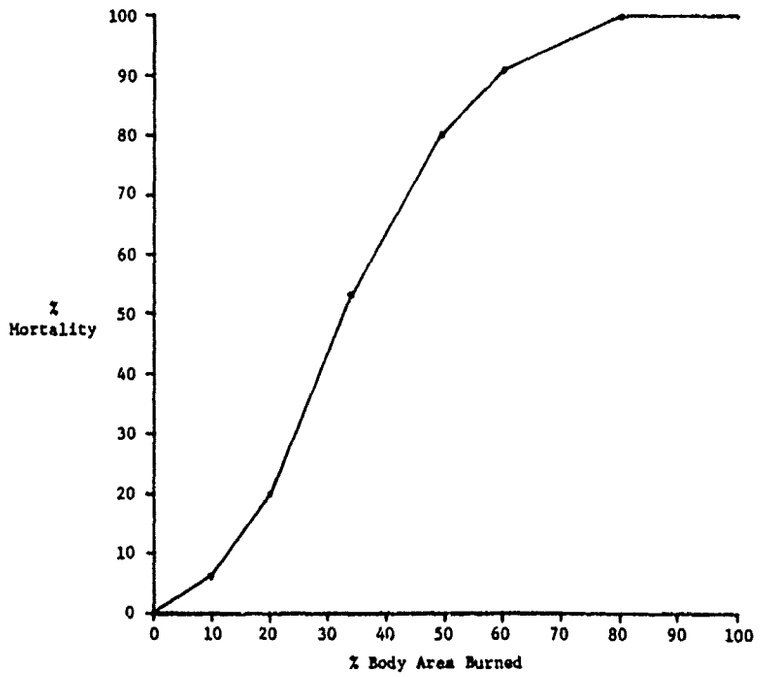

FIGURE 8-38. Linear Segment Relationship Between Percent Mortality and Percent Body Area Burned

Furthermore, the Longinow model relates burn mortality to the free-field overpressure for a 1-Mt nuclear weapon. Although it would probably be possible, with some effort, to relate weapon overpressure to the corresponding thermal radiation environment, that effort was deemed unwarranted in this case considering the other deficiencies of the model for use in the VM. Finally, treatment of the modification of the thermal radiation environment by intervening structures is not done in an adaptable manner in the model and may not be considered at all. Because of these various problems related to using this model in the VM, it was decided to develop another model, based on a similar philosophy, for the VM.

The VM Model for Indoor Burn Injury

The approach chosen for the Vulnerability Model is that the response of persons indoors to thermal radiation is described by the radiation damage model developed for outdoor populations; the problem therefore reduces to determining the indoor radiation environment. The various mechanisms by which external radiation is reduced before impinging on indoor occupants are shown schematically in Figure 8-39.

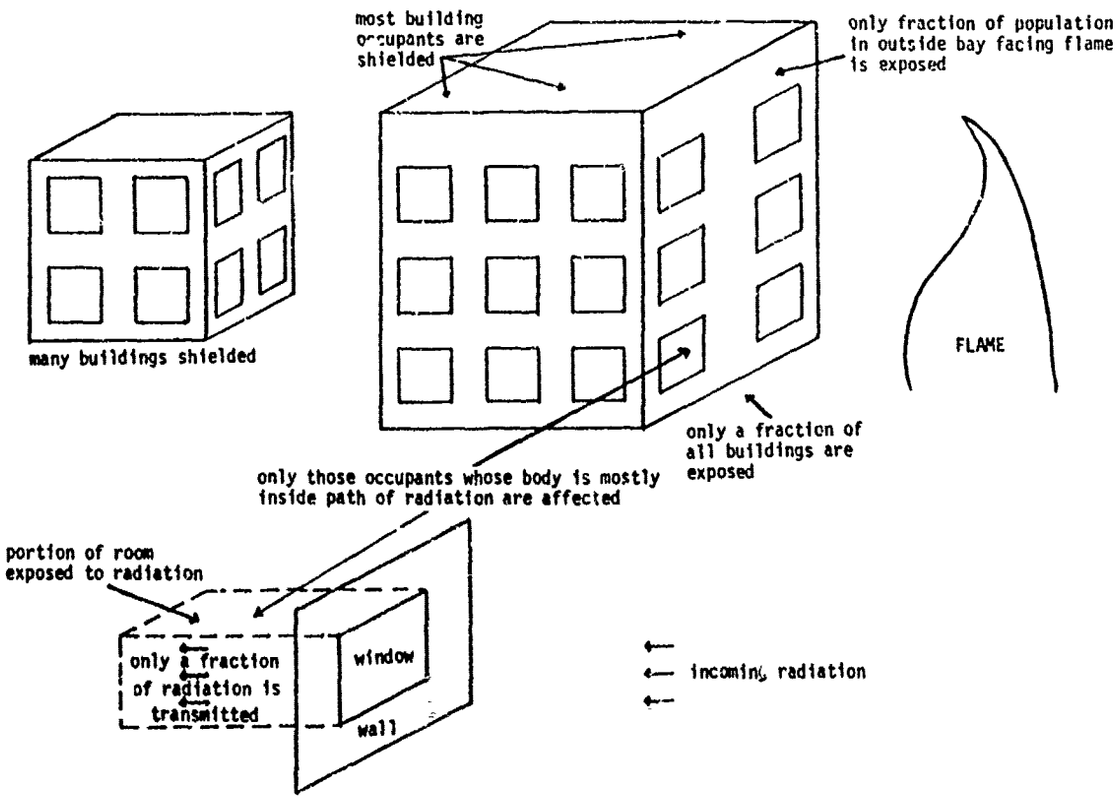

FIGURE 8-39. Schematic of Various Mechanisms Modifying the External Thermal Radiation Environment

The effects considered are:

(1) Shielding of the building in question by other buildings between it and the fire,

(2) Lack of exposure of parts of an exposed building,

(3) Shielding of part or all of the body of persons in exposed portions of the building, and

(4) Reduction of thermal radiation intensity by glass and screens.

The number of persons outdoors estimated to experience lethal burns is given by the following equation.

$$N_{B_O} = N F_O F_D (I,t) \tag{8-44}$$

where: N_{B_O} is the number outside killed by fire; N is the number of persons in the given cell; F_O is the fraction outdoors; and F_D is the fraction killed as a function of the thermal radiation intensity, I, and time, t (see reference [1], Ch. 6 and App. D). For indoor populations, this formulation is revised as follows.

$$N_{B_i} = N F_i f_1 f_2 f_3 F_D (f_4 I,t) \tag{8-45}$$

where: N_{B_i} is the number inside killed by fire; F_i is the fraction indoors; f_1 is the fraction of buildings unshielded in the cells; f_2 is the fraction of building occupants exposed in those buildings not shielded; f_3 is the fraction of body not shielded for those persons exposed; and f_4 is the factor reducing the level of thermal radiation; i.e., factors f_1 through f_4 correspond to the four effects listed above.

To determine the mitigating factors, f_1 through f_4, we proceed as follows. The problem of the shielding of buildings by intervening structures was considered at length in Chapter 4, Improved Method for Structural Ignition. The same considerations apply here. However, to simplify the problem we conservatively assume that the level of thermal radiation calculated for the cell center will occur throughout the cell, except for shielding effects. Thus, the entire cell is assumed always to be potentially involved in the cell center experiences a sufficiently high level of radiation. The fraction of buildings not shielded, f_1, varies between b and 1, where $0 < b < 1$. As in Chapter 4, we consider three shielding scenarios: maximum, minimum, and random. For the maximum shielding, only those buildings on the cell edge facing the fire are exposed; they, in turn, shield the interior buildings. For maximum shielding, $f_1 = b$, where b is the fraction of buildings on the front face of the cell. The method for finding b is detailed in Chapter 4.

For the minimum shielding scenario, $f_1 = 1$, and no structures are considered to be shielded by others. For random shielding, $b < f_1 < 1$, and the method for finding f_1 is explained in Chapter 4.

The fraction of building occupants exposed to radiation in those buildings that are not shielded is taken to be 1/8. For a typical structure, we assume that one-half of the occupants are in interior spaces or bays and are thereby shielded from external radiation. Furthermore, only one of the four external faces of the building is assumed capable of exposing occupants; thus an additional factor of 1/4 is applied. For thermal radiation not impinging on a building face, but arriving obliquely on a corner, it could be argued that 1/2, not 1/4, of the exterior space may be subject to high radiation levels. However, if the radiation does arrive oblique to a window, it will not irradiate as large a fraction of the room nor will it be as effective in producing damage. Thus we take $f_2 = 1/8$. To estimate the effect of partial shielding the body by exterior walls, we take

$$f_3 = \frac{A_{window}}{A_{wall}} \tag{8-46}$$

where A_{window} is the total window area and A_{wall} is the total wall area for an exterior wall. For most buildings, f_3 will range between 0 and 0.95. Some exterior walls are blank, hence the value 0. Glass-walled buildings still have some occluding features on the exterior, such as floor structures, air-handling equipment, and structural supports; hence the value $0.95 < 1$. As a typical value, we take $f_3 = 0.5$. If more specific information is available for a given cell, this factor can be modified. Although fraction of body exposed is, in general, not equivalent to fraction of persons exposed, the two are used interchangeably here, as in Longinow's model, to account for the phenomenon without developing models of unwarranted complexity.

Unlike the other factors, the factor accounting for attenuation of the external radiation by glass and screens, is applied directly to the radiation level, I, and not to the damage fraction. According to nuclear weapon effects research [32], window glass (including dirt and dust films) and screens can reduce the amount of transmitted radiant energy by a factor of 20 to 60 percent. Thus, for conservatism, we choose a value of 0.8 for f_4.

Closing Remarks

The assessment method for burn death to indoor population is summarized by equation (8-45). The mitigating effects of buildings are represented by the factors f_1 through f_4. Numerical values for these factors, or the mean by which these numerical factors may be calculated

have been presented. The modeling approach of using factors to quantify the effects of buildings is similar to that used by other investigators of indoor burn damage related to nuclear weapons. Several of the values used in this modeling are also based on nuclear weapon effects research. This model is considered to be reasonably representative of the state of the art in modeling these types of phenomena.

Chapter 9

SUMMARY OF REVISIONS TO VULNERABILITY MODEL COMPUTER PROGRAMS

INTRODUCTION

Major programming revisions to accommodate improvements and modifications to the Vulnerability Model have been made to several of its subroutines. A general overview of each modification and changes to the user input are given in this chapter. (Flowcharts of selected programs and subroutines are presented as figures at the end of the chapter.)

PHASE I

Executive Program, VMEXEC (Figure 9-1)

The main program of the Vulnerability Model (VM), called VMEXEC, initializes the data files and controls the execution of the various simulation submodels (MODA, MODC, etc.) over each time step for each geographic cell. VMEXEC now calls the improved spill development models, MODF and MODQ, if their path is specified. It has also been modified by adding a section which processes the secondary fire models and the improved structure ignition model. If ignition of a primary fire source (either flash fire or pool burning) occurs, the program calls the secondary fire model, SECFIR, which determines whether ignition of secondary fire sources will occur. The program then computes a time-weighted average radiation flux and a time/radiation-weighted average distance for each geographic cell based on a summation of primary and secondary fire parameters. Using these averages, VMEXEC then calls STRIG, which computes structural ignition criteria for each cell. VMEXEC then produces a time history of radiation intensity and duration from all fires for all cells. These data are written to a file for damage assessments in Phase II.

Subroutine, COORDS

This subroutine reads and stores data from the geography file, including the coordinates and spill assessment data (i.e., cell number, water depth, etc.) of each cell. Instructions have been added which read and store secondary fire source data and transform the longitude and latitude coordinates to x-, y-coordinates with respect to the spill origin and wind direction. A secondary source flag has been added to the user input data, which indicates whether the user has created a secondary source file to be read.

Subroutine, FLFIRE (Figure 9-2)

Subroutine FLFIRE calculates the effective radiation intensity level and effective duration of the radiation for each cell from the flash fire. The subroutine has been modified to compute the radiation flux from the flash fire at all cells, not just at the ignition cell and at other cells containing a vapor concentration between flammable limits as was done previously. Computation of the radiation flux at distant cells requires the use of the newly developed algorithm used to calculate view factor for the flash fire. In addition, for the secondary fire model, the subroutine now computes the distance from the flash fire to each secondary source and the radiation flux from the flash fire received at the secondary source location.

Subroutine, PLBURN (Figure 9-3)

This subroutine simulates the burning of a pool of flammable liquid floating on the surface of the water. It computes the magnitude and duration of the thermal radiation emitted from the pool burn. A modification was made to the section which calculates the emissive power, view factor, and radiation intensity at each cell of a pool burn. Using the old method, emissive power was calculated in subroutine JHHRF which was called by MODE2 which was called by PLBURN in a loop on cells. This calculation needs to be done only once, however, since emissive power is not dependent on the distance of the observer from the flame. Hence, two new subroutines, MODE3 and FLMOUT, were written to calculate emissive power. MODE3, which calls FLMOUT, is called in PLBURN before entering the loop on cells. Emissive power is now stored in the State File and used in subroutine JHHRF to calculate the radiation flux by taking the product of view factor and emissive power. A section has also been added to PLBURN to compute both the distance from the pool burn to the secondary source and the radiation flux from the pool burn to each secondary source location for the secondary fire model.

Subroutine, PATH (Figure 9-4)

This subroutine determines which path the spilled chemical will take. It has been modified to flag a path for both floating (MODF, V, and W) and sinking and spreading (MODQ) liquids with boiling point above ambient for spills in a nontidal river. Previously, for a sinking liquid with boiling point above ambient, the VM only printed a message stating that no model had been developed for this path; while for a floating liquid, only models V and W were used.

Subroutine, WATMIX (Figure 9-5)

This subroutine controls the cell and time loops for the water-mixing models. It previously considered only MODP. It now calls either MODP, MODF, or MODQ, depending upon which path is chosen.

Subroutine, DILUN

Subroutine DILUN computes the concentration of a water-miscible chemical at any point downstream from the spill. When running test cases for an instantaneous methanol spill in still water, an error condition occurred in this subroutine in line 66. The value for the argument of EXP is very small for large values of X, Y, and Z. That is, for a large distance from the spill site, the concentration is essentially zero. The value for C = EXP[-(X**2 + Y**2 + Z**2)/(4.*DIFCO*T)] for DIFCO = 1.56 E - 5 and T + 20 seconds becomes too small to evaluate. This has been corrected by checking this function before using it as an argument for EXP and setting the concentration to zero if the argument is less than -100.

Subroutine, SVEIW

An additional problem was encountered in subroutine SVEIW. In this subroutine, the view factor is computed for a distance of an observer from a flame. The model previously computed the view factor for distances equal to, or greater than, flame radius; however, for the tank failure models, distances within the flame itself may be considered. Previously, for distances within the flame diameter, SVEIW printed a message stating the "Observer Distance Is Less Than Flame Diameter" and continued processing. Because there was no path for this condition, errors such as negative arguments of a square root occurred. Now the subroutine has been modified to accept a distance less than flame diameter by setting view factor equal to 1.0, which is a perfect view factor.

New Model, SECFIR (Figure 9-6)

This new model is called by VMEXEC following the primary fire calculations. It determines whether ignition of secondary sources by the primary fire(s) will occur if the user has created and specified a secondary source file to be read. These secondary sources may be wood, cotton, paper, polymers, or light hydrocarbons. The first step in the program combines the duration and radiation intensity from the primary fire(s) and sorts these parameters on time of ignition. Then, by using a time-incremented radiation intensity algorithm, it determines if sufficient radiation occurs for ignition of the secondary source to obtain. The final step determines the distance and radiation flux from each secondary fire to each geographic cell and sorts the secondary fire parameters on time of ignition.

Tank Failure Subroutines (Figure 9-7)

These subroutines, named TNKFL, XMATL, XSTLD, AWBMV, XSAT, XDATA, XLAMDA, XUL, and XHV, are a part of the secondary fire model. They predict whether a cryogen tank subjected to external thermal radiation from

a flash fire and/or pool burning will fail. The model will accept a lading of propane stored in a steel tank of the following geometries:

- insulated dual-wall tank
- spherical shell
- vertical cylindrical shell
- horizontal cylindrical shell

However, by incorporating appropriate tables, the model could be modified to handle other ladings and tank materials.

Structural Ignition Criteria Model, STRIG (Figure 9-8)

This model computes the fraction of a geographic cell within the primary fire(s) ignition contour and the fraction of the cell's front face that is within the ignition contour. The inputs to this model are the time-weighted average radiation flux and the time/radiation-weighted average distance from the primary and secondary fires to the cell as computed in VMEXEC. The reasons for choosing these time-weighted parameters are as follows.

(1) The evaluation of structural ignitions will depend on a summation of radiation intensities from both primary and secondary fires which will occur at a varying distance and for varying durations.

(2) Rather than selecting an effective distance and/or duration based on any one fire, a distance algorithm was developed which would weight the average distance by both time and radiation intensity and which would weight radiation intensity by effective duration.

Improved Spill Development Models (Figures 9-9, 9-10)

Subroutines to treat the behavior of spills of liquids of finite solubility in nontidal rivers have been added. Both floating and sinking liquids with boiling points above ambient are considered. Subroutines SINK1, SINK2, and SINK3 calculate, respectively: (1) sinking time, distance traveled downstream while sinking, area of bottom covered by sunken liquid, and streamwise length of sunken pool; (2) dissolution rate and time for complete dissolution; and (3) the downstream water concentration of spilled liquid as a function of time and position. Subroutines SINK1 and SINK2 correspond to Chapter I in *Development of Additional Hazard Assessment Models* (ADL, December 1975). Subroutine SINK3 is described in Chapter II. Subroutine CDIFW computes the diffusion coefficient of the spilled material in water which is needed in SINK1. Subroutine FTCON, also described in Chapter II, computes the concentration of spilled liquid resulting from a floating pool of finite solubility.

The addition of these new spill development models allows for two additional paths in Phase I. Since these models apply to low vapor pressure chemicals only, dissemination of the hazardous material is limited to the water when these models are employed. Subroutines SINK1, SINK2, SINK3, and CDIFW are called by subroutine MODQ which is called by WATMIX if this path is chosen. Subroutine MODF, also called by WATMIX, calls FTCON if its path is chosen.

PHASE II

Executive Program, PHASEII (Figure 9-11)

The executive program, PHASEII, reads the spill assessment data from the files set up in Phase I and calls the appropriate damage assessment subroutines for each time step and geographic cell. It has been modified to accommodate additional output from Phase I. Included are the file containing the time history of radiation intensity and the structural ignition criteria. A loop was added to allow special "beach" cells to be included in the geographical file so that damage assessment, including ingestion of toxic substances, could be accomplished in these cells.

Subroutine, PRCONC (Figure 9-12)

This subroutine now determines both outside and inside concentration in units of parts per million and accumulates the weighted sum over time. It then stores these concentration arrays for later processing and passes them to subroutine PRTABL which prints out tables of concentration over the time intervals.

New Subroutine, INCONC (Figure 9-13)

This new subroutine computes the actual time-varying concentration inside a building produced by the passage of a cloud resulting from a spill. The buildup and dissipation of this concentration depend on the air temperature and wind velocity which affect the number of air changes per hour for an inside volume of air.

Subroutine, PRASSM

This subroutine prints out the various damage assessments. It has been modified to print the inside concentration of a toxic chemical (which was previously zero) and to print the damage assessment based on time-varying radiation from all fires, instead of a separate damage assessment for each fire.

Subroutine, SADTA (Figure 9-14)

This subroutine, previously called SADT, now computes deaths, injury, and irritation from a toxic cloud and deaths due to a simple asphyxiant for both inside and outside populations.

Subroutine, SADF (Figure 9-15)

This subroutine, which previously performed personnel damage assessments from both flash fires and pool burning, now performs these assessments based on an accumulation over time of a summation of radiation intensities from all fires and from solar radiation.

Subroutine, SADS (Figure 9-16)

This subroutine determines the damage to structures from explosions and assesses structural ignition from radiation intensity (for all primary and secondary fires) based on the output from Phase I subroutine STRIG. The previous damage computations were based on separate assessments for flash fire and pool burning only.

New Subroutine, PSHLD

This new subroutine computes the percent of structures within a cell that are shielded from radiation from all fires for three possible shielding situations: minimum, intermediate, and maximum shielding.

New Subroutine, BEACH (Figure 9-17)

This new subroutine performs damage assessment for special beach cells in which 50% of the population is on the beach and 50% is in the water. Those in the water are vulnerable to ingestion of water-soluble toxicants, as well as being vulnerable to radiation, explosion, and toxic clouds as are those on the beach. The special grid cells containing data on beach populations are to be placed at the front of the geographic file by the user, having the same format as other water cells but containing the total number of people in the cell.

USER INPUT

Several additional user input variables have been necessitated by changes in the VM. These are given in Table 9-1.

TABLE 9-1. ADDITIONAL USER INPUT VARIABLES

Field No.	Default Value	Unit[a]	Variable Name	Comment
3004	0	ND	NSF	Secondary Fire Source Indicator
3006	2	ND	LSHLD	Shielding Situation 1 = Maximum 2 = Minimum 3 = Intermediate
5004	0	ND	ITOX	Toxicity and Simple Aspyxiant Indicator 0 = Nontoxic 1 = Toxic 2 = Simple Asphyxiant
5036	100.0	ND	T4A	LD_{50} for Ingestion of Contaminated Water in ppm

[a]All units are nondimensional.

SECONDARY FIRE SOURCE FILE

The secondary fire source file is set up in the format shown below.

(I2,1x,F7.0,1x,F7.0,I2,1x,8E7.1)

SOURCE NUMBER - In I2 format, this is the unique number of the secondary source. There is a limit of 10 secondary fire sources.

BLANK SPACE

SCURCE LATITUDE - In F7.0 format, the latitude of the secondary fire source.

BLANK SPACE

SOURCE LONGITUDE - In F7.0 format, the longitude of the secondary fire source.

SOURCE CODE - In I2 format, the code specifying the type of secondary fire source. These are:

1 = Polymers
2 = Wood
3 = Cotton
4 = Paper
5 = Propane Tank

BLANK SPACE

(The following 8 input variables are in E7.1 format)

SOURCE MASS (g) or TANK LENGTH (cm)	- The mass of the secondary source material for codes 1-4; for a propane tank, this position is used for tank length.
SOURCE HEIGHT (cm) or OUTER RADIUS (cm)	- The height of the secondary source material for codes 1-4; for a propane tank, this position is used for the outer radius of the tank.
SOURCE DIAMETER (cm) or INNER DIAMETER (cm)	- The diameter of the secondary source material for codes 1-4; for a propane tank, this position is used for the inner diameter of the tank.
ΔTS (°C) or INITIAL ULLAGE RATIO	- The change in surface temperature needed to cause ignition of polymer fires (see Table 9-2). For a propane tank, this position is used for the ratio of ullage to tank volume. For wood, cotton, and paper sources, this position and all following positions may be left blank
ΔH (°C) or RELIEF VALVE SETTING ($dyne/cm^2$)	- The ratio of total heat radiated by the flame and heat of combustion for polymer sources (see Table 9-3). For a propane tank, this position is used for relief-valve setting.
$\kappa\rho c$ or RELIEF-VALVE OPENING (cm)	- The thermal inertia for polymer sources (see Table 9-2). For a propane tank, this position is used for relief-valve opening.
β	- Mass transfer driving force (see Table 9-3). May be left blank for sources other than polymers. For a propane tank, this position is used for tank geometry. Any of the following may be used: 1 = Insulated Dual-Wall Tank 2 = Spherical Shell 3 = Vertical Cylindrical Shell 4 = Horizontal Cylindrical Shell
γ	- Proportionately constant for polymers only (see Table 9-3).

TABLE 9-2. THERMAL INERTIA AND IGNITION TEMPERATURE DIFFERENCES OF SEVERAL POLYMER MATERIALS

Material	$(k\rho c)^{.75}$	ΔT_g (°C)
Gum Rubber	$[(2.9 \times 10^{-4})(0.99)(0.475)]^{.75} = 1.26 \times 10^{-3}$	240
Cellulose Acetate Butyrate	$[(6.0 \times 10^{-4})(1.2)(0.35)]^{.75} = 2.0 \times 10^{-3}$	180
Lexan	$[(4.6 \times 10^{-4})(1.19)(0.30)]^{.75} = 1.45 \times 10^{-3}$	800
Bakelite	$[(5.5 \times 10^{-4})(1.37)(0.375)]^{.75} = 2.18 \times 10^{-3}$	460
Silicone Rubber	$[(5 \times 10^{-4})(1.35)(0.35)]^{.75} = 1.90 \times 10^{-3}$	720
Polypropylene	$[(3.5 \times 10^{-4})(0.905)(0.50)]^{.75} = 1.41 \times 10^{-3}$	410
Polyethylene	$[(10 \times 10^{-4})(0.933)(0.55)]^{.75} = 3.41 \times 10^{-3}$	250
Plexiglas	$[(5 \times 10^{-4})(1.19)(0.35)]^{.75} = 1.73 \times 10^{-3}$	260
PVC	$[(5 \times 10^{-4})(1.40)(0.24)]^{.75} = 1.48 \times 10^{-3}$	220
Polystyrene	$[(2.9 \times 10^{-4})(1.63)(0.325)]^{.75} = 1.38 \times 10^{-3}$	350
Polymide (Nylon 6/6)	$[(5.9 \times 10^{-4})(1.14)(0.4)]^{.75} = 2.10 \times 10^{-3}$	460
Polyoxymethylene Delrin	$[(5.5 \times 10^{-4})(1.43)(0.35)]^{.75} = 2.36 \times 10^{-3}$	320

TABLE 9-3. PROPERTIES[a] OF POLYMERS AND THEIR FIRES

Polymer	f	ΔH (Kcal/gm)	B	γ	ψ	B_C	Q (cal/gm)
Polymethylmethacrylate (Plexiglas)	0.523	6.03	1.412	0.177	0.070	1.32	385
Polyamide (Nylon 6/6)	0.191	7.17	0.818	0.038	0.015	0.81	220
Polycarbonate (Lexan)	0.440	7.36	1.206	0.102	0.040	1.16	455
Polypropylene	0.292	11.00	0.940	0.213	0.084	0.87	534
Polyethylene	0.276	9.84	0.640	0.215	0.085	0.59	622
Polyoxymethylene (Delrin 500)	0.938	3.47	0.813	0.079	0.031	0.79	720
XX Phenolic, Natural	0.414	7.16	0.448	0.191	0.076	0.42	750
Fir (Wood)	0.938	4.00	0.572	0.169	0.067	0.54	710

[a]Property definitions:

f = grams of fuel per gram of oxygen

ΔH = heat of reaction (Kcal/gm)

B = mass transfer driving force

γ = fraction of heat radiated

ψ = radiative fractional feedback

B_C = mass transfer driving force uncorrected for radiative feedback

Q = latent heat of depolymerization

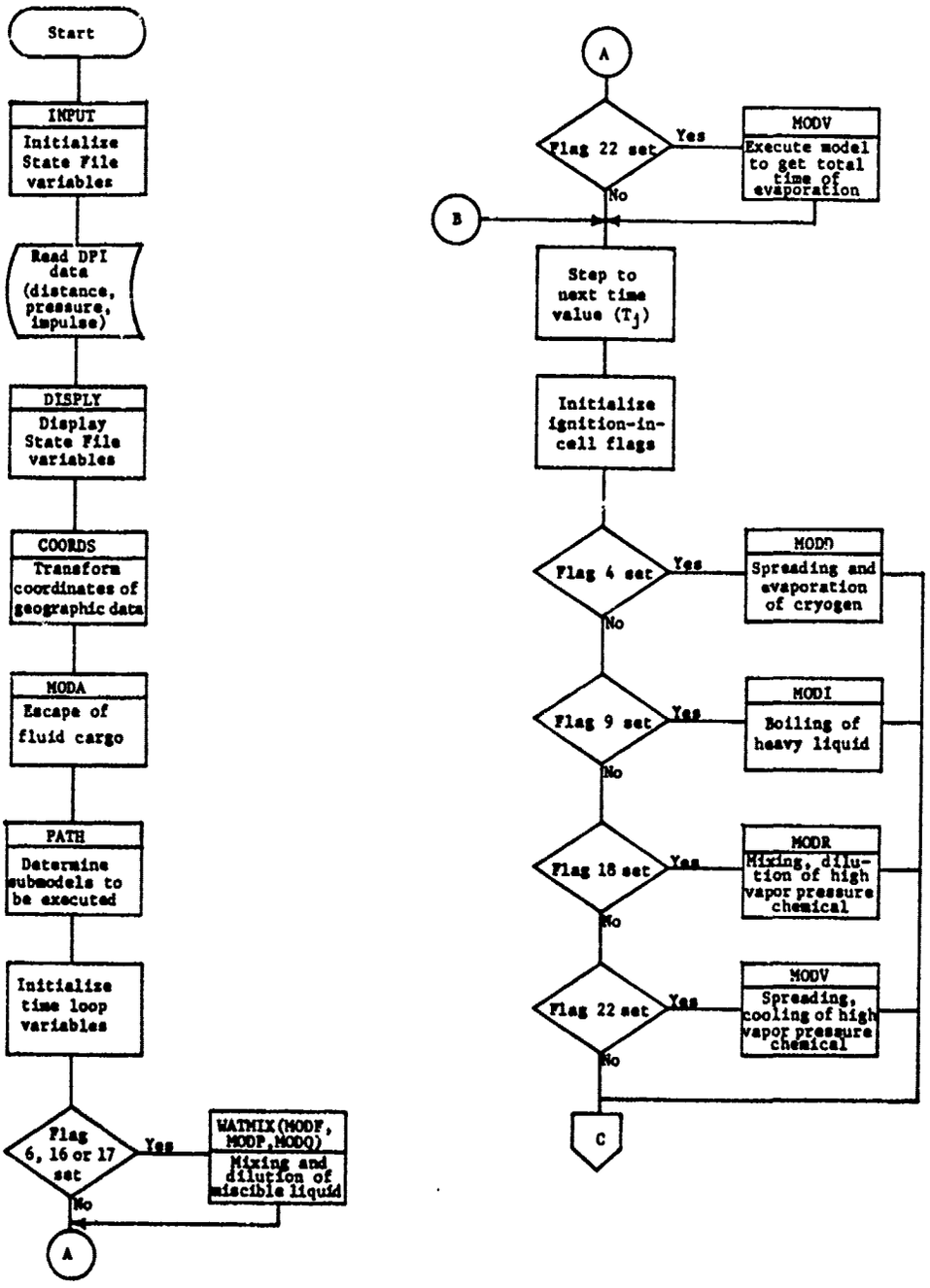

FIGURE 9-1. Flowchart of VM Executive Routine, VMEXEC

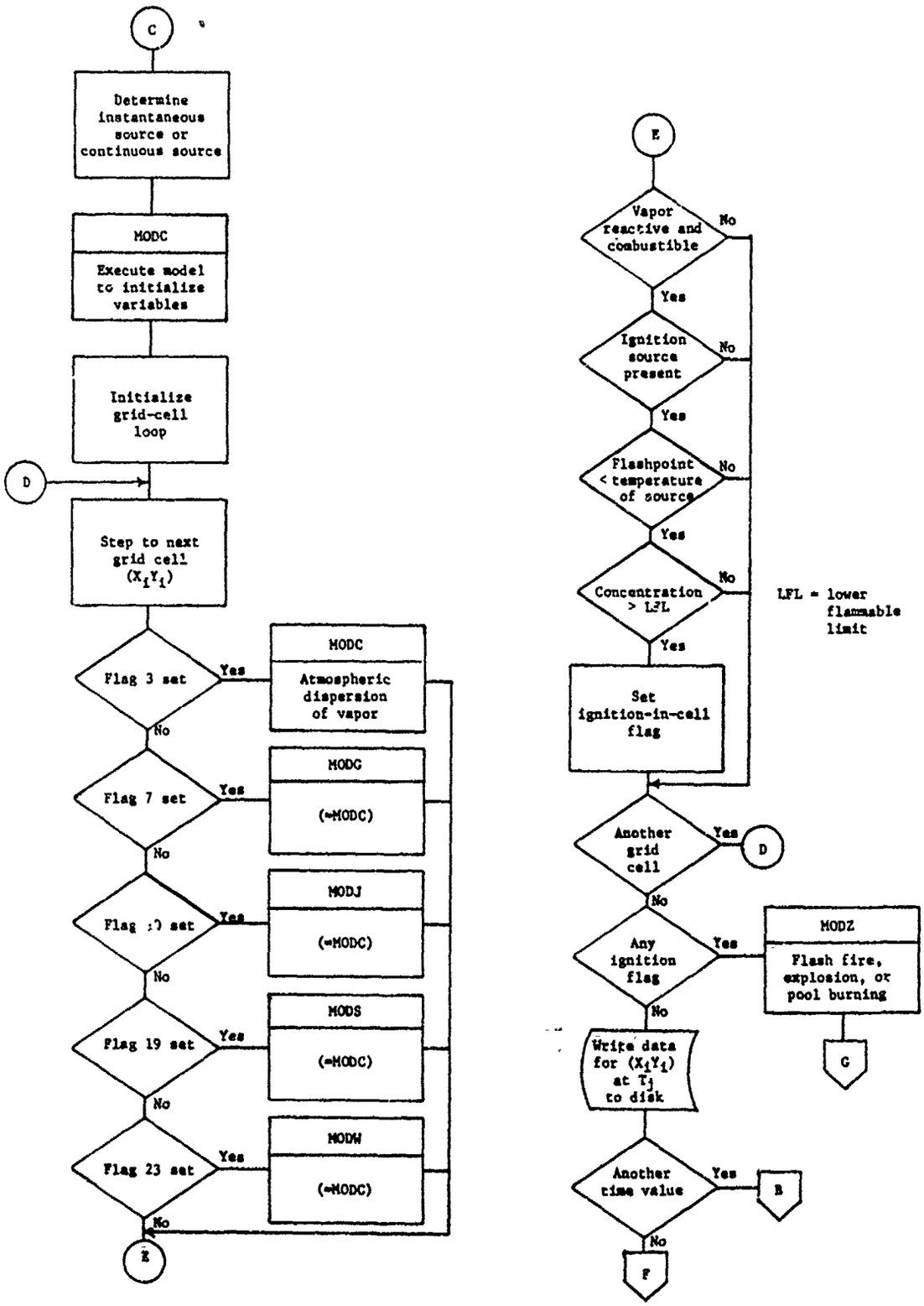

FIGURE 9-1 (continued). Flowchart of VM Executive Routine, VMEXEC

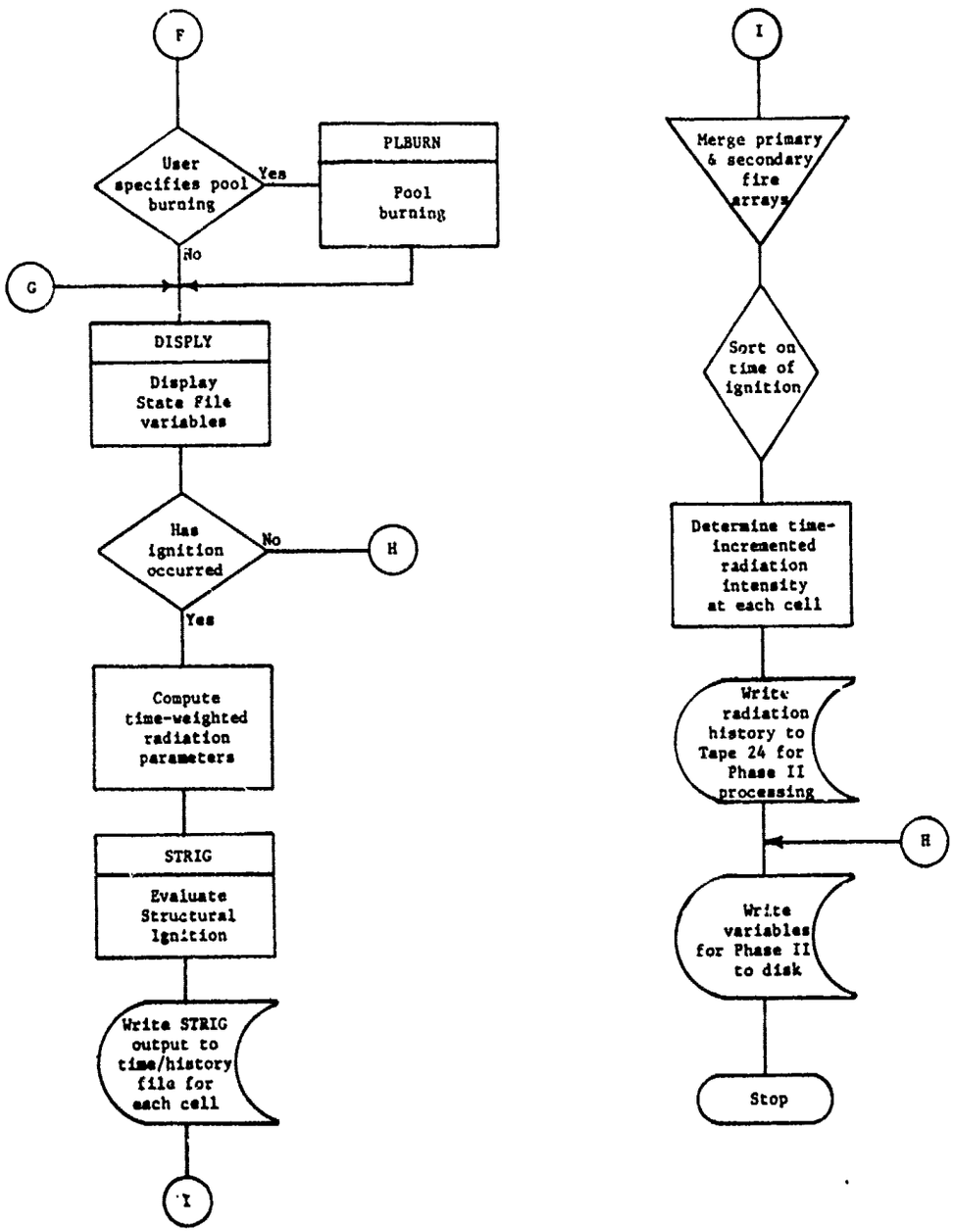

FIGURE 9-1 (continued). Flowchart of VM Executive Routine, VMEXEC

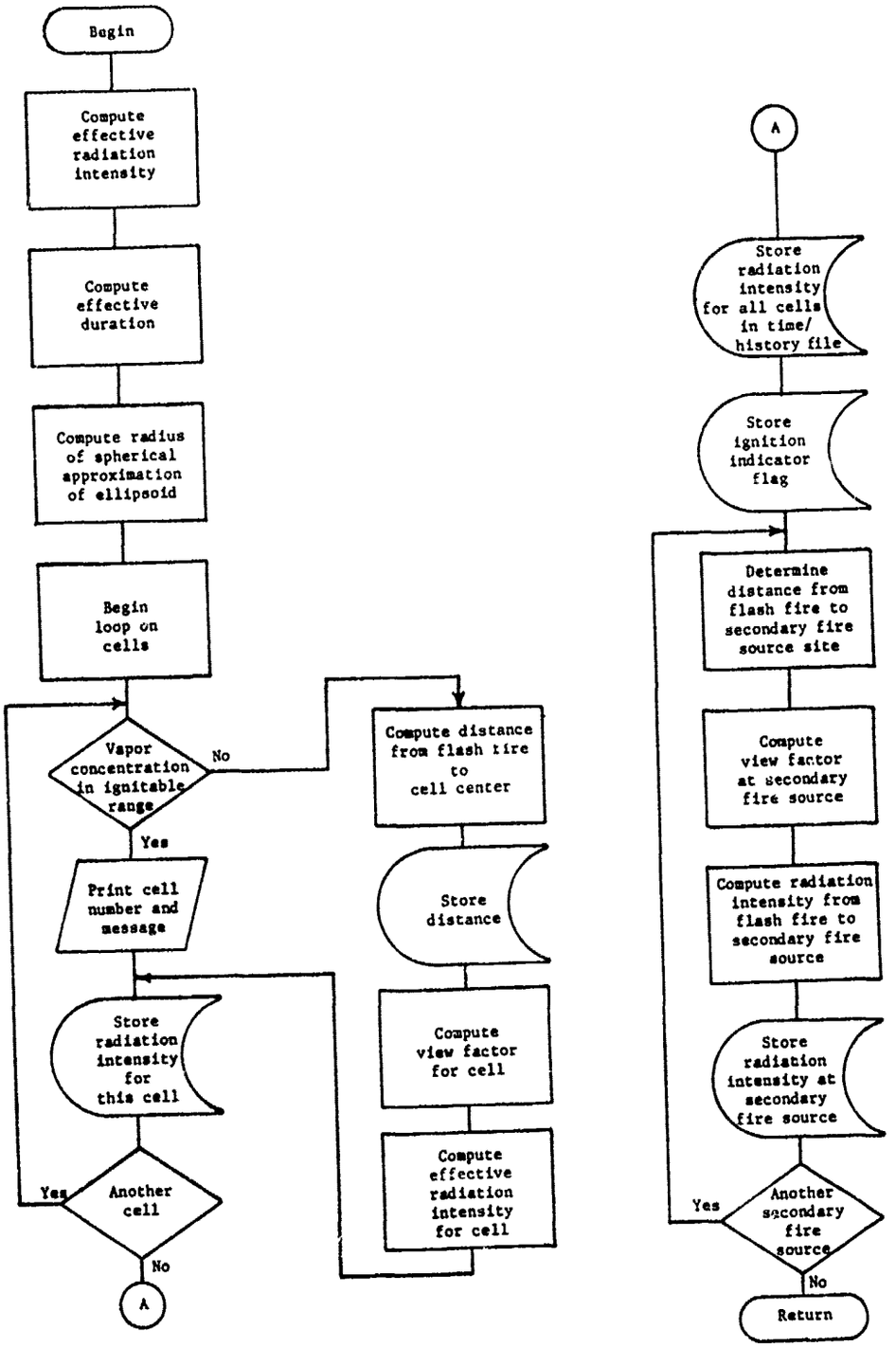

FIGURE 9-2. Flowchart of Flash Fire Subroutine, FLFIRE

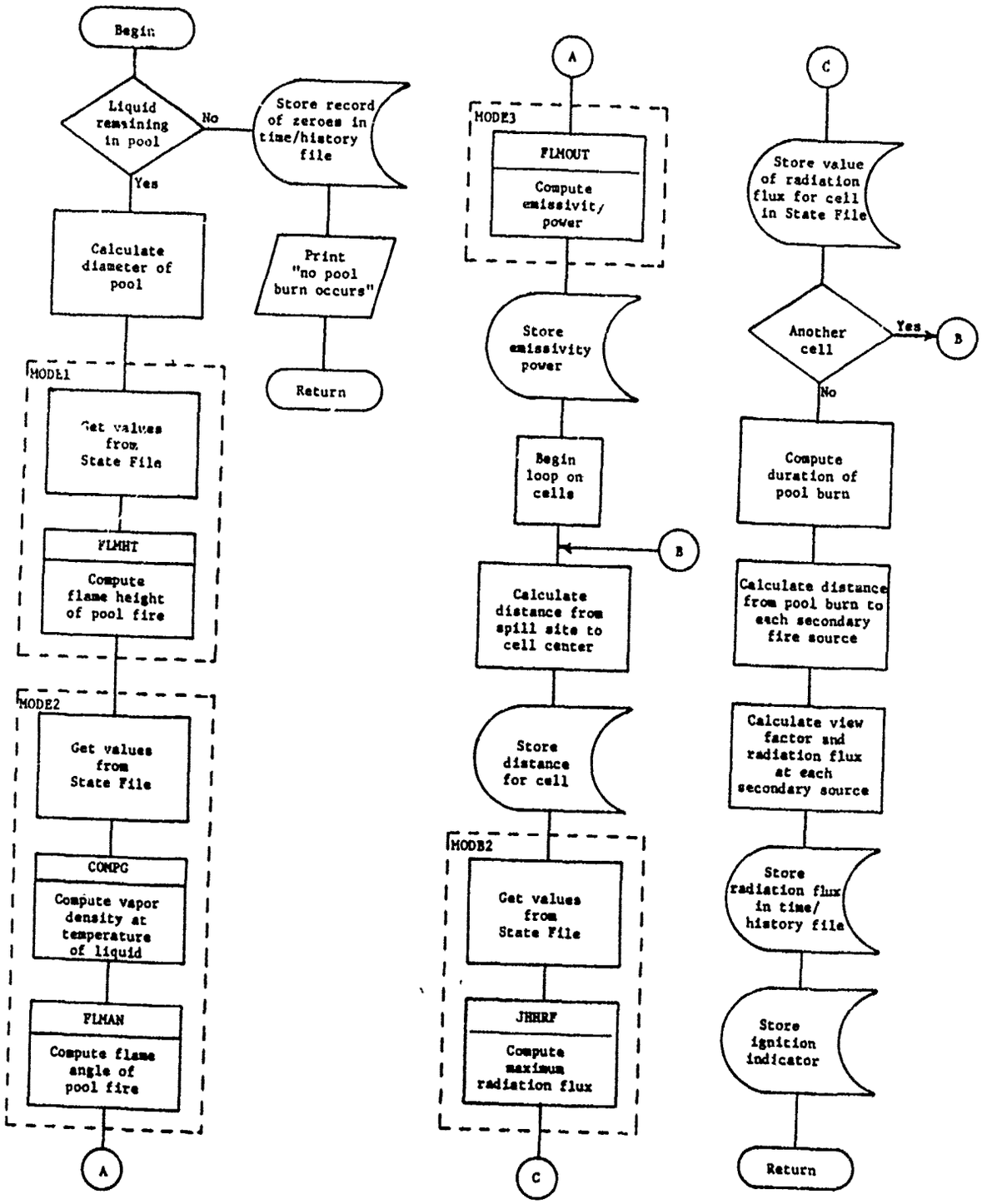

FIGURE 9-3. Flowchart of Pool Burn Subroutine, PLBURN

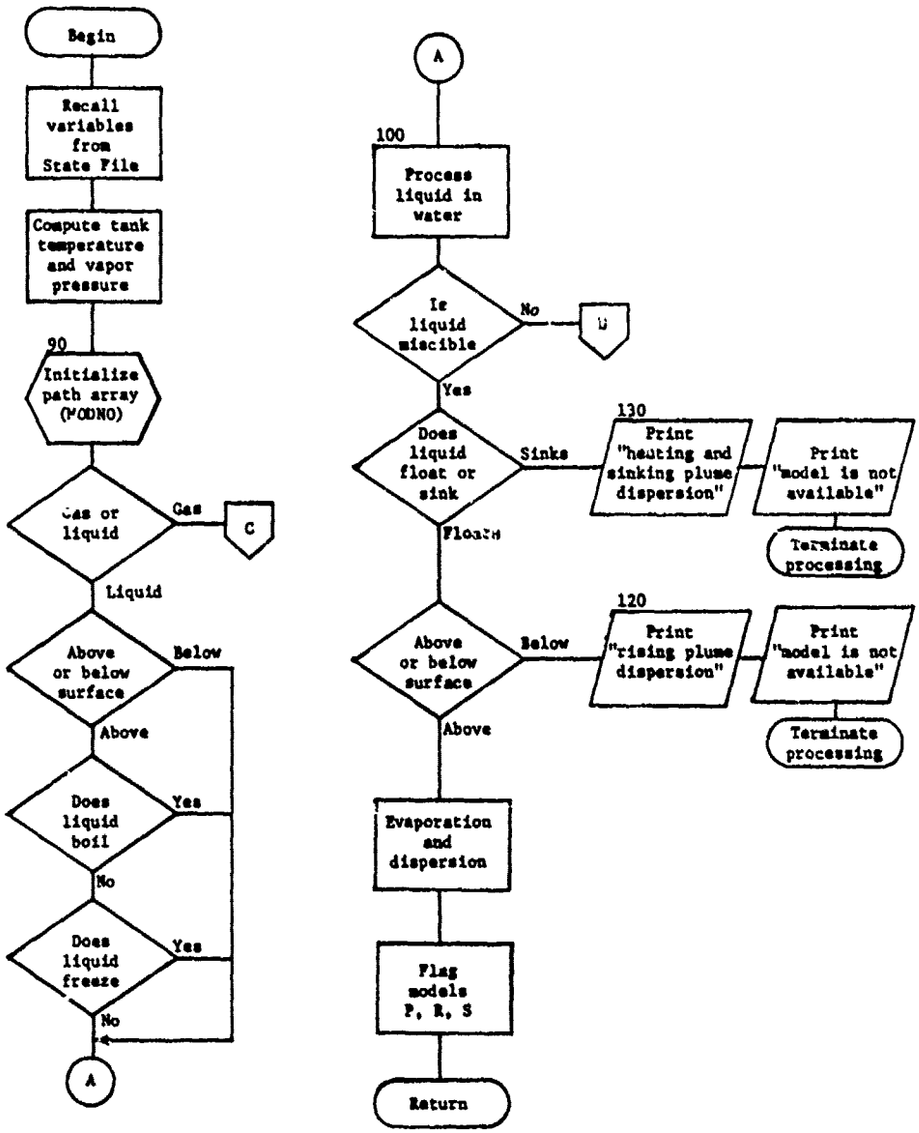

FIGURE 9-4. Flowchart of Subroutine, PATH

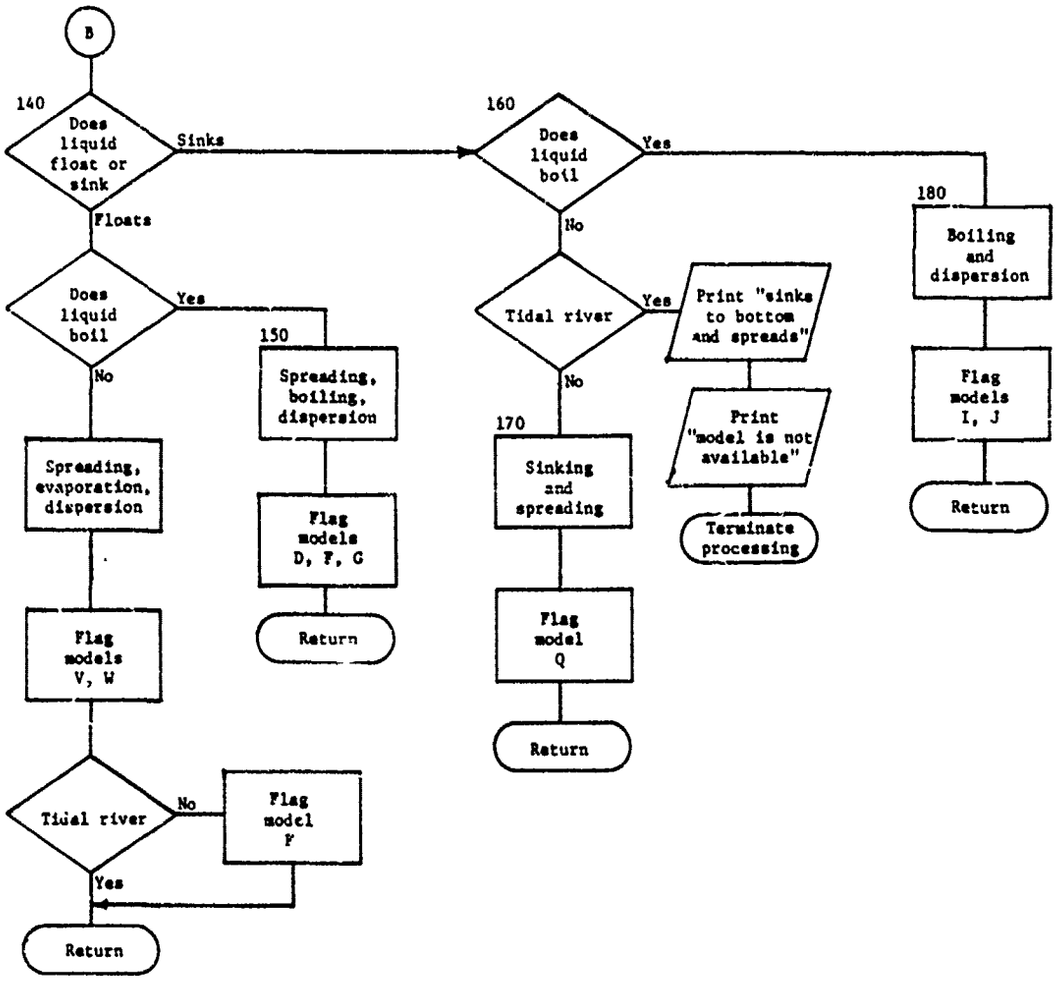

FIGURE 9-4 (continued). Flowchart of Subroutine, PATH

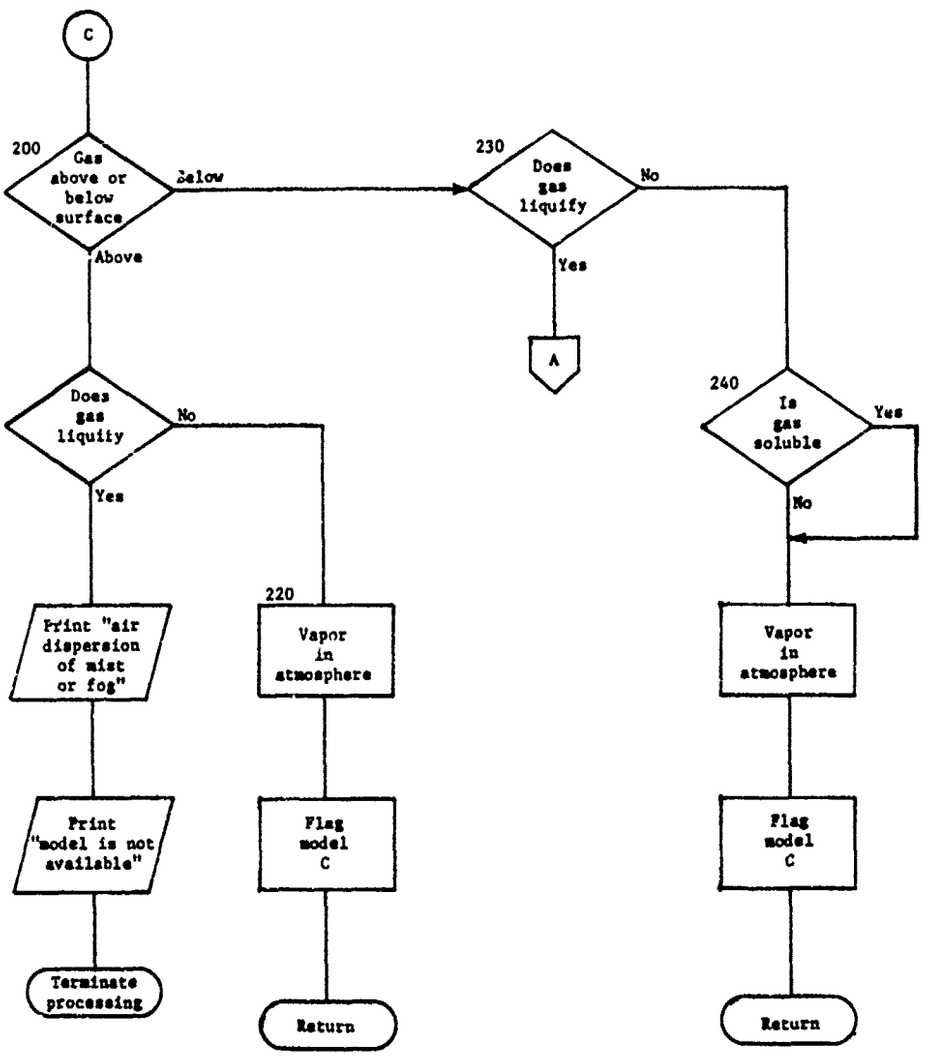

FIGURE 9-4 (continued). Flowchart of Subroutine, PATH

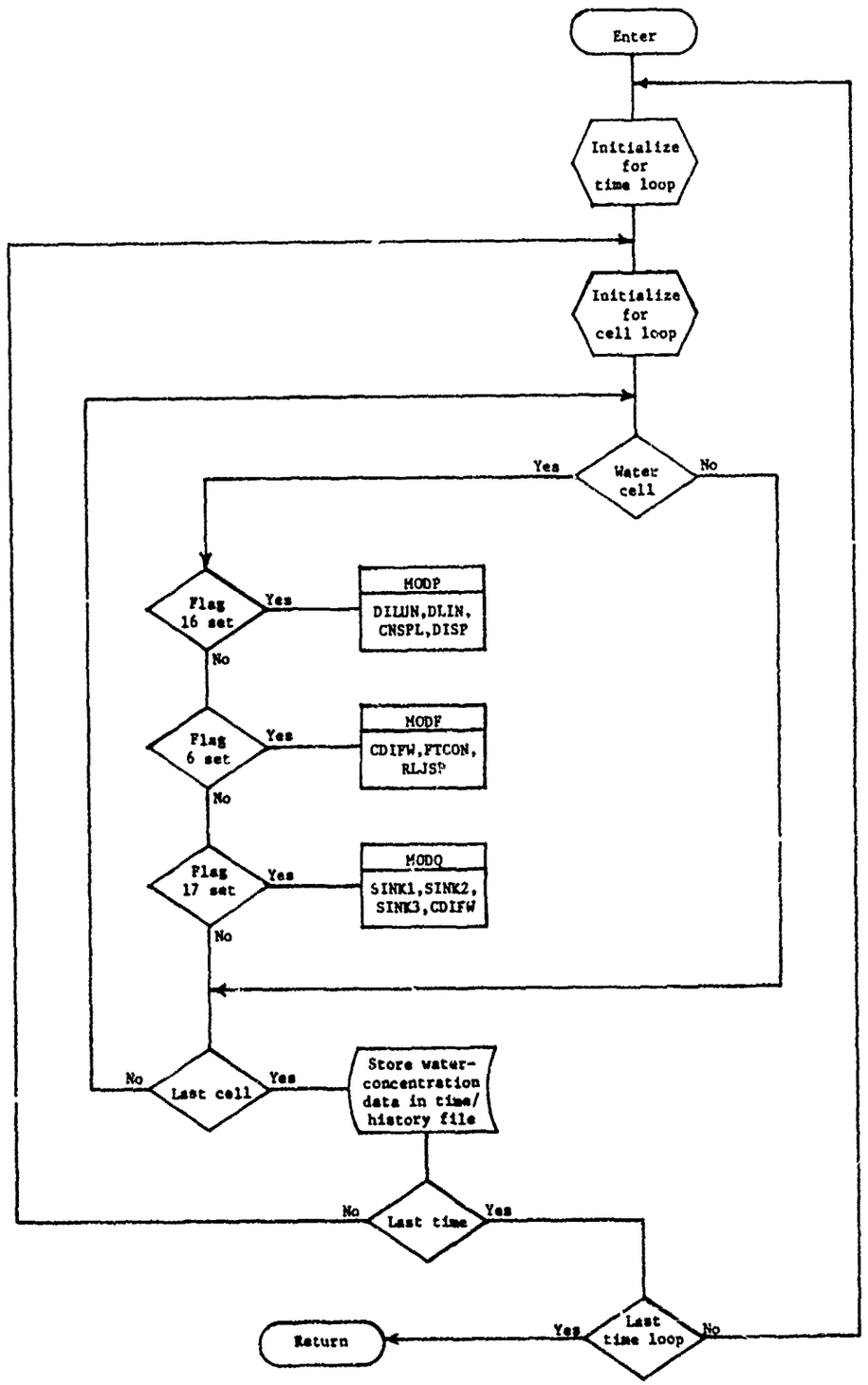

FIGURE 9-5. Flowchart of Water-Mixing Submodel Subroutine, WATMIX

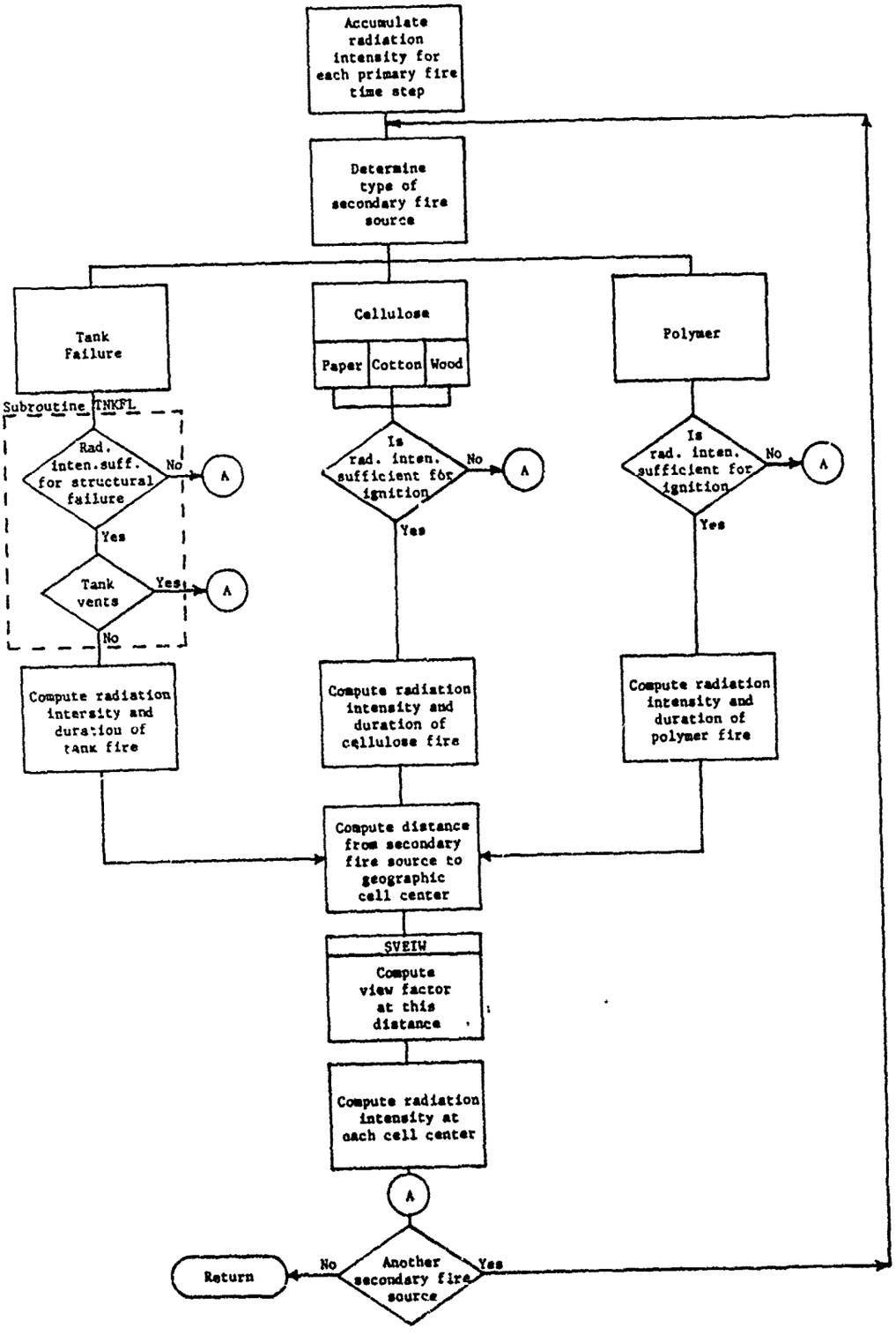

FIGURE 9-6. Flowchart of Secondary Fire Model, SECFIP

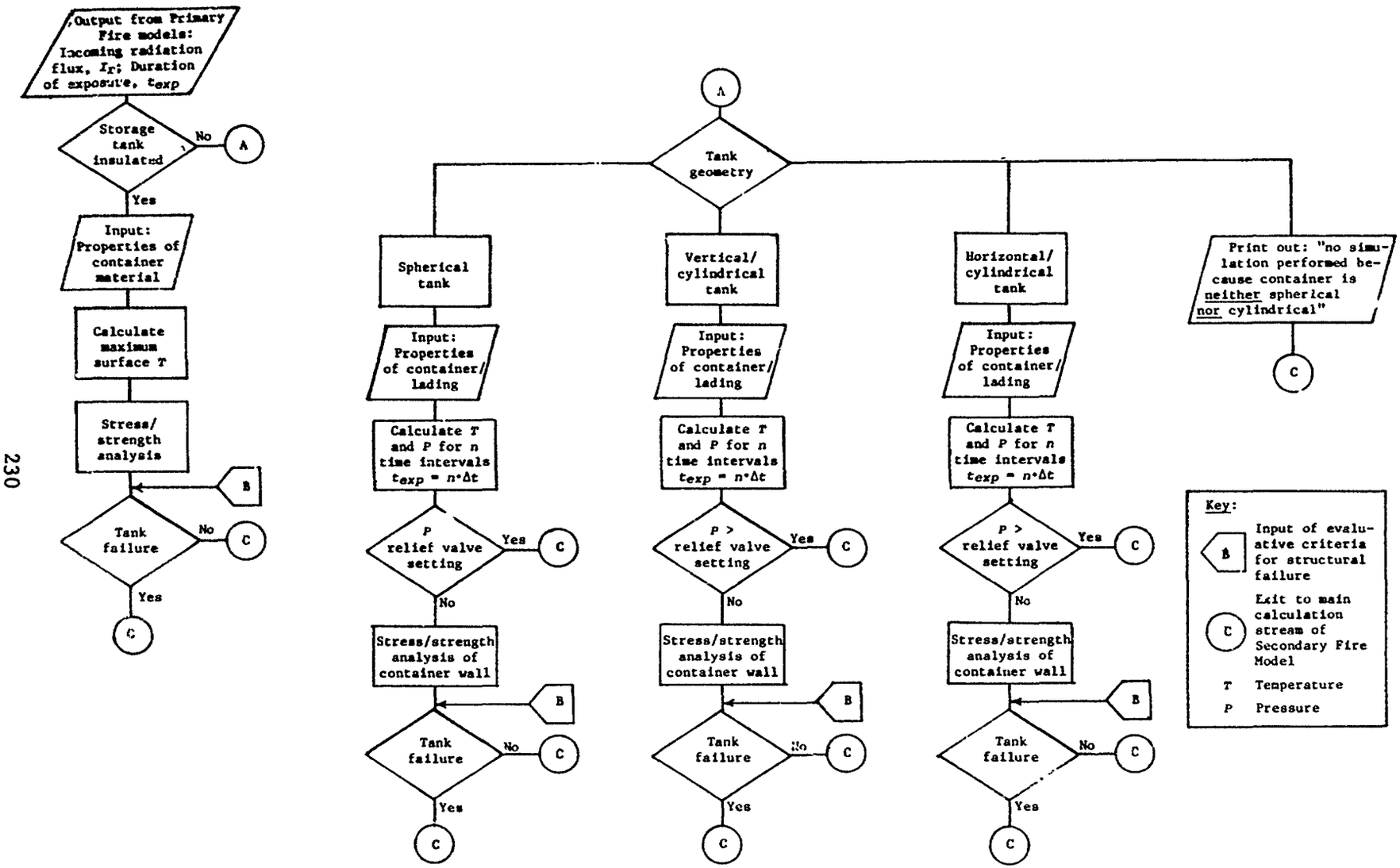

FIGURE 9-7. Flowchart of Tank Failure Subroutine, TNKFL

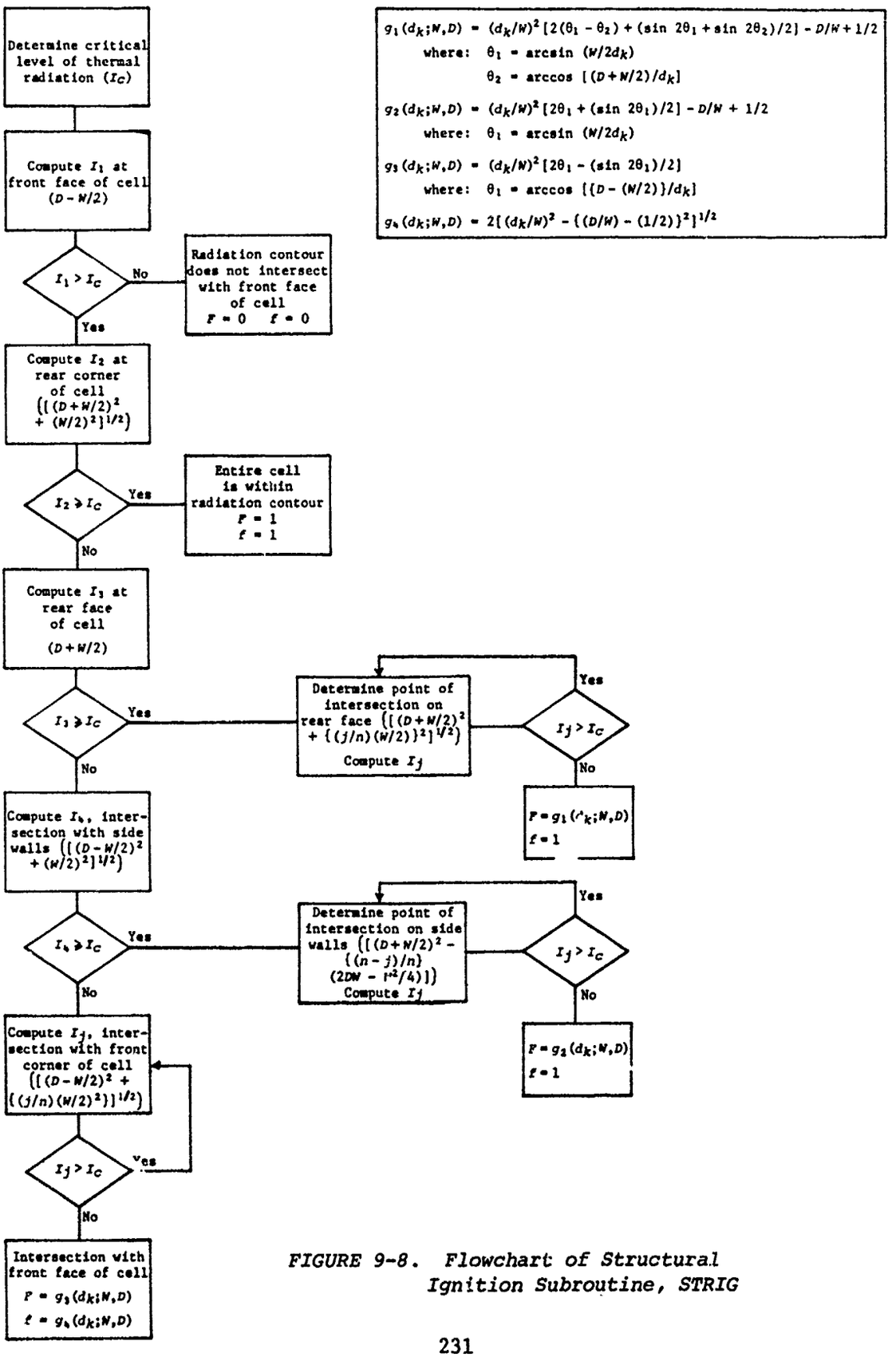

FIGURE 9-8. Flowchart of Structural Ignition Subroutine, STRIG

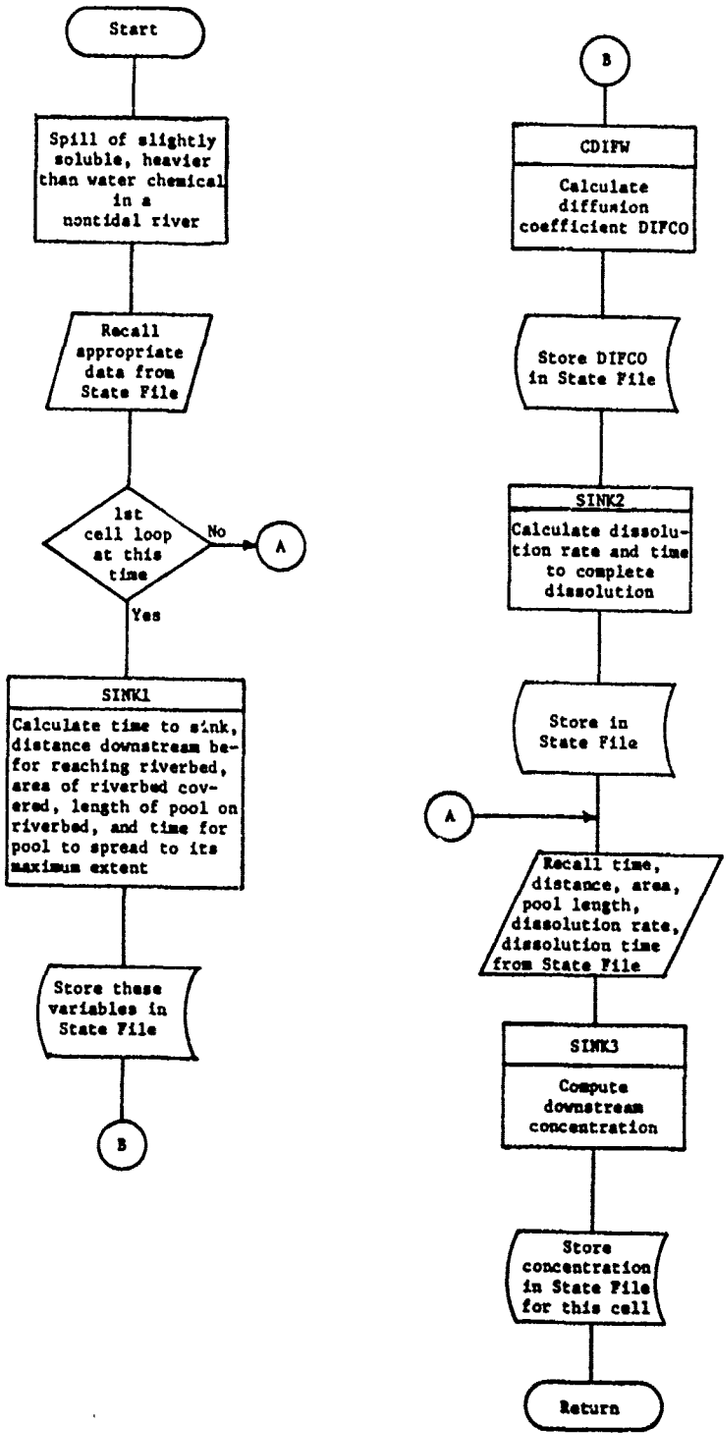

FIGURE 9-9. Flowchart of Subroutine, MODQ

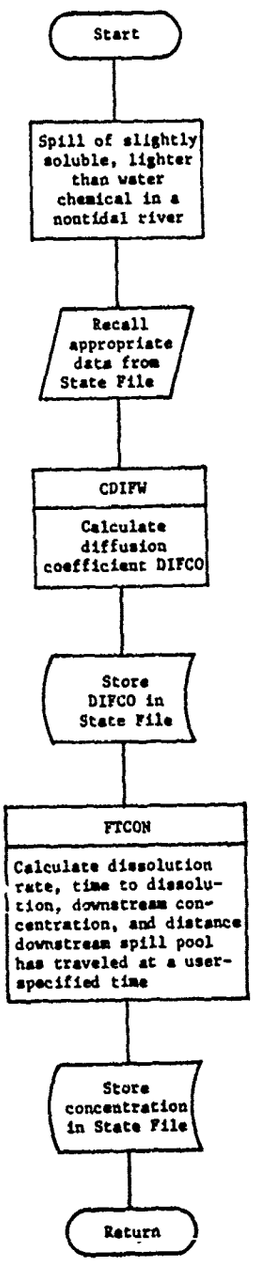

FIGURE 9-10. Flowchart of Subroutine, MODF

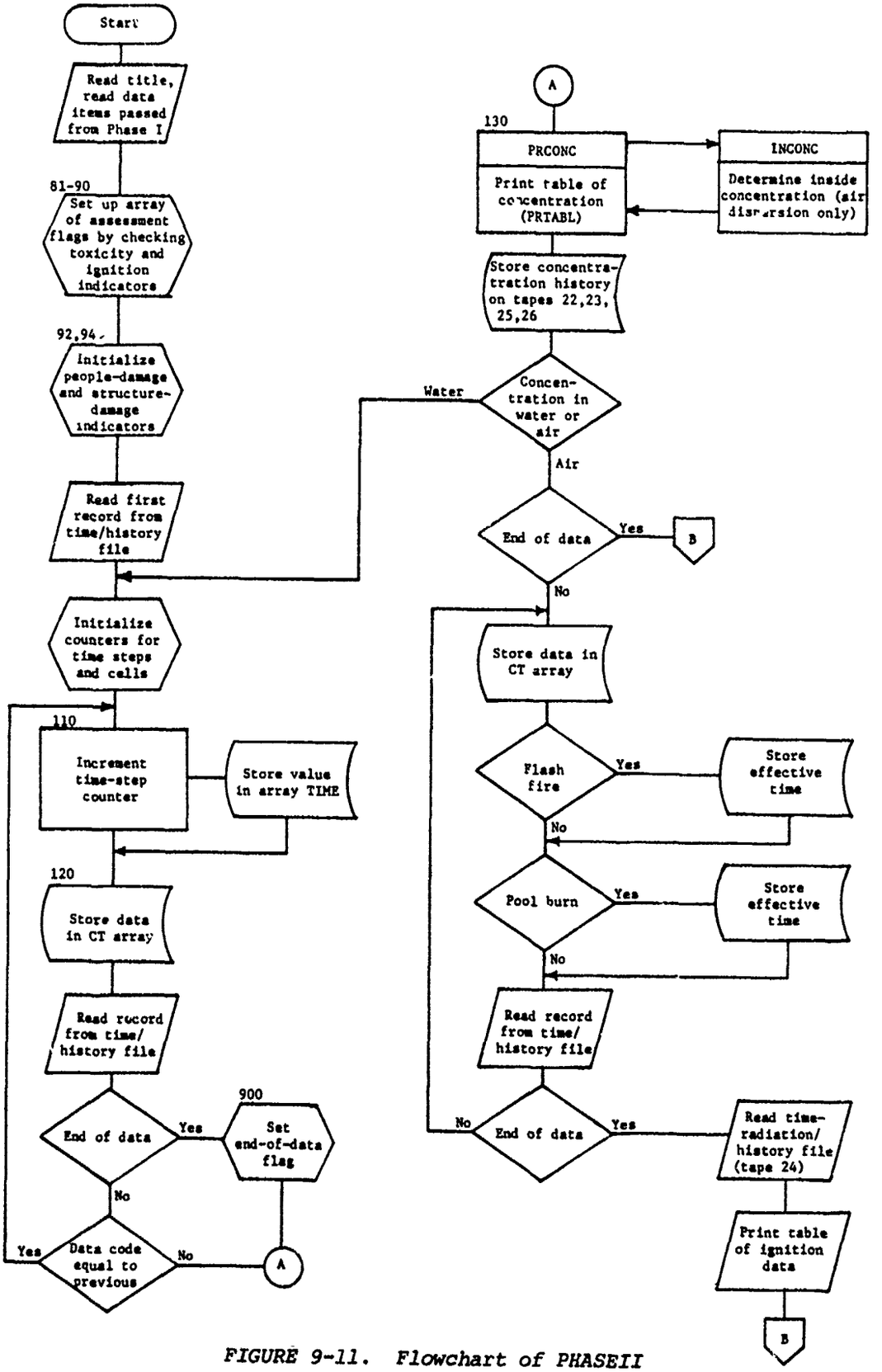

FIGURE 9-11. Flowchart of PHASEII

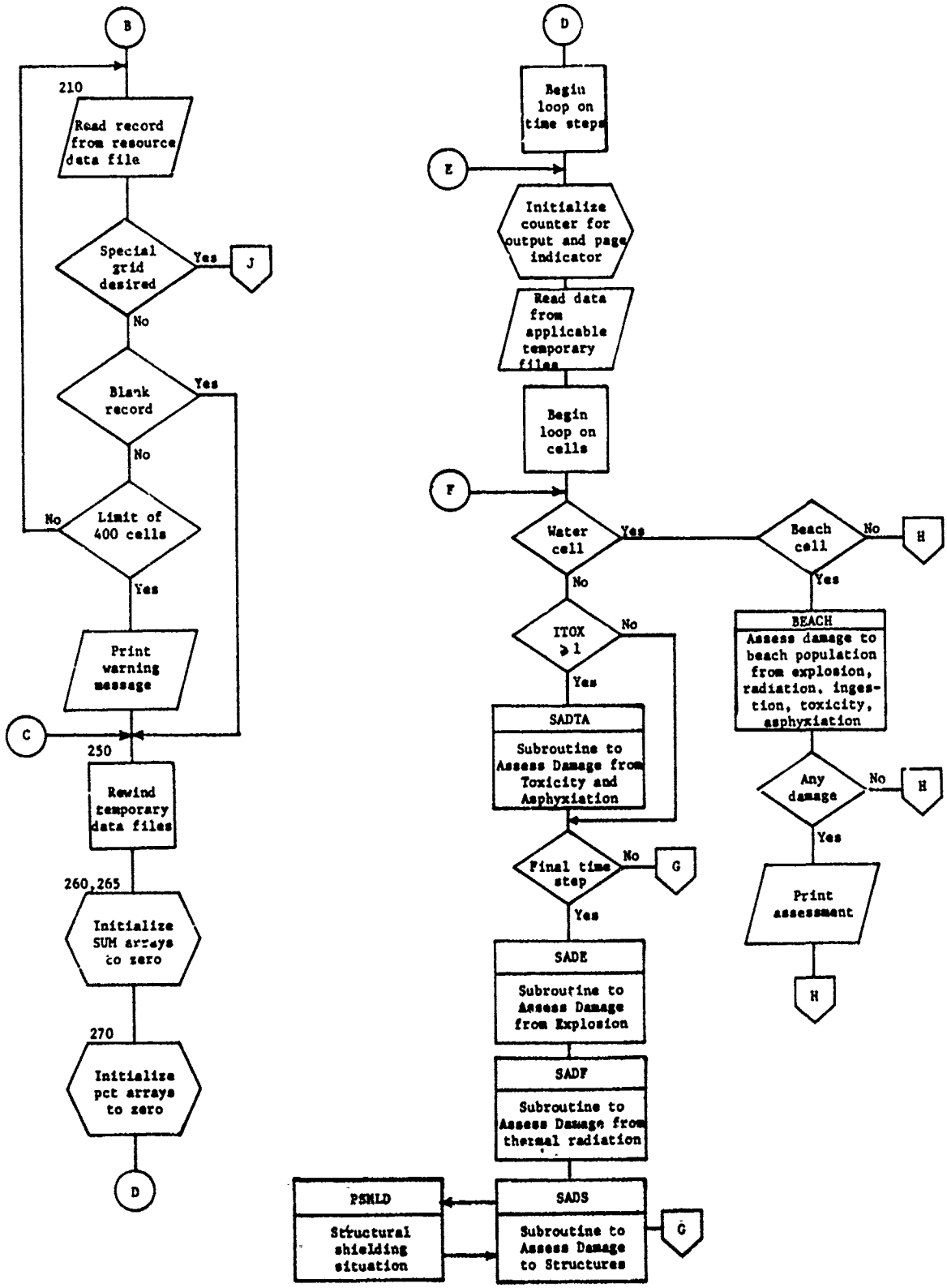

FIGURE 9-11 (continued). Flowchart of PHASEII

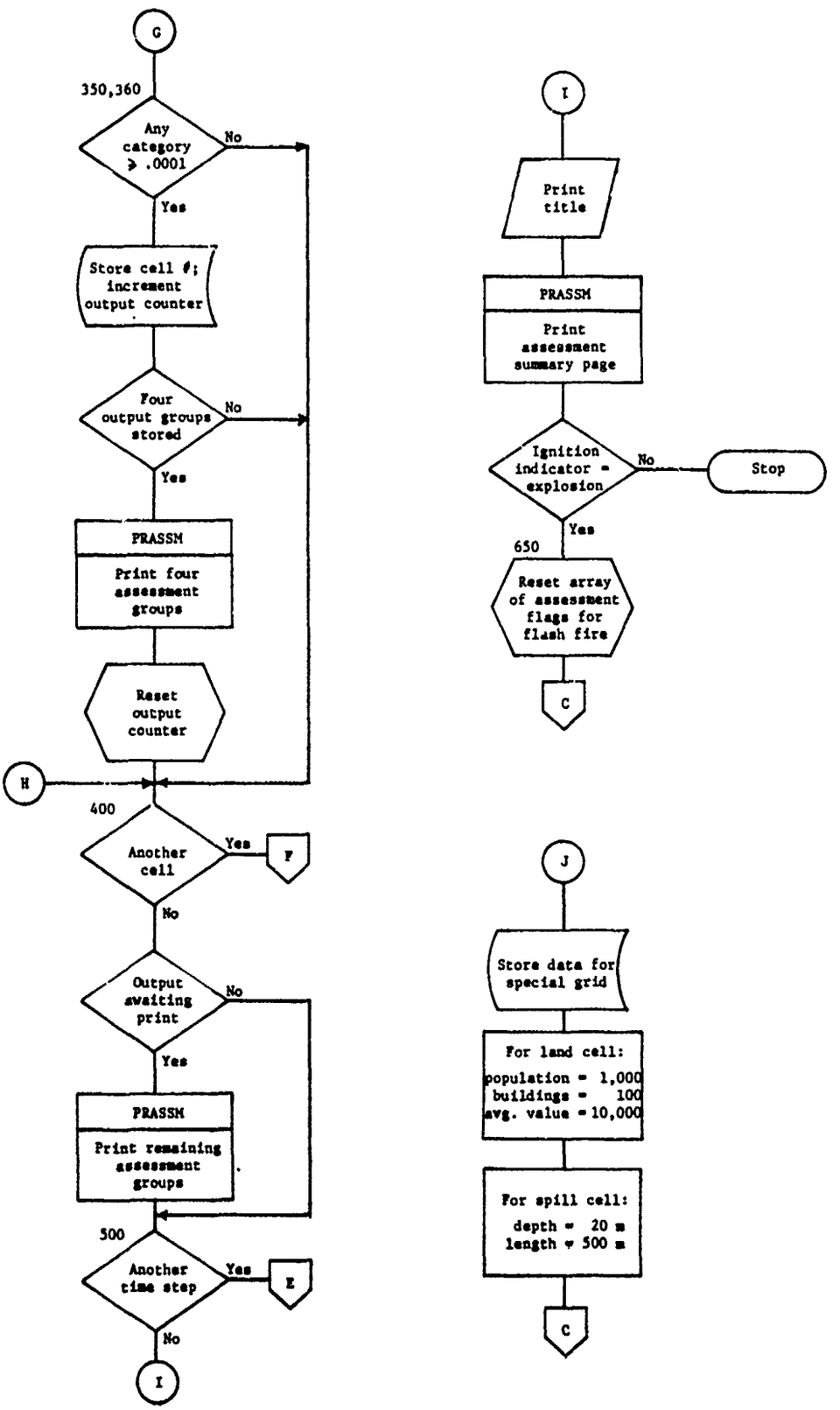

FIGURE 9-11 (continued). Flowchart of PHASEII

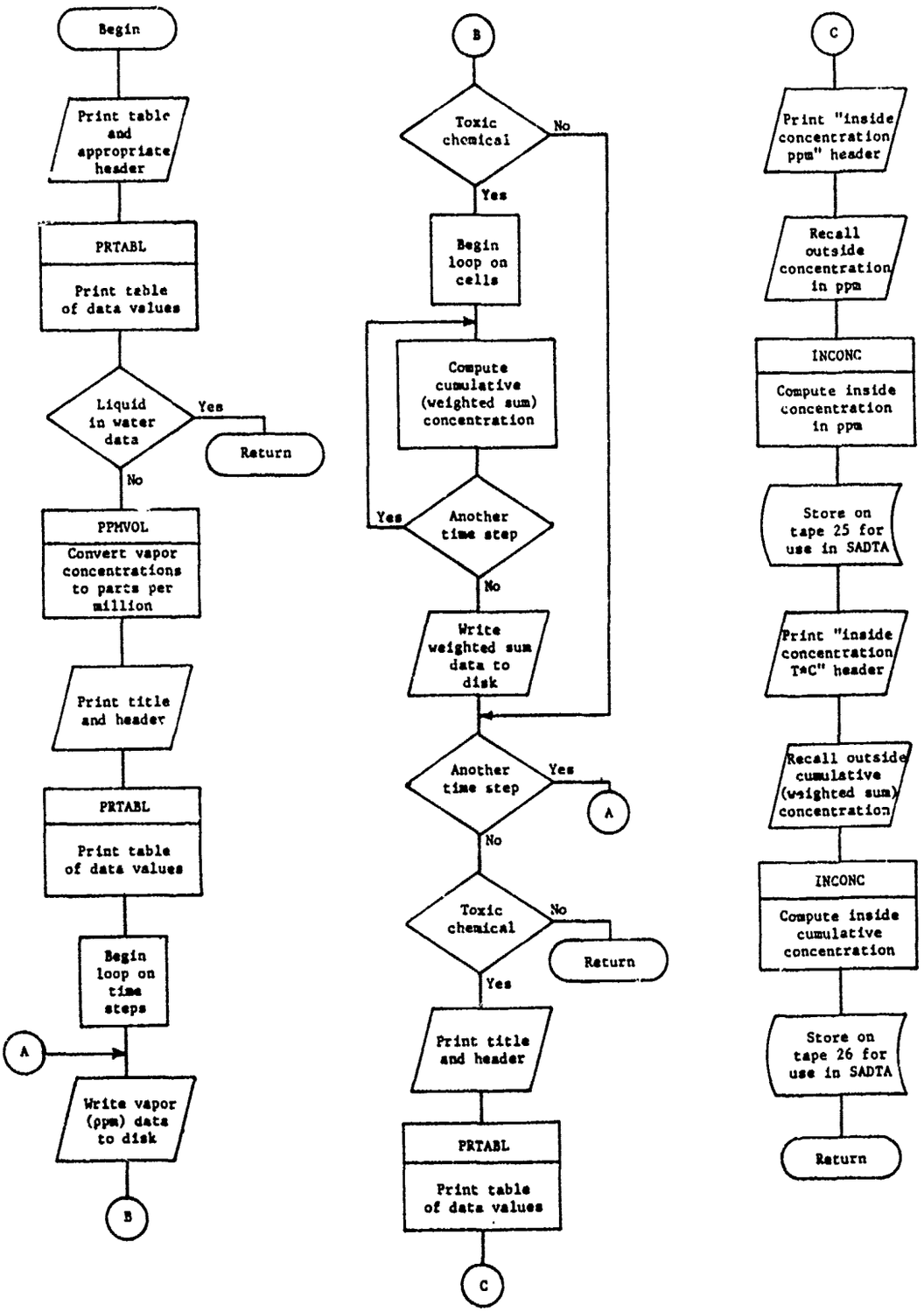

FIGURE 9-12. Flowchart of Subroutine, PRCONC

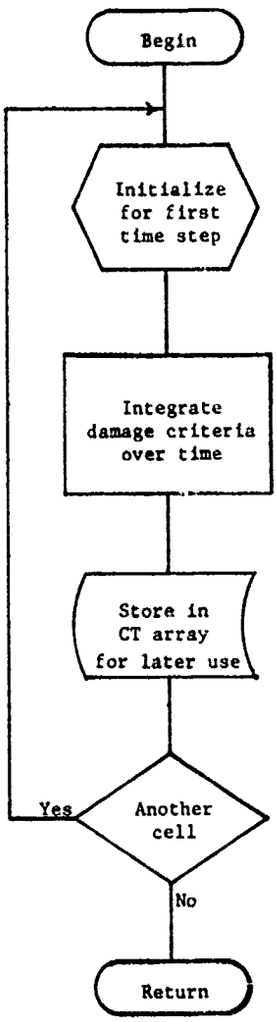

FIGURE 9-13. Flowchart of Subroutine, INCONC

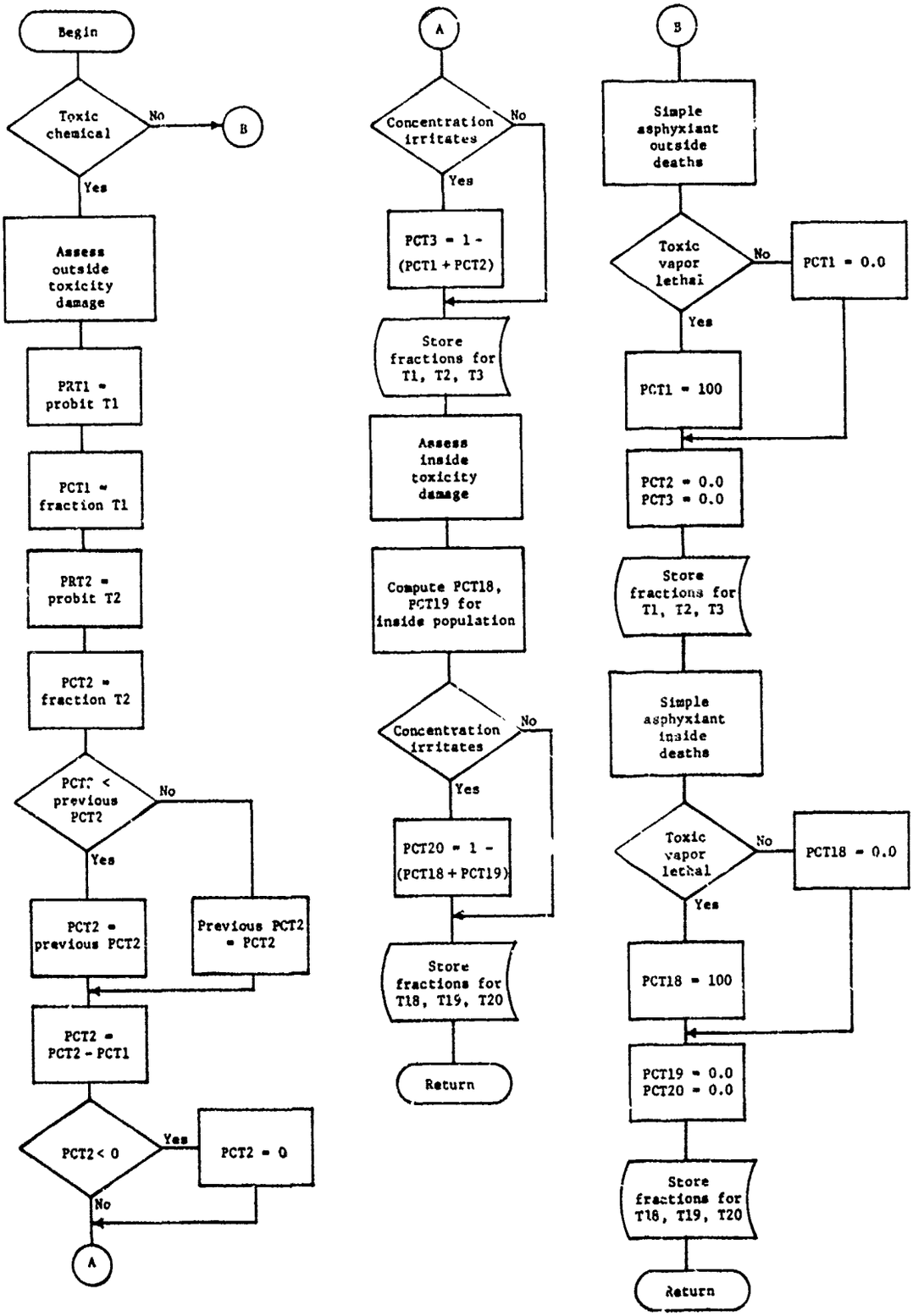

FIGURE 9-14. Flowchart of Subroutine, SADTA

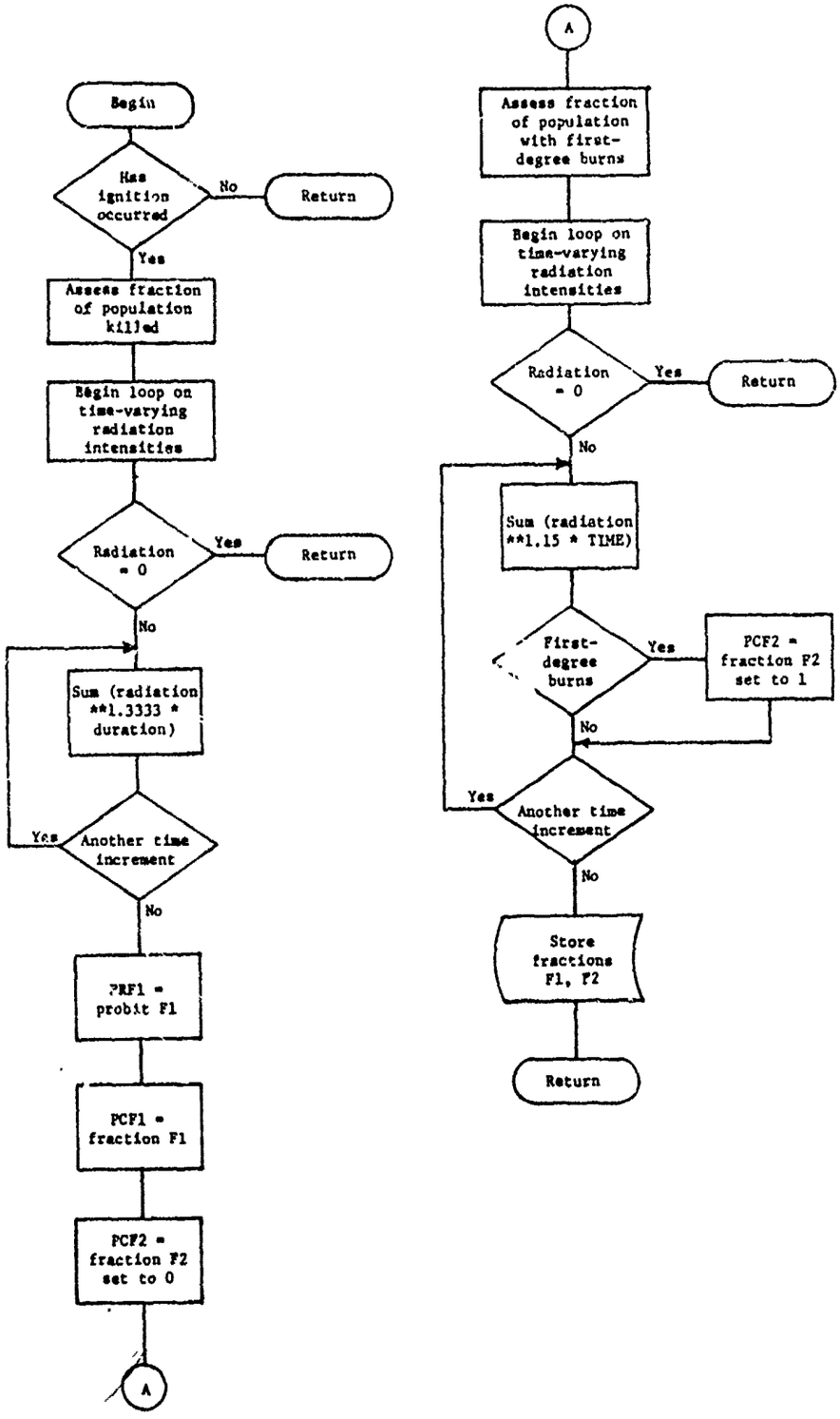

FIGURE 9-15. Flowchart of Subroutine, SADF

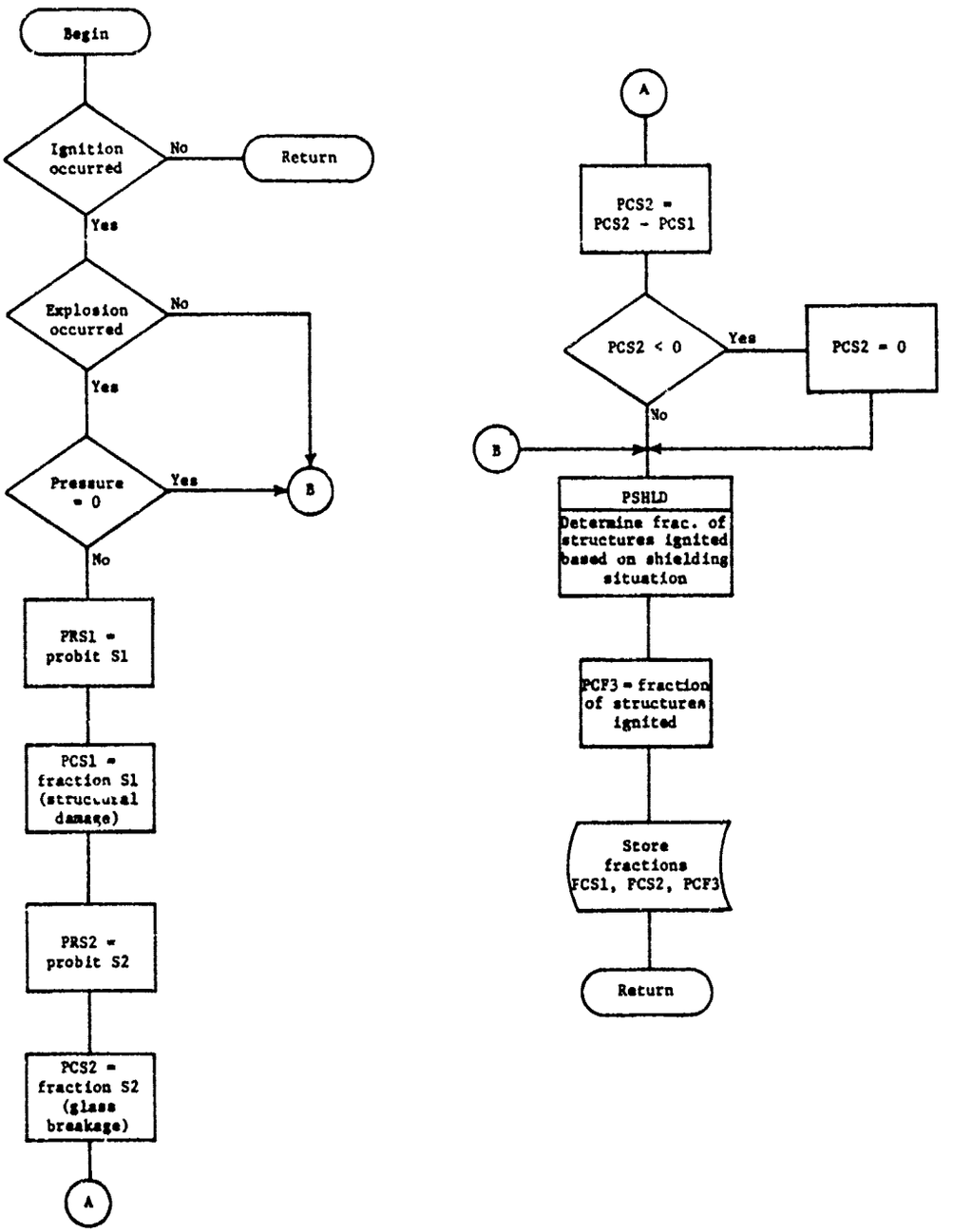

FIGURE 9-16. Flowchart of Subroutine, SADS

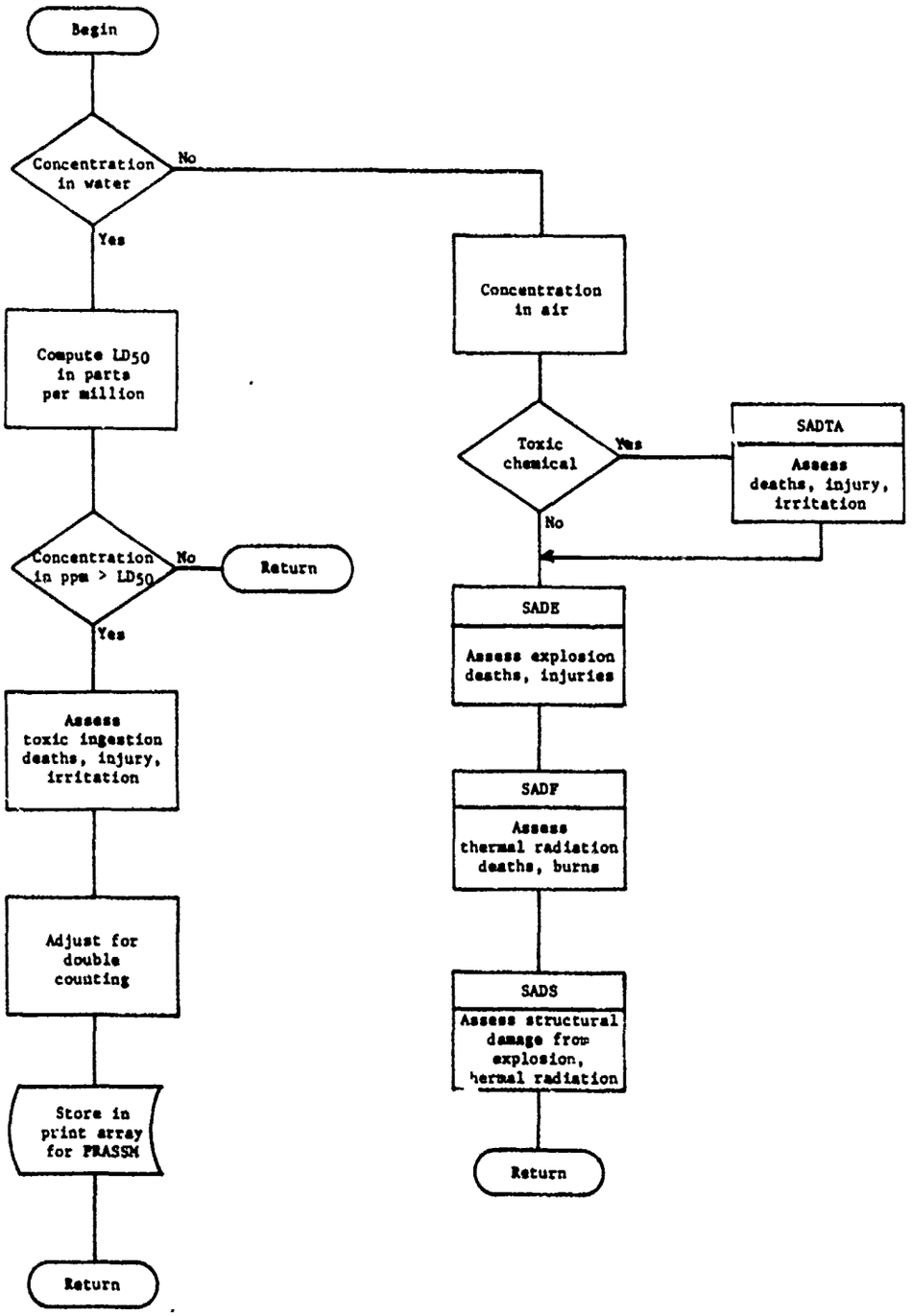

FIGURE 9-17. Flowchart of Subroutine, BEACH

Appendix A

ENCLOSURE MODEL

The Enclosure Model consists of four submodels:

- Submodel (1) Dual-Wall Container
- Submodel (2) Spherical Container
- Submodel (3) Vertical/Cylindrical Container
- Submodel (4) Horizontal/Cylindrical Container

Submodels (2), (3), and (4) are all single-wall containers. In this appendix we will treat in considerable detail material properties, characteristics of thermal radiation, and stress and strength analysis relative to the different submodels.

DUAL-WALL CONTAINER

An insulated dual-wall container submitted to a constant thermal radiation influx is an analogue of a slab subjected to a constant heat flux on one surface and with no heat transfer on the opposite surface. Therefore, thermal energy absorbed by the wall or slab is used to raise the temperature of the wall. A cross section of this type of container is shown in Figure A-1. The solution of Carslaw and Jaeger [A1], derived by rigorous mathematical treatment, is as follows.

$$T_w(x) = \frac{I_r t}{\rho_w c_w \ell} + \frac{I_r \ell}{k_w}\left\{\frac{3x^2 - \ell^2}{6\ell^2} - \frac{2}{\pi^2}\sum_{n=1}^{\infty}\frac{(-1)^n}{n^2}\exp\left[-\frac{k_w n^2 \pi^2 t}{\rho_w c_w \ell^2}\right]\cos\left(\frac{n\pi x}{\ell}\right)\right\} \tag{A-1}$$

where

$T_w(x)$ = wall temperature at x-distance from the inner surface

I_r = incoming thermal radiation flux

t = time

ρ_w = density of wall

c_w = specific heat of wall

ℓ = thickness of outer wall

and k_w = thermal conductivity of wall.

[A1] Carslaw, H. S., and J. C. Jaeger, *Conduction of Heat in Solids*, 2nd ed., p. 112, Oxford University Press, 1959.

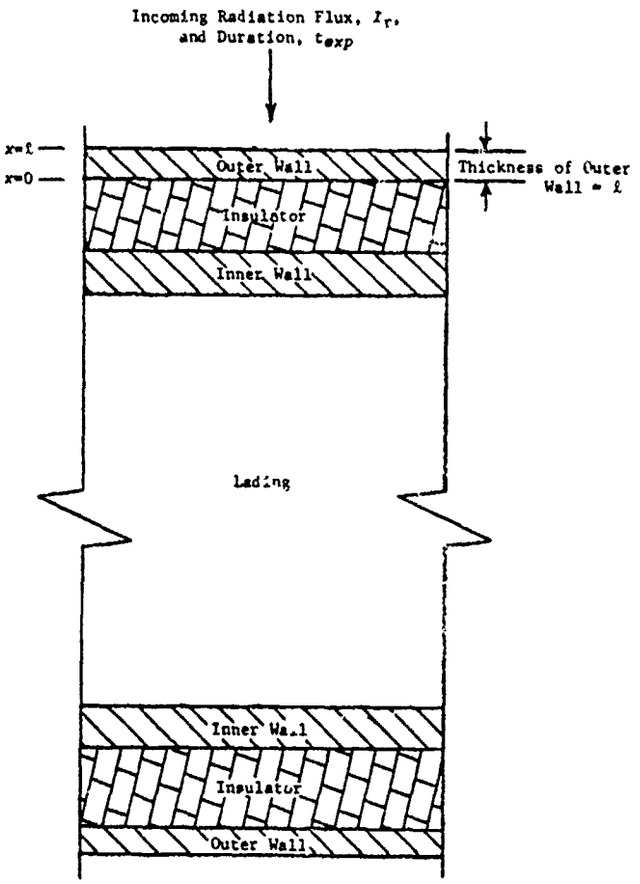

FIGURE A-1. Cross Section of Insulated Dual-Wall Container

Equation (A-1) can be reduced to describe the time-history of outer surface temperature by equating x's to ℓ.

$$T_{wo} = \frac{I_r t}{\rho_w c_w \ell} + \frac{I_r \ell}{k_w}\left\{\frac{1}{3} - \frac{2}{\pi^2}\sum_{n=1}^{\infty}\frac{1}{n^2}\exp\left(-\frac{k_w n^2 \pi^2 t}{\rho_w c_w \ell^2}\right)\right\} \qquad \text{(A-2)}$$

where

T_{wo} = temperature of outer surface.

The surface temperature calculated from equation (A-2) is then used in stress and strength analysis for the container wall. A comparison

between stress and strength determines the stability of the container. A detailed discussion of stress and strength analysis for a container is given in the last section of this appendix.

SINGLE-WALL CONTAINERS

A single-wall container subjected to external thermal radiation or engulfed by a fire is illustrated symbolically in Figure A-2. The heat transfer and mass transfer in this case are rather complicated. Heat transfer is indicated by wavy lines and mass transfer is represented by arrows. The sequential events in the heating process of the container are discussed as follows with appropriate mathematical equations.

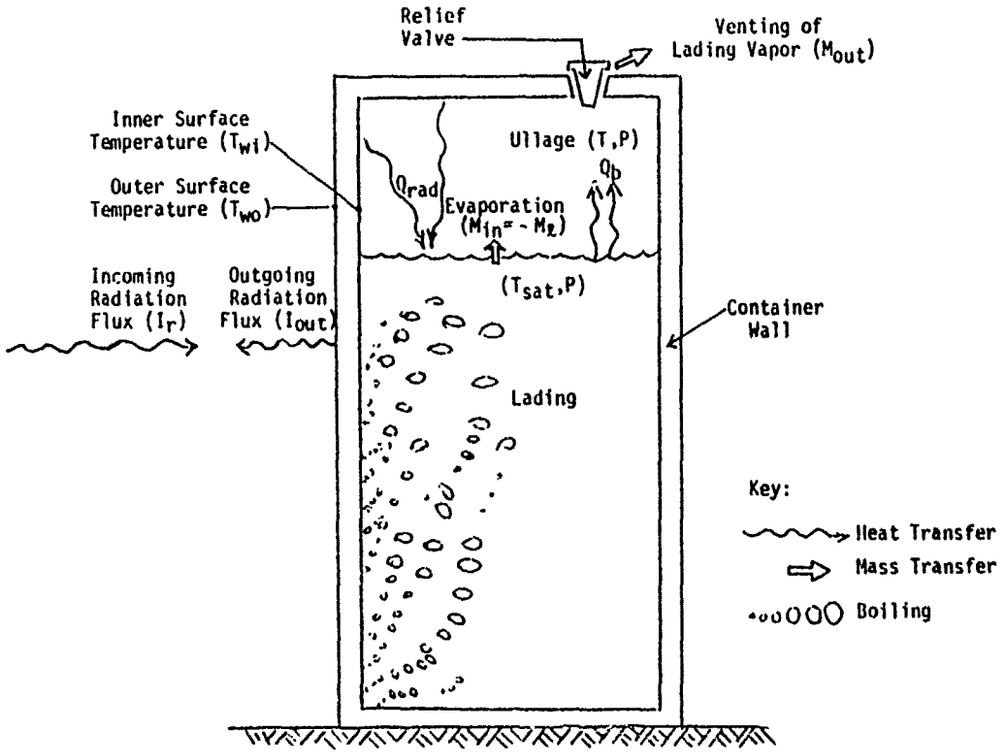

FIGURE A-2. Cross Section of Single-Wall Container

The incoming radiation energy heats up the container wall and causes its temperature to rise. The rate of absorption of thermal energy (Q_{abs}) by the wall is the difference between incoming radiation

flux (I_r) and outgoing radiation (I_{out}) which is determined by the outer surface temperature (T_{wo}) as shown in Figure A-2 and represented in the following equation.

$$Q_{abs} = I_r - I_{out} = I_r - \varepsilon \sigma T_{wo}^4 \qquad \text{(A-3)}$$

where

ε = thermal emissivity of wall

σ = Stephan-Boltzmann constant

and

T_{wo} = outer surface temperature

Part of the thermal energy absorbed by the wall is used to raise its own temperature; the re . of it is transmitted inwardly by thermal conduction, the rate of which depends on the temperature difference between the outer (T_{wo}) and inner (T_{wi}) surfaces. The inward heat flux raises the temperatures of both ullage volume and liquid lading. Because the specific heat of vapor is much less than that of liquid, the temperature of the inner surface in contact with the ullage subsequently is much higher than that of the wetted inner surface. When the temperature difference between the inner surface of the container wall and the saturated liquid lading is sufficiently high, boiling of the liquid lading can occur. This leads to loss of liquid due to evaporation which, in turn, contributes an increase in internal pressure. If internal pressure exceeds the relief valve setting, venting of vapor will take place. To represent the system more satisfactorily, the model does take evaporation and venting of lading into consideration. For problem solving, it is convenient to consider ullage and liquid lading separately in heat transfer analysis. Linkage between the two phases, i.e., gaseous and liquid phases, is then provided by heat and mass exchanges between them. To alleviate confusion, heat transfer and mass transfer are discussed separately below.

Heat Transfer

Thermal energy provided to liquid lading (Q_ℓ) includes convection (Q_b) from the boiling of liquid in contact with the heated container wall, and radiation (Q_{rad}) originating from the inner surface in contact with ullage and incident upon the meniscus between the liquid and vapor phases. It can be expressed as follows.

$$Q_\ell = Q_b + Q_{rad} \qquad \text{(A-4)}$$

The heat flow in vapor phase (Q_v) is the difference between heat conducted inwardly and heat absorbed by liquid lading (Q_ℓ). The heat conduction rate is governed by the thermal conductivity of the wall (K_w), tank surface area exposed to fire (A_w), and temperature difference between the outer wall and the inner wall ($T_{wo} - T_{wi}$). In analytical form, heat flow in the vapor phase is represented by the following equation.

$$Q_v = K_w A_w (T_{wo} - T_{wi}) - Q_\ell \qquad \text{(A-5)}$$

where K_w, A_w, T_{wo}, T_{wi}, and Q_ℓ have previously been defined.

It is obvious that the solution of Q_v depends on equation (A-4). Therefore, heat transfer by convection (Q_b) and radiation from the inner surface (Q_{rad}) will be discussed.

There are two types of boiling: namely, nucleate boiling and film boiling. Both of them depend solely on the temperature difference (ΔT) between the heating element, which is the inner surface of the wall in our case, and the saturation temperature of the liquid lading. Taking water as an example, if ΔT ranges from 0° to 4°F, pure vaporization without boiling takes place. The liquid is superheated, and heat transfer in the liquid phase is predominated by pure convection. In the ΔT range from 4° to 65°F, nucleate boiling with bubbles takes place, and ebullition increases with increasing ΔT. For ΔT larger than 65°F, film boiling occurs. The heating element is surrounded by a film of steam. As ΔT increases, film boiling changes from a metastable condition to a stable condition until the melting point of the heating element is reached [A2].

From experiments such as fire tests of railroad tank cars filled with liquefied petroleum gases [A3-A5], film boiling is very unlikely

---

[A2] Hsu, S. T., *Engineering Heat Transfer*, pp. 418-423, D. Van Nostrand Co., Inc., Princeton, N.J., 1963.

[A3] Anderson, C., W. Townsend, J. Zook, and G. Cowgill, *The Effects of a Fire Environment on a Rail Tank Car Filled With LPG*, prepared for U.S. Department of Transportation, Federal Railroad Administration, by Ballistic Research Laboratories, September 1974.

[A4] Anderson, C., and E. B. Norris, *Fragmentation and Metallurgical Analysis of Tank Car RAX 201*, prepared for U.S. Department of Transportation, Federal Railroad Administration, by Ballistic Research Laboratories, April 1974.

[A5] Anderson, C., W. Townsend, W. Wright, and G. Cowgill, *Railroad Rank Car Fire Test: Test No. 7*, prepared for U.S. Department of Transportation, Federal Railroad Administration, by Ballistic Research Laboratories, December 1973.

to occur in terms of the magnitude of radiation flux associated with common fires. Therefore, only nucleate boiling is considered in this model.

Correlation studies of heat transfer data for nucleate boiling have revealed that the heat transfer rate (q) by nucleate boiling is a function of ΔT and the thermodynamic properties of liquid lading. The correlation function is given as follows [A6,A7].

$$q = (3.25 \times 10^5) \frac{\lambda \mu_\ell}{B} \left\{ \frac{c_{p\ell} (T_{wi} - T_{sat})}{\lambda} \left(\frac{T_r}{N_{Pr}} \right)^{1.18} \right\}^{2.89} \tag{A-6}$$

where

λ = latent heat (erg/g)

μ_ℓ = viscosity of liquid (g/cm sec)

$$B = \left\{ \frac{\sigma_\ell}{g (\rho_\ell - \rho_v)} \right\}^{1/2} = \text{Laplace length (cm)} \tag{A-7}$$

in which

σ_ℓ = surface tension of liquid (dyne/cm)

g = gravitational acceleration = 980.7 (cm/sec^2)

and

ρ_ℓ, ρ_v = densities of liquid and vapor, respectively (g/cm^3)

$c_{p\ell}$ = specific heat of liquid (erg/g °K)

T_{wi} = inner surface temperature (°K)

T_{sat} = saturation temperature (°K)

$T_r = T_{sat}/T_{crit}$ = reduced temperature (dimensionless)

in which

T_{crit} = critical temperature (°K) (A-8)

[A6] Sciance, C. T., C. P. Colver, and C. M. Sliepcevich, Boiling of methane between atmospheric pressure and the critical pressure, *Adv. Cryog. Eng. 12*:395, 1967.

[A7] Rohsenow, W. M., A method of correlating heat-transfer data for surface boiling of liquids, *Trans. Am. Soc. Mech. Eng. 74*:969, 1952.

and

N_{Pr} = Prandtl number of liquid (dimensionless)

$$= \frac{c_{p\ell}\mu_\ell}{k_\ell}$$

in which

k_ℓ = thermal conductivity of liquid (erg/cm sec °K) (A-9)

The heat transfer rate due to nucleate boiling is then described by the following equation.

$$Q_b = A_b\, q \tag{A-10}$$

where q is defined in equation (A-6) and A_b is the total surface area where boiling takes place (cm^2).

The surface area of boiling (A_b) varies with the geometry of a container and is assumed to be the area exposed to the fire and wetted by liquid lading. Values of A_b as a function of ullage volume for submodels (2), (3), and (4) are given in the subsection, Geometry of Container, later in this appendix.

The thermal radiation flux (Q_{rad}) to the meniscus is determined by the following equation, assuming that the product of view factor and emissivity is unity.

$$Q_{rad} = A_m \sigma\, (T_{wi}^4 - T_{sat}^4) \tag{A-11}$$

where

A_m = surface area of the liquid-vapor meniscus

and

σ = Stephan-Boltzmann constant

The surface area of the meniscus depends on the geometry of the container and the ullage volume, and it is discussed in the subsection, Geometry of Container.

Mass Transfer

To establish mass balance for the vapor phase, one has to consider the vaporization rate $[(dM_{in})/(dt)]$ and the boiling process or the evaporation loss of liquid $[(dM_\ell)/(dt)]$. They are calculated by the following equation.

$$\frac{dM_{in}}{dt} = -\left(\frac{dM_\ell}{dt}\right) = \frac{Q_b + Q_{rad}}{h_g - u_\ell} \tag{A-12}$$

where

h_g = specific enthalpy of saturated vapor (erg/g)

and

u_ℓ = specific internal energy of subcool liquid (erg/g)

When internal pressure exceeds the relief-valve setting, venting of the vapor occurs. The mass venting rate $[(dM_{out})/(dt)]$ can be approximated by the following equation.

$$\frac{dM_{out}}{dt} = A_0 \left\{1 - \frac{\exp(P - P_{set})}{0.44}\right\} \left\{\frac{\gamma}{R_g}\left(\frac{2}{\gamma+1}\right)^{(\gamma+1)/(\gamma-1)}\right\}^{1/2} \frac{P}{\sqrt{T}}$$

when $P \geq P_{set}$ (A-13)

$$\frac{dM_{out}}{dt} = 0 \qquad \text{when} \quad P < P_{set} \tag{A-14}$$

where

A_0 = opening of relief valve (cm^2)

P_{set} = relief-valve setting ($dyne/cm^2$)

γ = ratio of specific heats of vapor (dimensionless)

R_g = gas constant of vapor (dyne cm/g °K)

P = internal pressure ($dyne/cm^2$)

T = temperature of vapor (°K)

General Solution

After the preceding considerations on heat transfer and mass balance of a container, one can define the problem by five independent variables: i.e., pressure (P), temperature (T), ratio of ullage volume and container volume (β), and temperatures of the inner (T_{wi}) and outer (T_{wo}) surfaces of the wall. The changing rates of these five variables with respect to time, in finite differential forms, are given as follows.

$$\frac{\Delta P}{\Delta t} = \frac{\alpha_4(\alpha_6 - Q_V) - \alpha_3\alpha_7}{\alpha_4\alpha_8 + \alpha_5\alpha_7} \tag{A-15}$$

$$\frac{\Delta T}{\Delta t} = \frac{Q_V + \alpha_8 \, (\Delta P/\Delta t) - \alpha_6}{\alpha_7} \tag{A-16}$$

$$\frac{\Delta \beta}{\Delta t} = \alpha_9 + \frac{1}{V} \left\{ \alpha_4 \left(\frac{\Delta T}{\Delta t} \right) + \alpha_5 \left(\frac{\Delta P}{\Delta t} \right) \right\} \tag{A-17}$$

$$\frac{\Delta T_{wi}}{\Delta t} = 2 \left\{ \left(\frac{\Delta T}{\Delta t} \right) - \alpha_2 \left(\frac{\Delta P}{\Delta t} \right) \right\} \tag{A-18}$$

$$\frac{\Delta T_{wo}}{\Delta t} = \alpha_1 - \left(\frac{\Delta T_{wi}}{\Delta t} \right) \tag{A-19}$$

where

V = volume of the container

P, T, β, T_{wi}, T_{wo}, and Q_V have been defined previously; and α_1 through α_9 are parameters defined in equations (A-20) through (A-28) shown below.

Rigorous mathematical treatment of the problem and the derivation of the preceding five equations are given in the study report (reference [A8]) and will not be repeated here.

$$\alpha_1 = \frac{2}{C_w} \left[(I_r - I_{out}) - K_w \, (T_{wo} - T_{wi}) \right] \tag{A-20}$$

$$\alpha_2 = \frac{1}{2} \left(\frac{dT}{dP} \right)_{sat} \tag{A-21}$$

$$\alpha_3 = \left(\frac{dM_{in}}{dt} \right) (v_v - v_\ell) - \left(\frac{dM_{out}}{dt} \right) v_v \tag{A-22}$$

$$\alpha_4 = \frac{\beta V}{v_v} \left(\frac{dv_v}{dT} \right)_P \tag{A-23}$$

$$\alpha_5 = \frac{\beta V}{v_v} \left(\frac{dv_v}{dP} \right)_T \tag{A-24}$$

[A8] Arthur D. Little, Inc., *Development of Additional Hazard Assessment Models*, prepared for the U.S. Department of Transportation, U.S. Coast Guard, December 1975.

$$\alpha_6 = \left(\frac{dM_{in}}{dt}\right)\{h_v - P(v_v) - h_g\} + \left(\frac{dM_{out}}{dt}\right)P(v_v) \qquad \text{(A-25)}$$

$$\alpha_7 = \frac{\beta V}{v_v}\left\{c_p - P\left(\frac{dv_v}{dT}\right)_P\right\} \qquad \text{(A-26)}$$

$$\alpha_8 = \frac{\beta V}{v_v}\left\{v_v + P\left(\frac{dv_v}{dP}\right)_m\right\} \qquad \text{(A-27)}$$

$$\alpha_9 = \left\{\left(\frac{dM_{in}}{dt}\right) - \left(\frac{dM_{out}}{dt}\right)\right\}\frac{v_v}{V} \qquad \text{(A-28)}$$

As can be seen in the preceding equations, the α-parameters are functions of vapor pressure-temperature, equation of state, thermodynamic properties of liquid and vapor, geometry and thermodynamic properties of the container, etc. Detailed discussion and input requirements for α-parameters will be given later for propane and various container geometries as defined in submodels (2), (3), and (4). The physical meaning of each α-parameter is discussed below.

α_1 = thermal capacity of container wall

$$C_w = \text{thermal mass of container wall} = c_w \rho_w (r_o - r_i) \quad (\text{erg/cm}^2\ ^\circ\text{K}) \qquad \text{(A-29)}$$

where

c_w = specific heat of container wall (erg/g °K)

ρ_w = density of container wall (g/cm^3)

and r_o and r_i are outer and inner radii of the container, respectively (cm).

$$I_{out} = \sigma T_{wo}^4 = \text{outgoing radiation flux} \quad (\text{erg/cm}^2\ \text{sec}) \qquad \text{(A-30)}$$

$$K_w = \text{radial thermal conductance of container wall (erg/cm}^2\ \text{sec}\ ^\circ\text{K}) = k_w/(r_o - r_i) \qquad \text{(A-31)}$$

where

k_w = thermal conductivity of the wall (erg/cm sec °K).

α_2 = slope of saturated temperature-pressure curve

$\left(\frac{dT}{dP}\right)_{sat}$ is calculated from the derivative of saturation vapor pressure-temperature relationship with respect to pressure.

α_3 = net accumulation rate of vapor

$\left(\frac{dM_{in}}{dt}\right)$ is calculated from equation (A-12).

$\left(\frac{dM_{out}}{dt}\right)$ is determined from equation (A-13).

v_v and v_ℓ are specific volumes (cm^3/g) of superheated and subcool liquid, respectively, and are calculated from equation of state.

α_4 = changing rate of ullage volume with temperature along an isobar in the pressure-volume-temperature (P-v-T) diagram

β = ratio of ullage volume and total container volume (dimensionless).

$\left(\frac{dv_v}{dT}\right)_P$ is calculated from the derivative of equation of state ($cm^3/g\ °K$).

α_5 = changing rate of ullage volume with pressure along an isotherm in the P-v-T diagram

$\left(\frac{dv_v}{dP}\right)_T$ is calculated from the derivative of equation of state (cm /g dyne).

α_6 = accumulation rate of thermal energy in vapor phase

h_v = specific enthalpy of superheated vapor

$$= h_g(T_{sat}, P) + \int_{T_{sat}}^{T} c_p(z)dz \qquad \text{(A-32)}$$

where

h_g = specific enthalpy of saturated vapor

c_p = specific heat of vapor under constant pressure as a function of temperature

and

z = dummy variable to facilitate integration.

α_7 and α_8 are important parameters in the determination of $\Delta P/\Delta t$ and $\Delta T/\Delta t$ but do not have explicit physical meaning

α_9 = net effect of boiling and venting of vapor on β value

Numerically integrating equations (A-15) through (A-19) with respect to time yields the changes of pressure, temperature, β, T_{wi}, and T_{wo}. However, to perform the integration, initial conditions have to be known. The initial conditions include:

outer surface temperature $(T_{wo})_{t=0}$

inner surface temperature $(T_{wi})_{t=0}$

temperature $(T)_{t=0}$

pressure $(P)_{t=0}$ and

$(\beta)_{t=0}$

at time zero. In addition, incoming radiation flux (I_r) and time of duration (t_{exp}), the area of opening of relief valves (A_0), and relief-valve setting (P_{set}) have to be given.

In the computerized enclosure model, the numerical integration will be performed in n steps to encompass the whole period of external radiation or fire. Selection of time steps n will then depend on the accuracy of computation required and computer time available for each simulation.

Specific Inputs and Auxiliary Functions for Submodels (2), (3), and (4)

There are three distinctive groups of input data required for the Enclosure Model, namely: (a) geometry of the container; (b) thermodynamic properties of liquid lading, vapor, and container; and (c) incoming radiation flux and duration, which are given from Phase I of the VM. The first group of data is collected for three different container geometries defined in submodels (2), (3), and (4). The second group of data is prepared for propane contained in either a steel or an aluminum container. Similar approaches and data sources can be taken for ladings other than propane.

(a) Geometry of Container

Only three types of containers are considered here: hollow sphere, horizontal cylinder, and vertical cylinder. It is felt that these three shapes of containers would encompass most of the containers used for storage of flammable liquids or cryogens. A spherical container can be defined by its inner (r_i) and outer (r_o) radii. However, a cylindrical container has to be described by its height or length (L) in addition to its inner and outer radii. There are five parameters required by the model that are related to container geometry: surface area of the wall exposed to fire (A_w), surface area where nucleate boiling takes place (A_b), surface area of the liquid-vapor meniscus (A_m), ratio (β) of ullage volume and container volume, and total container volume (V). They are presented in analytical forms for the three submodels as follows.

(i) Spherical Container -- Submodel (2)

$$A_w = \pi r_o^2 \quad (cm^2)$$

$$A_b = \pi (1 + \cos\phi) r_i^2 \quad (cm^2)$$

$$A_m = \pi (r_i \sin\phi)^2 \quad (cm^2)$$

$$\beta = \frac{1}{4}(1 - \cos\phi)^2 (2 + \cos\phi) \quad \text{(dimensionless)}$$

$$V = \frac{4}{3}\pi r_i^3 \quad (cm^3)$$

where ϕ is the angle (radians) between the vertical centerline and the edge of the meniscus as shown in Figure A-3.

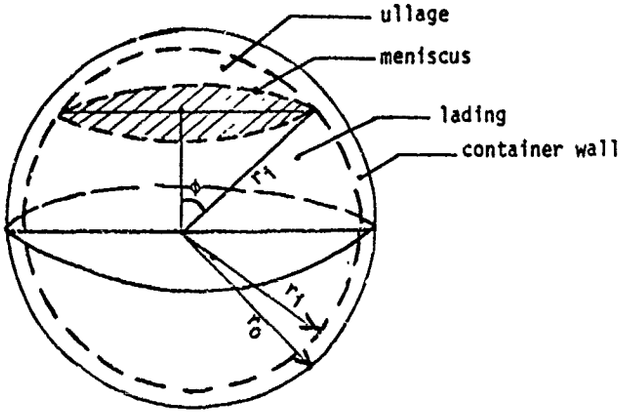

FIGURE A-3. Spherical Container

(ii) Vertical Cylindrical Container -- Submodel (3)

$$A_w = \pi r_i L \quad (cm^2)$$

$$A_b = (1 - \beta)\, \pi r_i L \quad (cm^2)$$

$$A_m = \pi r_i^2 \quad (cm^2)$$

$$\beta = (\beta)_{t=0} + \left(\frac{\Delta\beta}{\Delta t}\right) \cdot \Delta t \quad \text{(dimensionless)}$$

$$V = \pi r_i^2 L \quad (cm^3) \qquad \text{(See Figure A-4)}$$

(iii) Horizontal Cylindrical Container -- Submodel (4)

$$A_w = \pi r_i L \quad (cm^2)$$

$$A_b = (\pi - \phi)\, r_i L \quad (cm^2)$$

$$A_m = 2\,(r_i \sin\phi)\, L \quad (cm^2)$$

$$\beta = \left[(\pi - \phi) + \frac{\sin 2\phi}{2}\right] \frac{1}{\pi} \quad \text{(dimensionless)}$$

$$V = \pi r_i^2 L \quad (cm^3) \qquad \text{(See Figure A-5)}$$

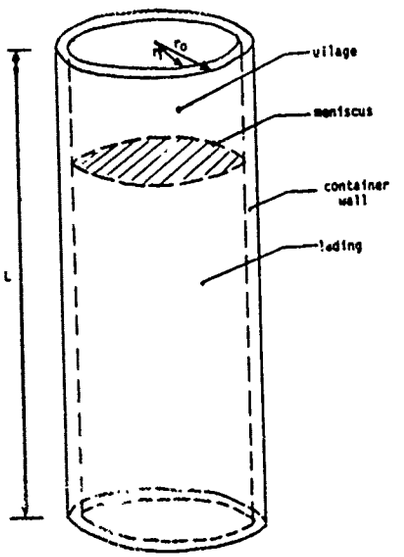

FIGURE A-4. Vertical Cylindrical Container

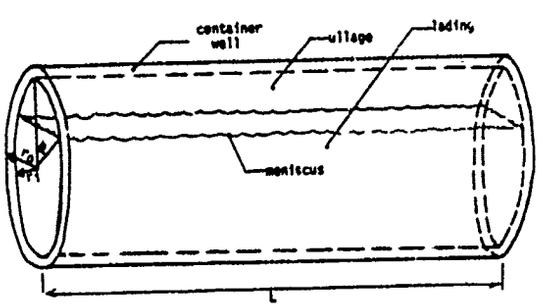

FIGURE A-5. Horizontal Cylindrical Container

(b) Thermodynamic Properties:

(i) Steel and aluminum. The thermodynamic properties of container material required for the model are specific heat, thermal conductivity, density, and coefficient of linear thermal expansion, as shown in Table A-1.

TABLE A-1. THERMODYNAMIC PROPERTIES OF STEEL AND ALUMINUM

Thermodynamic Properties	Steel	Aluminum
c_w [specific heat (erg/g °K)]	4.52×10^6	9.0×10^6
k_w [thermal conductivity (erg/cm sec °K)]	0.803×10^7	2.37×10^7
ρ_w [density (g/cm^3)]	7.87	—
k_e [coefficient of linear thermal expansion ($°K^{-1}$)]	12×10^{-6}	25×10^{-6}

(ii) Liquid propane and gaseous propane. The thermodynamic properties of propane are given for the liquid and gaseous states in Table A-2. See also Tables A-3 through A-6 which are presented on the following pages. (References [A9] through [A14] are utilized in these tables.)

[A9] Kwok, Y. C., and K. E. Starling, New equation of state for methane and propane from study of isochoric data and multiproperty analysis, art. C-1, *Adv. Cryog. Eng. 16*:54-63, 1971

[A10] Canjar, L. N., and F. S. Manning, ch. 4, pp. 33-43 in *Thermodynamic Properties and Reduced Correlations for Gases*, Gulf Publishing Co., Houston, Texas.

[A11] American Petroleum Institute Research Project 44, *Selected Values of Physical and Thermodynamic Properties of Hydrocarbons and Related Compounds*, Carnegie Press, 1952.

[A12] Spencer, H. M., and J. L. Justice, *J. Am. Chem. Soc. 56*:2311, 1934.

[A13] Spencer, H. M., and G. N. Flannagan, *J. Am Chem. Soc.* [illegible] 2511, 1942.

[A14] Gallant, R. W., *Physical Properties of Hydrocarbons*, vol. 1, Gulf Publishing Co., Houston, Texas, 1968.

TABLE A-2. THERMODYNAMIC PROPERTIES OF PROPANE

(1) Equation of State [A9]

$$P = R_g T \rho + (A_1\rho^2 + A_2\rho^3 + A_3\rho^6) + (B_1\rho^2 + B_2\rho^3 + B_3\rho^4 + B_4\rho^5) R_g T + C_3\rho^2 T^{-2}$$
$$+ \rho^2 T^{-2} (C_1\rho + C_2\rho^3 + C_3\rho^5) \exp(-C_4\rho^2) + D_3\rho^2 T^{-3} + \rho^2 T^{-3} (D_1\rho + D_2\rho^2 + D_3\rho^3) \exp(-D_4\rho)$$

where coefficients A_1, A_2, A_3, B_1, B_2, B_3, B_4, C_1, C_2, C_3, C_4, C_5, D_1, D_2, D_3, D_4, and D_5 are given in reference [A9], and $\rho = 1/v_v$.

(2) Vapor Pressure-Temperature Relationship [A10]

$$\ln P \text{ (dyne cm}^{-2}) = 22.921 - \frac{1872.5}{T\ (^\circ K) - 25.16} + \varepsilon$$

where $\varepsilon = 0$ for $T \leq 250^\circ K$

and $\varepsilon = 0.019\ (10^6)\ (T - 250)^3$ for $T > 250^\circ K$

(3) $$\left(\frac{dT}{dP}\right)_{sat} = \frac{[T\ (^\circ K) - 25.16]^2}{1872.5\ P} \quad \text{for } T \leq 250^\circ K$$

$$= \frac{[T\ (^\circ K) - 25.16]^2}{1872.5\ P} + \frac{1}{5.7\ (10^6)\ P\ [T\ (^\circ K) - 250]^2} \quad \text{for } T > 250^\circ K$$

(4) $\left(\frac{dv_v}{dP}\right)_T$ is obtainable by differentiating the equation of state with respect to pressure and solving for $(d\rho/dP)_T$.

(5) $\left(\frac{dv_v}{dT}\right)_P$ is obtainable by differentiating the equation of state with respect to temperature and solving for $(d\rho/dT)_P$.

(6) $$c_p = 0.410 + 64.710\ (10^{-3})\ T\ (^\circ K) - 225.82\ (10^{-7})\ [T\ (^\circ K)]^2 \quad \text{(cal/mole °K)}$$

$$c_v = c_p - R_g \quad \text{(reference [A11])}$$

$$\gamma = \frac{c_p}{c_v} = \frac{c_p}{c_p - R_g} \quad \text{(references [A12] and [A13])}$$

(7) $h_g(T_{sat}, P)$ can be satisfactorily represented by a mean value of $-1557.5\ (10^7)$ erg/g for temperature range from 42°C to critical temperature of 96.8°C.

(8) $$h_v = -1557.5\ (10^7) + 5.7329\ (10^6)\ (T - T_{sat}) + 18{,}794\ (T^2 - T_{sat}^2) \quad \text{(erg/g)}$$

(9) $R_g = 1.8857 \times 10^6$ (dyne cm/g °K) (reference [A10])

(continued)

TABLE A-2 (continued). THERMODYNAMIC PROPERTIES OF PROPANE

(10) $v_v \approx \frac{P}{R_g T} = 5.30\,(10^{-7})\,(P/T)$ (cm^3/g)

(11) $c_{p\ell}$ (see Table A-3)

(12) $k_\ell \approx 12{,}600$ (erg/cm sec °K) from 30°C to 100°C

(13) T_{crit} = critical temperature = 96.81°C = 369.97°K (reference [A10])

(14) $u_\ell = h_\ell - P\,(\Delta v_\ell)$ is obtainable from Table A-4.

(15) $v_\ell = \frac{1}{\rho_\ell}$ (see Table A-3)

(16) σ_ℓ (see Table A-5)

(17) λ (erg/g) = T (°K) P (dyne/cm^2) v_{fg} (cm^3/g) $\frac{d \ln P\ (\text{dyne/cm}^2)}{d T\ (°K)}$

where v_{fg} can be obtained from reference [A10]

$$\frac{d \ln P}{d T} = 1872.5\,[T\,(°K) - 25.16]^{-2} \quad \text{for} \quad T < 250°K$$

and $$\frac{d \ln P}{d T} = 1872.5\,[T\,(°K) - 25.16]^{-2} + 5.7\,(10^4)\,[T\,(°K) - 250]^2 \quad \text{for} \quad T > 250°K$$

(18) μ_ℓ (see Table A-6)

TABLE A-3. HEAT CAPACITY, DENSITY, AND SPECIFIC VOLUME OF LIQUID PROPANE

T (°C)	$c_{p\ell}$ (cal/g °K)	ρ_ℓ (g/cm^3)	v_ℓ (cm^3/g)
-50	0.590	0.590	1.69
-40	0.60	0.575	1.74
-30	0.615	0.565	1.77
-20	0.63	0.555	1.80
-10	0.645	0.545	1.83
0	0.66	0.530	1.89
10	0.68	0.515	1.94
20	0.705	0.500	2.00
30	0.73	0.485	2.06
40	0.755	0.465	2.15
50	0.790	0.445	2.25
60	0.835	0.425	2.35
70	0.895	0.400	2.50
80	0.970	0.365	2.74
90	1.060	0.315	3.17
96	1.145	0.220	4.56

TABLE A-4. ENTHALPY AND SPECIFIC VOLUME OF LIQUID PROPANE [A10]

T_{sat} (°F)	P (psia)	v_v (cm^3/g)	h_ℓ ($\times 10^7$ erg/g)
-43.73	14.696	1.718	-2050.0
-30	20.338	1.742	-2033.3
-20	25.395	1.767	-2020.7
-10	31.376	1.786	-2007.9
0	38.371	1.804	-1994.5
10	46.470	1.829	-1980.7
20	55.807	1.854	-1967.7
30	66.460	1.879	-1952.8
40	78.577	1.911	-1938.4
50	92.231	1.935	-1924.2
60	107.59	1.967	-1909.6
70	124.73	2.004	-1894.4
80	143.82	2.042	-1878.6
90	164.99	2.079	-1862.8
100	188.32	2.117	-1846.5
110	214.02	2.154	-1830.7
120	242.19	2.204	-1814.7
130	273.08	2.254	-1797.9
140	306.76	2.304	-1780.5
150	343.52	2.385	-1762.3
160	383.45	2.472	-1743.7
170	450.01	2.579	-1724.9
180	474.06	2.728	-1704.2
190	525.10	2.941	-1680.7
200	580.46	3.253	-1644.4
206.26	617.47	4.545	-1590.9

TABLE A-5. SURFACE TENSION OF LIQUID PROPANE [A11,A14]

T (°C)	σ_ℓ (dyne/cm)
-50	16.49
-40	15.15
-30	13.8
-20	12.4
-10	11.0
0	9.7
10	8.4
20	7.2
30	6.1
40	5.0
50	4.0
60	3.1
70	2.2
80	1.5
90	0.8
96	0

TABLE A-6. VISCOSITY OF LIQUID PROPANE [A11,A14]

T (°C)	μ_ℓ ($\times 10^{-2}$ g/cm sec)
-50	0.228
-40	0.205
-30	0.195
-20	0.180
-10	0.160
0	0.135
10	0.130
20	0.115
30	0.100
40	0.090
50	0.080
60	0.070
70	0.060
80	0.050
90	0.040
100	0.030

STRESS AND STRENGTH ANALYSIS OF A CONTAINER SUBJECTED TO EXTERNAL RADIATION

In this section the stress and strength of container materials are discussed. The inputs required here are essentially the outputs from the two preceding main sections of this appendix. The time-histories of temperature and pressure of a container are linked with governing equations of stress and strength of materials which are delineated in the following discussions. Besides stress and strength, failure criteria are also discussed in this section.

Strength of Material and Safety Factor

The strength of a metal, in terms of ultimate tensile strength, generally decreases with increasing temperature. However, ferritic steels and nickel are exceptions; they generally show maximum tensile strength at 300°F to 700°F. The yield properties of metals also decrease with increasing temperature [A15]. Unfortunately, an analytical relationship between strength and temperature has not yet been established. Therefore, for a given material, the strength-temperature diagram is approximated either by a series of straight line segments or by a table. For a temperature other than the values listed in the table, an interpolation method is used to calculate the corresponding strength. This approach is proposed to be used in the model.

[A15] American Society of Mechanical Engineers, *ASME Handbook - Metals Engineering Design* (O. J. Horger, ed.), McGraw-Hill Book Co., 1953.

According to either the ASME Pressure Vessel Code or the API-ASME Code generally applicable to liquefied-petroleum gas containers, the design pressures for propane and butane are 250 and 125 psi, respectively, and a safety factor of 4:1 has been used since 1952 [A16]. Therefore, the safety factor (f) of 4:1 is used throughout the model.

Stress Analysis and Failure Criteria

For a container subjected to a fire, a pressure buildup inside the container and a temperature difference between the outer and inner surfaces of the wall are the two major factors attributable to the development of stresses. The stresses for (a) a spherical shell and (b) a cylindrical shell and their failure criteria are discussed separately below.

(a) Spherical Shell - Submodel (2)

The stresses acting on a finite element of the wall material of a spherical shell are radial stress (σ_r) and tangential stress (σ_t). The radial and tangential stresses induced by the action of internal pressure (P) and external atmospheric pressure (P_{atm}) are given in the following equations [A17].

$$\sigma_{r,P} = \frac{P_{atm}\, r_o^3\, (r^3 - r_i^3)}{r^3\, (r_i^3 - r_o^3)} + \frac{P\, r_i^3\, (r_o^3 - r^3)}{r^3\, (r_i^3 - r_o^3)} \tag{A-33}$$

$$\sigma_{t,P} = \frac{P_{atm}\, r_o^3\, (2\, r^3 + r_i^3)}{2\, r^3\, (r_i^3 - r_o^3)} - \frac{P\, r_i^3\, (2\, r^3 + r_o^3)}{2\, r^3\, r_i^3 - r_o^3)} \tag{A-34}$$

The stresses in the radial and tangential directions induced by the thermal gradient are given below, as in [A17].

$$\sigma_{r,T} = \frac{K_e\, E\, (T_{wi} - T_{wo})}{1 - \nu} \left(\frac{r_i\, r_o}{r_o^3 - r_i^3}\right) \left[r_i + r_o - \frac{1}{r}\,(r_o^2 + r_o\, r_i + r_i^2) + \frac{r_o^2\ r_i^2}{r^3}\right] \tag{A-35}$$

[A16] National Fire Protection Association, *National Fire Codes - Gases*, vol. 2, app. C, 1973-74.

[A17] Timoshenko, S., *Theory of Elasticity*, McGraw-Hill Book Co., New York and London, 1934.

$$\sigma_{t,T} = \frac{k_e E (T_{wi} - T_{wo})}{1 - \nu} \left(\frac{r_i r_o}{r_o^3 - r_i^3} \right)$$

$$\cdot \left[r_i + r_o - \frac{1}{2r} (r_o^2 + r_o r_i + r_i^2) - \frac{r_o^2 r_i^2}{r^3} \right] \qquad \text{(A-36)}$$

where

k_e = coefficient of linear thermal expansion ($^\circ K^{-1}$)

E = modulus of elasticity of material (dyne/cm^2)

and

ν = Poisson's ratio (dimensionless)

which can be taken equal to 0.25 for many materials and is usually taken equal to 0.3 for structural steel.

The radial stresses, $\sigma_{r,P}$ and $\sigma_{r,T}$, can be considered as shear stresses. In the design of general structures, the working shear stress is taken equal to 40% of the yield strength of the material [A18]. The tangential stresses are tensile stresses in most cases. The working tensile stresses for elastic design are commonly taken as equal to 60% of the tensile strength of the material at the yielding point [A18]. Therefore, the failure criteria can be written in the following mathematical form:

$$\sigma_r = (\sigma_{r,P} + \sigma_{r,T}) > (40\%) \left(\frac{\sigma_{Y.P.}}{f} \right) \qquad \text{(A-37)}$$

$$\sigma_t = (\sigma_{t,P} + \sigma_{t,T}) > (60\%) \left(\frac{\sigma_{Y.P.}}{f} \right) \qquad \text{(A-38)}$$

where subscript $Y.P.$ means yielding point and f = safety factor. Satisfying either of equations (A-37) or (A-38) means the failure of the container. The time when the failure criteria are met is the time of failure, t_{fail}.

[A18] Yau-Shian Ho, Ph.D. and P.E. in structural engineering, private communication, February 1976.

(b) Cylindrical Shell - Submodels (3) and (4)

Any finite element of the wall material of a cylinder is subjected to three normal principal stresses: axial stress (σ_z), radial stress (σ_r), and tangential stress (σ_θ). The stresses induced by the action of internal pressure (P) and external atmospheric pressure (P_{atm}) are described by the following equations [A17].

$$\sigma_{r,P} = \frac{r_i^2 r_o^2 (P_{atm} - P)}{r_o^2 - r_i^2} \left(\frac{1}{r^2}\right) + \frac{P r_i^2 - P_{atm} r_o^2}{r_o^2 - r_i^2} \tag{A-39}$$

$$\sigma_{\theta,P} = - \frac{r_i^2 r_o^2 (P_{atm} - P)}{r_o^2 - r_i^2} \left(\frac{1}{r^2}\right) + \frac{P r_i^2 - P_{atm} r_o^2}{r_o^2 - r_i^2} \tag{A-40}$$

$$\sigma_{z,P} = \frac{(P - P_{atm}) r_i^2}{r_o^2 - r_i^2} \tag{A-41}$$

Stresses induced by temperature difference between the outer and inner surfaces of the wall are given in the following equations [A17]. The thermal stress in the axial direction is zero because most cylindrical shells are allowed to expand freely in the axial direction.

$$\sigma_{r,T} = \frac{- k_e E (T_{wo} - T_{wi})}{2 (1 - \nu) \log (r_o/r_i)} \left\{ -\log \frac{r_o}{r} - \frac{r_i^2}{(r_o^2 - r_i^2)} \left(1 - \frac{r_o^2}{r^2}\right) \log \frac{r_o}{r_i} \right\} \tag{A-42}$$

$$\sigma_{\theta,T} = \frac{- k_e E (T_{wo} - T_{wi})}{2 (1 - \nu) \log (r_o/r_i)} \left\{ 1 - \log \frac{r_o}{r} - \frac{r_i^2}{(r_o^2 - r_i^2)} \left(1 + \frac{r_o^2}{r^2}\right) \log \frac{r_o}{r_i} \right\} \tag{A-43}$$

The total axial, radial, and tangential stresses, respectively, are calculated by the following equations.

$$\sigma_z = \sigma_{z,P} \tag{A-44}$$

$$\sigma_r = \sigma_{r,P} + \sigma_{r,T} \tag{A-45}$$

$$\sigma_\theta = \sigma_{\theta,P} + \sigma_{\theta,T} \tag{A-46}$$

According to maximum distortion energy theory, yielding of material under triaxial stress will occur when the following equation is satisfied [A19].

$$\left(\frac{\sigma_{Y.P.}}{f}\right) < \frac{\sqrt{2}}{2}\left[(\sigma_r - \sigma_\theta)^2 + (\sigma_\theta - \sigma_z)^2 + (\sigma_z - \sigma_r)^2\right]^{1/2} \qquad \text{(A-47)}$$

where $\sigma_{Y.P.}$ is the yield strength of the material as determined from a uniaxial tension test, and f is the safety factor.

[A19] Juvinall, R. C., *Stress, Strain, and Strength*, p. 118, McGraw-Hill Book Co., New York, 1967.

Appendix B

TOXICOLOGY OF SELECTED HAZARDOUS CARGOES

The first report on the Vulnerability Model [B1] discussed the toxicology of ammonia and chlorine, and derived dose-response estimates for use in the VM. This work has been extended to:

- Acrolein
- Asphyxiating gases -- methane and propane
- Carbon tetrachloride
- Hydrogen chloride
- Methyl bromide
- Phosgene

The following sections of this appendix present the detailed evidential basis and method of analysis for arriving at the exposure-response estimates presented in Chapter 5.

ACROLEIN

Acrolein is a liquid with a boiling point of 52.5°C. It polymerizes readily, especially in light, to form a plastic solid. It has a disagreeable choking odor, and the vapor is strongly irritant to the respiratory mucosa and to the eyes, acting as a powerful lacrimator. It was introduced as a harassing war gas by the French in January of 1916 [B2], but was soon dropped because its instability made it impractical for field use. Although the vapor has some potential as a lung injuriant, it was considered solely as a temporary incapacitant, which may account in part for the paucity of estimates for human lethal effects in Table B-1.

[B1] Eisenberg, N. A., C. J. Lynch, and R. J. Breeding, *Vulnerability Model: A Simulation System for Assessing Damage Resulting from Marine Spills*, Report No. CG-D-136-75, prepared for the Department of Transportation, U.S. Coast Guard, by Enviro Control, Inc., NTIS AD-A015 245, June 1975.

[B2] Prentiss, A. M., *Chemicals in War*, 1st ed., McGraw-Hill Book Co., Inc., New York and London, 1937.

TABLE B-1. EFFECTS OF ACROLEIN IN MAN

Concentration mg m^{-3}	Concentration ppm	Time min	Dosage mg min m^{-3}	Effects	Reference
0.23	0.1	--	--	Threshold Limit Value	1
0.6	0.25	5	3	Moderate irritation	2
2.3	1	--	--	Irritation of eye and respiratory tract	3
2.3	1	--	--	Low limit of toxicity	4
2.3	1	immediate	--	Detection	5
2,3	1	2-3	6	Eye and nose irritation	2
2.3	1	4	9	Moderate eye irritation and lacrimation	2
7	3	--	--	Minimum lacrimatory	6
7	3	--	--	Lacrimation, nose irritation	2
7	3	--	--	Lacrimation, irritation of conjuctiva	7
13	5.5	1/3	4	Painful eye and nose irritation	2
13	5.5	--	--	Intense irritation	5
23	10	short	--	Lethal (?)	5
50	21.8	--	--	Intolerable	2
50	21.8	1	50	Limit of tolerance	6
55	24	--	--	Unbearable	5
350	153	10	3500	Lethal	7
Selected Data for Experimental Animals					
18.4	8	240	4400	ca. $L(CT)_{50}$ for rats	8
24.4	10.5	360	8700	$L(Ct)_{50}$ for mouse	4
300	130	30	9000	$L(Ct)_{50}$ for rat	9
350	156	10	3500	$L(Ct)_{60}$ for mouse	2

References:

1 ACGIH, 1971
2 Patty, 1962
3 Casarett & Doull, 1975
4 Pattle & Cullumbine, 1956
5 Henderson & Haggard, 1943
6 Wachtel, 1941
7 Prentiss, 1937
8 Carpenter et al., 1949
9 Skog, 1950

The following levels of concentration and corresponding effects are based on Table B-1.

Concentration, mg m^{-3}	*Effects*
0 - 0.4	Negligible
0.4 - 4	Readily perceptible, and disagreeable to general population
4 - 20	Temporary incapacitation after 1 to 2 minutes of exposure, primarily because of lacrimation; dangerous to susceptible persons in longer exposure
20 - 50	Severe harassment; complete (temporary) incapacitation with extreme discomfort; very dangerous for susceptible persons and also for normal subjects in long exposures

Some dosage (*Ct*) figures are given in Table B-1, but we do not believe that this is a useful measure of exposure for immediate irritation or, indeed, that Haber's Law (constant *Ct* for a given level of effect) would be expected to apply to this strongly irritant agent. The general pattern of response to this type of agent is that increasing levels of concentration produce increasingly intense degrees of harassment, which build up rapidly on exposure and then tend to level off as exposure continues; time factors are of lesser importance and are seen in more rapid onset at higher concentrations and more prolonged aftereffects following longer exposure. The response, however, may be regarded as coinciding with the duration of exposure, without serious inaccuracy, for nonhazardous concentrations.

At high concentrations, the assault on the senses is violent and not voluntarily tolerable. An estimate of lethal exposure for man is given in Table B-1: 10 minutes of exposure at 350 mg m^{-3} (which is seven times the threshold level for intolerable irritation). Lethality here may be interpreted as the consequence of almost complete cessation of breathing through respiratory spasm; the victim dies of hypoxia rather than a chemical toxic action.

The intermediate zone of concentrations (55 to 350 mg m^{-3}), for which no estimates of effect are shown, presents difficult problems of judgment. It is undoubtedly a zone of increasing hazard, probably with significant risk of lethality in susceptible individuals at the lower border and threatening healthy adults in its middle and upper levels. The most immediate hazard is that the impairment of ability to breathe will induce serious hypoxia; this is obviously most likely in those with chronic respiratory disease or cardiovascular deficiency. Note also the severe stress of a highly unpleasant and alarming experience. There is also a possibility of short- or long-term aggravation of respiratory disease through lung irritation. Further possibilities are mutagenic effects [B3], which could lead to tumor growth, and permanent degenerative "aging" of lung tissue [B4]. Acrolein has a molecular structure which indicates the ability to react disruptively with cellular genetic material and to participate in "oxidative" destruction of the lung parenchyma.

Skog [B5] gives a dose-response graph for lethality in rats by inhalation (see Figure B-1). Lethalities read from his graph are:

[B3] Kodama, J. K. (Shell Chemical Co.), personal communication, 1976.

[B4] Wands, J. C. (National Academy of Sciences), personal communication, 1976.

[B5] Skog, E., A toxicological investigation of lower aliphatic aldehydes. I. Toxicity of formaldehyde, acetaldehyde, proprionaldehyde and butyraldehyde; as well as of acrolein and crotonaldehyde. *Acta Pharmacol. Toxicol.* (Copenhagen) 6:299-318, 1950.

mg min m^{-3}	*% Dead*
15,000	95
12,500	85
9,000	50
6,600	15
5,500	5

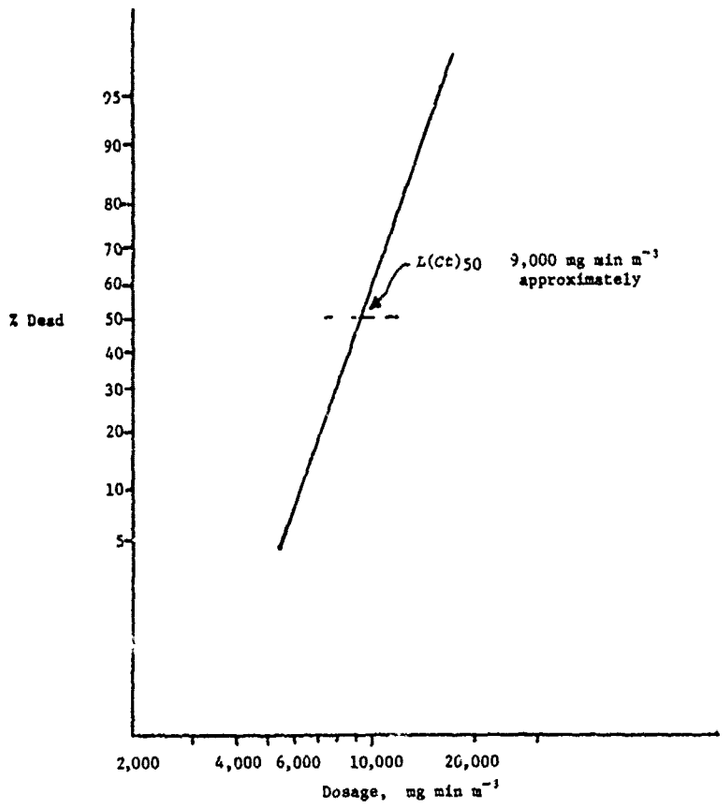

FIGURE B-1. Lethality of 30-Minute Inhalation Exposure of Rats to Acrolein (after Skog [B5])

Unfortunately, he presents this only as a rather small graph without grid and without any indication of the scatter of points. He says only that 88 rats were exposed to concentrations in the range of 0.1 to 0.7 mg per liter and that 28 died; the number of concentration levels and

the mortality in each group are not given. The most interesting observation is that the deaths were substantially delayed, none occurring during or immediately after exposure:

	No. Dead (cumulative)
6 to 24 hours after exposure	15
Second day	26
Fourth day	28

This was similar to the effects of formaldehyde and crotonaldehyde and quite dissimilar to acetaldehyde, propionaldehyde, and butyraldehyde, in which all deaths were during exposure or within six hours. The mechanism of the lethal toxic effect by acrolein appears to have been damage to the gas-exchange tissues of the lung, with consequent edema and catastrophic impairment of function.

The evidence suggests that two quite different lethal mechanisms may operate in human exposure to acrolein, similarly to the toxicology of chlorine which we reviewed previously. Over a certain range of concentration, the subject is able to continue breathing--although with extreme distress--and accumulates a dangerous dosage in the lower respiratory tract; pulmonary edema develops, and the outcome may be fatal in a day or two. This mechanism would be expected to show a normal type of dose-response relationship. At higher concentrations, the irritation of the upper respiratory tract is so extreme that reflex respiratory spasm causes a hazardous reduction or cessation of breathing, so that resulting fatalities occur immediately or very soon. In those cases, the subject may be regarded as the victim of "strangulation" and the slower deep-lung toxic mechanism cannot of course develop. This lethal mechanism would be expected to be concentration-dependent rather than dosage-dependent. In survivors of the "strangulation" effect, the delayed deep-lung toxicity would develop in those who had accumulated a sufficient inspired dosage. It will be apparent that Skog [B5] exposed his rats at concentrations which permitted the delayed deep-lung effect to take place, resulting in delayed deaths and a normal dose-response regression over a concentration range of 1 to 7. Caution is necessary in attempting to extrapolate from this to man: sensitivity to irritants varies enormously between species, and one may see, for example, a dog trot unconcerned through a cloud of ω-chloracetophenone (a lacrimator) which is immediately incapacitating for humans.

We have arrived tentatively at the dose-response estimates of Table B-2, which structurally resembles the table for chlorine and ammonnia in the Final Report of the VM [B1, Table 6-4, p.86]. It will be clear from the foregoing discussion and the deficiency of estimates for human lethal effects in Table B-1 that our estimates are highly judgmental and should be treated accordingly. However, we believe that they present a credible and coherent picture of the possible consequences of acute exposure of the general population to acrolein.

TABLE B-2. PROPOSED DOSE-EFFECT RELATIONS FOR THE VM: ACROLEIN

CH_2:CHCHO Concentration, mg m^{-3}	Time	Effect	Deaths, %	
			General Population	High-Risk Population
0.4	any	Negligible	0	0
0.4-4	any	Complaint, no risk	0	0
4-20	0.5 hr	Severe harassment, risk to susceptibles	0	0
	1 hr		0	25
20-50	0.5 hr	Severe harassment (risk)	0	25
	0.5-1 hr	Lethal	3	50
	1-2 hr	Lethal	50	100
50-150	0.5 hr	Lethal	3	50
	0.5-1 hr	Lethal	50	100
	1-2 hr	Lethal	97	100
150-450	5 min	Lethal	3	50
	5-15 min	Lethal	50	100
	15-30 min	Lethal	97	100

References for Acrolein

American Conference of Governmental Industrial Hygienists (ACGIH). *Documentation of Threshold Limit Values for Substances in Workroom Air*, 3rd ed. ACGIH, P.O. Box 1937, Cincinnati, Ohio, 1971.

Carpenter, C. P., H. F. Smyth, Jr., and U. C. Pozzani. The assay of acute vapor toxicity and the grading and interpretation of results on 96 chemical compounds. *J. Ind. Hyg. Toxicol. 31*:343, 1949.

Casarett, L. J., and J. Doull (eds.). *Toxicology - The Basic Science of Poisons*. Macmillan, New York, 1975.

Henderson, Y., and H. W. Haggard. *Noxious Gases and the Principles of Respiration Influencing Their Action*, 2nd ed. Reinhold Publishing Corp., New York, 1943.

Kodama, J. K. (Shell Chemical Co.). Personal communication, 1976.

Pattle, R. E., and H. Cullumbine. *Br. Med. J. 2*:913, 1956.

Patty, F. A. (ed.). *Industrial Hygiene and Toxicology*. Interscience Publishers, New York, 1962.

Prentiss, A. M. *Chemicals in War*, 1st ed. McGraw-Hill Book Co., Inc., New York and London, 1937.

Skog, E. A toxicological investigation of lower aliphatic aldehydes. I. Toxicity of formaldehyde, acetaldehyde, proprionaldehyde and butyraldehyde; as well as of acrolein and crotonaldehyde. *Acta Pharmacol. Toxicol.* (Copenhagen) 6:299-318, 1950.

Wachtel, C. S. *Chemical Warfare*. Chemical Publishing Co., Inc., Brooklyn, N.Y., 1941.

Wands, R. C. (National Academy of Sciences). Personal communication, 1976.

ASPHYXIATING GASES -- METHANE AND PROPANE

General Discussion

Nontoxic gases such as methane are a respiratory hazard if they considerably reduce the oxygen supply to the lungs by dilution of the air. The lower concentration of inspired oxygen leads to lower partial pressure of oxygen in the alveolar spaces and, hence, to less effective oxygenation of the blood and to impaired cellular respiration. This is similar to the effect of low pressure at high altitude or of obstructed air supply as in strangulation. The consequences are various incapacitating symptoms, unconsciousness, and death; if the oxygen deprivation is effectively complete, incapacitation occurs in about 0.25 minute, unconsciousness in 1 minute, and death in 5 minutes. Oxygen deficiency at the cellular level can be caused by many things and is generally referred to as hypoxia. If the cause is inadequate oxygen supply to the lungs, it is called anoxic hypoxia or aerohypoxia.

Methane is classified by toxicologists and industrial hygienists as a "simple asphyxiant," and other examples of this category are ethane, propane, butane, ethylene, nitrogen, and the inert gases. Some of these gases are significant hazards in the context of the Vulnerability Model (VM) because they are handled in sufficient bulk and have such properties that they can establish very high concentrations in the vicinity of an accidental release. Properties of a material such as LNG that favor development of high concentrations are high volatility and the high density of the cold vapor which reduces its tendency to disperse away from the surface.

VM Conditions Compared With Other Situations Inducing Hypoxia

Anoxic hypoxia has been studied in a variety of circumstances in which it is an important physiological hazard. Deprivation of oxygen supply to the lungs may be due to reduced intake of normal air, as in choking; to reduced pressure, as in aviation and mountaineering; or to changed composition of the air due to oxygen depletion and dilution with "asphyxiating" gases, as in firefighting in enclosed spaces. It is necessary to consider these situations here, even though they differ in various ways from the conditions of the VM, because our data come from studies related to them. A typical victim of oxygen deprivation in the context of the VM will suffer rapid onset of depleted oxygen intake; the degree of depletion may be very high but is unlikely to be complete; the ambient atmosphere will be at normal pressure throughout; and there will probably be no aggravating factors such as toxic gases. It is also to be noted that effective help and protective measures will very seldom be available. These characteristics are compared with other situations in Table B-3. As can be seen, there is no complete match for the VM. Firefighting is perhaps the closest but only for low degrees of hypoxia, because combustion of most common materials is suppressed at oxygen concentrations below about 14%, which is only the threshold for marked physiological effects. Aerial ascent differs because the development of hypoxia is slow enough for significant physiological compensation. Rupture of pressurized aircraft matches the rapid onset of the VM conditions but is accompanied by different effects of explosive decompression.

An important point about decompression is that its effect is immediately apparent at the lung surface. In contrast, exposure to an oxygen-depleted atmosphere at normal pressure results in an exponential decrease of alveolar oxygen as breathing continues. Most of the alveolar oxygen depletion is accomplished in less than one minute, but it is certainly not immediate.

Since most of the data we will use come from aviation medicine, the effects of reduced pressure (cabin altitude) should be converted to dilution of air by inert gas at sea level. The equivalence must be in terms of alveolar gas which is at 37°C and saturated with water vapor. The vapor pressure of water is 47 mm Hg at 37°C. Consequently, at ambient pressure P mm Hg, only $P - 47$ mm is "available" for gases other than water vapor. At 63,000 feet, the pressure is 47 mm Hg of which 9 mm is O_2, but *none* of this O_2 is available to the lung surface; consequently, the corresponding "dilution" of air at sea level is 100% inert gas. Dilutions of air vs. P_{O_2} in saturated air are shown in Figure B-2.

TABLE B-3. CHARACTERISTICS OF VARIOUS CIRCUMSTANCES CAUSING ANOXIC HYPOXIA

Characteristic	Vulnerability Model	Fire-Fighting	Aerial Ascent	Mountain-eering	Rupture of Pressurized Aircraft	Choking
Speed of onset	Rapid	Rapid	Relatively slow	Relatively very slow	Rapid to instantaneous	Rapid to instantaneous
Degree of oxygen deprivation	Low to high	Low	Low to high	Low to moderate	Moderate to effectively total	High to total
Ambient pressure	Normal	Normal	Slow drop	Very slow drop	Instant drop, may be large	—
Other ambient factors	None	Toxic gases likely	None	None	None	None
Physiological condition of subjects	Average (i.e., normal range)	Average to good	Average to good	Good	Average to good	Average
Availability of help and protective measures	No	Yes	Perhaps	Probable	Yes	—

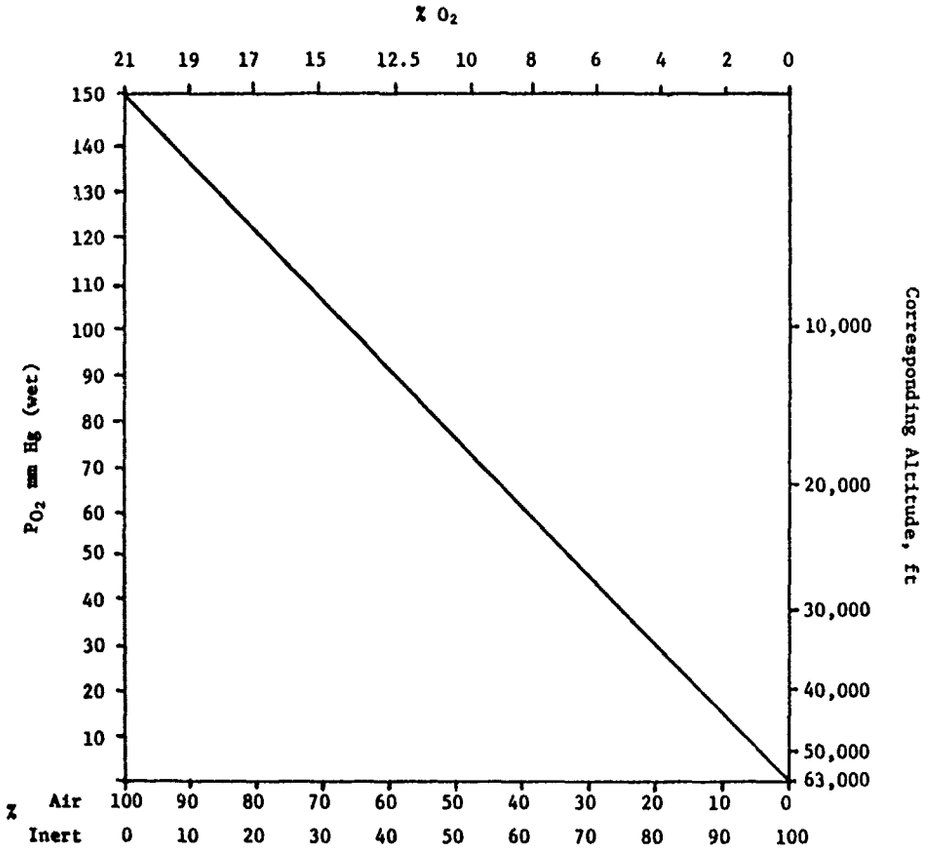

FIGURE B-2. Mixtures of Air and Inert Gas Vs. P_{O_2} in Saturated Atmosphere at 760 mm Hg

Effects of Hypoxia

A series of physiological endpoints has been recognized in aviation medicine [B6]. These endpoints are usually expressed in terms of cabin altitude, which can be converted for our purposes to asphyxiant concentration in air at sea level and corresponding O_2 concentration.

The time of useful consciousness (TUC) in Table B-4 and Figure B-3 is taken from the onset of anoxic conditions in decompression, when the decrease of oxygen partial pressure in the alveoli is immediate. As

---

[B6] Mohler, S. R., *Physiologically Tolerable Decompression Profiles for Supersonic Transport Type Certification*, FAA Report AM 70-12, 1970.

already mentioned, the decrease is not immediate when anoxia is due to inhalation of oxygen-depleted air. TUC is defined as the time beyond which the victim is not competent to take protective action, such as putting on an oxygen mask.

TABLE B-4. PHYSIOLOGICAL ENDPOINTS

Cabin Altitude (feet)	$P_{I_{O_2}}$	Equivalent Proportions at Ground Level (%)		Physiological Significance (in brief)
		Asphyxiant	O_2	
8,000	108	28	15.0	Ceiling for no impairment
10,000	100	33	14.0	Computational ability impaired
12,000	91	39	12.7	Errors of omission; short-term memory impaired
14,000	83	44	11.7	All persons impaired; intellectual and emotional alteration
15,000	79	47	11.1	Some seriously impaired
20,000	63	58	8.8	TUC, 10 min
25,000	50	67	6.9	TUC, 2.5 min
30,000	37	75	5.2	TUC, 30 sec
34,000	29	81	4.0	TUC, 22 sec
37,000	25	83	3.6	TUC, 18 sec
40,000	20	87	2.7	TUC, 15 sec

$P_{I_{O_2}}$ = partial pressure of inhaled O_2, mm Hg.

Asphyxiant = proportion of asphyxiant in normal air at sea level to give the same $P_{I_{O_2}}$.

O_2 = proportion of oxygen by volume in air-asphyxiant mixture.

TUC = time of useful consciousness. If exposure at the given oxygen partial pressure continues beyond this time, ability for purposeful activity, such as putting on an oxygen mask, is lost. See Figure B-3.

Figure B-3 shows a minimum TUC of about 15 seconds. This consists of the time for unoxygenated blood to reach the cerebral cortex and for metabolism to deplete the cellular oxygen reserve below the level of ability to sustain "useful" consciousness. The cortex is the most vulnerable tissue to hypoxia (see Table B-5).

It is to be noted that "revivable" does not necessarily mean without impairment, especially for the brain in which irreversible damage is likely after four minutes of total anoxia and invariably occurs after five minutes. The brain is the most important target for damage, because it normally functions with only small marginal reserves of cellular oxygen, and is the first tissue to suffer impairment; furthermore,

partial damage has devastating effects. Davies and Bronk [B7] note that the cortex of the mammalian brain is normally on the verge of oxygen insufficiency.

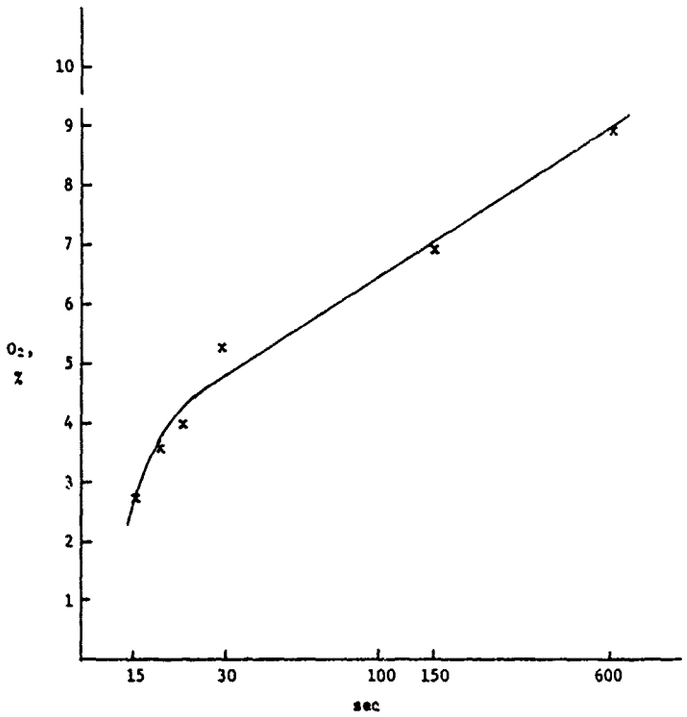

FIGURE B-3. Time of Useful Consciousness
(data from [B6])

TABLE B-5. TIME FOR EFFECTS OF ANOXIA IN VARIOUS ORGANS

Tissue		Minutes After Total Anoxia	
		Functioning	Revivable*
Brain, awake:	Cortex	0.3	5
	Medulla	4.0	15
Heart, at work		5	10
Heart, at rest		10	
Liver			50
Kidney			60
Skeletal muscle, at rest		120	480

*See discussion in text.

[B7] Davies, P. W., and D. W. Bronk, *Fed. Proc., Fed. Am. Soc. Exp. Biol. 16*:689, 1957.

The data for irreversible damage and death in man are based on accidental exposure and are supported by extensive animal experiments. The data for TUC are based on numerous exposures made by investigators on themselves and on other volunteers. As long as the point of no return is not reached, the aftereffects of disorientation, nausea, headache, etc., although unpleasant, are transitory and there is no permanent harm.

The effects of hypoxia short of unconsciousness are not necessarily unpleasant, nor are they harmful if appropriate help is at hand. About 70 years ago a British Chief Inspector of Mines, walking unprotected in an area of high CO concentration after a conflagration in a coal mine, lost all initiative, sat down, and began writing farewell messages. A World War I pilot at about 19,000 feet waved cordially to an enemy pilot and took no further action despite his observer's vehement protests. A team of mountaineers was returning from over 28,000 feet when one collapsed; a companion remarked, with complete unconcern, "Poor old Tom; he's had it." The point of this is that, in the context of the VM, victims of hypoxia may not be aware of their impairment or of imminent loss of consciousness. They will not feel "shortness of breath" and may even become euphoric. However, they may perceive some abnormality in the inspired air, such as an unusual odor or a sudden drop in temperature.

For the purposes of the VM, we can neglect effects short of unconsciousness. There may be some unpleasant immediate and briefly persistent reactions, but no lasting harm is expected except perhaps in a small minority of exceptionally sensitive subjects (e.g., those with severe respiratory, cerebrovascular, or cardiovascular disease).

"Dose-Response" Relationships

The responses with which we are concerned are unconsciousness and death. Expert opinion [B8] is that the tolerable time of unconsciousness is probably about the same at various levels of severe hypoxia: i.e., if the cerebral cortex is deprived of oxygen for four minutes at a level sufficient to induce unconsciousness, then permanent cell damage will occur regardless of the extent of the oxygen deficit.* Note that this applies to unconsciousness in which the oxygen concentration remains low. If the oxygen is restored to a safe level of 14% to 16%

[B8] Mohler, S. R., personal communication, 1975.

*There is probably a zone of oxygen concentration marginally insufficient for maintaining consciousness, for which this generalization is not applicable, so that substantially longer exposure after loss of consciousness would not have permanent effects. However, not enough is known quantitatively about this for useful application in the VM.

within the critical period, nc permanent damage is expected, although the subject may remain unconscious for a much longer period of time. For example, a volunteer was exposed to total anoxia and lost consciousness after about 15 seconds. Within one minute he was restored to normal air, but he remained unconscious for 30 minutes. He then passed through a stage of confusion and disorientation for a quarter of an hour and lacked coordination for a further 15 minutes. A few hours later there was no detectable aftereffect.

As already noted, all persons are impaired at a cabin altitude of 16,000 feet, and some are seriously impaired at 15,000 feet. (They may not be conscious of impairment unless they get up and move about or undertake moderately demanding mental tasks.) This is in the O_2 range of 11.7% to 11.1%. At 10,000 to 12,000 feet (14.0% to 12.7% O_2), there is some impairment of cerebral function, enough to require use of supplementary oxygen by aircraft flight crew members but not by others. As a baseline for the VM, we propose 12% O_2 (58% air, 42% asphyxiant) as the safe level above which the exposed population will suffer no significant harm, regardless of the duration of exposure. A small minority with severe respiratory or circulatory deficiencies, or undertaking extreme and unaccustomed exertion, might be at risk, but to offset this the time of exposure is likely to be quite short.

At the other extreme, exposure to 100% asphyxiant would lead in a few inhalations to alveolar oxygen depletion sufficient to induce loss of consciousness; the depletion would continue and the cerebral cortex would suffer permanent damage or death would occur in four to five minutes after losing consciousness. The time to loss of consciousness would be about one minute or less in the absence of breath-holding. (Hyperventilation would be more likely in the context of the VM, because of alarm induced by awareness of abnormal conditions.) If the victim were restored to a level of 15% O_2 (28% asphyxiant) or more within a short time, no permanent harm would be experienced. This time would be not more than about five minutes from the onset of exposure. (The "safe" level of 12% is not considered adequate for reoxygenation after experiencing hypoxia.)

If no loss (or very brief loss) of consciousness is used as the criterion of safe exposure, we can estimate a set of concentration/time figures by (1) allowing for the time taken to deplete alveolar oxygen after exposure and (2) using two to three times the TUC as time to loss of consciousness (see Table B-6). (Breathing 100% inert gas, the TUC is 15 seconds and the time to unconsciousness is 45 to 90 seconds; at levels of incomplete anoxia, the difference may be less.)

The safe period of unconsciousness and continued exposure may be taken to be four minutes at any of these oxygen levels, provided that the victim is exposed after four minutes to not less than 15% O_2.

TABLE B-6. ESTIMATED TIMES TO UNCONSCIOUSNESS AT VARIOUS OXYGEN LEVELS

O_2 (%)	Time to Unconsciousness
0	45 seconds
3	45 seconds
4	60 seconds
5	90 seconds
6	3 minutes
7	5 minutes
8	8 minutes

These estimates are shown in Figure B-4. For the VM, it is suggested that the interval between unconsciousness and the point of no return might be ignored: i.e., the unconsciousness curve equated with death. This would allow for (1) the unlikelihood of rapid return to air below the threshold of impairment after exposure at these high levels of asphyxiant concentration, (2) the probable absence of any supportive treatment, (3) the likely presence of more sensitive subjects than the healthy adults to which these estimates apply, and (4) possible physical injuries during impairment and loss of consciousness.

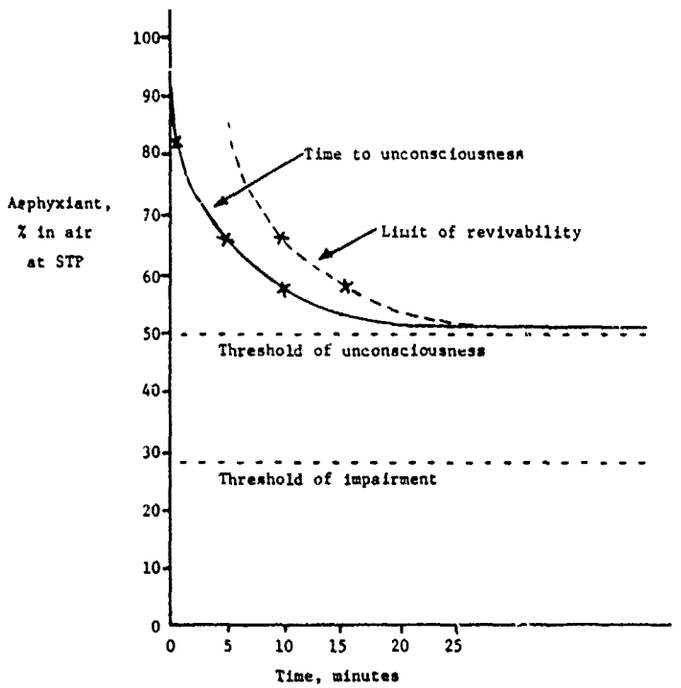

FIGURE B-4. Estimates of Time to Effect Vs. Asphyxiant Concentration

It is emphasized that these estimates, except for the extreme conditions of total anoxia and safe exposure, are not supported by direct experimental evidence. They are guesses which may be supported by future experiment or observation of accidental exposure.

Application to the Vulnerability Model

On the basis of the foregoing discussion, it is proposed that the concentration-effect relationships in Table B-7 be used for true "simple asphyxiants" in the VM.* The numerical values may well change with future inputs of new information, but it is believed that the proposed structure will continue to be the most acceptable. It is to be noted that the values in Table B-7 apply to exposure in the context of the VM: i.e., exposure times likely to be well under one hour.

TABLE B-7. CONCENTRATION-EFFECT RELATIONSHIPS FOR USE IN THE VM, FOR TRUE "SIMPLE ASPHYXIANTS" ONLY

Asphyxiant (%)	Effect
42	Ceiling for safe exposure; some mental impairment, but unlikely to result in harm (except to extremely susceptible individuals)
50	Threshold for unconsciousness in the more susceptible segment of the population; a few cases of lasting impairment and perhaps death
60	8 minutes to unconsciousness for an average individual; time to unconsciousness may be about one-half that in the more susceptible segment; recovery unlikely in absence of immediate medical aid[a]
65	5 minutes to unconsciousness
70	3 minutes to unconsciousness
75	1.5 minutes to unconsciousness
80	1 minute to unconsciousness
85	0.75 of a minute to unconsciousness

[a]As already noted, it is unlikely that the return to "safe" air would be rapid after exposure at those levels.

*I.e., for gases whose adverse influence is essentially limited to diluting atmospheric O_2. Methane is an example (although it has a slight toxic effect in addition). Nitrogen and the inert gases are other examples. Propane has a sufficiently toxic effect to require modified treatment in the VM.

It is of interest to compare our estimates with some published figures. Sax [B9] gives the following:

% *Asphyxiant*	*Effect*
33	Symptomatic threshold
50	Marked symptoms
75	Fatal in minutes

Mohler [B6] reports on three subjects "raised" from 8,000 feet to 25,000 feet in two minutes, held for one minute at 25,000 feet, and "lowered" back to 8,000 feet in three minutes. This corresponds to approximately 25% asphyxiant increased to 65%. It "brought the subjects to the brink of physiologic incapacitation."

Methane

Methane (LNG) is generally regarded as a "simple asphyxiant," capable of diluting the atmosphere so as to cause oxygen deprivation but having no other hazardous effect. The latest evidence available to us (see the discussion on propane below) indicates that this is not strictly true. However, the difference is not sufficient to invalidate the simple concept for use in the VM. The concentration-effect relationships for air dilution in Table B-7 are therefore applicable to methane.

Propane

Propane has a characteristic natural gas odor which, however, does not give adequate warning of hazardous concentrations [B10,B11]. The "commercial" grade has a minimum purity of 65.0 mole % propane (other grades are 96% and up), the main impurity being propylene.

Some observations from the literature relevant to various concentrations in air (otherwise clean) are shown on the following page.

[B9] Sax, N. I., *Dangerous Properties of Industrial Materials*, 3rd ed., Van Nostrand Reinhold Co., New York, 1968.

[B10] Braker, W., and A. L. Mossman, *Effects of Exposure to Toxic Gases - First Aid and Medical Treatment*, Matheson Gas Products, East Rutherford, N.J., 1970.

[B11] Braker, W., and A. L. Mossman, *Matheson Gas Data Book*, 5th ed., Matheson Gas Products, East Rutherford, N.J., 1971.

0.1% by volume: Threshold Limit Value (TLV) recommended by the American Conference of Governmental Industrial Hygienists [B12] (concentration to which nearly all workers may be repeatedly exposed during an 8-hour day without adverse effects)

1% for brief periods: Has produced no symptoms [B13]

3% to 5% for several hours: No hazard [B14]

10%: Slight dizziness in a few minutes; not noticeably irritating [B15]

33%: Threshold of noticeable anoxia

50%: Soon incapacitated

75%: Quickly fatal

(The last three levels of exposure are from Henderson and Haggard [B14]; Sax [B9] gives similar information.)

The consensus among established authorities is to treat methane (CH_4) and ethane (C_2H_6) as inert gases, toxicologically, in modeling their effects, on the assumption that their only action, physiologically, is to dilute the air and so cut down the concentration of available oxygen. It is recognized that, as molecular size increases, the higher members of this series of hydrocarbons have a narcotic action, acting on the central nervous system to induce dizziness, stupor, and loss of consciousness. However, the balance of opinion has been to regard this as significant for pentane (C_5H_{12}) and above, but not for propane (C_3H_8)

[B12] American Conference of Governmental Industrial Hygienists (ACGIH), *Documentation of Threshold Limit Values for Substances in Workroom Air*, 3rd ed., ACGIH, P. O. Box 1937, Cincinnati, Ohio, 1971.

[B13] FWPCA, *Oil and Hazardous Materials. Emergency Procedures in the Water Environment*, FWPCA, North Atlantic Water Quality Management Center, Edison, N.J., 1968.

[B14] Henderson, Y., and H. W. Haggard, *Noxious Gases and the Principles of Respiration Influencing Their Action*. 2nd ed., Reinhold Publishing Corp., New York, 1943.

[B15] Patty, F. A. (ed.), *Industrial Hygiene and Toxicology*, Interscience Publishers, New York, 1962.

and butane (C_4H_{10}). Some authorites describe methane and ethane as inert and ascribe slight narcotic properties to propane and butane; others--including the American Conference of Governmental Industrial Hygienists (the long-established authority on occupational exposure)--describe all four as inert.

When we first reviewed propane for the VM, we treated it simply as an atmospheric diluent (in the 22nd Monthly Report, February 1976). However, we later received a paper by Forney and Harger [B16] on the experimental exposure of mice to the series methane-butane, which was presented at a meeting in Edinburgh, Scotland in 19/2 but has not been published; our attention was drawn to it by Dr. Steven C. Lewis of Exxon Corporation's Toxicology Division. It shows that all four hydrocarbons have a depressant effect on the central nervous system, the potency of which rises with increasing molecular weight. Oxygen deficiency is the chief factor in the narcotic action of methane, and we saw no need to revise our earlier treatment of LNG. However, Forney and Harger's results show that oxygen deficiency played no part in the narcotic action of butane, which was entirely a toxic effect, and that the effect of oxygen deficiency was accompanied by a substantial toxic action in propane. We therefore revised the treatment of propane to accommodate this property.

It will be noted that this new evidence depends solely on experiments with mice. We do not feel that there would be justification for applying the results directly to man--i.e., assuming that a given concentration of propane would produce the same effect in the same exposure time. The general run of experience in laboratory comparison of animal species is that the scale of effects is similar, but that the level of effect for a given exposure differs (especially with uncomplex agents such as these hydrocarbons). Accordingly, we propose to modify the predicted response in man, which was based on simple oxygen deprivation, in similar proportion to the different responses of mice exposed to oxygen deprivation alone and with propane exposure.

Forney and Harger's results (for methane and propane only) are shown in Table B-8. They exposed all mice for 60 minutes, observing the most severe response and the time for it to take effect. All mice that survived were transferred to clean air and recovered completely within three minutes, with no deaths in the following 24 hours.

There are three series of experiments shown in Table B-8. The first three columns show the effect of increasing hydrocarbon concentrations in air: the response is more marked to propane than to methane.

[B16] Forney, R. B., Jr., and R. N. Harger, Reaction of mice from acute exposure to various concentrations of methane, ethane, propane and butane in air, or in oxygen, paper presented at Sixth International Meeting of Forensic Sciences, September 20-26, 1972, Edinburgh, Scotland.

TABLE B-8. RESPONSE OF MICE IN 60-MIN EXPOSURE TO VARIOUS GAS MIXTURES

(1) % Air/Hydrocarbon	(2) Resulting % Oxygen	(3) Response		(4) % Air/Nitrogen	(5) Response	(6) % Air/Hydrocarbon	(7) Response	
		Methane	Propane				Methane	Propane
90/10	18.9	0	0					
80/20	16.9	0	0					
70/30	14.8	0	1	70/30	0			
60/40	12.6	1	1	60/40	1	60/40	0	0
50/50	10.5	1	2	50/50	1	50/50	1	1
40/60	8.4	1	4	40/60	1	40/60	1	2
30/70	6.3	4	4	30/70	2	30/70	1	3
20/80	4.2	5	5	20/80	5	20/80	1	3
						10/90	1	4

Key to responses:

0 No effect.
1 Mild depression, including humped appearance and marked decrease of locomotion.
2 Loss of muscular coordination, but still able to maintain balance.
3 Loss of ability to remain upright on tilting surface; loss of consciousness.
4 Some mice dead.
5 All mice dead.

Column (5) shows the response to similar mixtures of air and nitrogen, an inert diluent. Comparing this with column (3), it will be seen that methane differs in having a more severe response at one level (30/70) only and that the response to propane is generally more severe. The time to death at 20/80 also showed a significant difference:

	Time (min)
Nitrogen	6 to 8
Methane	7 to 8
Propane	2 to 5

The oxygen/hydrocarbon exposures show the extent to which response in the air/hydrocarbon mixtures was due to oxygen deficiency (validating the conclusions already indicated by the nitrogen results). Column (7) shows that there was only a slight effect in methane, even at 90% CH_4, but a marked effect in propane. Comparing this and column (5) with column (3) shows that the dominant mechanism of action in methane is oxygen deficiency with an indication of only slight toxicity, but that in propane the toxic action makes a substantial contribution. We decided accordingly to retain the treatment of methane as a simple diluent and to make due allowance for the toxicity of propane.

Responses in propane and nitrogen mixtures are given in Table B-9. It will be seen that the limit for mild depression in propane is 40% and

TABLE B-9. RESPONSES IN AIR MIXTURE WITH PROPANE AND NITROGEN COMPARED

Air/Diluent	Response	
	Propane	Nitrogen
70/30	Mild depression	None
60/40	Mild depression	None
50/50	Loss of coordination (10 min)	None
40/60	3 out of 12 dead (29-50 min)	Mild depression
30/70	4 out of 6 dead (15-23 min)	Loss of coordination (30 min)
20/80	All dead (2-5 min)	All dead (6-8 min)

in nitrogen is 60%, and that there is a similar difference in the level for loss of coordination. In the lethal zone, the difference is less. Assuming a similar proportionality in man, we propose to apply a correction of 15% to all levels of concentration: e.g., the response predicted for 60% of simple asphyxiant in air will be attributed to 45% of propane in air. Modifying Table B-7 accordingly, we get Table B-10.

TABLE B-10. CONCENTRATION-EFFECT RELATIONSHIPS FOR PROPANE

Propane (%)	Effect
27	Ceiling for safe exposure; some mental impairment, but unlikely to result in harm (except to extremely susceptible individuals)
35	Threshold for unconsciousness in the more susceptible segment of the population; a few cases of lasting impairment and perhaps death
45	8 minutes to unconsciousness for an average individual; time to unconsciousness may be about one-half that in the more susceptible segment; recovery unlikely in absence of immediate medical aid
50	5 minutes to unconsciousness
55	3 minutes to unconsciousness
60	1.5 minutes to unconsciousness
65	1 minute to unconsciousness
70	0.75 of a minute to unconsciousness

Asphyxiating Gases: Acknowledgments

We had helpful discussions with the following experts, who are however in no way responsible for the conclusions which are entirely ours.

Dr. Stanley R. Mohler, Chief, Aeromedical Applications Division, Federal Aviation Administration.

Dr. Rechnitzer, Dr. R. C. Bornmann, Dr. Lawton, and Dr. Homer Carhart; U.S. Navy, NMRI, and NRL.

Surg. Cdr. Ian Young, United Kingdom Royal Navy.

Dr. Merrill Goodwin, Aerospace Medical Association.

Asphyxiating Gases: Bibliography

The following texts were used by us or were quoted by our advisers.

Armstrong, H. G. (ed.). *Aerospace Medicine*. Williams and Wilkins, Baltimore, 1961. (See U. C. Luft for explosive decompression and C. F. Gell for time of useful consciousness.)

Armstrong, H. G. *Principles and Practice of Aviation Medicine*, 3rd ed., p. 201. Williams and Wilkins, Baltimore, 1952.

Brown, J. H. O. (ed.). *Physiology of Man in Space*, p. 155. Academic Press, 1963.

Comroe, J. H., et al. *The Lung*. Year Book Medical Publishers, Chicago, 1962.

Fenn, W. O., and H. Rahn (eds.). *Handbook of Physiology*, sec. 3, vol. 2. American Physiological Society, Washington, D.C., 1965.

Van Liere, E. J., and J. C. Stickley. *Hypoxia*. Univ. of Chicago Press, Chicago and London, 1963.

White, C., and O. Benson (eds.). *Physics and Medicine of the Upper Atmosphere*. Symposium, Lovelace Foundation, Univ. of New Mexico Press, Albuquerque, 1952.

CARBON TETRACHLORIDE

Carbon tetrachloride (CTC) is a liquid of medium volatility: its boiling point is 77°C, and its vapor pressure at 21°C is 100 mm Hg. Since the vapor density is high (ca. 5.4), air saturated with CTC at normal temperatures is about 60% heavier than clean air.

The present discussion is limited to inhalation toxicity. There is also a significant percutaneous hazard from contact with the liquid, and CTC in contact with flames or hot surfaces may form dangerous concentrations of phosgene. Ingestion of the liquid is highly dangerous.

CTC used to be handled in many industrial and domestic applications which resulted in substantial and repeated inhalation exposures, and it was also used as an anesthetic (being similar to chloroform, though less effective). When it became apparent that chronic exposure or even a heavy single exposure might cause serious and lasting injury, a large number of toxicological studies were made. CTC has been replaced by less toxic solvents for such operations as degreasing and dry cleaning, but the amount manufactured has not changed much because of its extensive use in fluorocarbon manufacture and other applications. U.S. production is about one billion pounds annually.

Because it was in occupational exposures that toxic effects were most often observed, the majority of animal experiments with CTC and epidemiological studies of human exposure relate to successive substantial doses over a period of time or to lower level chronic exposure and are consequently not very helpful for our purposes. There is, however, a fair body of experimental data for man in single exposures below the level of loss of consciousness and some data for heavier single exposures. One difficulty in combining and interpreting these observations arises from the extreme variation in individual susceptibility, "...some persons appearing to be unaffected by exposures which seriously poison their fellow-workers" [B9]. Susceptibility is considerably enhanced by intake of alcohol at around the same time, and habitual drinkers are highly susceptible; there is an accepted metabolic explanation for this, and the same effect can result from preexisting disorders of the liver or kidney which are not alcohol-related. It was therefore to be expected that we would find data on dose-response relationships from different reports showing wide variations, and this proved to be the case.

In the context of the VM, we are concerned with the consequences of a single exposure lasting probably less than an hour. (A spill in water will sink; the specific gravity of CTC is about 1.6.) CTC can work through at least two different toxicological mechanisms with quite different syndromes. One is its effect as a depressant of the central nervous system, in which it acts like many other inhalation anesthetics. A heavy concentration leads rapidly to loss of consciousness and, if the exposure continues, to death through respiratory failure. Lighter

exposures may lead to dizziness, vertigo, and stupor, and the experience is not necessarily disagreeable; CTC has been voluntarily inhaled for its euphoric intoxicating effect. The stupefying effect (narcosis), with or without loss of consciousness, clears up quite soon after exposure, although there may be some general malaise and gastrointestinal upset for a day or so.

The other mechanism is tissue injury, particularly to the liver and kidney, developing after some hours or days and perhaps lasting for a long time. (This mechanism is complex, including at least two quite distinct pathogenic processes, but this need not concern us.) The overt signs of liver or kidney damage are a range of metabolic and excretory disorders which may persist for a considerable time but are probably rarely or never permanent. Hamilton and Hardy [B17] say:

> The prognosis in severe cases of carbon tetrachloride poisoning has improved markedly since the availability of dialysis has become common. The simultaneous presence of hepatic failure with impaired urea synthesis and ammonia intoxication is obviously unfavorable. Recovery may require months but may be eventually complete. There is no universal agreement as to whether or not acute hepatorenal injury...may result in chronic impairment...

but the authors believe that it is possible in some cases. The International Agency for Research on Cancer (WHO) has noted that occasional case reports of liver tumors in man following acute intoxication with CTC are of doubtful significance but that they cannot be disregarded [B18].

In summary, the immediate narcotic effects of CTC may be harassment through mental and sensory disturbances, incapacitation through heavy stupor or complete loss of consciousness, or death if deep narcosis is prolonged into respiratory failure. After exposure, survivors of the narcosis will recover quite quickly and completely *from that effect*. There is the different effect of injury, primarily hepatorenal, developing after hours or days and persisting for some time; if severe, this injury would require hospitalization. Recovery from the narcotic effects would usually require no more than supportive first aid.

[B17] Hamilton, A., and H. L. Hardy, *Industrial Toxicology*, 3rd ed., Publishing Science Group, Inc., Acton, Mass., 1974.

[B18] International Agency for Research on Cancer (WHO), *Monographs on the Evaluation of the Carcinogenic Risk of Chemicals to Man. Carbon Tetrachloride, Vol. 1*, pp. 53-60, WHO/IARC, 1949.

In preparation for the development of dose-response expressions for the VM, we tabulated all the serviceable data we had compiled for man (Table B-11). The criteria for inclusion were: (1) that the source we referred to reported both concentration and time as single figures, or as a range of no more than 2:1; (2) that the exposure time did not exceed 60 minutes; and (3) that the source described the observed or estimated response in reasonably definite terms (e.g., "dangerous" was acceptable but "tolerated"--with no indication of degree of harassment--was rejected). The data in Table B-11 are presented in order of decreasing dosage (Ct). To avoid large numbers, dosages are in units of 10^3 mg min m^{-3} instead of the more usual mg min m^{-3}. (It helps to see where CTC is on the general scale of toxicity, if we note that the dosages we have analyzed elsewhere for phosgene are roughly 1/5000 of these for CTC at similar levels of response.) In Table B-11, data given by the source as a range are shown as the midpoint: e.g., 1,000-2,000 would appear as 1,500. The column "Effect Categorized" shows our best estimate of the category into which the reported effects should fall:

0	=	No effect - other than acceptable odor
sl.H	=	Slight harassment
H	=	Harassment - discomfort, but voluntary activity continues
I	=	Incapacitation - loss of consciousness
D	=	Danger - heavy narcosis, lethal to susceptible subjects
L	=	Lethal - respiratory failure in normal subjects

We did not attempt to include categories for delayed or long-term incapacitation from liver or kidney injury, or for delayed death from the same cause. There is no sound basis for quantitative estimates of exposure; the clinical evidence is from cases in which no measurements (or reconstructions) were made of CTC concentrations.

It will be seen that the intensity of effect generally increases with the increasing dosage, but there are some reported effects which are badly out of place. Ordering by concentration (Table B-12) is perhaps a little better. We prefer, however, to use the dosage because it is likely that liver or kidney injury, a more serious consequence than temporary narcosis, is dose-dependent.

The effects categorized in Table B-11 are displayed against time and concentration in Figure B-5. In an attempt to bring some order into this scattered display, it was divided into zones by lines sloping at 45°; i.e., conforming to Haber's law of constant Ct for any given level of effect. The points were then marked according to whether they fell into their correct zone or not (Figure B-6). It will be seen that the outcome was quite good. There are two points conspicuously out of place--the 0 in the lethal zone, and the H in the danger zone--but the

TABLE B-11. EFFECTS OF CTC EXPOSURE IN MAN, IN ORDER OF INCREASING DOSAGE

Dosage, 10^3 mg min m^{-3}	Concentration, mg m^{-3}	Time, min	Effect	Effect Categorized[a]	Reference[b]
31	1,560	20	Slight odor	0	1
31	1,030	30	One case of slight nausea	sl.H	2
33	1,650	20	No effect	0	3
39	3,900	10	Vertigo, headache	H	1
62	2,050	30	Nausea, headache	H	2
77	92,000	0.84	Immediate paresthesia, loss of consciousness, unwell 2.5 hr later	I	3
77	61,800	1.25	Paresthesia of extremities, fainting	I	4
78	31,200	2.5	Intoxication, slight sickness, stupor	H	4
78	15,500	5	Dizziness, nausea, vomiting	H	4
82	62,000	1.3	Moderate fainting	I	3
83	82,500	1	Paresthesia, unconsciousness	I	4
93	7,750	12	Dizziness, nausea, vomiting	H	6
104	20,700	5	No effect	0	6
114	56,800	2	Some incapacitation	I	3
114	11,400	10	Irritation, vertigo, headache, fatigue	H	4
117	3,900	30	Dizziness	H	1
124	41,400	3	Some incapacitation	I	3
124	4,130	30	Irritation, vertigo, headache, fatigue	H	4
125	41,600	3	Paresthesia of extremities, stupor	H	4
150	15,000	10	Dizziness, nausea, vomiting	H	4
155	31,000	5	Slight somnolence	sl.H	3
438	9,750	45	Fatalities reported	D	5
1,950	32,500	60	Maximum time without serious disturbance	H	6
2,438	325,000	7.5	Fatal	L	6
3,366	74,800	45	No immediate or later consequence	0	7
7,313	162,500	45	Dangerous	D	6
8,190	182,000	45	Dangerous	D	6
8,760	146,000	60	Fatal or serious injury	L	8
21,060	463,000	45	Immediate or later death	L	6

Note: Paresthesia is the usual term for a range of abormal feelings such as burning and prickling sensations in the skin. It is worth noting that this kind of sensation may be quite disturbing to a human but is not an observable response in animal exposure.

[a]Key for Effect Categorized appears in text.

[b]References key:

1 Lehmann and Schmidt-Kehl, 1936
2 Davis, 1934
3 Von Oettingen, 1964
4 King, 1949
5 FWPCA, 1968
6 McNally, 1937
7 Patty, 1962
8 Deichmann and Gerarde, 1969

TABLE B-12. EFFECTS OF CTC EXPOSURE IN MAN, IN ORDER OF INCREASING CONCENTRATION

Concentration, mg m^{-3}	Time, min	Effect	Effect Categorized
1,030	30	One case of slight nausea	sl.H
1,560	20	Slight odor	0
1,650	20	No effect	0
2,050	30	Nausea, headache, vomiting	H
3,900	10	Vertigo, headache	H
3,900	30	Dizziness	H
4,130	30	Irritation, vertigo, headache, fatigue	H
7,750	12	Dizziness, nausea, vomiting	H
9,750	45	Fatalities reported	D
11,400	10	Irritation, vertigo, headache, fatigue	H
15,000	10	Dizziness, nausea, vomiting	H
15,500	5	Dizziness, nausea, vomiting	H
20,700	5	No effect	0
31,000	5	Slight somnolence	sl.H
31,200	2.5	Intoxication, slight sickness, stupor	H
32,500	60	Maximum time without serious disturbance	H
41,400	3	Some incapacitation	I
41,600	3	Paresthesia of extremities, stupor	H
56,800	2	Some incapacitation	I
61,600	1.25	Paresthesia of extremities, fainting	I
62,000	1.3	Moderate fainting	I
74,800	45	No immediate or later consequence	0
82,500	1	Paresthesia, unconsciousness	I
92,000	0.84	Immediate paresthesia, loss of consciousness, unwell after 2.5 hr later	I
146,000	60	Fatal or serious injury	L
162,500	45	Dangerous	D
182,000	45	Dangerous	D
325,000	7.5	Fatal	L
463,000	45	Immediate or later death	L

other four are not far out. The main defect in this treatment is that a zone at this slope must embrace both harassment and incapacitation, which is too wide a range of hazards. However, King [B19], using many of the same data, estimated a zoning of responses which corresponds much more closely with a compromise at a slope of 22.5°, halfway between Haber ($Ct=k$ for a given level of effect) and concentration-dependence ($C=k$), than it does with Haber: see Figure B-7.

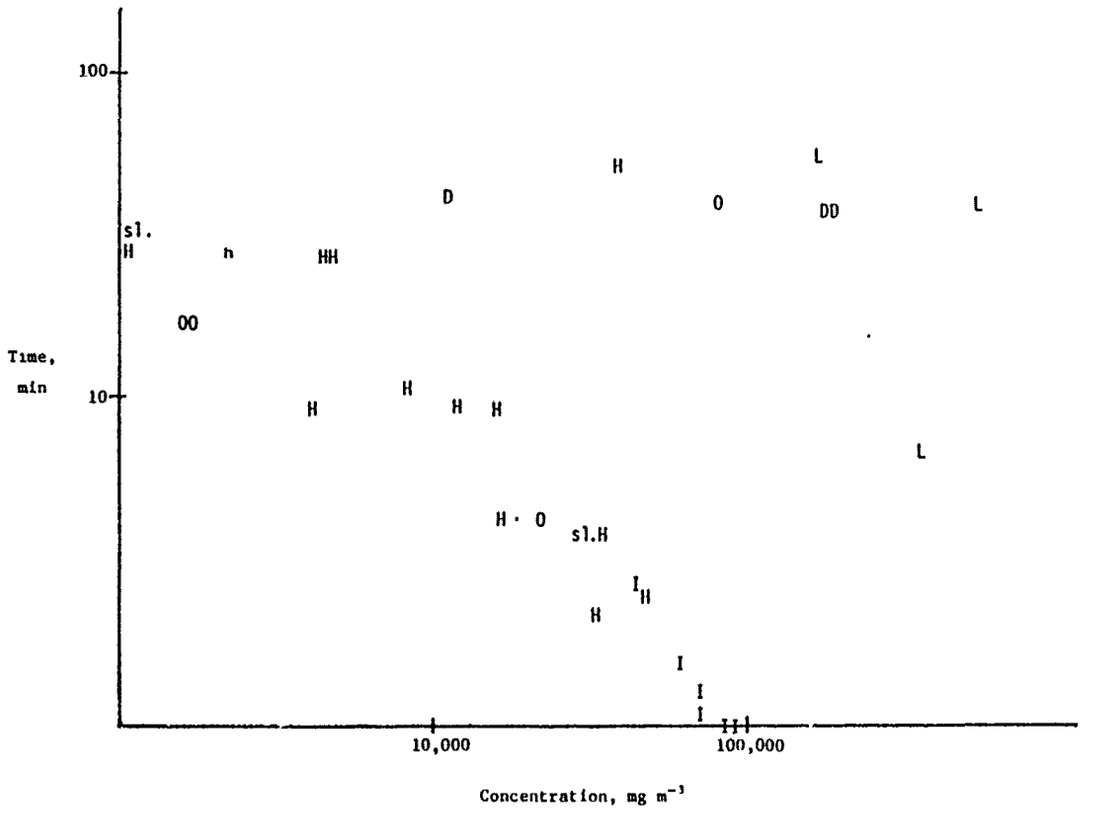

FIGURE B-5. Response Vs. Time and Concentration

[B19] King, B. G., High concentration - short time exposures and toxicity, *J. Ind. Hyg. Toxicol.* *31*(6):365-375, 1949.

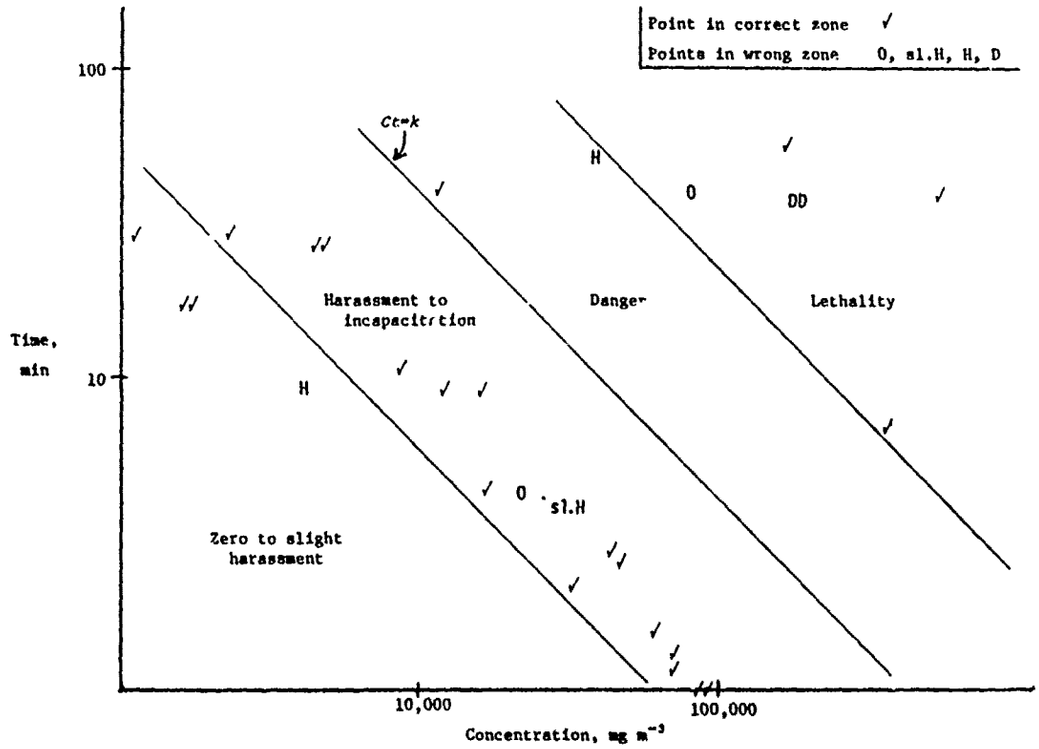

FIGURE B-6. Responses Zoned (the response descriptions apply to the zones in which they appear)

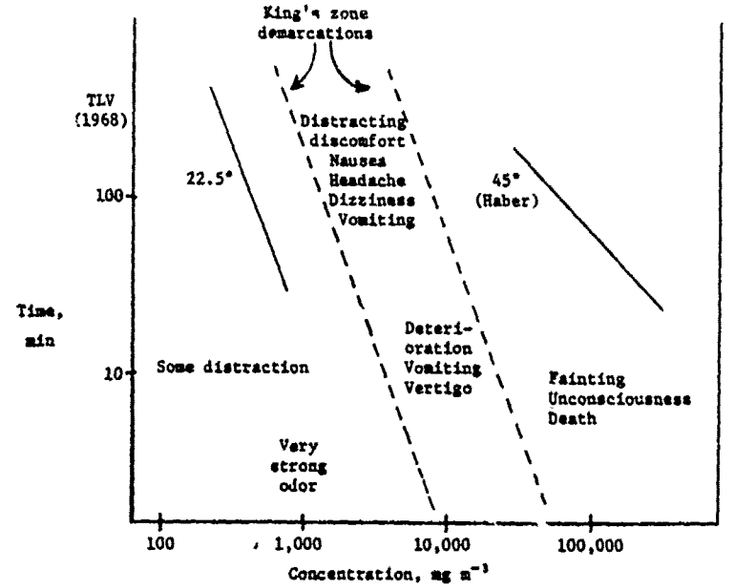

FIGURE B-7. Responses Zoned (adapted from King [B19]; the response descriptions apply roughly to their locations on the chart)

Accordingly, we revised Figure B-6, using the 22.5° slope and redefining the zones (see Figure B-8). This represents a dosage (Ct) response relationship with greater dependence of response on concentration than on time, which seems to us acceptable for the conditions of the VM: namely, single, short-time exposure and concern primarily for narcosis.

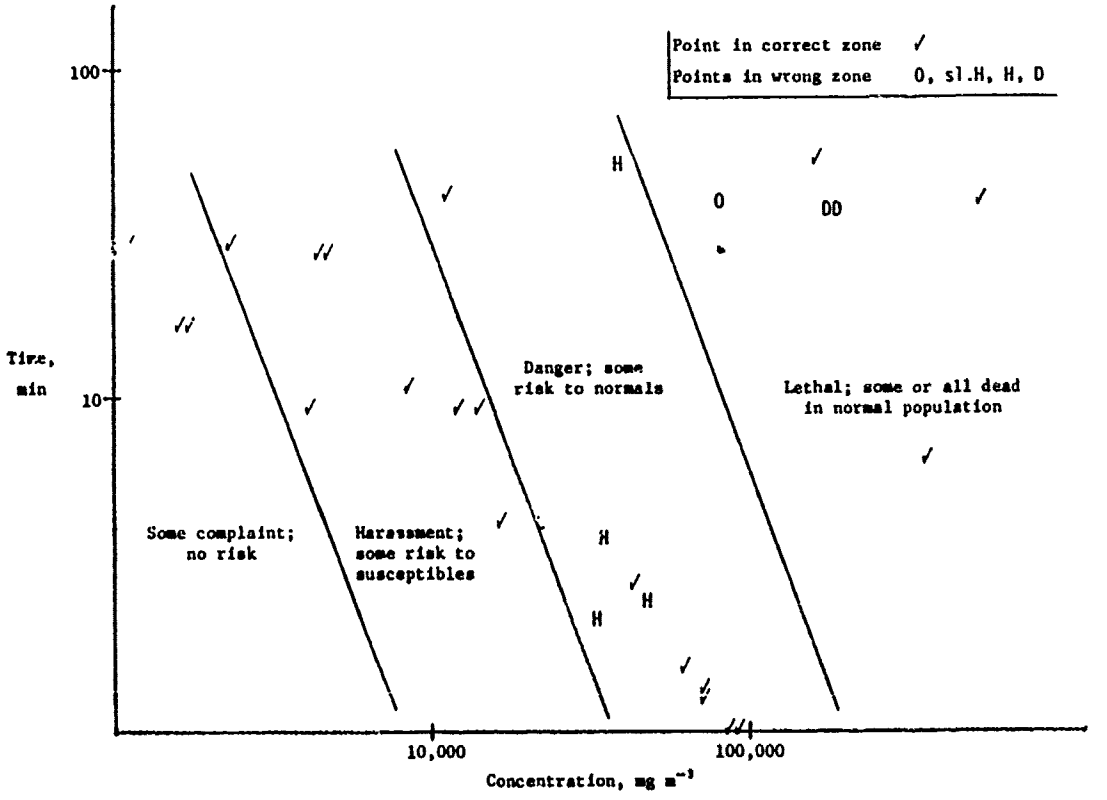

FIGURE B-8. Figure B-6 Revised

Using Figure B-8, the dose-response relationships shown in Table B-13 have been estimated. It must be emphasized that these estimates are not at the level of reliability that the use of two significant figures might suggest; this will, in fact be obvious from a cursory examination of Table B-11. However, we believe that they are reasonable estimates, and probably not much different in reliability from the dosage predictions with which they will be used.

TABLE B-13. DOSE-RESPONSE RELATIONSHIP FOR INHALED CTC IN MAN

Effect	Concentration, 10^3 mg m^{-3}			
	Time, min			
	5	15	30	60
Complaint; no risk	2.1	1.4	1.0	0.8
Harassment; LC_5 for susceptibles	9.5	6.3	4.5	3.6
Severe harassment; LC_{50} for susceptibles, LC_5 for normals	42	28	20	16
Lethal, LC_{100} for susceptibles, LC_{50} for normals	210	140	100	80

References for Carbon Tetrachloride

Davis, P. A. Carbon tetrachloride as an industrial hazard. *J. Am. Med. Assoc. 103*:962-966, 1934.

Deichmann, W. B., and H. W. Gerarde. *Toxicology of Drugs and Chemicals*. Academic Press, New York, 1969.

FWPCA. *Oil and Hazardous Materials. Emergency Procedures in the Water Environment*. FWPCA, North Atlantic Quality Management Center, Edison, N.J., 1968.

Hamilton, A., and H. L. Hardy. *Industrial Toxicology*, 3rd ed. Publishing Science Group, Inc., Acton, Mass., 1974.

International Agency for Research on Cancer (WHO). *Monographs on the Evaluation of the Carcinogenic Risk of Chemicals to Man. Carbon Tetrachloride. Vol. 1*, pp. 53-60. WHO/IARC, 1949.

King, B. G. High concentration - short time exposures and toxicity. *J. Ind. Hyg. Toxicol. 31*(6):365-375, 1949.

Lehmann, K. B., and L. Schmidt-Kehl. [The thirteen most important chlorinated aliphatic hydrocarbons from the standpoint of industrial hygiene]. *Arch. Hyg. 116*:132-200, 1936.

McNally, W. D. *Toxicology*. Industrial Medicine, Chicago, 1937.

Patty, F. A. (ed.). *Industrial Hygiene and Toxicology*. Interscience Publishers, New York, 1962.

Sax, N. I. *Dangerous Properties of Industrial Materials*, 3rd ed. Van Nostrand Reinhold Co., New York, 1968.

Von Oettingen, W. F. *The Halogenated Hydrocarbons of Industrial and Toxicological Importance*. Elsevier, Amsterdam (and Elsevier Publishing Co., New York), 1964.

HYDROGEN CHLORIDE

The anhydrous gas is transported as a liquid under about 40 atmospheres of pressure; the boiling point at one atmosphere is -85°C. On release into the air, the gas combines with water vapor to form a white cloud of hydrochloric acid droplets; if there is insufficient water vapor, some of the hydrogen chloride (HCl) will remain as anhydrous gas. In either state, the chemical is extremely aggressive because it dissolves in bodily moisture to form strongly acid conditions, reacting with and disturbing the normal alkalinity. The effects are highly irritant and destructive, and the anhydrous gas also has a dehydrating action which augments its aggressiveness. The main sites of attack are the eyes and the moist mucous surfaces of the respiratory tract. Because of its high solubility, the gas is trapped mainly in the upper respiratory tract. However, acid droplets of less than 5 microns in diameter may escape impaction in the upper tract and be deposited by settling or diffusion in the lower tract--i.e., in the alveolar region responsible for respiratory gas exchange.* (The hydration of the HCl gas to form hydrochloric acid droplets may take place in the atmosphere, as already indicated, or in the oronasal region which is highly effective in hydrating inspired air.) The droplets are, of course, accompanied by hydrochloric acid vapor.

The skin is also vulnerable, especially to the anhydrous vapor, and it is evident that not only moist skin surfaces but also overlying clothing can trap and retain the acid. This can cause severe burns and necrosis, and subsequent dermatitis may develop. Industrial safety practices recommend removal of contaminated clothing and thorough showering. Eyes should be thoroughly irrigated. First aid for inhalation casualties is removal to clean air, artificial respiration if required, oxygen if breathing with difficulty, and rest. Direct contact with liquid anhydrous HCl causes the additional hazard of severe frostbite.

The accompanying table (Table B-14) displays toxic effect in man, based on experiment at lower concentrations and on estimates (from accidental exposures and animal experiments) at higher concentrations.

---

*This mechanism, by which the HCl can attack the lower lung, does not seem to be widely appreciated. Possibly because the immediate irritant effect is felt most in the upper respiratory tract and at high concentrations may lead at once to spasm of the larynx, most descriptions of the toxicology of HCl give the impression that it is entirely an upper respiratory irritant. It is clear, however, that the small airways and alveoli are also seriously at risk; this may be important for high-risk subjects, as we shall see later.

TABLE B-14. HCl EXPOSURE AND EFFECTS

Concentration		Time	Dosage,	Effect	Reference[a]
mg m^{-3}	ppm		mg min m^{-3}		
1.5-15	1-10	--	--	Various estimates of odor threshold	1
3	2	30 min	90	Short-Term Public Exposure Limit (STPL); below discomfort level	1
3	2	60 min	180	STPL	1
5	3	30 min	150	Public Emergency Limit (PEL); temporary discomfort	1
5	3	60 min	300	PEL	1
6	4	10 min	60	STPL	1
7	5	--	--	Ceiling Threshold Limit Value (TLV)	2
7-15	5-10	--	--	Disagreeable	3
10	7	10 min	100	PEL	1
15	10	Long	--	Maximum allowable concentration; man can work undisturbed	3,4
>15	>10	--	--	Irritation	1
15-75	10-50	1 hr	2,700	Work difficult but possible	3
15-75	10-50	Few (3) hr	(8,100)	Maximum tolerable	4
52	35	Short	--	Irritation of throat	3,4
75-150	50-100	--	--	Impossible to work	3
75-150	50-100	1 hr	6,780	Maximum tolerable	4,5
75-150	50-100	1 hr	6,780	Tolerable but normal work impossible	1
150	100	30-60 min	6,750	Endurable	6
1000	670	2 hr	120,000	Lowest reported exposure lethal to mammals	7
1500	1000	$\leq$1 hr	$\leq$90,000	Dangerous	1
1500	1000	30-60 min	67,500	Dangerous	6
1500-1900	1000-1300	30-60 min	76,500	Dangerous	8
1500-3000	1000-2000	Short (5 min)	(11,250)	Dangerous	4,5
1900-3000	1300-2000	Few (5) min	(12,250)	Lethal	8
1900	1300	30 min	57,000	Lowest lethal estimate for man	9
4500	3000	5-10 min	33,750	Fatal	6

NOTES: Conversion of concentrations is on the approximate basis of 1 ppm = 1.5 mg m^{-3} (more exactly, 1.49 mg m^{-3}). Where original publications give vague times such as "few hours," we have allowed ourselves a guess at what is meant: this is shown in parentheses, and the calculated dosage is also in parentheses.

[b] *References:*

1 NAS-NRC, 1971
2 ACGIH, 1971
3 Patty, 1962
4 Henderson and Haggard, 1943
5 Sax, 1968
6 McNally, 1937
7 Machle et al., 1942
8 Jacobs, 1969
9 Lefaux, 1968

Table B-14 shows dosages--i.e., concentration (C) multiplied by time (t)--but this is not meant to imply that Haber's law, $Ct = k$ for a given level of response, is expected to apply. On the contrary, the effect of a primary irritant such as HCl is highly concentration-dependent. (We met this kind of toxicological response previously with ammonia, and in part with chlorine also.) In simple terms, the agent exerts its effect immediately at the point of contact with the body. If the rate of dosing (i.e., the concentration) is low enough, the body deals continually with it and disperses the agent without effect at the site of contact; this is the level of indefinite tolerance without discomfort. The body does not build up a harmful level at the contact site or in another organ, because the agent is disposed of by dilution and reaction. If the concentration is somewhat above the discomfort level, irritation is immediate and continues throughout exposure; after exposure, recovery is rapid. At higher levels, the time of exposure begins to be important because the effect of continued irritation builds up, with longer-lasting consequences. At the very high concentration levels which induce complete or near-complete cessation of respiration, another time effect comes into play: oxygen deprivation has rapidly fatal effects, and it is the time which the body can survive this hypoxia which determines the outcome of an exposure.

Table B-14 is divided into exposure ranges which may be summarized as follows.

Concentration, mg m^{-3}	*Effect*
< 5	Negligible
5 - 15	Temporary discomfort
15 - 75	Endurable for a few hours
75 - 150	Endurable for 1/2 to 1 hour
150 - 1000	There is a gap here, for which no useful figures are available
1000 - 2000 approx.	Dangerous in 1/2 to 1 hour
2000 approx. - 4500	Fatal in 5 to 30 minutes

We have concluded that this may be modified to the same structure of effect levels that we have used previously for chlorine and ammonia; this involves closing the gap in the above table by use of best estimates, as in the following summary.

Concentration, mg m^{-3}	*Time*	*Effect*
< 5	Any	Negligible
5 - 75	Any	Complaint, but no risk
75 - 200	ca. 1 hr	Severe harassment of normal population; lethal hazard to high-risk population
200 - 700	ca. 1 hr	Partial lethality in normal population; high lethality in high-risk population
700 - 2000	ca. 1 hr	50% lethality in normal population; 100% in high-risk population
> 2000	ca. 15 min	Lethal

The estimates in this summary (and it is emphasized that they are highly judgmental, except at the lowest concentrations) are set out in Table B-15 in the same form as the former chlorine and ammonia estimates.

TABLE B-15. PROPOSED DOSE-EFFECT RELATIONS FOR THE VM: HYDROGEN CHLORIDE

HCl Concentration, mg m^{-3}	Time	Effect	Deaths, %	
			General Population	High-Risk Population
< 5	any	Negligible	0	0
5-75	any	Complaint, no risk	0	0
75-200	ca. 1 hr	Severe harassment (some risk)	0	25
200-700	< 0.5 hr	Severe harassment/risk	0	25
	0.5-1 hr	Lethal	3	50
	1-2 hr	Lethal	50	100
700-2000	< 0.5 hr	Lethal	3	50
	0.5-1 hr	Lethal	50	100
	1-2 hr	Lethal	97	100
> 2000	< 5 min	Lethal	3	50
	5-15 min	Lethal	50	100
	15-30 min	Lethal	97	100

We have considered the possibility of long-term or permanent injury and have concluded that this may be neglected in the context of the VM. This is not to say that there will be no such injury (which is more likely among the high-risk sectors), but that it will be negligible in proportion to the incidence of temporary incapacitation and of death if exposures are severe.

References for Hydrogen Chloride: Table B-14

1. National Academy of Sciences-National Research Council, Committee on Toxicology. *Guides for Short-Term Exposure of the Public to Air Pollutants. II. Guide for Hydrogen Chloride.* NAS-NRC, Washington, D.C., 1971.
2. American Conference of Governmental Industrial Hygienists (ACGIH). *Documentation of Threshold Limit Values for Substances in Workroom Air*, 3rd ed. ACGIH, P.O. Box 1937, Cincinnati, Ohio, 1971.
3. Patty, F. A. (ed.). *Industrial Hygiene and Toxicology.* Interscience Publishers, New York, 1962.
4. Henderson, Y., and H. W. Haggard. *Noxious Gases and the Principles of Respiration Influencing Their Action*, 2nd ed. Reinhold Publishing Corp., New York, 1943.
5. Sax, N. I. *Dangerous Properties of Industrial Materials*, 3rd ed. Van Nostrand Reinhold Company, New York, 1968.
6. McNally, W. D. *Toxicology.* Industrial Medicine, Chicago, 1937.
7. Machle et al., *J. Ind. Hyg. Toxicol. 24*:222, 1942.
8. Jacobs, M B. *The Analytical Toxicology of Drugs and Chemicals.* Academic Press, New York, 1969.
9. Lefaux, R. *Practical Toxicology of Plastics.* Chemical Rubber Co., Cleveland, Ohio, 1968.

METHYL BROMIDE

Methyl bromide (MeBr) is a gas, its boiling point being 4°C; it is shipped in liquid form under 1 atmosphere excess pressure. It is odorless except at high concentrations, when it has an inoffensive sweetish smell rather like chloroform. It is described as highly toxic (see Braker and Mossman [B10]), but this is slightly misleading; for example, the Threshold Limit Value (TLV) recommended by the American Conference of Governmental Industrial Hygienists [B12] for workroom exposure is 20 parts per million (ppm), which may be compared with 10 ppm for carbon tetrachloride and 0.1 ppm for phosgene. MeBr is better desribed as highly *hazardous*, because it is insidious and can produce lasting injury.

Its toxic action has four characteristics that make it exceptionally hazardous:

- No warning; the slight odor and absence of immediate irritation result in "the possibility of experiencing a fatal exposure without any awareness of exposure at all" [B20].*
- Delayed action; "the onset of symptoms is usually delayed for 4 to 6 hours, though the latent period may vary from 2 to 48 hours" [B9].

[B20] Collins, R. P. Methyl bromide poisoning. A bizarre neurological disorder. *Calif. Med. 103*(2):112-116, 1965.

*Collins [B20] gives an interesting example from Clarke et al. [B21] of how little warning may be received of a serious exposure.

> "Clarke, Roworth and Holling described dramatically such an occurrence in the British Navy. A leaking methyl bromide fire extinguishing system exposed four officers while they were eating lunch in the wardroom. All four became ill and two died. The two officers exposed the longest noted smarting of the eyes, but did not become seriously ill until four hours later, when both vomited and one became unconscious. After they were admitted to hospital, a hearing officer was sent to hold an inquiry into the cause of this illness. The third of the four officers summoned to the hearing, which was held in the same wardroom, was perverse, uncooperative, and unconcerned at his fellow officers' serious plight. The hearing ended with some suspicion that the steward had poisoned the two officers, since he was under punishment and had discarded the remains of the meal. It was only later, when the hearing officer noted smarting of his own eyes, that the atmosphere in the wardroom and the fire extinguishing system was suspected."

[B21] Clarke, C. A., C. G. Roworth, and H. E. Holling. Methyl bromide poisoning: An account of 4 recent cases met with in one of H.M. ships. *Br. J. Ind. Med. 2*:17-23, 1945.

- Multiple organ targets; the gas "is a delayed pulmonary irritant and neurological effects are more common, often severe..." [B17]. In addition to attacking the lungs and the central nervous system, "the kidneys may be damaged and...the liver may be enlarged" [B9].
- Lasting injury; "Recovery is frequently prolonged and there may be permanent injury, such as sensory disturbances, weakness, disturbances of gait, irritability, and blurred vision" [B11].

In the conditions of single exposure which concern us, fatalities usually result from lung irritation although there are accompanying neurological symptoms, especially latterly. Nonfatal cases exhibit variable symptoms which may include headache, nausea and vomiting, visual and other sensory disorder, weakness, muscular incoordination, and epilepsy-like seizures. All these symptoms have been seen to persist. The sequence of responses commonly observed in the case of inhalation poisoning by MeBr is:

- Headache, nausea, vomiting, etc.; in mild cases this may be all, with full recovery soon following.
- Neurological disturbances such as impairment of vision, hearing, and speech; manifestations of irrationality and drowsiness which may be mistaken for alcohol or marijuana intoxication are characteristic of more severe cases, which may lead to fatal outcome or lasting injury.
- Death, usually within 24 to 48 hours, probably from effusion of fluid into the lung (pulmonary edema) or perhaps from circulatory failure; in survivors from "dangerous" exposures, neurological or psychiatric symptoms may persist for months or years.

The mechanism of MeBr's toxic action is of some interest because of its relation to the characteristic response after exposure. An obvious hypothesis is that it decomposes (is hydrolyzed) into methanol (methyl alcohol, MeOH) and bromine ion (Br^-). Bromides are well known for their action on the central nervous system; however, measured blood bromine levels in MeBr poisoning never equal those reached in inorganic bromide poisoning. Nor is there evidence of the optic nerve damage caused by methyl alcohol poisoning. Furthermore, exposure of rabbits and rats to methyl alcohol vapor and simultaneous administration of bromide, over a period of months, did not simulate MeBr exposure [B22]. The hypothesis is not in accordance with these observations nor with "the striking

---

[B22] Irish, D. D., E. M. Adams, H. C. Spencer, and V. K. Rowe. Methyl bromide intoxication of a large group of workers. *J. Ind. Hyg. Toxicol.* *23*:408-411, 1941.

similarity between the toxicity of methyl bromide and methyl chloride. There is the same delay in the onset of symptoms and the same convulsions" [B20]. These compounds share the physical properties of being slightly soluble in water and freely soluble in fat and the chemical property of being strong methylating agents (i.e., they insert Me-groups into organic molecules, changing their nature). So MeBr and MeCl can be carried by the blood, in solution, to the central nervous system, where they penetrate the nerve cells by dissolving in the fatty (lipid) layer and inactivate enzymes by methylation. Irritation and destruction of lung cells can occur similarly. This is consistent with the type and location of injury and with the delayed action.

The following section analyzes the available data to arrive at best estimates for dose-response relations for use in the VM. It will be clear from the foregoing discussion that the toxic effects are all delayed, so that no response is to be expected during exposure. There will, therefore, be no category of effect corresponding to the immediate harassment and incapacitation caused by primary irritants. We shall, however, be able to distinguish between delayed death and delayed incapacitation.

Analysis of Data

The earliest reports available to us on MeBr come mostly from Germany in the 1920's and are mainly clinical studies plus a few animal experiments. In 1929, Sayers et al. [B23] at the U.S. Bureau of Mines reported the first substantial animal experiments; they exposed several guinea pigs at each of several concentrations and times. Eleven years later, a group at Dow Chemical (Irish et al. [B24]) exposed rats and rabbits in a well-conducted series of experiments which, however, were published in terms of exposures for 100% deaths or 100% survival, rather than intermediate levels of partial response which would be more useful to us. We have some data from estimated exposures in fatal and nonfatal industrial accidents and some published estimates of human response based on animal experiments, and some further animal data. This information was analyzed in the following way.

All the useful data were tabulated by species (Table B-16) in order

---

[B23] Sayers, R. R., W. P. Yant, B. G. H. Thomas, and L. B. Barger. *Physiological Response Attending Exposure to Vapors of Methyl Bromide, Methyl Chloride, Ethyl Bromide, and Ethyl Chloride.* U.S. Public Health Bulletin No. 185, 56 pp., 1929.

[B24] Irish, D. D., E. M. Adams, H. C. Spencer, and V. K. Rowe. The response attending exposure of laboratory animals to vapors of methyl bromide. *J. Ind. Hyg. Toxicol. 22*(6):218-230, 1940.

of increasing dosage within species. "Useful" data were those including a numerical value for both concentration (C) and time (t), so that a dosage value (Ct) could be assigned. In a few cases, times were estimated from statements such as "a few hours," and these estimates are shown in parentheses. Some of the values for human exposure were estimated by their authors from postaccident investigation and some from animal exposures; there are, of course, no controlled exposures of humans to hazardous dosages. Some of the reports give ranges for concentration or time; we used the midrange as, for example, in recording "30-60 min" as "45 min."

It was immediately apparent that the ordering of data by increasing dosage gave on the whole a rational gradation of effects from negligible to lethal, although there were some anomalies. (Arrangement by increasing concentration gave a disordered array; this was to be expected, since the toxicology of MeBr was much more likely to be dose-dependent than concentration-dependent.) A very rough estimate was possible, for most species, of the dosage fatal to 50% of those exposed ($L(Ct)50$).

Species	$L(Ct)50 (10^3 mg\ min\ m^{-3})$
Man	1,000
Rat	250
Rabbit	750
Guinea pig	400
Mouse	500
Dog	300

It must be emphasized that these figures are not to be viewed as if they were calculated 50% lethal dosages. Their purpose was simply to get an idea of the consistency of the experimental animal data and of their relation to the estimates for man. The animal values are, in fact, a reasonably consistent group. The value for man is higher than that for any of the animals. Since it is based entirely on estimates, unlike the experimental animal data, it seemed prudent to assume a somewhat lower $L(Ct)50$ (higher toxicity) for man. A provisional figure of 500×10^3 mg min m^{-3} was adopted.

The next step was to learn more about the nature of the dose-response relationship; in particular, the slope of the curve. The difficulty here is that the data include very few in the form best suited to our purpose; they are mostly either 100% response or none, or a partial response in nonquantitative terms. Accordingly, we took the following approach, in which we first established that response at hazardous and lethal levels was consistent with Haber's law (constant Ct for a given effect) and then made an estimate of the slope of the dose-response curve.

TABLE B-16. RESPONSE TO INHALATION OF METHYL BROMIDE IN VARIOUS SPECIES

Species	Dosage, Ct, 10^3 mg min m^{-3}	C, 10^3 mg m^{-3}	t, min	Effect	Reference[a]
Man	37	0.078	480	TLV	1
	41	0.195	210	Slight; maximum tolerable in long exposure	2
	47	31.2	1.5	Skin sensation, erythemia, vesication	3
	91	0.378	(240)	Slight	4
	132	17.6	7.5	Narcosis; fatal if more than a few minutes	5
	176	3.9	4.3	Dangerous to life	6
	206	0.429	480	Slight	7
	225	1.073	210	Several hours without serious disturbance	5
	234	3.9	60	Maximum without serious disturbance	2
	351	7.8	45	Dangerous	2
	410	1.95	210	Injurious	5
	527	11.7	45	Dangerous	4
	362	1.17	480	Neurological effects	5
	870	29.0	30	Lethal or serious injury	8
	<1,170	<15.6	75	1 out of 2 dead (using inefficient masks)	5
	2,136	137	4	Survival	5
	<2,746	<31.2	88	1 out of 3 dead	5
	2,808	31.2	90	1 out of 2 dead	5
	>11,200	>31.2	360	Death	5
	50,000	93.2	540	6 out of 8 dead	5
"Animal"	585	117	(5)	Kills most	4
Rat	120	20	6	Survival	9
	150	50	3	Survival	9
	240	2	120	Survival	9
	240	10	24	Survival	9
	300	50	6	Death	9
	420	10	42	Death	9
	480	2	240	Death	9
	480	20	24	Death	9
Rabbit	250	10	25	Survival	10
	475	19	25	Survival	10
	600	10	60	Survival	9
	600	50	12	Survival	9
	720	2	360	Survival	9
	720	20	36	Survival	9
	750	25	30	Death (3 days)	10
	900	36	25	Death (2.5 hours)	10
	1,320	2	660	Death	9
	1,320	10	132	Death	9
	1,500	50	30	Death	9
	1,680	20	84	Death	9
	2,744	98	28	Death	11
Guinea pig	120	0.4	300	None	2
	189	2.1	90	None	2
	211	21.1	10	None	2
	240	0.4	600	None	2
	252	8.4	30	1 out of 4 dead (9 hours)	2
	324	0.6	540	3 out of 4 dead (2-3 days)	2
	324	1.2	270	None (0 out of 4 dead)	2
	360	1.2	300	1 out of 2 dead (3 days)	2
	422	21.1	20	2 out of 2 dead (6 days)	2
	486	0.6	810	None (0 out of 6 dead)	2
	567	2.1	270	4 out of 4 dead (2 days)	2
	581	2.1	279	Slight	4
	648	1.2	540	6 out of 6 dead	2
	748	11	68	Death (several hours)	10
	756	8.4	90	4 out of 4 dead (2-5 hours)	2
	819	27.3	30	Death (1-2 hours)	2
	972	1.2	810	6 out of 6 dead	2
	1,008	2.1	480	6 out of 6 dead (during or soon after exposure	2
	1,200	80	15	Death (15 minutes after exposure)	10
	1,365	273	(5)	Death	4
	1,428	8.4	170	6 out of 6 dead (during exposure)	2
	1,500	25	60	Death (2-5 hours)	10
	2,460	27.3	90	2 out of 2 dead (immediate)	2
	2,574	85.9	30	Cough at 7 minutes; retch at 8 minutes; weak at 30 minutes	4

(continued)

TABLE B-16 (continued). RESPONSE TO INHALATION OF METHYL BROMIDE IN VARIOUS SPECIES

Species	Dosage, Ct, 10^3 mg min m^{-3}	C, 10^3 mg m^{-3}	t, min	Effect	Reference[a]
House	234	5.2	45	Death (10 hours)	12
	539	49	11	Survival	12
	2,100	28	28	Narcosis 35 minutes; death overnight	12
	2,304	1.6	1,440	Death (after 6 hours)	11
	2,375	95	25	Death (after 75 minutes)	11
	3,468	204	17	Narcosis 3 minutes; death 1 hour	12
	4,370	115	38	Light narcosis	11
Dog	210	6	35	Survival	10
	350	10	35	Death (5-6 hours)	10
	570	19	30	Death (3.75 hours)	10
	798	21	38	Death (68 minutes later)	10
	2,100	35	60	Death (80 minutes later)	11
	4,680	52	90	Death (90 minutes later)	11
	7,644	98	78	Death (20 hours)	12
Cat	440	20	22	Survival	12
	951	31.7	30	Survival	12
	1,200	120	10	Survival	12
	1,750	70	25	Death (80 minutes)	12
	4,080	340	12	Survival	12
Porpoise	230	23	10	Death (8 days)	13
	366	61	6	Death (1.75 hours later)	13
	1,220	61	20	Death (1.25 hours later)	13

[a] *References:*

1 ACGIH, 1971
2 Sayers et al., 1929
3 Von Oettingen, 1964
4 McNally, 1937
5 King, 1949
6 Manufacturing Chemists Association, 1968
7 Henderson and Haggard, 1943
8 Deichmann and Gerarde, 1969
9 Irish et al., 1940
10 Beyne and Goett, 1934
11 Flury, 1931
12 Glaser and Frisch, 1929
13 Schwarz, 1928

King [B19] tabulated human tolerance values in two categories: (1) "maximum tolerable limits without injury" and (2) "deterioration, serious injury or death." The dosages in the first group ranged from 41×10^3 mg min m^{-3} to 234×10^3 mg min m^{-3}; in the second, from 351 up to $50{,}000 \times 10^3$ mg min m^{-3}. He drew a chart (Figure B-9 is a simplified version) which indicated a dose-response relation more dependent on concentration than on time (cf. our analysis of carbon tetrachloride in this report), with the transition from tolerable to hazardous exposure occurring in a dosage range of about 100 to 300×10^3 mg min m^{-3} in the middle area of the chart.

We made a trial plotting of selected data for man, dog, guinea pig, rabbit, and rat (this plot is not shown here), which indicated that the data might in fact be consistent with a Haber's law fit (unlike King's estimates for man). The animal $L(Ct)50$ rough estimates, given earlier, show a range of about 250 to 500×10^3 mg min m^{-3}. This band of dosage values fitted quite well with the data on the trial plot and encouraged further analysis along these lines.

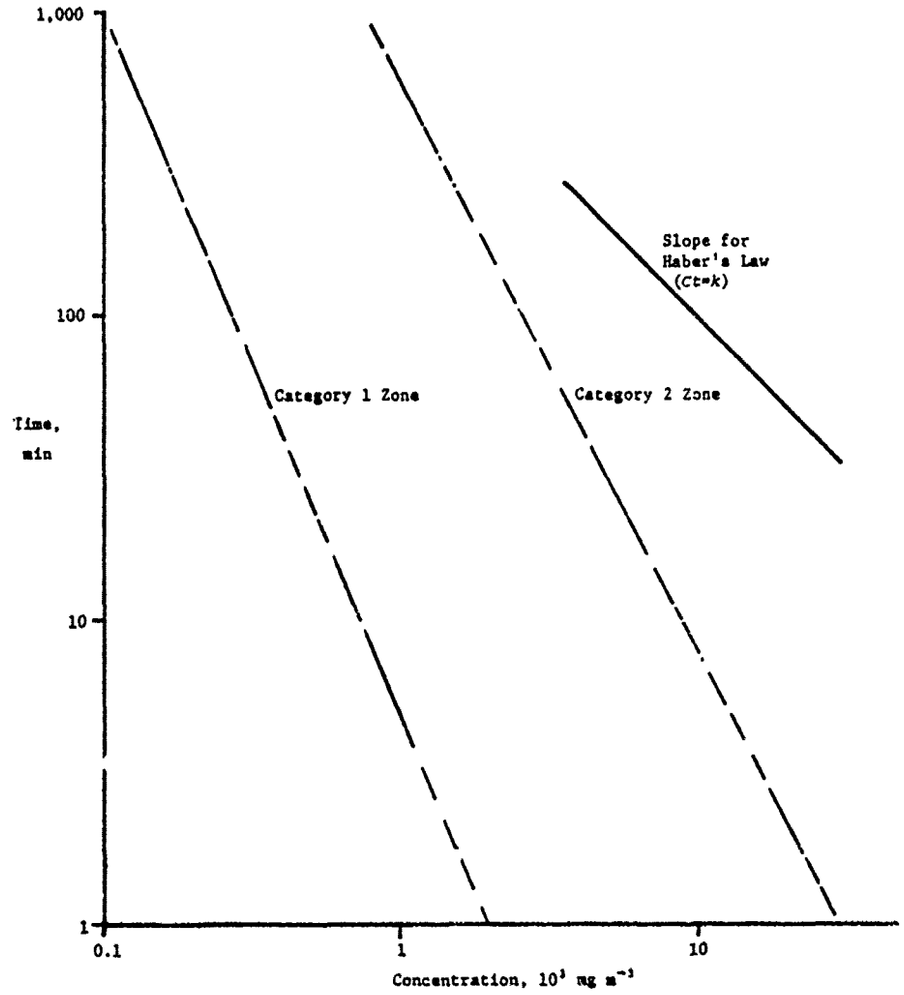

FIGURE B-9. Category of Response Vs. Concentration and Time (simplified from King [B19])

The best and most useful animal data were those of Sayers et al. [B23] and of Irish et al. [B24]. Both groups had arrived at graphs of response on log concentration and log time axes, with straight line demarcation between zones of increasing response. These are shown in Figure B-10, where the zone demarcations are as follows.

Sayers et al. (guinea pig)

1. Demarcation between serious and lethal response
2. Demarcation between not serious and serious

Irish et al. (rat and rabbit, combined)

1. Lower limit for 100% lethality
2. Upper limit for zero lethality

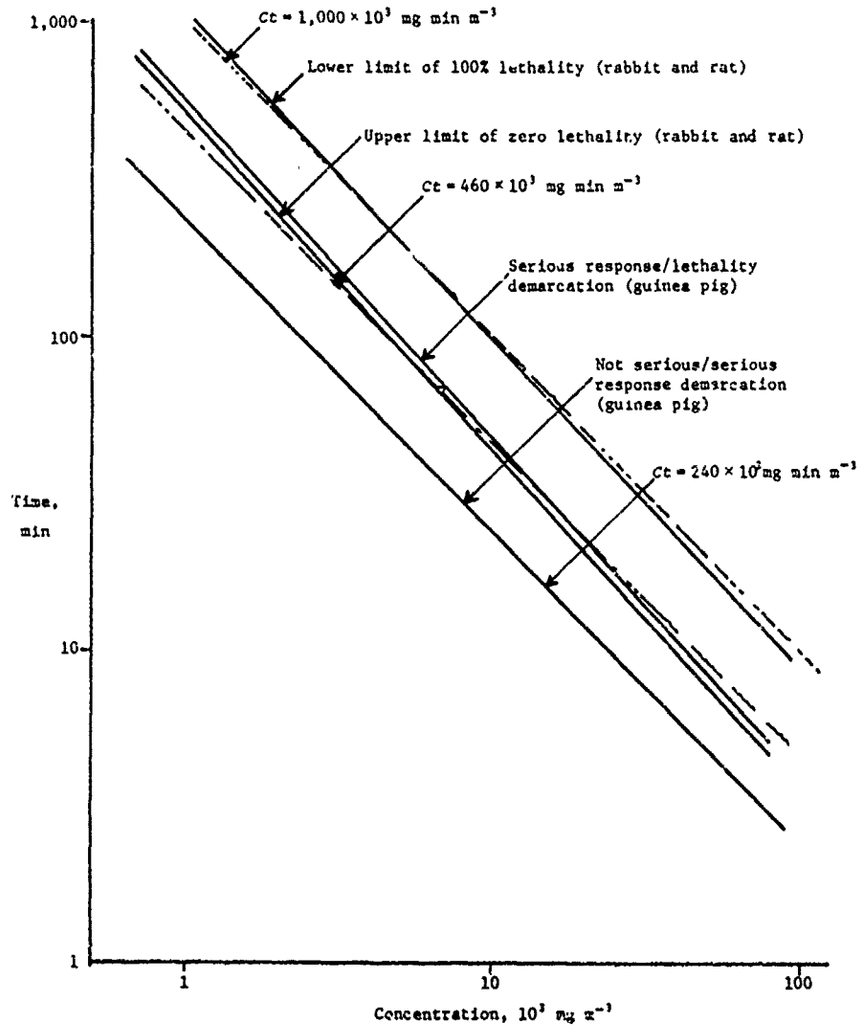

FIGURE B-10. Levels of Response Vs. Concentration and Time (after Sayers et al.[B23] and Irish et al.[B24])

Lines are also given for the following *Ct* values:

$1{,}000 \times 10^3$ mg min m^{-3}
460×10^3 mg min m^{-3}
240×10^3 mg min m^{-3}

It will be seen that the slopes of both the Sayers and the Irish data fit closely with Haber's law, which thus applies to sublethal as well as lethal effects. We are therefore justified in applying the same relationship to man. It is also apparent that the slope of the response is steep; the separation between the upper limit of no deaths and the

lower limit of 100% deaths is only a twofold increase in dose, and the same applies to the separation between no serious effect and lethality.

The difficulty in analyzing the figures is that we have to use responses of 0% and 100%. It is possible by grouping results to get two or three intermediate points of partial response from the Sayers et al. data, but not enough to derive a dose-response curve with any confidence. The way we overcame this difficulty was as follows.

We assigned Ct values to the demarcation lines in Figure B-10:

	10^3 mg min m^{-3}
Guinea pig	
Upper limit of serious response	500
Lower limit of serious response	240
Rat and rabbit	
Lower limit of 100% lethality	1,000
Upper limit of zero lethality	460

The assumption was made that the upper limit of serious response in guinea pigs corresponded to 98% of the animals showing this effect, and the lower limit to 2%. Similarly, the lethality limits were treated as 98% and 2%. These figures were plotted on log/probability paper (see Figure B-11), the purpose being to arrive at an estimate of the dose-response slope. It will be seen that the two lines agreed surprisingly well, in view of their rather dubious basis (which was accepted only for lack of more suitable data to work from).

The $L(Ct)50$ for man of 500×10^3 mg min m^{-3} was plotted and a line drawn through it at the same slope as the others. This intercepted the 2% response level at 340×10^3 mg min m^{-3}. The assumption was made that this dosage corresponded also with 98% incapacitation and a further line was added to Figure B-10, passing through the 50% incapacitation level, $I(Ct)50$, at 240×10^3 mg min m^{-3}.

Using these lines, we arrived at the dose-response figures in Table B-17, in which the various concentration ranges are narrow enough for a single percent value to approximate the response level within each. The responses were taken to apply to normal adults and we added quite arbitrary estimates for the most sensitive sectors of the population, which may include the very young and very old and those with severe preexisting impairment of the lung, liver, kidneys, or central nervous system.

NOTE: It is recognized that the basis for the numbers in Table B-17 is extremely weak. However, we have searched a considerable amount of literature--covering about a half-century and coming from several countries in three languages--without finding any more useful data. Some of the papers, especially the earlier ones, give results for groups of 2 or 3 animals only, which are not adequate; and the majority are even less

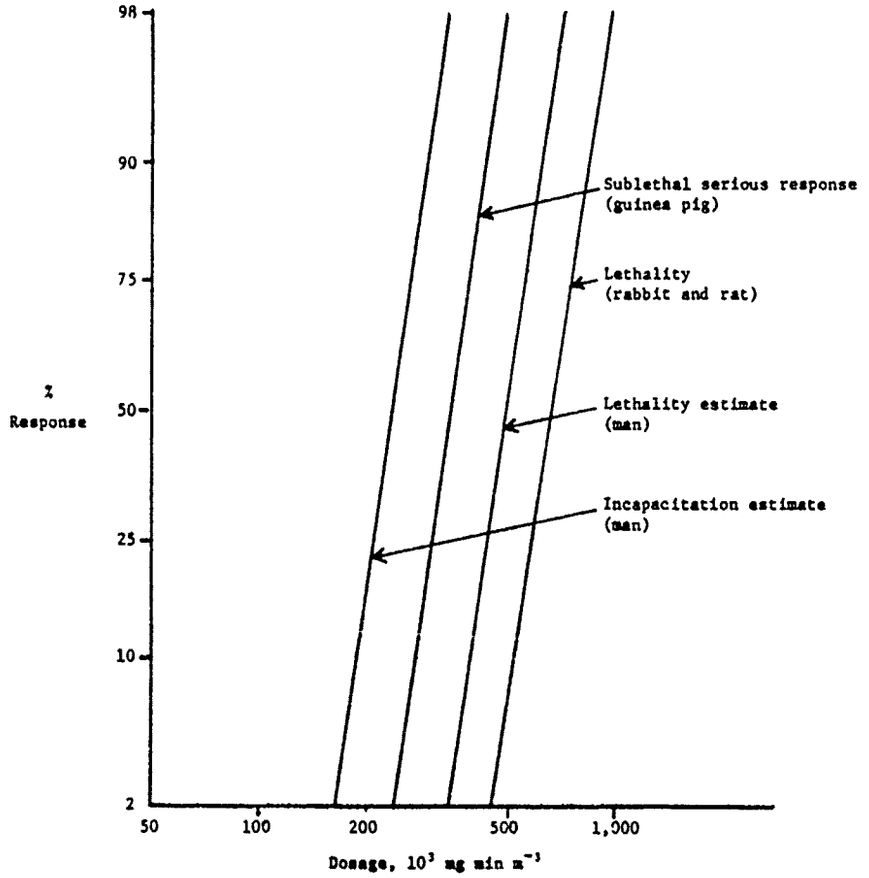

FIGURE B-11. Dose-Response Estimates

TABLE B-17. INHALATION EXPOSURE OF HUMANS TO METHYL BROMIDE: ESTIMATED RESPONSES IN NORMAL AND SENSITIVE SECTORS OF THE POPULATION

Dosage, *Ct*, 10^3 mg min m^{-3}	Lethality		Dosage, *Ct*, 10^3 mg min m^{-3}	Incapacitation	
	Normal	Sensitive		Normal	Sensitive
> 740	100		> 340	100	
740-580	90		340-280	90	
580-430	50	100	280-200	50	100
430-340	10	50	200-160	10	50
340-280	0	25	160-130	0	25
< 280		10	< 130		10

informative about the intermediate levels of partial response which we need for a sounder treatment. So the alternative to the method by which Table B-17 was derived is to make no estimate.

We do, however, feel that the slope of the response curves is reasonably plausible and that the $L(Ct)50$ estimate for man is not likely to be off by a large factor. If we are right, Table B-17 is acceptable for its intended use in the VM (although not necessarily for any other application).

References for Methyl Bromide: Table B-16

1. American Conference of Governmental Industrial Hygienists (ACGIH). *Documentation of Threshold Limit Values for Substances in Workroom Air*, 3rd ed. ACGIH, P.O. Box 1937, Cincinnati, Ohio, 1971.
2. Sayers, R. R., W. P. Yant, B. G. H. Thomas, and L. B. Barger. *Physiological Response Attending Exposure to Vapors of Methyl Bromide, Methyl Chloride, Ethyl Bromide, and Ethyl Chloride.* U.S. Public Health Bulletin No 185, 56 pp., 1929.
3. Von Oettingen, W. F. *The Halogenated Hydrocarbons of Industrial and Toxicological Importance.* Elsevier Publishing Co., Inc., New York, 1964.
4. McNally, W. D. *Toxicology.* Industrial Medicine, Chicago, 1937.
5. King, B. G. High concentration - short time exposures and toxicity. *J. Ind. Hyg. Toxicol. 31*(6):365-375, 1949.
6. Manufacturing Chemists Association. *Methyl Bromide. Safety Data Sheet SD-35.* MCA, 1825 Connecticut Ave., N.W., Washington, D.C., 1968.
7. Henderson, Y., and H. W. Haggard. *Noxious Gases and the Principles of Respiration Influencing Their Action*, 2nd ed. Reinhold Publishing Corp., New York, 1943.
8. Deichmann, W. B., and H. W. Gerarde. *Toxicology of Drugs and Chemicals.* Academic Press, New York, 1969.
9. Irish, D. D., E. M. Adams, H. C. Spencer, and V. K. Rowe. The response attending exposure of laboratory animals to vapors of methyl bromide. *J. Ind. Hyg. Toxicol. 22*(6):218-230, 1940.
10. Beyne and Goett. Toxicité de certains appareils extincteurs d'incendie et précautions qu'ils compartent dans leur emploi. *Arch. Med. Pharm. Nav. 124*:409, 1934.
11. Flury, F., and F. Zernik. *Schädliche Gase.* Springer, Berlin, 1931.
12. Glaser, E., and S. Frisch. Ein Beitrag zur Kenntnis der Wirkung technisch und hygienisch wichtiger Gase und Dämpfe auf der Organismus. Über gebromte Kohlenwasserstoffe der Fettreihe. *Arch. Hyg. 101*:48, 1929.
13. Schwarz, F. Die Brommethyl vergiftung. *Schweiz Z. Unfallmed. 249*: 56, 1928.

PHOSGENE

Phosgene has a boiling point of 8°C and is transported as a liquid under less than 1 atmosphere excess pressure (if at 21°C). The gas is much heavier than air (3.4 times) and this, together with the cooling which accompanies evaporation (latent heat of 59 cal g^{-1}), means that the cloud from a spill has a strong tendency to hug the ground.

It is highly toxic, being lethal at about one-sixteenth of the concentration required for chlorine [B14], and it is much more insidious than chlorine because it is less irritating and has a delayed effect. A fatal dose can be inhaled without serious discomfort; and there are several cases on record where the victim, even under medical care, was released after first aid, only to collapse and die within the next day or two. Phosgene is not severely irritant so that, at concentrations which are in the dangerous zone for prolonged breathing, it passes through the upper respiratory tract with no more than some difficulty in breathing accompanied by slight lacrimation. Higher concentrations cause immediate incapacitating distress, but not to the point of involuntary cessation of respiration as with strong irritants such as hydrogen chloride. The gas which enters the lung is absorbed and reacts slowly with intensely irritant and destructive consequences. There is therefore no strong avoidance reflex to protect the victim and no immediate serious symptoms to warn that a hazardous dose has been taken. After some time, 2 to 24 hours, pulmonary edema develops and the victim, as is often said, drowns in his own body fluid. If this does not occur, there is still a grave risk of pneumonia because the damaged lung tissue's defenses against invasive pathogens are seriously impaired.

Phosgene was introduced as a war gas in World War I in December of 1915, and it displaced chlorine as the preferred lethal agent. Prentiss [B2] reports details of 28 attacks (by both sides), and we have analyzed his figures. They show a total of 13,183 casualties, with 2,454 dead (19%); the range of percent dead in 25 of the cases is from 6% to 46%. It will be understood that these figures are unlikely to be very accurate and that the conditions were different from those likely in a VM incident. For example, gas masks were developed and the amount of gas expended per casualty rose considerably from 1915 to 1918; however, the mortality ratio did not show any trend. So these figures give us an idea of the casualty rate and the proportion of fatalities for large releases in favorable meteorological conditions (which were selected for the attacks and which could occur by chance during a spill).

First aid naturally starts with removal to clean air. Emphasis is placed by many authorities on minimizing activity, so that the patient must be carried and not allowed to walk, even if he feels fit to do so. However, others believe that the risk of dangerous respiratory stress is exaggerated. Oxygen is the principal treatment (to offset impaired uptake in the damaged lung) and supplementary oxygen is recommended if

artificial respiration is required. Treatment and close medical surveillance must be continued for 24 hours, because of the latent period before onset of detectable edema.

A selection of exposure levels and corresponding effects, observed or estimated for man, is given in Table B-18. We have also compiled and reviewed a considerable amount of animal data, but we have not used them except where we have no choice in estimating dangerous and lethal exposures for man. The animal data generally substantiate the dose-response figures of Table B-18.

TABLE B-18. EFFECTS OF PHOSGENE EXPOSURE IN MAN

Concentration mg m^{-3}	Concentration ppm	Time	Dosage mg min m^{-3}	Effect	Reference[a]
0.4	0.1	—	—	Threshold Limit Value for workroom exposure	1
2	0.5	—	—	Recognizable odor	2
4	1	—	—	Readily noticed	2
4	1	—	—	Maximum allowable concentration	3
4	1	0.5-1 hr	180	Endurable	4
8	2	—	—	Strong odor	2
10	2.5	—	—	Throat irritation	4
5-10	1.25-2.5	Long	—	Dangerous	2
12	3	Immediate	—	Minimum for throat irritation	3
12-20	3.5	—	—	Irritation of eyes and throat	5
15	3.75	—	—	Lacrimation	4
16	4	Immediate	—	Eye irritation	3
19	4.75	Immediate	—	Cough	3
20	5	1 min	20	Cough	2
20	5	30 min	600	Probably fatal (questionable)	6
20	5	50 min	1,000	May be fatal	7
22	5.5	Immediate	—	Detection of odor (questionably high concentration)	3
40	10	Few (5) sec	(200)	Incapacitation by lacrimation and respiratory irritation	8
40	10	Few (5) sec	(200)	Fighting efficiency diminished	7
40	10	<1 min (45 sec)	(30)	Eye and respiratory irritation (questionably nigh)	2
40	10	1 min	40	Serious irritation of lower respiratory tract	9
40	10	25 min	1,000	May be fatal	7
50	12.5	0.5-1 hr	2,250	Dangerous	2
80	20	1-2 hr	7,200	Serious lung injury (effect probably understated)	2
80	20	>1-2 min	>160	Definite bronchial and pulmonary lesions	8
80	20	2 min	160	May damage lung	9
100	25	30 min	3,000	Very dangerous	9
100	25	0.5-1 hr	4,500	Dangerous	4
100	25	0.5-1 hr	4,500	Dangerous	3
100	25	0.5-1 hr	4,500	Very dangerous	5
132	33	—	—	Very dangerous	6
160	40	1 hr	960	Highly toxic	7
200	50	5-10 min	1,500	Fatal	4
200	50	Short	—	Rapidly fatal	3
200	50	Short	—	May be fatal	9
200	50	Short	—	Rapidly fatal	5
>200	>50	—	—	May be fatal	9
360	90	<30 min	<10,800	Rapidly fatal	2
500	125	10 min	5,000	Lethal	6
668	167	2 min	1,336	May injure	6
1,000	250	—	—	Casualties certain, fatal if > few minutes	8

[a] *References:*

1 ACGIH, 1971
2 Patty, 1962
3 Henderson and Haggard, 1943
4 McNally, 1937
5 Sax, 1968
6 Jacobs, 1967
7 Wachtel, 1941
8 Vedder, 1925
9 Braker and Mossman; 1970, 1971

Table B-18 Notes: Wachtel [B25] gives $L(Ct)$ (percentage not specified) of 1,000 mg min m^{-3}. Rothschild [B26] gives MLD (median lethal dosage) of 3,200 mg min m^{-3} and MID (median incapacitating dosage) of 1,600 mg min m^{-3}. These were the standard figures used by the Americans and British in World War II. In the table, estimates have been made of a reference's meaning intended by "few sec" and "<1 min" and the resulting dosages are shown in parentheses.

It will be seen that there is fair agreement among the authorities; some egregious estimates of effect are commented on parenthetically in Table B-18. It will also be seen that the effects, especially at higher dosage levels, are generally more in proportion to the dosage than to the concentration level. Table B-18 may be summarized as follows.

Dosage, mg min m^{-3}	*Concentration mg m^{-3}*	*Effect*
20-40	up to 40	Cough, serious eye and respiratory irritation
--	40	Incapacitating concentration
100-160+	up to 80	Cough, respiratory injury
200	40	Incapacitation
960-1500	up to 200	Highly toxic to fatal
1600	--	Median incapacitating dosage (MID)
2250-4500	up to 100	Dangerous to fatal
3200	--	Median lethal dosage (MLD)

There is a considerable amount of laboratory evidence from experimental animals, on which we have drawn to estimate dose-response relationships for man. It may be noted that the estimated slope of the dose-response in man is more likely to be correct than the absolute value of the estimated $L(Ct)50$ (or any other level of lethality). The reason is that the slope generally reflects the type of toxicological mechanism: simple and specific effects giving a steep slope, and complex, multiple-cause toxicity given a less steep slope [B27]. The toxic mechanism for phosgene is probably very similar in man and other mammals.

[B25] Wachtel, C. S., *Chemical Warfare*, Chemical Publishing Co., Inc., Brooklyn, N.Y., 1941.

[B26] Rothschild, J. H., *Tomorrow's Weapons*, McGraw-Hill Book Co., New York, Toronto and London, 1964.

[B27] Casarett, L. J., and J. Doull (eds.), *Toxicology - The Basic Science of Poisons*, Macmillan, New York, 1975.

On the other hand, estimates of lethal exposure levels for man depend on unverified assumptions such as, for example, equality of lethal dose in mg/kg of body weight for man and goat.

Boyland et al. [B28] give data for mice, rats, and guinea pigs exposed for times increasing twofold from one-fourth of a minute to 64 minutes. They found a marked increase in the dosage required for lethality at the shorter times, especially below about 2 minutes; the explanation apparently being breath holding, which would be more marked at the high concentrations necessary to establish a lethal dose in these short exposures, and which would have a proportionately larger effect in reducing intake during short exposures. We have, therefore, rejected their results at the 1/4-, 1/2-, and 1-min times which are, in any case, shorter than we would consider typical of exposure in a VM incident. We have also rejected the results at 16, 32, and 64 min, not so much because these times might be atypical for the VM but rather to use results from a region of reasonably similar $L(Ct)50$s in exposures for 2, 4, and 8 min. We were left with 13 to 15 groups of animals (totaling 4 to 40 in each) for each species, with various dosages and mortalities, which give the dose-response lines shown in Figure B-12.

Karel and Weston [B29] give data for 28 goats exposed to various dosages of phosgene at a concentration of approximately 2 mg per liter, of which 7 survived, and for 30 goats exposed at approximately 10 mg per liter, of which 12 survived. We have grouped the results into four dosage ranges, each including 6 or 7 animals, for each of the two concentration levels, and have plotted the dose-response graphs as shown in Figure B-12.

It will be seen that the slopes of all the dose-responses agree very tolerably except for the "10-mg" goats, which we chose arbitrarily to reject. Taking the widely accepted estimates of 3,200 mg min m^{-3} as the $L(Ct)50$ or 50% lethal dosage for man, and 1,600 mg min m^{-3} as the $I(Ct)50$ or 50% incapacitation dosage, we have drawn lines through these points at the same slope as the average of the four animal series to arrive at our best estimate of dose-response for man. The graphs yield the following estimates.

	Dosage, mg min m^{-3}	
% Response	*Lethality*	*Protracted Incapacitation*
85	4,400	2,200
50	3,200	1,600
15	2,200	1,150

[B28] Boyland, E., F. F. McDonald, and M. J. Rumens, Inhalation toxicity of phosgene for small animals, *Br. J. Pharmacol. 1*:81, 1946.

[B29] Karel, L., and R. E. Weston. Biological assay of inhaled substances, *J. Ind. Hyg. Toxicol. 29*:23, 1947.

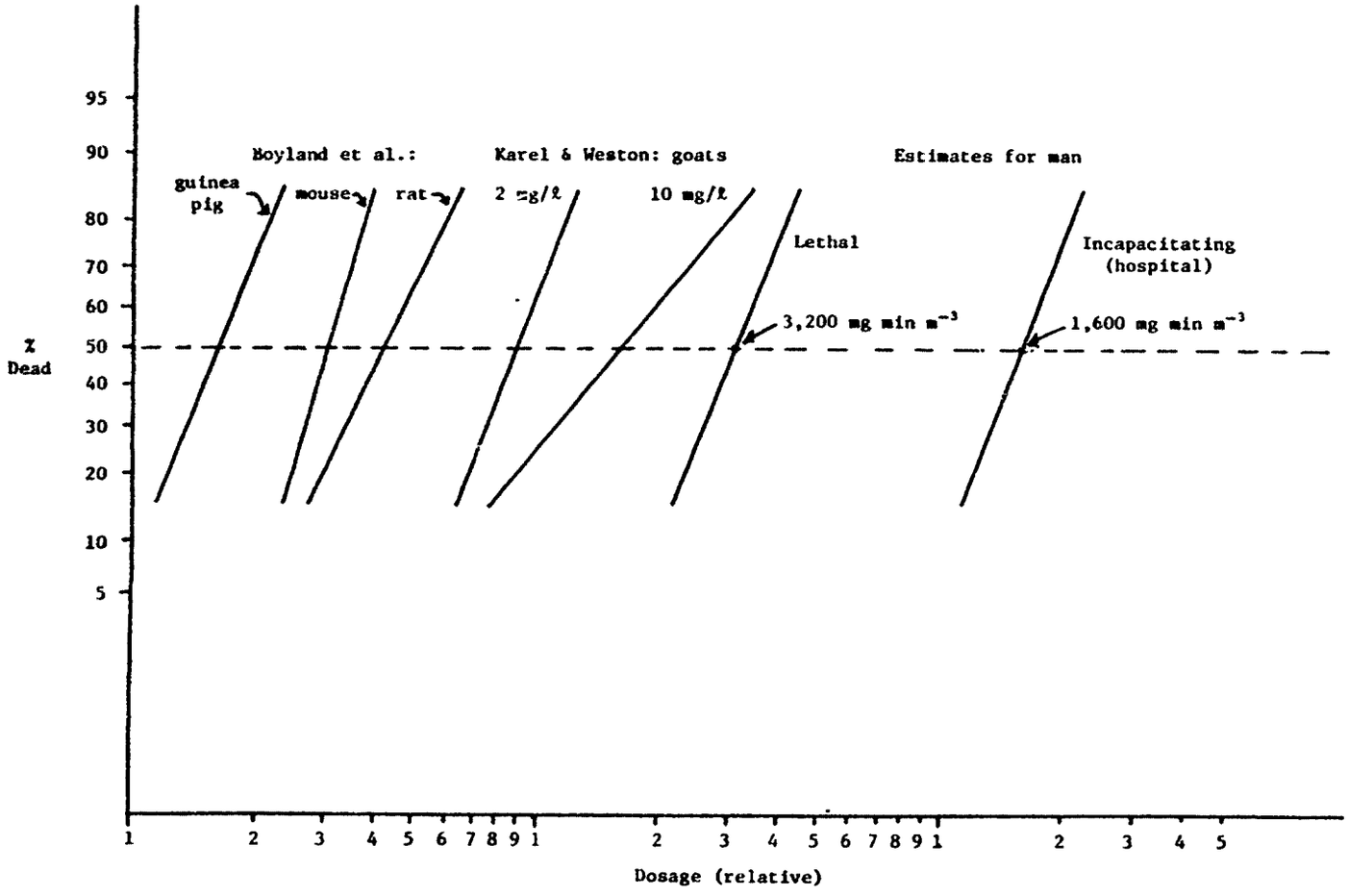

FIGURE B-12. Dose-Response to Phosgene

Incapacitation is used here in the military sense of being out of action for a substantial time after exposure (in the VM context, being hospitalized for a week or more), rather than with reference to temporary incapacitation during and briefly after exposure. Temporary incapacitation is the result of immediate irritation, with lacrimation, throat irritation, cough, etc. Protracted incapacitation is the result of deep-lung tissue damage which is slow to heal.

The question of long-term effects requires careful consideration. Opinions are divided about this. Macnamara [B30] says that, if the patient survives beyond 48 hours, the pulmonary edema resorbs and recovery is complete. Sax [B9] says that no permanent residual disability is thought to occur. Jacobs [B31], however, says that coughing with bloody sputum and weakness may last for months; this is not inconsistent with the previous opinions but puts the matter in a less favorable light. Vedder [B32] and Prentiss [B2] both conclude against permanent disability on the basis of World War I and postwar observations. It may not be unfair to point out that most of those opining against permanent disability must have had a background of unavoidable and frequent defensiveness about chemical warfare; and a similar possibility of bias is seen in the British Ministry of Pensions maintaining (after World War I) that serious structural aftereffects did not occur, provided the lungs were healthy before gassing. This British opinion is quoted by Galdston et al. [B33] in a study of residual effects after acute exposure; on the other side, they note that numerous reports in the French and American literature present evidence of residual lung damage in phosgene casualties: chronic bronchitis, pulmonary emphysema, obliterative bronchiolitis, peribronchiolitis, bronchiectasis and suppuration of the lungs. (It is to be remembered, however, that these conditions are all common in non-gassed subjects and that the causal relation with gassing is therefore not easy to prove.)

The Galdston et al. paper is an important one, although the evidence is limited to six volunteers who had previously been exposed and developed symptoms of acute poisoning. Galdston et al. note that during World War I the British Chemical Warfare Medical Committee recognized a syndrome which resembled the "Irritable Heart" or "Effort Syndrome."

[B30] Macnamara, B. J., Edgewood Arsenal Technical Report, 1961.

[B31] Jacobs, M. B., *The Analytical Toxicology of Industrial Inorganic Poisons*, John Wiley & Sons, New York, 1967.

[B32] Vedder, E. G., *The Medical Aspects of Chemical Warfare*, Williams and Wilkins Co., Baltimore, Md., 1925.

[B33] Galdston, M., J. A. Luetscher, Jr., W. T. Longcope, and N. L. Ballich. A study of the residual effects or phosgene poisoning in human subjects. I. After acute exposure, *J. Clin. Invest. 26*: 145-168, 1947.

Haldane and his co-workers observed that rapid, shallow breathing was a conspicuous feature, but there was scant evidence of structural disease of the lungs. (There is a reflex--the Hering-Breuer reflex--which regulates the excursions of the respiratory cycle. If this reflex is exaggerated under gassing--i.e., shallow breathing--blood oxygen deficiency produces a general nervous upset which may perpetuate the exaggerated reflex and the accompanying anoxemia.) Galdston et al. observed that this breathing pattern was the most striking feature of their studies. They recorded clinical abnormalities in all six subjects, at 3 to 14 months after exposure. An important feature was the correlation of psychiatric abnormalities with the severity of symptoms, and they remark that "Although compensation was rarely mentioned, the potential financial and psychological gains of invalidism loomed large to the insecure patients."

It appears that there may be a significant proportion of long-term or permanent disabilities, even though the clinical (or postmortem) evidence to validate disability may be lacking. However, there is no way that we can see to treat this on any sort of quantitative basis. One imponderable is outcome of any arbitration between patient's subjective feelings and expert clinician's judgment. The etiology of chronic respiratory disease in aging persons is another difficult area.

We have also to consider the problem of high-risk sectors of the population. There is no quantitative evidence but it will be obvious that those whose respiratory or cardiovascular functions are already impaired, so that they are at the brink of serious or catastrophic cellular oxygen deficiency (especially in the cerebral cortex or heart muscle), are likely to show a much higher casualty rate than normally healthy adults.

The exposure ranges and accompanying effects that we propose for present use are discussed below. It is emphasized that, with the exception of the lowest exposures--which are based on adequate volunteer experiments--all the values are highly judgmental and must be regarded as no better than well-informed guesstimates.

Boyland et al. [B28] found that Haber's law, $L(Ct)50 = k$, held reasonably well for longer exposures of their small experimental animals, but not for short exposures. They introduced a concentration baseline correction and a time constant, the modified expression being:

$$\frac{L(Ct)50 - C_0 t}{1 + t_0/t}$$

The t_0 may be regarded as a species constant connected with breath holding at the onset of exposure. The C_0 implies that this concentration would be fatal only at infinite time and that lower concentrations would be nonfatal. Unadjusted and adjusted $L(Ct)50$s are shown in Table B-19, together with the appropriate constants.

TABLE B-19. LETHALITY: HABER'S LAW (H) AND HABER'S LAW MODIFIED (H_{mod})

Exposure Time, min		Rat		Mouse		Guinea Pig	
	C_0, mg m^{-3}		10		0		20
	t_0, min		4		1.6		0.8
		H	H_{mod}	H	H_{mod}	H	H_{mod}
1/4		39,000	2,300	15,000	2,020	5,500	1,310
1/2		18,000	2,000	10,000	2,380	3,000	1,130
1		14,000	2,800	5,400	2,080	2,000	1,190
2		7,000	2,320	3,400	1,900	1,800	1,260
4		4,000	1,980	3,000	2,140	1,500	1,180
8		3,000	1,950	2,500	2,080	1,400	1,130
16		2,400	1,740	2,200	2,000	1,660	1,270
32		2,200	1,670	2,000	1,900	1,700	1,090
64		2,800	2,040	1,900	1,850	2,900	1,570

From Boyland et al. [B28].

We could possibly estimate a C_0 value for man but the t_0 constant, which has such a large effect in short exposures, is of course unavailable. It is considered justifiable to assume that VM exposures will generally be not less than a few minutes and that the unmodified Haber's law is applicable. This is for the lethal or incapacitating effect of phosgene brought about by damage to the gas-exchange region of the lung, which might reasonably be expected to be proportional to dosage (Ct) except at very low concentration/long time when there would be opportunity for continuous dissipation of the irritant. We have also to consider concentration alone for irritant effects on the eyes and upper respiratory tract (without regard for time of exposure, except that this must be long enough to set up the physiological response and not so long as to become hazardous). The following provisional dose-response estimates represent our best judgment at the present time.

Harassment zone: concentration-dependent rather than dosage-dependent, but time cannot be ignored; a few minutes are required to build up effect, especially at the lower concentrations, and long exposures may be hazardous, especially at the upper end of the concentration range.

Effect	*Time*	*Normal Population* C, mg m^{-3}	*High-Risk Population* C, mg m^{-3}
Negligible	Up to 1 hr	0 - 4	0 - 2
Complaint but no serious risk	Few min to 1 hr	4 - 10	2 - 5
Severe harassment: temporary incapacitation	Up to 15 min	10 - 20	5 - 10

Temporary incapacitation means inability to continue normal activities because of lacrimation, coughing, and respiratory discomfort.

Dangerous-to-lethal zone: dosage-dependent; incapacitation is protracted, from a week or so to several months.

Dosage, mg min m^{-3}	*Normal Population, %* *Incapacitated*	*Dead*	*High-Risk Population, %* *Incapacitated*	*Dead*
800			15	
1,150	15	--	50	--
1,600	50	--	85	15
2,200	85	15	50	50
3,200	50	50	--	90-100
4,400	--	90-100		

This is for exposure times from a few minutes to one hour; the dose for a given effect would be expected to increase both below that time range (because of breath holding) and above it (because of detoxification). The high-risk responses have been derived from the normal responses by assuming that 15% normal corresponds to 50% high risk and that the slope is the same.

References for Phosgene: Table B-18

1. American Conference of Governmental Industrial Hygienists (ACGIH). *Documentation of Threshold Limit Values for Substances in Workroom Air*, 3rd ed. ACGIH, P.O. Box 1937, Cincinnati, Ohio, 1971.
2. Patty, F. A. (ed.). *Industrial Hygiene and Toxicology*. Interscience Publishers, New York, 1962.
3. Henderson, Y., and H. W. Haggard. *Noxious Gases and the Principles of Respiration Influencing Their Action*, 2nd ed. Reinhold Publishing Corp., New York, 1943.

4. McNally, W. D. *Toxicology*. Industrial Medicine, Chicago, 1937.

5. Sax, N. I. *Dangerous Properties of Industrial Materials*, 3rd ed. Van Nostrand Reinhold Co., New York, 1967.

6. Jacobs, M. B. *The Analytical Toxicology of Industrial Inorganic Poisons*. John Wiley & Sons, New York, 1967.

7. Wachtel, C. S. *Chemical Warfare*. Chemical Publishing Co., Inc., Brooklyn, N.Y., 1941.

8. Vedder, E. G. *The Medical Aspects of Chemical Warfare*. Williams and Wilkins Co., Baltimore, Md., 1925.

9. Braker, W., and A. L. Mossman. *Effects of Exposure to Toxic Gases - First Aid and Medical Treatment*. Matheson Gas Products, East Rutherford, N.J., 1970. And *Matheson Gas Data Book*, 5th ed. Matheson Gas Products, East Rutherford, N.J., 1971.

Appendix C

ASSESSMENT METHOD FOR DAMAGE-PRODUCING FACTORS VARYING IN TIME

INTRODUCTION

For many of the damage mechanisms considered in the VM, the degree of damage inflicted on the exposed vulnerable resources depends not only on the level of a causative variable existing in the environment, but also on the time-history of that variable. Among the damage mechanisms in this category are:

- lethal burns from thermal radiation,
- ignition of structures by thermal radiation,
- death from exposure to asphyxiating gases, and
- death and injury from inhalation of toxic gases.

For example, death from inhalation of chlorine depends not only upon the peak concentration achieved as the cloud passes over the subject population, but also upon passage time of the cloud and the resulting time-history of concentration.

Because the damage-causing phenomena inherently involve time as a significant causative variable, the damage assessment methods developed for use in the VM quantitatively estimate the degree of damage as a function of both causative variable level and time. However, the assessment methods determine the expected degree of damage for a *constant* level of causative variable experienced for a given length of time, although the hazard environments predicted in Phase I of the VM are, in general, characterized by *changing* levels of causative variables. The algorithm developed here is a general method that may be applied to various damage-producing mechanisms, so that laboratory results for constant levels of causative variables may be used to predict vulnerable resource response to the time-varying damage environments simulated in the VM. Among the advantageous characteristics of this algorithm are that:

- It is readily computerized.
- It reduces to the original data for constant level exposures.
- It partially accounts for the nonlinear behavior of the damage mechanisms.

A more accurate algorithm would obtain the response to time-varying damage environments by an analysis based on first principles of physics, engineering, chemistry, and/or physiology. However, the physical science analyses are apt to be very complex and difficult and the required physiological principles unknown or incomplete. Thus the approach derived here was deemed to be most suitable at this time, since the

deeper approach would be out of step with the developmental philosophy and cost for the VM and since this approach does incorporate, to some degree, the nonlinear behavior of the damage mechanisms.

STATEMENT OF THE PROBLEM

In assessing damage in the VM, the response of the vulnerable resource may be digital, i.e., injury either occurs or does not occur. Examples of such damage mechanisms include: (a) ignition of materials, (b) production of first-degree burns in people, and (c) asphyxiation mortality. In all of these cases, the production of damage depends upon: (1) exceeding a certain theshold value of environmental factor (e.g., thermal radiation must be above so many cal/cm^2 s, or asphyxiant concentration must exceed 50%) and (2) maintaining the elevated level of environmental factor for at least the critical time, t_c, which in general depends upon the level of environmental factor. This is stated more clearly graphically, as shown below.

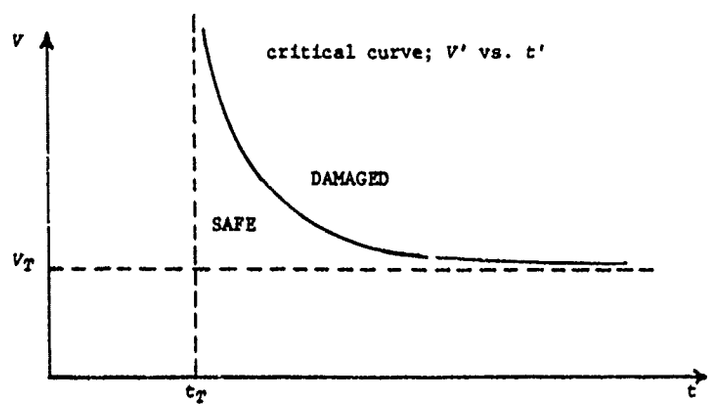

The critical curve is defined as follows. For each value of the environmental variable, V' (e.g., concentration or radiation intensity), there is a value of time, t', such that the vulnerable resource is damaged if it is exposed to the level V' for a time equal to or greater than t'. For most damage mechanisms, a threshold value, V_T, must be exceeded or no damage will be possible. For some damage mechanisms, notably asphyxiation, the duration of exposure must exceed the time, t_T, regardless of the level of the variable, V, or no damage will result. For all the damage mechanisms of this type considered so far in the VM, the duration required, t', decreases as the environmental factor, V', is increased.

The curve of V' vs. t' is generated from data from experiments in which the vulnerable resource (or an animal model in the case of human response) is exposed to a constant level of environmental factor, V', and the corresponding time, t', of critical response (e.g., ignition or death) is determined. In general, the critical curve can be described by an equation of the form:

$$(V' - V_T)^n \ (t' - t_T) = K \qquad \text{(C-1)}$$

where n and K are fitted constants.

The problem that repeatedly arises in the VM is that vulnerable resources are exposed not to a constant level of environmental factor, V, but to a time-varying level, and it is the response to the time-varying level that must be determined.

For illustrative purposes, consider the following numerical example. Suppose the data defining the V' vs. t' curve are as given in Table C-1 and as graphed in Figure C-1. These data are described by the equation

$$(V' - 1)^2 \ t' = 100 \qquad \text{(C-2)}$$

i.e., using the notation of equation (C-1), $t_T = 0$, $V_T = 1$, and $n = 2$.

TABLE C-1. CRITICAL CURVE: NUMERICAL EXAMPLE

V'	t' (sec)
2	100.00
3	25.00
4	11.11
5	6.25
6	4.00
7	2.78

Now suppose that a vulnerable resource experiences an environment in which V is not constant but is time-varying. Suppose, for example,

$V = 0$ $\quad t < 0$
$V = 5$ $\quad 0 \leqslant t < 5$ sec
$V = 4$ $\quad 5$ sec $\leqslant t < 10$ sec
$V = 0$ $\quad 10$ sec $\leqslant t$

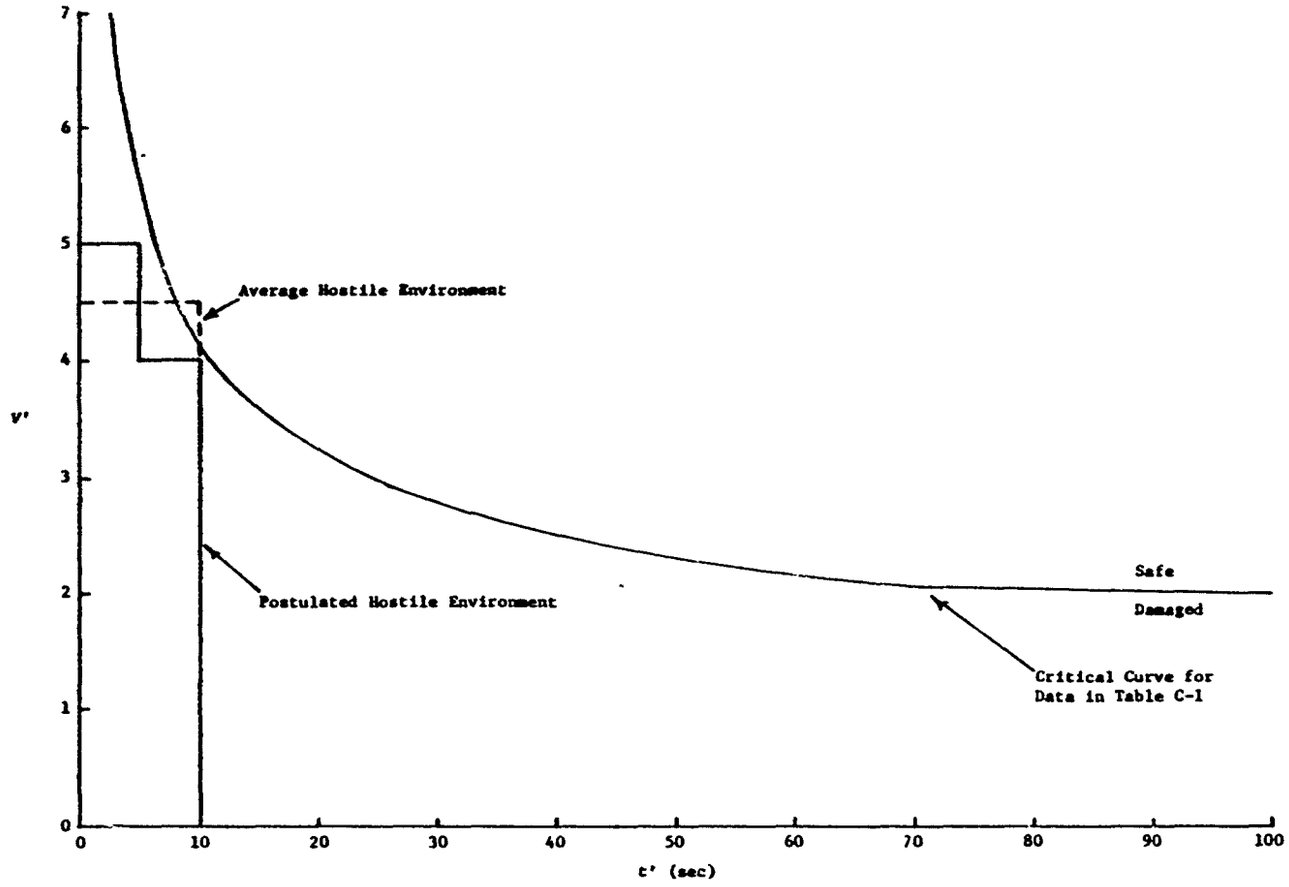

FIGURE C-1. Example of Critical Curve of Vulnerability and Postulated Hostile Environment (such that no single level of causative variable exceeds the damage criteria, but where the combined effects of several levels would appear to cause damage)

As a first test to determine whether damage would be produced by this postulated environment, we can examine the duration of each level of the causative variable. Since V is greater than or equal to 5 for only 5 sec, which is less than the required 6.25 sec, it cannot be deduced that damage will result. Also, since V is greater than or equal to 4 for only 10 sec rather than the required 11.11 sec, it cannot be deduced that damage will result. But such reasoning considers only components of the exposure, rather than the entire exposure history. It seems reasonable that the combined exposures at levels 4 and 5 might result in damage, even though the exposure at each level fails to satisfy the criterion.

To pursue this line of reasoning, consider the simple arithmetic (i.e., time-weighted) average exposure. Thus,

$$\overline{V} = \frac{\sum_{i=1}^{n} V_i \Delta t_i}{\sum_{i=1}^{n} \Delta t_i} \qquad \text{(C-3)}$$

where V_i are the various levels of exposure, and Δt_i are the duration of exposure at each level.

For this numerical example, we have

$$\overline{V} = \frac{(5)(5) + (4)(5)}{(5 + 5)} = \frac{45}{10} = 4.5$$

Inserting the value $\overline{V}$ for V' into equation (C-2) and solving for t' (the time duration required to cause damage for the average value of causative variable) yields

$$t' = \frac{100}{(V' - 1)^2} = 8.16 \text{ sec}$$

Since the average exposure level $\overline{V}$ persists for 10 sec, we might conclude from this approach that damage does indeed occur (see Figure C-1). Heuristically, this appears to be the correct result; damage should occur. However, the method of computation leaves something to be desired.

DERIVATION OF THE ALGORITHM

The average level defined by equation (C-3) is based on simple linear weighting. It would be more satisfying to have an averaging method that more directly reflects the nonlinear behavior of the phenomena, as exhibited explicitly in equation (C-1) via the exponent n. To

obtain such a method, let us restate the linear averaging method in a slightly different form; then we will generalize to the nonlinear case. Consider equation (C-2) and a constant exposure level, V^*, with a duration, t^*. Let us compute

$$q = (V^* - 1)^2 \, t^* \tag{C-4}$$

If $q \geq 100$, then damage occurs; if $q < 100$, then the vulnerable resource is safe. This is equivalent to calculating the critical time, t', corresponding to V^* and then comparing t' to t^*. For the linear average exposure level $\overline{V}$ and duration of the preceding example, we find from equation (C-4) that

$$q = (\overline{V} - 1)^2 \, \overline{t} = (4.5 - 1)^2 \, 10 \text{ sec} = 122.5$$

where $\overline{t}$ is duration of the average level $\overline{V}$. Since $q = 122.5 > 100$, we conclude, as before, that damage does indeed occur. Now in equation (C-1), if n were unity, the defining equation for q equivalent to (C-4) would be

$$q = (V^* - V_T) \, t^* \tag{C-5}$$

assuming, as before, that $t_T \equiv 0$.

Now consider the quantity

$$\overline{q} = \sum_{i=1}^{n} (V_i - V_T) \, \Delta t_i \tag{C-6}$$

which becomes

$$\begin{aligned} \overline{q} &= \sum_{i=1}^{n} V_i \, \Delta t_i - \sum_{i=1}^{n} V_T \, \Delta t_i \\ &= \sum_{i=1}^{n} V_i \, \Delta t_i - V_T \sum_{i=1}^{n} \Delta t_i \\ &= \sum_{i=1}^{n} V_i \, \Delta t_i - V_T \, \overline{t} \end{aligned} \tag{C-7}$$

And, from equation (C-3),

$$\overline{V} = \frac{\sum_{i=1}^{n} V_i \, \Delta t_i}{\sum_{i=1}^{n} \Delta t_i} = \frac{\sum_{i=1}^{n} V_i \, \Delta t_i}{\overline{t}}$$

hence,

$$\overline{V}\,\overline{t} = \sum_{i=1}^{n} V_i \Delta t_i$$

and substituting in equation (C-7) yields

$$\overline{\mathcal{F}} = \overline{V}\,\overline{t} - V_T\,\overline{t} = (\overline{V} - V_T)\,\overline{t} \qquad \text{(C-8)}$$

Thus we see that, in the linear case, the computation indicated by (C-6) is equivalent to substituting $\overline{V}$ and $\overline{t}$ into equation (C-5). The advantage of equation (C-6) is that it is more readily computed at each time step of the simulation and is computationally simpler than finding $\overline{V}$ and $\overline{t}$ and substituting these into equation (C-5). Futhermore, during a VM simulation, damage as a function of time will be computed, rather than just total damage at the end of the simulation.

For the nonlinear case, the analogue to equation (C-5) is

$$q = (V^* - V_T)^n\, t^* \qquad \text{(C-9)}$$

and, as discussed above, comparing q to the critical value q' is equivalent to computing the critical time t' for an exposure level V^* and comparing it to t^*. Extending these ideas to the nonlinear case gives the following as the analogue to (C-6):

$$\hat{q} = \sum_{i=1}^{n} (V_i - V_T)^n \Delta t_i \qquad \text{(C-10)}$$

It is suggested that this form be used to estimate damage by comparing $\hat{q}$ to the critical value q'. To examine how this might work, consider the previous numerical example. We have

$$\hat{q} = (5 - 1)^2\, 5 + (4 - 1)^2\, 5 = 80 + 45 = 125$$

Since $q' = 100$, we would conclude that damage does occur since $\hat{q} > q'$. Notice that $\hat{q}$ computed from equation (C-10) is slightly higher than $\hat{q} = 122.5$ computed by substituting $\overline{V}$ into equation (C-4). This appears to be desirable since it means that the higher exposure levels "count for more" in the algorithm expressed by equation (C-10) than those do for linear averaging. Since equation (C-10) is simpler computationally and more descriptive of the nonlinear phenomena considered, it will be adopted as the numerical algorithm for time-varying exposures. In the event that t_T is not identically zero as has been assumed in the above, $\hat{q}$ may be defined as follows:

$$\hat{q} = \sum_{i=1}^{n} (V_i - V_T)^n \, \Delta t_i - t_T \frac{\sum_{i=1}^{n} (V_i - V_T)^n \, \Delta t_i}{\sum_{i=1}^{n} \Delta t_i}$$

or as

$$\hat{q} = \left(1 - \frac{t_T}{t_d}\right) \sum_{i=1}^{n} (V_i - V_T)^n \, \Delta t_i \qquad \text{(C-11)}$$

where t_d is the total time for which $V_i > V_T$; i.e.,

$$t_d = \sum_{i=1}^{n} \Delta t_i$$

A FINAL EXAMPLE

As an example of how this algorithm would be used, let us consider the asphyxiation mortality data presented in Appendix B and shown below.

Concentration (%)	*Time to Death* (min)
100	5
85	5.75
80	6
75	6.5
70	8
65	10
60	13
50	∞

These data were described by a curve of the form:

$$911.9 = (C - 50\%)^{1.979} \; (t - 5 \text{ min})$$

In the terminology used previously in this appendix,

$$V \equiv C$$
$$t_T = 5 \text{ min}$$
$$V_T = 50\%$$
$$K = 911.9$$

Now let us consider the following two exposure histories.

Case 1	*Case 2*	*Time*
$C = 0$	$C = 0$	$t < 0$
$C = 90\%$	$C = 90\%$	$0 \leq t < 3$ min
$C = 75\%$	$C = 65\%$	3 min $\leq t < 6$ min
$C = 0$	$C = 0$	6 min $\leq t$

For both cases:

$$\left(1 - \frac{t_T}{t_d}\right) = \left(1 - \frac{5 \text{ min}}{6 \text{ min}}\right) = \frac{1}{6}$$

For Case 1:

$$\sum_{i=1}^{n} (V_i - V_T)\, \Delta t_i = 3[(90 - 50)^{1.979} + (75 - 50)^{1.979}] = 6194.64$$

and for Case 2:

$$\sum_{i=1}^{n} (V_i - V_T)^n\, t_i = 3[(90 - 50)^{1.979} + (65 - 50)^{1.979}] = 5079.88$$

Thus

$$\hat{q}_1 = 1032.44$$

and

$$\hat{q}_2 = 846.65$$

for Cases 1 and 2, respectively.

Comparing these values to $K = 911.9$, we would assess deaths in Case 1 but not in Case 2. Note that in Case 1 the concentration equals or exceeds 75% for a total of 6 minutes, whereas a duration of 6.5 minutes is required for that level of asphyxiant. However, the assessment method represented by equation (C-11) does assess deaths for Case 1 because exposure at the higher concentration ($C = 90\%$) is accounted for. This is just the type of behavior desired for the assessment method. Equation (C-11) also has the desired property that, if a constant level of exposure is experienced, damage will be assessed if the critical exposure time, t', for that particular level of exposure is exceeded.

That is, for a single exposure level, V, equation (C-11) becomes

$$\hat{q} = \left(1 - \frac{t_T}{t_d}\right)(V - V_T)^n \, t_d$$

or

$$\hat{q} = (t_d - t_T)(V - V_T)^n$$

and damage will be assessed if $t_d \geq t'$.

* U.S. GOVERNMENT PRINTING OFFICE : 1977 O-728-950/1312